

AD-A039 541 COLD REGIONS RESEARCH AND ENGINEERING LAB HANOVER N H F/6 13/13
FIELD STUDIES OF THE CONCRETE DAM AT THE BRATSK HYDROELECTRIC P--ETC(U)
APR 77 S Y EIDELMAN

UNCLASSIFIED

CRREL-TL-621

NL

4
AD
A039541



TL 621



ADA 039541

5

Draft Translation 621
April 1977

FIELD STUDIES OF THE CONCRETE DAM AT THE BRATSK HYDROELECTRIC POWER PLANT

S.Ya. Eidel'man

COPY AVAILABLE TO DDC DOES NOT
PERMIT FULLY LEGIBLE PRODUCTION



CORPS OF ENGINEERS, U.S. ARMY
COLD REGIONS RESEARCH AND ENGINEERING LABORATORY
HANOVER, NEW HAMPSHIRE

AD NO. _____
DDC FILE COPY

Approved for public release; distribution unlimited.

Unclassified

SECURITY CLASSIFICATION OF THIS PAGE (When Data Entered)

Unclassified

SECURITY CLASSIFICATION OF THIS PAGE(When Data Entered)

and stressed state, the opening of the structural seams of the dam and the effect of cementation on them. The standard thermal stress patterns of concrete and the development of thermal cracks are investigated. By comparison with the first edition, this book has been enlarged using the results of the field studies of the stresses in the casing and the reinforcing of the turbine conduit and data on the seepage heads in the foundation and in the body of the dam.

SECURITY CLASSIFICATION OF THIS PAGE(When Data Entered)

(14) CRREL-TL-621

DRAFT TRANSLATION 621

ENGLISH TITLE: FIELD STUDIES OF THE CONCRETE DAM AT THE BRATSK HYDROELECTRIC POWER PLANT

FOREIGN TITLE: NATURNNYE ISSLEDUVANIYA BETONNOY PLOTINY BRATSKOY GES

10
AUTHOR: S.Ya. Eidel'man

ACCESSION for	
HTB	White Section <input checked="" type="checkbox"/>
BSC	Buff Section <input type="checkbox"/>
UNARMED	
JUSTIFICATION	
BY	
DISTRIBUTION/AVAILABILITY CODES	
DISL	AVAIL. 200/OF SPECIAL
A	23
1/87Z	

SOURCE: Moscow, Energiya, 1975, 294p.

CRREL BIBLIOGRAPHY
ACCESSIONING NO.: 30-1860

Translated by Office of the Assistant Chief of Staff for Intelligence for U.S. Army Cold Regions Research and Engineering Laboratory, 1977, 295p.

(11) Apr 77

037 100

(12) 303po

NOTICE

The contents of this publication have been translated as presented in the original text. No attempt has been made to verify the accuracy of any statement contained herein. The translation is published with a minimum of copy editing and graphics preparation in order to expedite the dissemination of information. Requests for additional copies of this document should be addressed to the Defense Documentation Center, Cameron Station, Alexandria, Virginia 22314.

6/87

TABLE OF CONTENTS

	Page
FOREWORD	2
CHAPTER 1. BRIEF DESCRIPTION OF THE DAM	4
1.1. Natural Conditions of the Construction Zone	8
1.2. Concrete Dam	14
1.3. Organization of Concrete Work	19
1.4. Artificial Cooling of the Columnar Massifs and Cementation of the Intercolumnar Joints	20
1.5. Hydroelectric Power Plant Building, Reservoir and Startup of the Units	22
CHAPTER 2. MEASURING INSTRUMENTS, THEIR PLACEMENT AND INSTALLATION	22
2.1. Composition of the Observation and Locations of Measuring Instruments and Devices	22
2.2. Measurement of the General Displacement	26
2.3. Measuring the Piezometric Levels	30
2.4. Measurement of the Concrete Temperature	31
2.5. Measurement of Strains and Stresses in Concrete	32
2.6. Measuring the Pressure of the Seepage Water in the Horizontal Structural Joints at Monolithic Concrete	36
2.7. Study of the Static Operation of the Pressure (Turbine) Conduit	36
2.8. Receiving Instruments	39
2.9. Instrument installation	40
2.10 System of Monitoring and Measuring Instruments of the Operational Inspectorate and Its Organization	45
CHAPTER 3. DETERMINATION OF THE PHYSICAL-MECHANICAL AND THERMOPHYSICAL CHARACTERISTICS OF CONCRETE	48
3.1. Test Composition and Procedure	48
3.2. Compressive and Tensile Strength of Concrete	50
3.3. Young's Modulus of Concrete	53
3.4. Limiting Extensibility of Concrete	54

CONTENT [Continued)

Page

3.5. Measure of Creep	55
3.6. Calculation and Measurements of the Relaxation Stress Coefficients	55
3.7. Heat Release Characteristics of the Concrete	60
3.8. Thermophysical Characteristics of Concrete	62
3.9. Coefficient of Linear Expansion of Concrete	63
3.10 Effect of the Negative Temperature on the Physical-Mechanical Properties of Concrete	64
CHAPTER 4. TEMPERATURE REGIME OF THE DAM	
4.1. Air and Water Temperatures	68
4.2. Air Temperature Regime in the Cavities of the Expanded Joints	71
4.3. Planning Measures with Respect to Regulating the Temperature of the Concrete	74
4.4. Exothermal Heating of the Concrete	75
4.5. Dissipation of Exothermal Heat	80
4.6. Variation in Time and Temperature Distribution in Concrete Massifs	83
4.7. Freezing of the Dam Sections	88
4.8. Thermal Regime of the Dam During Permanent Operation of the Hydroelectric Power Plant	91
CHAPTER 5. GENERAL DISPLACEMENTS OF THE DAM	96
5.1. Vertical Displacements (Settling) of the Sections	96
5.2. Horizontal Displacements of the Dam Sections	102
5.3. Thermal Displacements of the Sections of the Dam	106
5.4. Calculation of the Deflection of the Dam from the Hydrostatic Pressure of the Reservoir Water	111
5.5. Horizontal Displacement of the Dam from Rotation of the Base	117
5.6. Deflection of the Dam in the Normal Operating Regime	120
5.7. Determination of the Young's Modulus of the Dam and the Rock Base	123
CHAPTER 6. STRESSED STATES OF CONCRETE MASSIFS	
6.1. Calculation of the Stresses with Respect to the Deformations Measured in Concrete	126
6.2. Stresses in the Blocks Next to the Rock	135
6.3. Stresses in the Blocks in the Extracontact Zone	146
6.4. Stresses on the Downstream Face	159
6.5. Stresses in the Blocks of the First Columns	162
6.6. Stresses in the Blocks During the Filling of the Reservoir, Effect of the Hydrostatic Load	166
6.7. Deformations in the Contact Zone of the Rock Base	178
6.8. Theoretical and Experimental Studies of the Stressed State of the Contact Zone of the Dam During Its Joint Operation with the Base	182

CONTENTS [Continued]

Page

CHAPTER 7. CRACK FORMATION IN THE DAM BLOCKS	189
7.1. Crack Formation in Dams Built in Locations with Sharply Continental Climate	189
7.2. Remote Strain Gage as a Crack Formation Indicator	190
7.3. Crack Resistance Criterion	191
7.4. Crack Formation in the Uncovered Blocks	195
7.5. Crack Formation Connected with Covering of the Blocks	202
7.6. Crack Formation for High Rates of Pouring Concrete	206
7.7. Crack Formation in the Concrete Massif Made of Old Concrete	208
7.8. Variation of the Opening of the Cracks in Time	209
7.9. Observations of the Surface Cracks	212
7.10 Probability of Through Crack Formation in the Blocks	217
CHAPTER 8. OPENING OF THE CONSTRUCTION AND STRUCTURAL JOINTS OF THE DAM	221
8.1. Conditions of Making the Dam Monolithic	221
8.2. Maximum Opening of the Intercolumnar Joints	222
8.3. Relation Between the Openings of the Intercolumnar Joints and Temperatures	228
8.4. Cementation of Intercolumnar Joints	228
8.5. Quality of Cementation	230
8.6. Role of the Toothed Couplings	237
8.7. Intersectional Joints	241
8.8. Joint Between the Dam and the Hydroelectric Power Plant Building	243
CHAPTER 9. STRESSES IN THE TURBINE CONDUIT	246
9.1. Calculated Loads. Calculated Stresses from the Internal Water Pressure	246
9.2. Thermal Stresses	247
9.3. Stresses from the Internal Pressure and Total Stresses	250
9.4. External Pressure on the Conduit Shell	254
9.5. Stresses in the Concrete and Reinforcing Around the Shell of the Spiral Chamber	254
CHAPTER 10. LEAKAGE REGIME IN THE BASE AND IN THE BODY OF THE DAM	257
10.1. Leakage Head in the Contact Zone	257
10.2. Effect of the Cementation on the Counterpressure in the Base of the First Column	261
10.3. Nature of Percolation Flow in the Traprocks	263
10.4. Effect of the Cementation Curtain and the Drainage Structures	265
10.5. Percolations through Concrete of the First Columns of the Dam	269

CONTENTS [Continued]

Page

CHAPTER 11. CONCLUSIONS AND PROPOSITIONS	272
11.1. State of the Dam	272
11.2. Effect of the Technological Factors on the Monolithic Nature of the Dam	275
11.3. Conclusions with Respect to the Problems of Planning, Design and Construction	276
11.4. Conclusions with Respect to Procedural Problems	279
BIBLIOGRAPHY	284

FIELD STUDIES OF THE CONCRETE DAM AT THE BRATSK HYDROELECTRIC POWER PLANT

Moscow NATURNYYE ISSLEDOVANIYA BETONNOY PLOTINY BRATSKOY GES [Field Studies of the Concrete Dam at the Bratsk Hydroelectric Power Plant] in Russian
1975 pp 3-285

[Book by S. Ya. Eydel'man, Second Enlarged and Revised Edition, Energiya]

A discussion is presented of the results of field observations and studies performed over a nine-year period during the construction, the temporary operation and six years of permanent operation of the concrete dam at the Bratsk Hydroelectric Power Plant imeni 50th Anniversary of the October Revolution.

The characteristics of the measuring instruments, the arrangement and placement of them and the methods of installing them are presented. The field data are presented for the general shifts of the dam, its thermal regime and stressed state, the opening of the structural seams of the dam and the effect of cementation on them. The standard thermal stress patterns of concrete and the development of thermal cracks are investigated. By comparison with the first edition, this book has been enlarged using the results of the field studies of the stresses in the casing and the reinforcing of the turbine conduit and data on the seepage heads in the foundation and in the body of the dam.

The book is designed for engineers working in design, construction, maintenance and research of hydroengineering structures.

FOREWORD

The technical progress in the design and construction of high concrete dams is continuously connected to the field studies and observations of their state and operation in the process of construction, operation and maintenance. The comprehensive field investigation of the structures is not only the most reliable means of controlling the satisfaction of the design specifications and construction quality, but it is also a source of information for making corrections to the calculation systems and the methods of designing and constructing analogous structures.

In the middle of the 1950's, an intense phase of hydroelectric power construction began in eight regions of our country. The absence of Soviet and foreign experience in the construction of large concrete structures under severe, sharply continental climatic conditions posed a number of complex problems requiring solution while designing and building high concrete dams under such conditions. The dam at the Bratsk Hydroelectric Power Plant imeni 50th Anniversary of the October Revolution was the first dam in the USSR higher than 120 meters built in Eastern Siberia, and these complex problems were solved for the first time on this project. The field observations and studies of the dam under construction acquired special urgency under these conditions.

The field studies of the concrete dam at the Bratsk Hydroelectric Power Plant were performed by the All-Union Scientific Research Institute of Hydroengineering imeni B. Ye. Vedeneyev (VNIIG) by the initiative of the Bratsk Hydroelectric Power Plant division of the Gidroproyekt Institute imeni S. Ya. Zhuk.

A broad system of monitoring and measuring instruments and devices have been installed in the Bratsk Hydroelectric Power Plant dam. The systematic observation of these instruments were carried out throughout the entire construction period and the temporary operation of the hydroelectric power plant, and they are continuing on the dam now under operation. Being the largest-scale studies of this type in our country, the field studies of the Bratsk Hydroelectric Power Plant dam have provided broad experimental data on a number of significant problems of the design and construction of concrete dams under severe climatic conditions. The results of this work

performed in all phases under the direct management and with the participation of the author were discussed in the first edition of this book which encompasses the first eight years of the observations. It is the first Soviet monograph devoted to studies of a concrete dam since the papers by Yu. A. Nilender on the Dnepr dam published at the beginning of the 1930's.

The second edition of the book contains discussions of the results of 15 years of observations, including the six years of normal operation of the dam. The book has been enlarged by two chapters, the material of which was not discussed in the first edition. Inasmuch as the size of the book has remained the same, the inclusion of the new material required condensation of the old. Thus, the material of the book has been to a significant degree revised and reworked.

The significance of the field studies is determined not only by their control functions and the information obtained, but to a significantly greater degree the new phenomena which are established by them and which arise in connection with these problems for future research. Among such problems it is necessary first of all to note the important influence of the temperature effects on the stress-strain state of high concrete dams under severe climatic conditions and the necessity for considering these effects. The problem stated by the given research regarding the stressed state of the contact zone of the first columns which at the present time has become the subject of a number of experimental and theoretical studies is no less important. Finally this work has revealed a change in the physical-mechanical properties of the hardened concrete and its effect on the static operation pattern of high concrete dams. Some of the results of the theoretical and experimental studies of these problems are discussed in the second edition.

The results of the investigation presented in the first edition of this book are being considered to one degree or another in the design and construction of analogous dams and also when performing experimental and field studies. It is to be hoped that the second edition will be useful to Soviet hydraulic engineers.

The author expresses his appreciation to Professor A. L. Mozhevitinov for a number of valuable comments which he made when reviewing the manuscript.

It is requested that all comments and suggestions be sent to the following address: 192041, Leningrad D-41, Marsovo pole d. 1, Leningrad division of Energiya Press.

CHAPTER 1. BRIEF DESCRIPTION OF THE DAM

1-1. Natural Conditions of the Construction Zone

The Bratsk Hydroelectric Power Plant was constructed on the Padunskoye narrows of the Angara River in the vicinity of Lake Baykal.

The climate in the construction zone is sharply continental. The mean annual temperature for many years is -2.6° C. The mean period from frost to frost lasting approximately from the middle of October to the second half of April is 182 days. For 109 days a mean diurnal temperature below -15° C is observed, and for 83 days, below -20° C. The lowest mean monthly air temperature of -23.8° C was recorded in January; the absolute minimum of -58° C was also recorded in January.

The average temperature in the warmest month -- July -- is 18.2° C; the absolute maximum temperature is 35° C.

The greater part of the annual precipitation, equal to 300 mm, falls in the warm part of the year.

The watershed area of the river from Lake Baykal to the dam site is about 1,200,000 km². The most important tributaries of the Angara in this section are the Irkut, Kitoy, Belya and Oka Rivers. The total mean flow rate of the tributaries over many years to the site is 870 m³/sec. The primary runoff of the tributaries occurs in the summer as a result of rain falling in the headwaters and falling of the high mountain snow. During the July-September period, this creates a number of sharply expressed but brief peaks on the hydrographs of the Angara River. The maximum annual flow rates of Angara in the dam section are also caused by the passage of these floods.

The mean flow rate of the river over many years is 2,906 m²/sec, and the most observed flow rate is 13,400 m³/sec. The maximum flow rates with a guarantee of 5, 1, 0.1 and 0.01% amount to 11,400, 14,000, 17,300 and 22,300 m/sec respectively. The minimum mean monthly flow rates usually come in March-April and are within the limits of 1060 to 2090 m³/sec [1].

The Padunskoye narrows along the section line have a trapezoidal cross section with a width at the base of 800 meters, and at the level of the cliff top about 900 meters. The height of the scarp beaches is 70-80 meters. The narrows are located in a massif of Siberian traprock represented by several varieties of diabases. The traps on the right bank are 100-130 meters thick, and on the left bank, about 200 meters thick. The traps in the channel are eroded, and they are 33-50 meters thick (Figure 1-1,b)

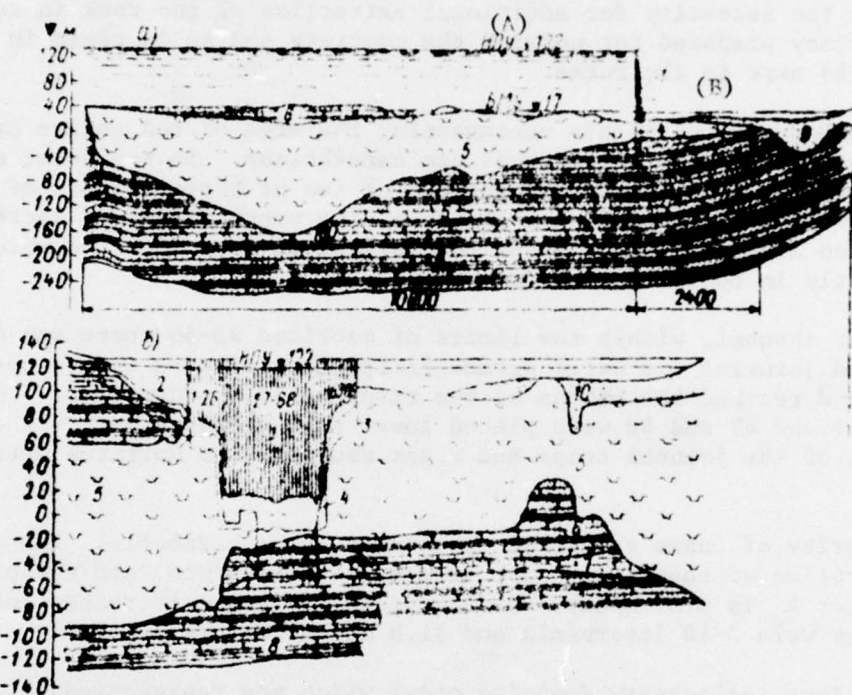


Figure 1-1. Geological sections through the axes of the dam:
 a -- transverse; b -- longitudinal. 1 -- concrete dam; 2 -- earthen dam; 3 -- drainage contour; 4 -- cementation curtain contour; 5 -- diabases; 6 -- sandstone; 7 -- aleurolites; 8 -- argillites; 9 -- sand and sandy loam; 10 -- talus.

Key: A. normal backwater level
 B. base low water level

The trap massif occurs in the form of a thick plate wedging out at a distance from the section equal to 11 km in the upstream direction and 2 km in the downstream direction (Figure 1-1,a). The trap series is dismembered by primary separation joints into blocks of different sizes and shapes. The parallelepiped, for the most part massive-block and columnar, is the predominant shape. The joints are filled with chlorite, calcite and other minerals.

In addition to the basic system of joints (two mutually perpendicular, close to vertical and a third close to horizontal), the traps contain secondary systems of original fissures and weathering joints. The traps are also characterized by very fine, latent jointing by which the rock easily exfoliates under the effect of additional external loads. This property of the rock was felt especially during blast operations in the pit as a result of which the primary partings opened up; and at a great distance from the blasting site a set of fine fissures appeared by which the rock exfoliated to a depth of several tens of centimeters. This led in a number of cases to the necessity for additional extraction of the rock in the foundations already prepared for pouring the concrete and an increase in size of the blocks next to the rocks.

No sustained horizontal joints encompassing the area of the entire cross section were detected in the channel dam excavations. In the worst case such joints extended to the foundations of two or three columns of individual sections. Within the limits of the sixth column of sections 32-38, sustained etchelon-like (convex upward) joints were detected which dropped gently in the downstream direction.

In the river channel, within the limits of sections 43-56 there was a zone of increased jointing and water permeability which plunged in the upstream direction and reached the bottom of the river below the dam site. The footings of sections 47 and 48 were placed lower than provided for by the plan as a result of the jointed traps and traps weathered to detritus detected here.

In the majority of cases the traps are weakly water permeable. The specific water absorption of them q does not exceed 0.2 liters/min, and the percolation factor k is 0.05 m/day. In the vicinity of the increased jointing, these values were 2-10 liters/min and 11.5 meters/day respectively.

Below the traps sedimentary deposits occur which are represented by fine grain sandstones. Within the limits of the narrows at a depth of 20-25 meters below the footing of the traps there is a layer of dark gray dense aleurolites about 15 meters thick below which sandstones again occur. The water permeability of the sandstones on the upper part of the aleurolites is characterized by values of q from 0.02 to 2 liters/min and $k = 12$ m/day. The lower footing of the aleurolites in practice is a confining bed ($q < 0.02$ liters/min) [2].

The mean mechanical properties of the rock in the foundation of the dam determined by the temperature testing of samples are presented in Table 1-1.

The trap deformation modulus determined by the seismic method is $(6-9) \cdot 10^6$ kg-force/cm², that is, it is close to the core testing results.

The Soil Mechanics Laboratory of the VNIIG Institute imeni V. Ye. Vedeneyev performed a number of field studies in vertical boreholes of the deformative properties of the rock foundation of the dam to a depth of 34 meters and also

BEST AVAILABLE COPY

the studies to investigate the mechanism of the development of stresses and strains in the contact zone of the dam with the rock bases. As a result, the following approximate empirical relations were obtained between the deformation modulus E (kg-force/cm²) and the depth h (m) for the diabases:

light jointing

$$E = 546000 h^{0.125}, \quad (1-1)$$

medium jointing

$$E = 170000 h^{0.893}, \quad (1-1')$$

Table 1-1

Rock	Specific weight, t-force/m ³	Volume metric mass, t/m ³	Water absorption, %	Temporary resistance to crushing, kg-force/cm ²	Deformation modulus, kg-force/cm ²
Traps	3.04	3.02	0.03	1700	500000
Sandstones	2.70	2.25	3.8	325-375	90000
Aleurolite	2.75	2.32	5.0	320	60000

For transmission of the vertical pressure to the concrete stamps the deformation modulus of the rock turned out to be equal to 11,400 kg-force/cm² for the weathered traps and 130,000-440,00 kg-force/cm² for the preserved traps.

In order to determine the modulus of deformation of the rock the author used vertical deformations measured by remote strain gages in the process of building up the first columns when the temperature in the contact zone was in practice stable. Beginning with the proposition that the mass of the concrete is uniformly distributed with respect to area of the base of the first column, it was established that the modulus of deformation of the rock increased as the vertical load increased and it grew sharply after prolonged breaks in pouring the concrete which can be explained by gradual compacting of the rock. The pliability of the latter in the base of different sections and their columns of the same section turned out to be different, and the stabilized values of the modulus of deformation of the rock in the contact zone were within the limits from $1.6 \cdot 10^6$ to $4 \cdot 10^6$ kg-force/cm² close to the values obtained using the stamps [19].

In substantiation of the shearing coefficient used in the stability calculations for the dam, D. D. Sapegan and K. V. Khoklov, under the direction of P. D. Yevdokimov performed broad field studies in mines and also directly in the excavation for the first stage at the marks for laying the footings of the dam. The studies were performed by the method of shift of the concrete stamps from 0.5 to 4 m² in size cemented to the rock base. With respect to geological structure the bases of the stamps were different:

from disintegrated to the gruss state to fully compact finely jointed and hard diabases, and with respect to nature of preparation, from minimum roughness (depressions, protrusions 0.5 cm) to maximum roughness (unevenness to 15 cm).

The results of the experiments with respect to the shear-slip of the stamps on the foundations of different roughness gave values of the parameters of the straight lines $t = c + \sigma \tan \phi$ presented in Table 1-2 [3].

Table 1-2

Roughness of the foundation	c, t/m ²		tg φ	
	shear	slip	shear	slip
Minimal	80	14	1.13	1.17
Medium	100	20	1.74	1.81
Maximum	140	42	1.82	2.04

The adopted calculated coefficient 0.8 was determined by the minimum value of $\tan \phi = 1.13$ with a safety margin of 1.4.

1-2. Concrete Dam

The pressure front of the Bratsk Hydroengineering Complex [1, 4, 5] includes the concrete dam (Figure 1-2) with the channel section II 924 meters long and the shore sections I with a total length of 506 meters and also the earthen dams with a total length of 3,710 meters.

The channel section II, which is the basic structure of the hydroengineering complex is a light type concrete gravity dam of triangular profile with vertical pressure face and a slope of the downstream face of 1:0.8. The maximum height of the dam is 125 meters.

The dam is sectioned by permanent transverse expansion joints in the section 22 meters long equal to the length of the hydroelectric power plant building block. On the inside, beginning with the rock foundation the joints are expanded to 7 meters. The dam is cut into columnar massifs by the temporary longitudinal joints every 13.8 meters. The concrete pouring block is 3 meters high; the joining of the adjacent blocks is toothed. Cementation reinforcing is installed in the intercolumnar joints through which the joints are cemented for making the dam a monolith.

In structural respects the channel section is divided into three parts: the station part IV, the spillway part V and the closed part III (Figure 1-2).

The station part comprises 20 sections (31-50), each of which has a steel turbine conduit 7 meters in diameter with wall thickness from 22 mm at the top to 28 mm at the bottom. Around the conduit there are reinforcing girders creating a reinforced concrete ring 1.5 meters thick. The water intake threshold is located at a depth of 42 meters from the normal backwater level, and the temporary water intake threshold of 6 units put into operation in the first stage was submerged 67 meters below the normal backwater level.

BEST AVAILABLE COPY

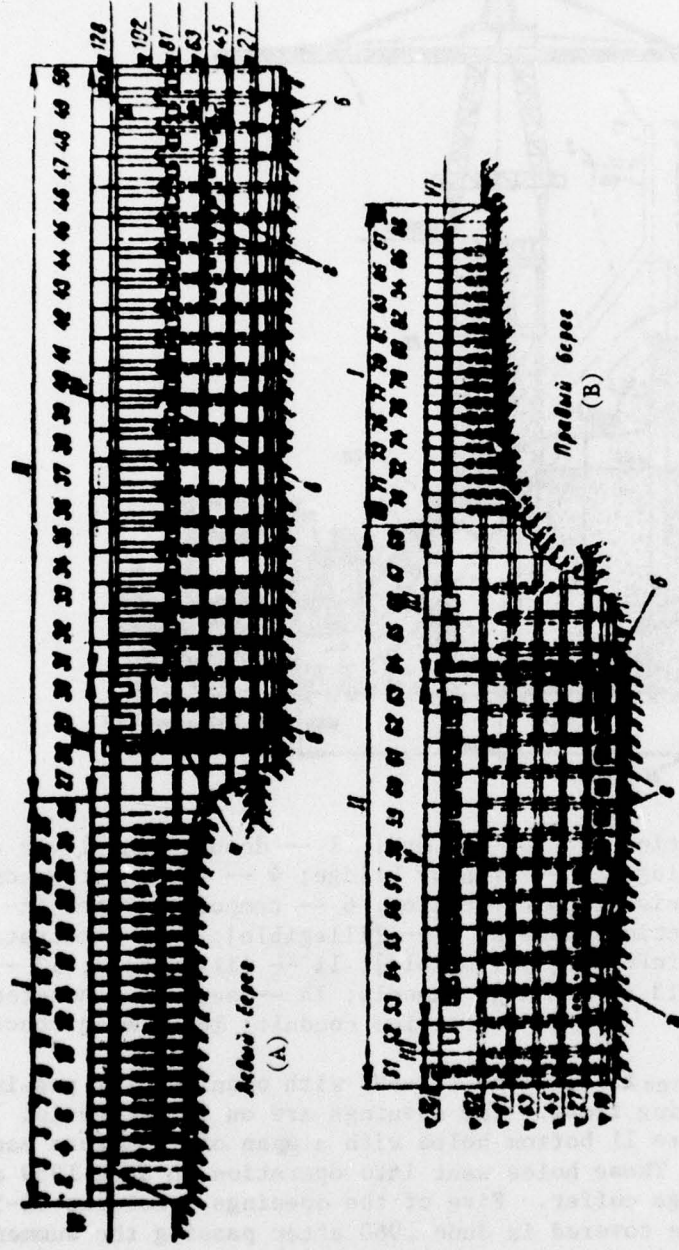


Figure 1-2. Concrete dam with sections: I -- shore; II -- channel; III -- closed part; IV -- spillway part; V -- station part; VI -- adjoining of the earthen dams, 1-89 -- section numbers; a -- elevator shaft; b -- pumping station; c -- permanent water intake openings; d -- temporary water intake opening; e -- deep floodgates; f -- bottom spillway.

Key: A. left bank B. right bank

For covering the water intake openings, flat gates, a repair enclosure and debris trapping gratings have been constructed (see Figure 1-3).

BEST AVAILABLE COPY

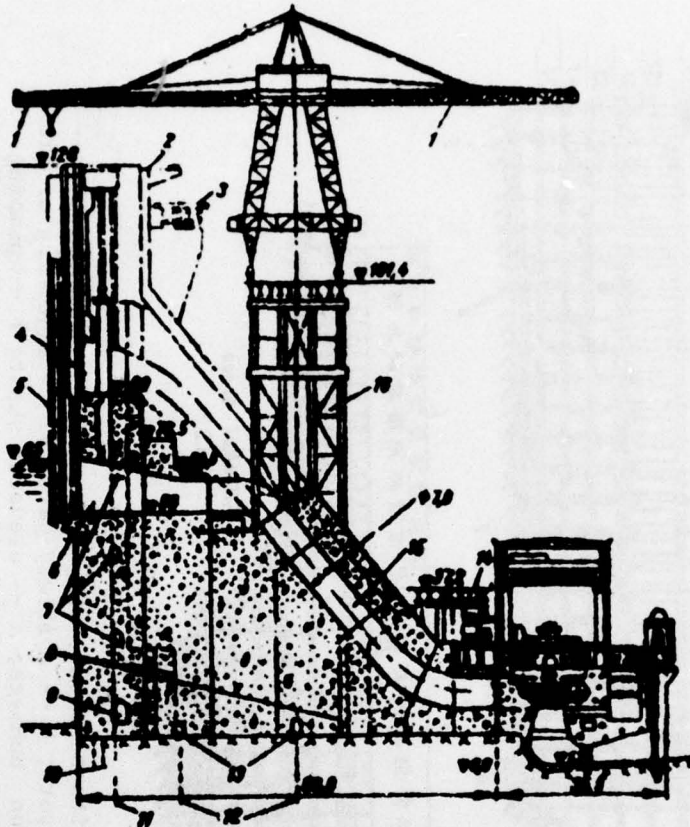


Figure 1-3. Station part of the dam. 1 -- double-cantilever crane; 2 -- railroad bridge; 3 -- highway bridge; 4 -- permanent water intake; 5 -- debris trapping grating; 6 -- temporary water intake; 7 -- inspection tunnels; 8 -- [illegible]; 9 -- cementation tunnel; 10 -- reinforcing [illegible]; 11 -- [illegible]; 12 -- drainage holes; 13 -- drainage tunnels; 14 -- auxiliary concrete carrier trestle; 15 -- turbine conduit; 16 -- main concrete trestle.

The spillway part comprises 11 sections (53-63) with openings for passing the construction and operating flows. The openings are on three levels. On the lower level there were 11 bottom holes with a span of 12 meters each and a height of 10 meters. These holes went into operation in June 1959 after building the second-stage coffer. Five of the openings (sections 53-57) in the form of a crest were covered in June 1960 after passing the summer floods. The remaining six openings (sections 58-63) in the form of bottom tunnels covered with reinforced concrete beams were successfully closed beginning on 1 September 1961 for filling the reservoir. The last of these openings was closed when the water level in the reservoir rose to the 55 meter mark, and the possibility of passing the flow through the deep spillways arose (Figure 1-2).

BEST AVAILABLE COPY

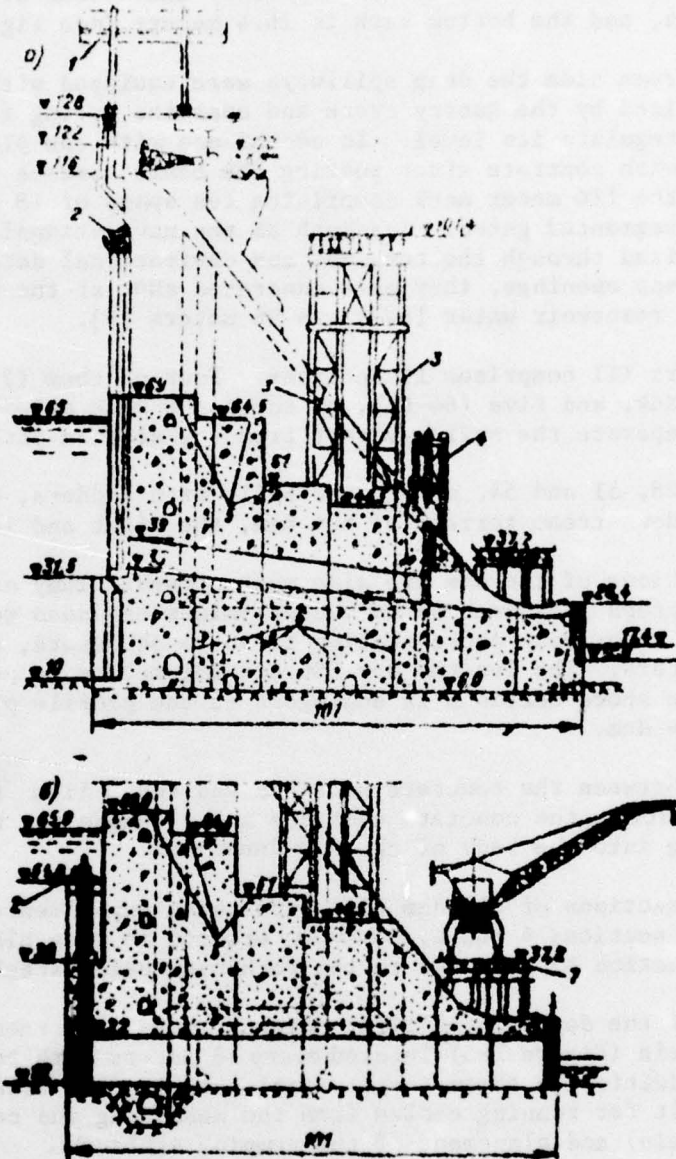


Figure 1-4. Spillway part of the dam: a -- with deep openings; b -- with bottom openings. 1 -- gantry crane; 2 -- [illegible]; 3 -- main concrete carrier trestle; 4 -- crane; 5 -- contour of the pass profile of the dam; 6 -- intercolumnar joint; 7 -- auxiliary trestle.

The ten deep spillways with the threshold mark at the input of 33 meters and dimensions of 3×6 meters were located two above the finished holes of the crest in sections 53-57. The spillway dimensions of the exit are 3×4.8 meters, and the bottom mark is 26.4 meters (see Figure 1-4).

On the downstream side the deep spillways were equipped with flat gates which were raised by the gantry crane and operated during filling of the reservoir to regulate its level. In accordance with the plan they were finished off with concrete after putting the basic surface spillway into operation at the 116 meter mark comprising ten spans of 18 meters each covered with segmented gates. Inasmuch as the navigational passes in 1964 could be realized through the turbines and cavitation deterioration occurred in deep openings, they were concreted shut at the beginning of 1964 when the reservoir water level was 96 meters [6].

The closed part III comprises 11 sections. Four of them (27-30) are located on the left bank, and five (64-68), on the right bank adjoinings, and two (51 and 52) separate the spillway part from the station part (Figure 1-2).

In sections, 28, 51 and 54, shafts are built with ladders, elevators and exits to the downstream terrace of the dam, the right and left banks.

The shore sections of the dam are also made closed. They are split into sections 11 meters long each by permanent joints expanded to 4 meters. The height of the right bank shore section is 33 to 54 meters, and the left bank 53-64 meters. The lengths are 286 and 231 meters respectively. The profile of the shore sections is analogous to the profile of the channel section of the dam.

The coupling between the concrete sections and the dirt sections is realized by cutting the concrete sections and a tongue and groove pattern 20 meters long into the body of the earthen dam.

In the shore sections of the dam there are three experimental sections: on the left bank sections 4 and 6, partially erected in long blocks, and on the right bank, section 85 anchored to the rock base using steel guys.

In the body of the dam and the first columns there are cementation and inspection tunnels (Figure 1-5) located every 18 meters with respect to the height. In addition to these longitudinal tunnels, the transverse tunnels have been built for running cables from the measuring and control equipment (the KIA tunnels) and placement of the pumping stations.

The drainage of the body of the dam comprises the vertical, tubular drains 30 cm arranged 2.75 meters apart at a distance of 7.5 meters from the pressure face. These drains collect the water which seeps through the horizontal structural joints, the cracks and seals in the expansion joints, and the discharge to the cementation tunnel.

For draining the base of the dam two drainage tunnels are built (in the second and fourth columns) with the flooding directly on the rock base.

Theee tunnels collect water which seeps through the base from the open surface of the expanded joints and through the charging holes of the deep drains. The latter 110 mm in diameter are drilled with spacing of 3 meters along the drainage tunnels to a depth of 23-35 meters in the first line drainage and 20-32 meters in the second line drainage.



Figure 1-5. Inspection tunnel

At the lowest points of the channel section of the footing of the dam in the central part (sections 48 and 49) and on the banks (sections 29 and 64) water collecting basins are made which communicate with the tail race by pipes 1 meter in diameter through which the seepage water freely discharges. Thus, in the expanded joints the water level should be maintained close to the maximum level of the tail race. In order to drain the expanded joints pumping stations are located in the same section with a total output capacity of $4.4 \text{ m}^3/\text{sec}$ by means of which it is possible to drain the cavities of the joints for three days and keep them dry. The same pumping stations drain the cementation tunnel which is isolated from the drainage system. During the construction period and the temporary operation of the hydroelectric power plant the expanded joints were kept dry.

The significant water permeability of the trap rock noted above excludes the possibility of any noticeable leakage of the water through the base of the dam and to the bypass. Therefore a deep (to the lower part of the aleurolites) cementation curtain was built in a single row with 4 meter spacing and only within the limits of the zone of increased water permeability (sections 44-65). The primary purpose of this curtain was to protect the drainage holes from overloading.

Under the remaining part of the channel dam a conjugate cementation curtain was constructed to 10 meters deep reinforced in the shore adjoinings. Under sections 29-33 the curtain depth is 15 to 20 meters. The reinforcing surface (area) cementation was done under sections 47-49.

Pressure turbine conduits 7 meters in diameter made of M16S steel with a yield point of $\sigma_{yield} = 2,300$ kg-force/cm² and a sheet thickness of 22 meters in the upper section and 25 meters in the lower section are built into the concrete massifs of the station sections of the dam next to its downstream face.

The stability of the steel shell when pouring the concrete and also under the effect of the external seepage pressure is insured by the T-cross section stiffening rings installed at a distance of 750 mm from each other. These rings are used to couple the shell to the surrounding concrete reinforced to a thickness of 1.7 meters by the annular reinforcing girders.

In view of the insignificance of the expected deformations in the joint between the dam and the hydroelectric power plant building, the packing gland compensator is replaced by the free section of pipe 536 cm long insulated from the concrete by an elastic felt insert 50 mm thick allowing displacement of the steel shell with respect to the concrete. This section of the pipe is made of 10KhSND steel with a yield point of 4,000 kg-force/cm² and a sheet thickness of 28 mm.

The water intakes of the conduits have a threshold at the 77.1 meter mark. Six pipes of the first stage units started on the reduced head at the reservoir level of 65 meters were made with temporary water intakes having the threshold at the 55 meter mark. In order to convert the water intake to the permanent system the steel elbow by which the temporary water intake made contact with the pipe (Figure 1-3) was cut out and replaced by a straight insert of the permanent pipeline, and the temporary water intakes were closed off with concrete.

1-3. Organization of Concrete Work

The organization of the concrete work at the Bratsk Hydroelectric Power Plant is described in [6, 7 and 11]. The total volume of concrete work for the hydroengineering complex was 4.86 million m³; of this 4.415 million m³ or 91% went to the channel and shore sections of the concrete dam. The volume of concrete in the channel section is 3.995 million m³ or 82% of the total volume of the concrete work. In order to start the first stage units (for the reduced profile of the dam with toothed downstream face) it was necessary to pour 2.8 million m³ of concrete [1].

The concrete was poured by construction years as follows:

1958	1959	1960	1961	1962	1963	1964
38.8	454.3	910.5	1126.5	1241	491.8	76 thousand m ³

The maximum actual monthly intensity of concrete pouring reached 135,000 m³ and the annual, 1,241,000 m³.

The order of erection of the dam arose from the established time for starting up the first stage units (November 1961) and the scheme for passing the construction flows.

In the initial stage the operations were performed in the pit of the first stage behind the right bank coffers: the longitudinal crib and transverse dirt (fill, 15 meters wide at the top). In this section the concrete was poured in only 11 sections of the spillway dam to a height of 13-14 meters above the bottom of the pit. The concrete sectional coffer was constructed simultaneously which became the base section of the longitudinal coffer of the second stage and was then used as the separating pier in the tail race. Between this coffer and the longitudinal coffer of the first stage an intermediate pit was built in which the operations were performed on going from the pits of stage 1 to the pit of stage 2.

The construction flows during this period were passed through the left-hand free part of the channel. The concrete was delivered by motor transport across the right bank foreshore and the downstream coffer.

In May 1959 the Angara channel was closed and the pit of stage 1 was flooded. Then the construction flows were passed through the openings of the crest and the bottom tunnels. The operations were performed in the pits, intermediate and stage, under the protection of the left bank coffers. During this period the entire volume of concrete was poured required to start the first units; the channel part of the dam was raised to starting profile and on 1 September 1961, at exactly the time provided for by the plan, the first bottom opening was covered and filling of the reservoir began.

The plan provided for pouring concrete in the channel section from two concrete carrier trestles -- the primary trestle (1370 meters long, 90 meters high, 18.7 meters wide, spacing of supports 44 meters) and auxiliary (850 meters long, 27 meters high, 13 meters wide, spacing of supports 22 meters). On the primary trestle (Figure 1-6) six double-cantilever cranes operated with a boom span of 50.5 meters and a load capacity of 22 tons, and on the auxiliary trestle (the small trestle) there were seven portal-boom cranes with a capacity of 10/7.5 tons and a boom span of 30/40 meters respectively.

The delay in the erection and mounting of the trestles forced the concreting to be done first by caterpillar cranes operating in the pits from the rock base, and then by the portal-boom cranes installed on the columns of the truncated lower part of the dam. This procedure without the use of trestles, which made it possible to operate in various parts of the pit and at different levels, was used to pour more than 1.5 million m^3 of concrete. The deficiencies of this procedure must be considered to include the necessity of remounting the cranes and bridges and also the nonuniformity of erection of the columns in the section in which the crane was installed as a result of which great disparities in height between them arose.

The concrete mix was transported by the MAZ-205 and the KrAZ-222 five and 12-ton dump trucks with concrete feeders and buckets of 3 and 6.4 m^3 capacity on the auxiliary trestle. The double-cantilever cranes on the main trestle, the operation of which on the dead-end access began in the first quarter of 1960 provided for pouring concrete at any point on the dam

to its full height with the exception of the space under the trestle covered by the bridge of the second level of the trestle through which during construction the main Tayshet-Lena railroad was laid. The pouring of the concrete for the dam in the space under the trestle and also the hydroelectric power plant building was done using the portal-boom cranes from the auxiliary trestle.



Figure 1-6. Station part of the dam and the concrete carrier trestle during construction.

The preparation of the blocks for pouring concrete consisted in treating the concrete surface before much aging with a water-air jet or brushing with steel brushes and then flooding with a high pressure stream of water. In the winter the surface treated with the steel brushes was not flooded with water, but it was blown with compressed air. The first layer of the concrete mix 15 to 20 cm thick with plasticity of 4-6 cm (without large gravel) was poured on the prepared surface. The concrete mix was compacted using the I-86 sonic vibrators modified by the Bratskgesstroy trust.

The following types of forms were used to build the dam: in the expanded joints, concrete blocks $150 \times 230 \times 70$ cm with projections on the inside (Figure 1-7); in the construction joints between columns, metal panels; in the remaining parts of the dam, panels 6×3.18 meters made of boards 2.5 cm thick fastened with metal rods.

In the winter the panels were insulated by a layer of shavings 5 cm thick and a second layer of boards 2 cm thick. The peripheral electric heating electrodes were attached to the surface of the panels. This heating was used during the setting of the concrete.

In the joints between columns, interblock toothed elements (coffins) were attached to the installed forms (see Figure 2-12). A wood cantilevered form made of panels 3.75×3 meters in size on metal girders was used on the pressure face.



Figure 1-7. Modular concrete forms.

The concrete mix for the basic structure was prepared at the concrete plant located on the lower terrace of the right bank 3.5 meters from the site. Eighteen concrete mixers with 2,400 liter each were operated at the plant. The storage capacity for the cement was 16,000 tons. The fillers were delivered by the gravel sorting plant. The mass of the gravel was screened wet in the summer, and dry in the winter. Under the pit conditions at the Bratsk Hydroelectric Power Plant the quality of the fillers screened in the winter, especially during the cold part of the year, differed little from the quality of the material screened in the summer [8, 9].

The insufficient content of the coarse (more than 40 mm) components in the gravel led to the necessity for preparing gravel from local diabases at the rock crushing plant and adding up to 50% fine grain sand to the concrete.

In order to decrease the cement consumption, the plan provided for sorting the coarse filler into four fractions: 5-20, 20-40, 40-80 and 80-100 mm, and the sand into two fractions: 0.15-0.8 and 0.8-5 mm. Actually for the fillers the concrete was prepared from two fractions of the sand and three fractions of gravel and crushed rock (5-20, 20-40 and 40-100 mm).

With respect to strength the concrete corresponded to types 100 and 200; with respect to water impermeability, types V-2, V-4 and V-8; with respect to frost resistance, types Mrz-100 and Mrz-250.

The type 100, V-2 concrete was poured in the inside part of the dam and concrete type 200, V-8 was used in the first columns (below the reservoir operation level) and also in the base of the station part of the dam. At the surface of the pressure face within the limits of variation of the water level and on the down stream face of the spillway part concrete type 200, V-8, Mrz-250 was used. The downstream faces of the station and the closed parts of the dam subjected to variable air temperatures were executed

from type 200, V-4, Mrz-100 concrete. Type 200 concrete was used for the hydroelectric power plant building, and type 400, V-12 was used for the discharge tubes.

Until 1960, cement from various plants, primarily the Irkutsk plant, was used in the concrete mix. In subsequent years two grades of cement from the Krasnoyarsk plant were used: the pure clinker BGS-A, activity 420-660 kg-force/cm², and the slag-portland cement BGS-B, activity 300-600 kg-force/cm², which had to satisfy the requirements indicated in Table 1-3 [13].

Table 1-3

Index	Grade of cement	
	A	B
Compressive strength R, kg-force/cm ²	>400	>300-400
Heat of hydration on the 7th day, cal/gram	≤60	≤60
Mineralogic composition of the clinker, %		
C ₃ S	45-55	45-55
C ₃ A	≤8	≤10
Alkali content (recalculated for Na ₂ O), %	≤0.6	≤0.6
MgO content, %	≤4.5	≤4.5

The established C₃A content exceeds the value of 6% recommended in [12]. However the Krasnoyarsk cement plant did not guarantee delivery of purely clinker cement with a C₃A content less than 7-8% [8].

The concrete compositions during the first years of construction were not stable. A large part of the concrete was made from gravel no more than 40 mm in diameter; stiff mixes were used with cone settling of close to zero, and for placeability the SNV air entraining additive was introduced. The compositions used from 1961 on [10] are presented below:

Type of concrete	100, V-2	200, V-8	200, V-8 Mrz-250
Type of cement	BGS-B	BGS-B	BGS-A
Calculated V:C ratio	0.8	0.55	0.5
Cone settlement, cm	0.5-3	0.5-3	3-5
Per 1 m ³ of concrete, kg of			
Cement.....	160	230	280
Water	128	126	140
Fine sand	284	270	--
Coarse sand	284	270	757
Gravel 5-20 mm	569	510	362
Gravel 40-40 mm	416	386	361
Gravel 40-100 mm	645	626	550
Crushed rock 40-100 mm.....	706	706	635

SSB plasticizer	0.2% of the weight of the cement
Density of the concrete mix, tons/m ³	2.44-2.53 2.42-2.50 2.45-2.53

The following requirements were imposed on the winter concrete, the volume of which exceeds half of the total volume of the concrete: before freezing it had to get 50% of its compressive strength after 28 days of aging, and the temperature of the mix poured could not be more than 8-10° C. Accordingly, the concrete mix was heated in the heating bins to 20° C; the bodies of trucks were equipped with double walls between which the exhaust gases were passed. The blocks were covered with tenths, inside which a positive temperature was maintained by using steam heaters. While the concrete was setting up, it was subjected to peripheral electrical heating. The winter forms were not removed until spring.

In the summer the temperature of the concrete mix leaving the plant had to be lowered to 10° C according to the plans. For this purpose it was proposed that the filler be cooled in the bins to 8° C and the water to 2° C. In addition, provision was made for the addition of crushed ice to the concrete mixes. The plant used only experimental addition of ice and then only to a small volume of the concrete (120,000 m³).

1-4. Artificial Cooling of the Columnar Massifs and Cementation of the Intercolumnar Joints

It is necessary to cement the intercolumnar joints at a concrete temperature close to the operating temperature at which their maximum opening is achieved. Inasmuch as under the conditions of natural cooling it did not appear possible to insure the appropriate temperature of the concrete by the beginning of cementation operations, the plan provided for artificial cooling of the columnar massifs. Here consideration was also given to decreasing the temperature gradients between central and peripheral zones of the massifs by equalizing the temperature with respect to their cross sections.

Beginning with the marks at about 30 meters, coils of inch tubing with a spacing with respect to height of 1.5-3 meters were laid beginning at the 30 meter mark through which brine was passed from the cooling units constricted on the right bank and equipped with three AK-4 compressors with a total output capacity of 4.5 million kcal/hour.

The refrigeration plant was put into operation only in 1962. Up to that time, in 1960 and 1961, the cooling of a limited number of the columns was accomplished either by the open loop using water from the Angara or by the closed loop using brine subjected to natural cooling of the outside air in pipes.

According to the plan, by the time of cementing of the intercolumnar joints the concrete massifs have to have a temperature close to the mean annual temperature in the dam during the operating period (about 2° C). It was difficult to insure this temperature especially under the conditions of

lagging of the cementation operations behind the schedule providing for setting up the first station units in 1961. Therefore the following cementation temperatures were permitted: 10° C for the zone 12 to 15 meters from the rock and from 10 to 2-4° C on approaching the base.

The cementation of the intercolumnar cements was accomplished through the feeder pipe system laid in the joints when pouring the concrete for the blocks. In order to release the mix into the joints, plate-type valves were used (one for every 5 m² of joint) which were opened as the joints opened. The ends of the feeder pipes emerging in the expanded joints were connected by collectors to which the mortar from the cement pumps was fed through the rubber-fabric hoses.

Vertically the intercolumnar joints were separated into cards 9 meters high encompassing three concrete pouring levels. The cards were insulated from adjacent cards and also from the open surfaces by water tight metal sheets (packing). An air exhaust tooth was built into the upper part of the card.

After flushing the joint with water and discovering its hydraulic possibility and seal, the mortar was fed to the system, the consistency of which was gradually increased from V:C = 5 to the thickness already taken by the joint. On increasing the viscosity of the mortar so much that the flow from the air exhaust tube is reduced, the tooth was covered and the joint was pressed with circulation of the mortar under constant pressure.

The cementation equipment was placed on the sites in the expanded joints at the level of the inspection tunnels; it comprises two mortar mixers and three cementation system pumps [14-15].

1-5. Hydroelectric Power Plant Building, Reservoir and Startup of the Units

The hydroelectric power plant building was located in the river channel on the left bank directly beyond the dam and separated from it by a structural joint 20 mm thick. It comprises 20 aggregate sections on two installation sites sections: shore and channel. The total length of the building is 515 meters, the width along the flow is 35.5 meters, the height of the underwater section is 26.3 meters, and above water, to the ridge of the roof 21.3 meters. The underwater part was made of monolithic reinforced concrete, and the above water part, from prefabricated reinforced concrete.

Eighteen hydraulic units were installed in the hydroelectric power plant building with radial-axial type RO-662-VM-550 turbines with a capacity of 230 megawatts each with a calculated head of 100 meters, with a rotor diameter of 5.5 meters, rpm 125 and maximum water flow rate through the turbine 257.7 m³/sec.

The turbines were connected by a vertical shaft to the SV 1190/250 flow rate suspended generators with 225 megawatt capacity each on a voltage of 13.75 kilowatts [5].



Figure 1-8. Bratsk Hydroengineering Electric Power Plant.
General view of the dam and a hydroelectric plant building.

The spindle chamber was welded steel. The exhaust pipes were bent, concrete with an elbow 2.6 D high and 3.56 D long and a metal facing on the cones.

The maximum backwater created by the dam for normal backwater level (the 122 meter mark) is 106 meters. The surface area of the reservoirs for a normal backwater level is 5470 km^2 ; the total capacity is 169.3 km^3 , the useful capacity is 48.2 km^3 , the depth of available capacity is 10 meters. The maximum flow rates in the flood (considering cutoff by the reservoir) with a probability of being exceeded 0.01% is $11,936 \text{ m}^3/\text{sec}$ and with a probability of being exceeded of 0.1% in $10,960 \text{ m}^3/\text{sec}$. The guaranteed mean daily pass (during navigation) is $2600 \text{ m}^3/\text{sec}$, and the minimum is $1800 \text{ m}^3/\text{sec}$.

The mean electric power output over many years with the installation of 4,100,000 kilowatts in 18 units was 22.6 billion kilowatt-hours; the mean for the critical low water period was 21.2 billion kilowatt-hours, the minimum head was 20 billion kilowatt-hours [5].

The filling of the reservoir began on the first of September 1961, and the normal backwater level was reached on 27 September 1967.

The first four units of the hydroelectric power plant were put under industrial load during the period from 28 November to 31 December 1961 on the temporary water intakes (Figure 1-3) with the headwater level 64.5-67.8 and a head of 48-52 meters. The power of each unit does not exceed 40 megawatts. On the temporary water intakes for the middle of 1962 two more units were started up. The remaining units were installed on the permanent water intake [6, 16].

In September 1967 the Bratsk Hydroelectric Power Plant (Figure 1-8) was put into industrial operation. The power output on 15 May 1974 was 220 billion kilowatt-hours.

CHAPTER 2. MEASURING INSTRUMENTS, THEIR PLACEMENT AND INSTALLATION

2-1. Composition of the Observation and Locations of Measuring Instruments and Devices

The research program provides for the equipment of the dam with the system of measuring and control instruments and devices for observing the state and operation of the high concrete dam under construction and operation under severe climatic conditions.

The observations of the dam under construction included first of all the measurements of the temperature and the thermal stresses in the concreting units. The basic maintenance inspection operations are measurements of the general shifts having great significance for determining the stability of the structure and nature of its joint operation with the foundation and also measurement of the piezometric levels permitting control of the counter pressure on the footing of the dam and the operating efficiency of the seepage control and unloading devices.

The operating observations must also include observations using a number of remote devices placed at characteristic locations in the dam and measuring the temperature of deformation (stress) of the concrete and the rock base and also the mutual displacements of the columns.

The technical plan for replacement of the instruments provided by the Moscow Division of the Gidroenergoprojekt with the participation of the author provided for measurements of the following:

- a) General displacements of the dam -- vertical (settling), absolute and relative horizontal displacements, angles of rotation and mutual displacements of the sections;
- b) Piezometric levels of the contact zone of the dam with the base;
- c) Temperature of the concrete and the rock foundation;
- d) Strains and stresses at a number of points of the transverse cross section of the dam and the deformations of the rock base;

- e) Pressure of the seepage water in the horizontal expansion joints and in the monolithic concrete;
- f) Stresses in the walls of the turbine, concrete and the circular reinforcing.

In order to establish the effect of the set of simultaneously operating factors on the displacement of the dam and its stressed state provisionally made for the placement of the instruments for different purposes in the same measuring section called the complete measuring section in contrast to other sections in which only some of the instruments or devices were located (for example, the piezometers). Beginning with the effort to have a clear system for static calculation in the section in which the instruments were located and to insure comparability of the results of the field studies with the calculation data, it was recognized as expedient to locate the complete measuring cross sections in the closed sections. In order to increase the observation reliability, to consider the various conditions performing the operations, introduce corrections into placement of the instruments and into the measurement procedure by the results of the first observations, it was decided to have three basic measuring cross sections: in the closed section 65 on the right bank (the first stage pit), in the closed section 51 between the spillway and station parts of the channel dam (the intermediate pit) and in the closed section 30 on the left bank (the second stage pit)¹. Thus, the placement of the instruments in each of the sections and the beginning of observations of them were shifted in time.

The plan provided for the placement of the instruments in the horizontal transverse sections, including the remote strain gages in the lowest section at the contact between the rock base and the footing of the dam and the tensometric rosettes in the two next sections -- one each per block, with the exception of the block of the first column in which three rosettes were planned. Piezodynamometers and the Carlson instruments for correct measurement of the compressive stresses were placed in these two sections. In the upper three sections the installation of remote thermometers was planned.

Inasmuch as the string devices placed in the lower three sections are also remote thermometers, the total number of sections in which the temperature can be measured was six.

The placement of the instruments in the horizontal transverse sections pursued the goal of establishing the stress distribution from the calculated loads -- the natural weight of the concrete and the hydrostatic pressure of the water. Beginning with the calculated operating scheme for the high monolithic gravity dam of triangular profile, this distribution appeared continuous, and the effect of the calculated loads, predominant by comparison with the thermal stresses.

¹ Hereafter we shall provisionally call these sections the experimental sections.

It must, however, be noted that in the instrument placement plan, the insufficiently clear concept of the peculiarities of performance of operations under the conditions under which the Bratsk Hydroelectric Power Plant was built was reflected.

A number of instruments called for by the plant turned out to be insufficient, and the placement was insufficiently successful. This was discovered after processing the readings with respect to the first instruments in section 65. Therefore in the process of installing the instruments the author had to make changes on location in the planned scheme for placement of the instruments in certain blocks. Thus, the remote crevice gages in the intercolumnar joints, remote strain gages in certain horizontal construction joints, groups of remote strain gages in the blocks next to the rock base and also in the intercolumnar joints, longitudinal and vertical sections of the instruments in a number of blocks emerging in the expanded joints, and so on were installed which were not provided by the plan (Figure 2-1).

The total number of instruments was increased as compared to the plan, but in a number of blocks, as a result of an insufficient number of instruments at the time of installation, the number had to be reduced.

During the construction process, a number of additional instruments for the explanation of problems not provided for by the plan were installed by request of the construction and design organizations. In particular these instruments provided for investigating the following:

- a) The temperature and stress in the successively laid, adjacent with respect to height experimental "long" blocks of section 63;
- b) The temperature and thermally stressed state in the blocks with wood and concrete modular forms;
- c) The temperatures and stresses in the successively laid, adjacent with respect to height, blocks of the columnar section;
- d) Stresses in the reinforcing and the concrete of the spiral chamber of unit No 13;
- e) Pressure distributions of the intercolumnar joint on cementation of it;
- f) Deformations in the horizontal construction joints of sections 84-86 and in the anchor rods of section 85;
- g) Stresses in the counterforces of the temporary water receivers of sections 43 and 45 and also in the plug concrete and on the conduit shell.

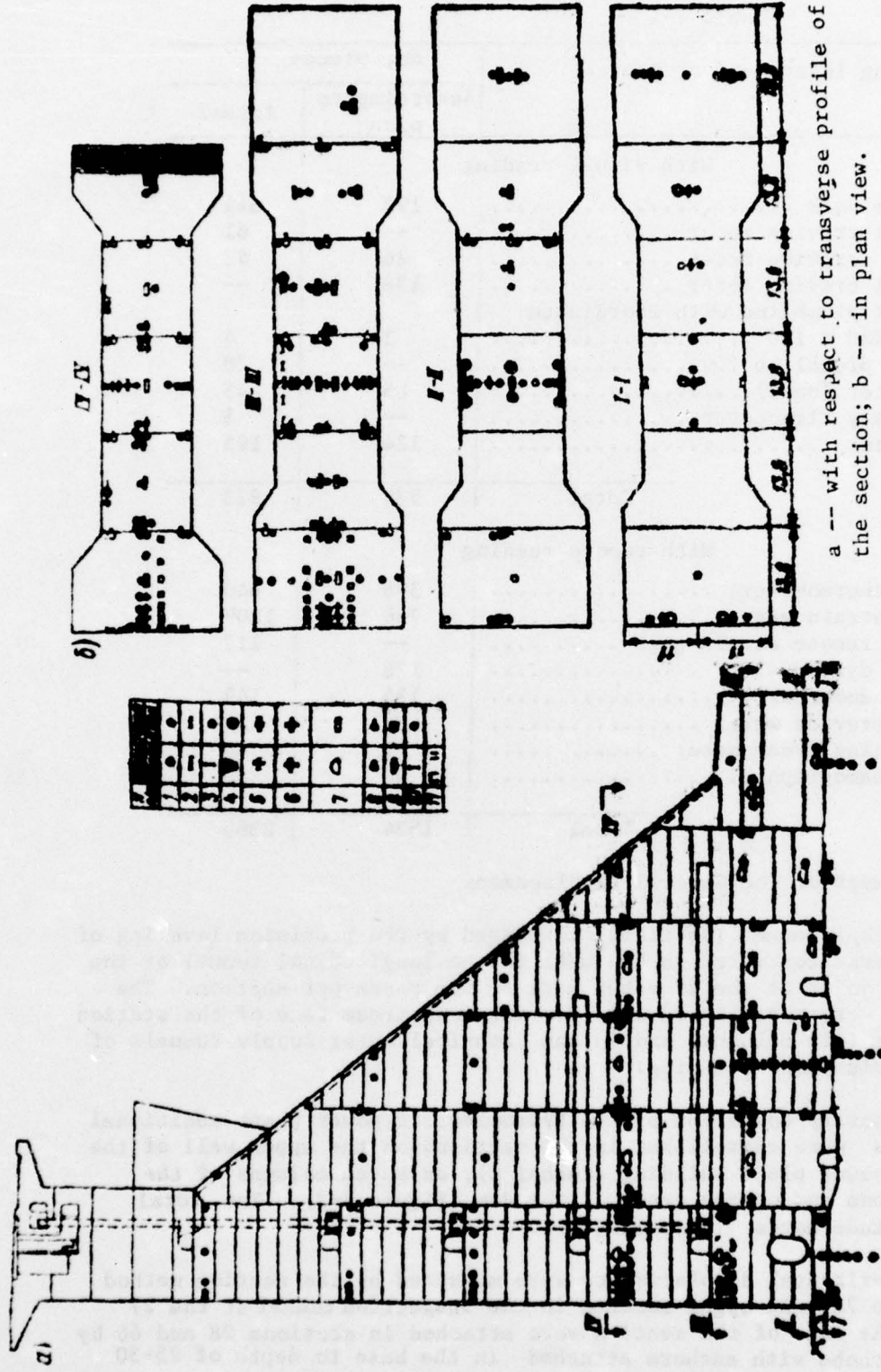


Figure 2-1. Schematic for placement of the instruments in section 30: I-I -- in the rock 20-40 cm below the cross section; II-II -- 1.5 meters below the contact with a base; III-III -- the same 12 m below; IV-IV -- the same 30 m below the base; 1 -- remote thermometer; 2 -- horizontal remote thermometer; 4 -- [illegible]; 5 -- two mutually perpendicular remote strain gages with housing; 6 -- three mutually perpendicular remote strain gages with housing; 7 -- group of remote strain gages from the "fan" rosette, longitudinal and two in housings; 8 -- remote [illegible]; 9 -- piezothermometer; 10 -- remote strain gage in the joint; 11 -- [illegible] remote strain gage.

Table 2-1

Measuring instrument or device	No. pieces	
	According to plan	Actual
With visual reading		
Altitude mark	192	541
Uniaxial crevice meter	--	61
Biaxial crevice meter	26	43
Triaxial crevice meter	178	--
Straight plumbline with coordinate gage K80 x 150	3	4
Inverse plumbline	--	28
Clinometer (base)	15	45
Stationary clinometer	--	5
Piezometer	124	195
Total	538	923
With remote reading		
Remote thermometers	378	640
Remote strain gages	764	1209
Mounted remote strain gage	--	117
Carlson dynamometer	126	--
Piezodynamometer	134	149
Remote crevice meter	--	136
Reinforcing dynamometer	72	64
IIPD dynamograph	50	50
Total	1524	2365

2-2. Measurement of the General Displacement

The vertical displacement (settling) is measured by the precision leveling of the altitude marks concreted in the wall of the longitudinal tunnel at the intersectional joint at the 27 meter mark -- two marks per section. The altitude marks were established also for the downstream face of the station part of the dam (six columns) and in the technical water supply tunnels of the hydroelectric plant building.

During the temporary operation of the hydroelectric power plant additional longitude marks were established in the sections on the upper wall of the hydroelectric power plant building (tunnel C), on seven columns of the spillway sections and on the crest of the dam (Figure 2-2). The total number of altitude marks reached 541.

The absolute horizontal displacements were measured by the section method with respect to 78 wall signs located in the inspection tunnel at the 27 meter mark. The ends of the section were attached in sections 28 and 66 by reversible plumbbobs with anchors attached in the base to depth of 25-30 meters from the 27 meter mark.

BEST AVAILABLE COPY

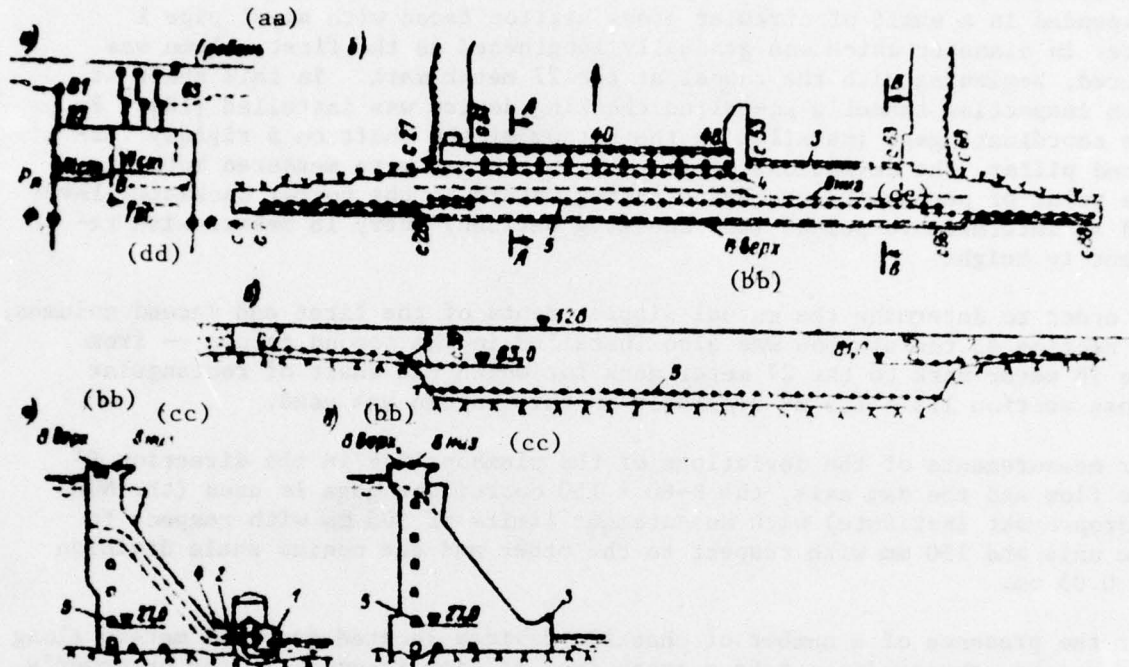


Figure 2-2. Schematic of the geodetic altitude sections on concrete structures: a -- survey system; b -- plan; c -- longitudinal section; d -- transverse section of the station section; e -- the same for the spillway section. Φ -- foundation reference point; P_x -- rock reference point; 1 -- TVS tunnel; 1 -- V tunnel; 2 -- V tunnel; 3 -- seven columns; 4 -- sixth column; 5 -- 27 meter mark tunnel; 6 -- the same for the 63 meter mark; 7 -- the same for the 81 meter mark; 8_{low} -- the low section crust; 8_{high} -- high section crust.

Key: aa. crest bb. 8_{high} cc. 8_{low} dd. TVS

The relative horizontal displacements are measured using plumbobs (inverse and straight). The structural design of the inverse plumbobs and the coordinate gages for them was developed at the Moscow Institute of Geodetic Areal Surveying and Cartographic Engineers (MIIGAiK) by Professor M. S. Murav'yev [17].

The 17 plumbobs of the first stage were installed, including the terminal plumbobs reinforcing the geodetic section (sections 28, 30, 35, 37, 41, 47, 50 and 66), five second stage plumbobs (sections 30, 35, 41, 47 and 64) six third stage plumbobs (sections 30, 35, 41, 47, 54 and 64).

All of the geodetic operations with respect to measuring the settling and the absolute horizontal horizontal displacements and also observations of the inverse plumbobs were performed before 1969 by the Angar Expedition of the Gidroproyekt Institute.

The relative horizontal displacements in each of the experimental sections 30, 51 and 65 were measured using the direct plumbobs. The plumbob was suspended in a shaft of circular cross section faced with steel pipe 1 meter in diameter which was gradually lengthened as the first column was poured, beginning with the tunnel at the 27 meter mark. In this shaft at each inspection tunnel a so-called checking device was installed [18]. By one coordinate gage installed on the bottom of the shaft on a rigidly fastened pillar, the deviations of the plumbob thread were measured both at the point of permanent attachment approximately at the normal backwater level and at intermediate points (the checking devices) every 18 meters with respect to height.

In order to determine the mutual displacements of the first and second columns, in section 65 the plumbob was also installed in the second column -- from the 76 meter mark to the 27 meter mark for which the shaft of rectangular cross section $1.5 \times 1.5 \text{ m}^2$ available in this column was used.

For measurements of the deviations of the plumbob line in the direction of the flow and the dam axis, the K-80 \times 150 coordinate gage is used (the NIS Gidroproyekt Institute) with measurement limits of 305 mm with respect to one axis and 150 mm with respect to the other and the nonius scale division of 0.05 mm.

For the presence of a number of checking devices located every 18 meters along the height, the readings take a great deal of time inasmuch as the observer's helper must successfully go from one inspection tunnel to another to put the plumbob line in the checking device. The electromagnetic mechanism that we used which permits this to be done remotely [19] was replaced during operation by the simpler and more reliable mechanical device [20].

The mutual displacement of the sections is measured using the simplest uniaxial crevice gages made according to the author's sketch on site. The crevice gage (Figure 2-3,a) comprises two 30 \times 30 mm angles built into the wall of the inspection tunnel on both sides of the joint. A steel ball 10 to 12 mm in diameter is welded on each end of the vertical webbs of the angles. The spacing between the balls is measured by the sliding calipers with precision of 0.05 mm. The uniaxial crevice gages are installed on 15 intersectional joints in all of the longitudinal inspection tunnels of the first column. The mutual displacement of the dam and the hydroelectric power plant building has been measured since July 1963. The biaxial crevice gages (Figure 2-3,b) installed in the tunnel of the hydroelectric power plant building in all sections.

The mutual displacement of the dam columns is measured using the DShch remote crevice gages designed by the NIS Gidroproyekt Institute (see Figure 2-4) installed in the same sections in which the temperature and deformation of the concrete are measured. In the majority of the cases in each joint the remote crevice gages are installed at three points: along the axis of the section and 1 to 1.5 meters from its edges (on the inside of the packing). There is a remote thermometer for each crevice gage. With respect to measuring principle the instrument is a rheostatic sensor. Measurement limits are 3

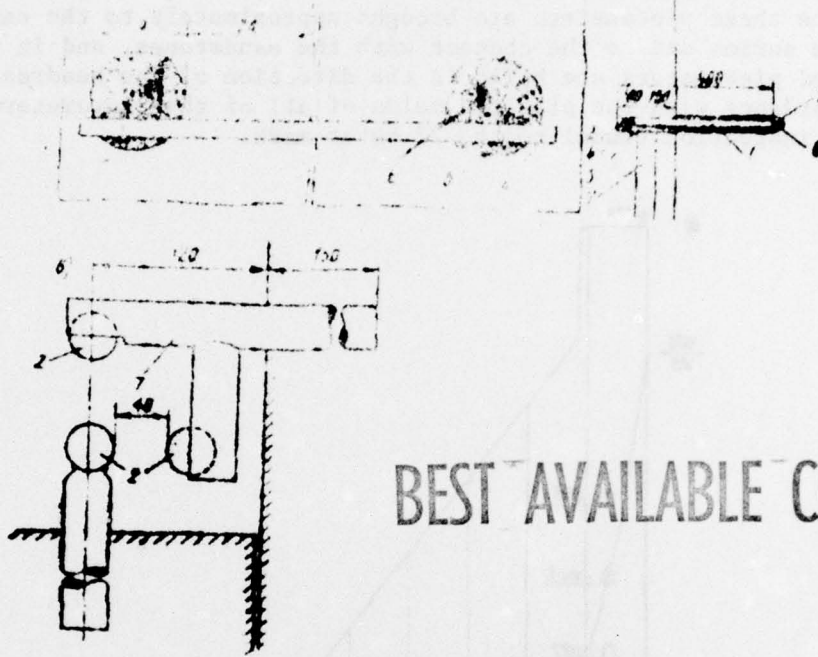


Figure 2-3. Crevice gages: a -- uniaxial; b -- biaxial. 1 -- 30 × 30 mm angle steel; 2 -- steel ball 10 mm in diameter; 3 -- perforated hole; 4 -- standard; 5 -- bolt; 6 -- mortar; 7 -- rod.

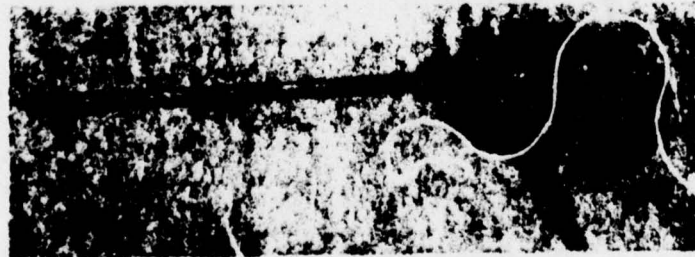


Figure 2-4. Remote crevice gage: 1 -- housing; 2 -- rod; 3 -- anchor.

and 6 mm, the rated error is ± 0.05 mm. The instrument is highly reliable in operation [18, 19].

2-3. Measuring the Piezometric Levels

The piezometric levels are measured by tubular piezometers drilled on an incline from the cementation tunnel. The working faces of the piezometers are in the contact zone 2-3 meters from the footing of the dam. In several sections these piezometers are brought approximately to the center of the diabase series and to the contact with the sandstones, and in 9 sections inclined piezometers are built in the direction of the headrace (Figure 2-5). In accordance with the plan the melds of all of the piezometers must emerge in the inspection tunnel to the 27 meter mark.

BEST AVAILABLE COPY

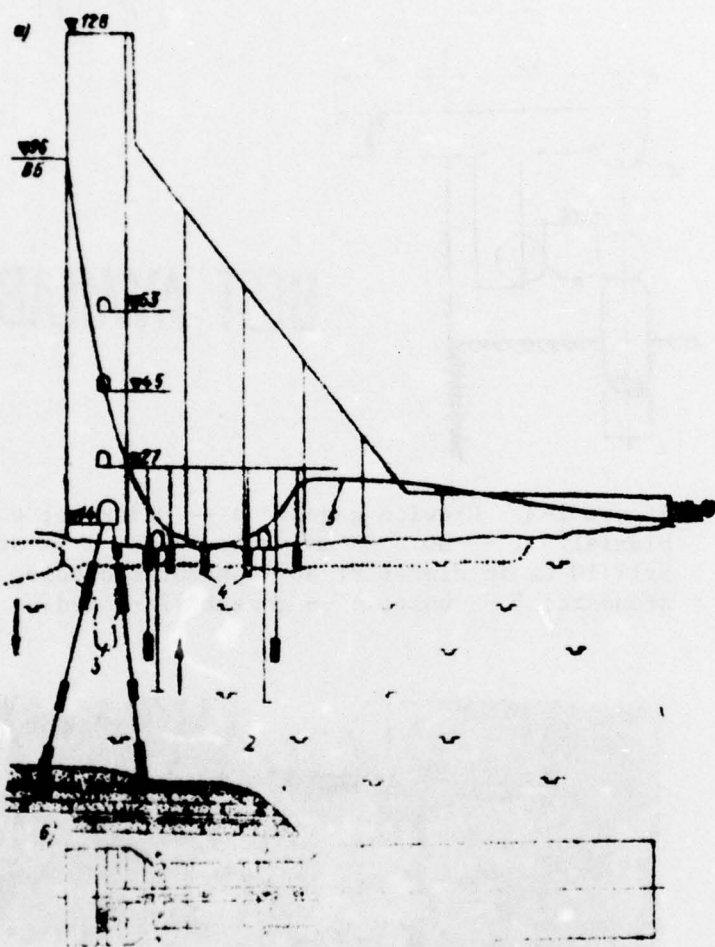


Figure 2-5. Schematic of the placement of the piezometers in section 30: a -- transverse section; b -- plan view. 1 -- sandstones; 2 -- diabases; 3 -- cementation curtain; 4 -- piezometer water intake; 5 -- piezometric level for January 1964. The light dots are the piezometers, the black dots are the drainage holes. The arrows indicate the direction of the seepage flow.

In addition to the indicated longitudinal¹ section of the piezometers, transverse lines for the point piezometers (Figure 2-5) are equipped in seven sections (28, 30, 36, 45, 51, 58 and 63), which permits the construction of the counterpressure diagram along the axis of the section and estimation of the operating efficiency of the cementation curtain and the discharge drainage.

The construction of the piezometers and the observation of the piezometric levels were accomplished by the Angara Expedition of the Gidroproyekt Institute under the direction of Chief Expedition Geologist N. M. Bolotina.

2-4. Measurement of the Concrete Temperature

In order to measure the concrete temperature in the dam blocks, electrical resistance thermometers were installed with a temperature coefficient of 3.5-5 ohm/deg and a resistance at 0° C within the limits of 800-1,200 ohm. These thermometers are in the form of coils of electromagnets of string devices. Overall, the temperature is measured at 1,300 points.

Resistance thermometers of two types are installed in the dam which are distinguished by structural design and method of running the cable. The thermometer is built by the NIS Gidroproyekt Institute have a brass housing, the sections of which are joined by soldering. The section of cable in lead sheathing is also soldered in. The thermometers built by the NIIG Institute have a housing in the form of a solid steel cylinder. The cable in rubber sheathing is sealed by a packing gland with rubber mass packing. The thermometers are placed in six longitudinal sections of the axial cross section of the experimental sections approximately every 18 meters with respect to height beginning with the rock base in which under the first, third and sixth columns of each experimental section remote thermometers are installed in the vertical section to a depth of six meters (see Figure 2-1,a). In addition, the remote thermometers are installed in the vertical and longitudinal sections of the first columns (Figure 2-6) and also in the columns bordering with the expanded joint (Figure 2-7).

In addition to the remote thermometers installed by us in the experimental sections, the Bratsk Expedition of Gidrospetsproyekt installed remote thermometers in the majority of sections of the dam for construction control of the concrete temperature in connection with the cementation of the inter-columnar joints. The total number of these remote thermometers remains 2,015. At the end of 1965 when observations were discontinued, 57% of them were still operating.

¹Here and hereafter the section will be called longitudinal which is parallel to the axis of the dam, and the section parallel to the axis of the section will be called transverse.

BEST AVAILABLE COPY

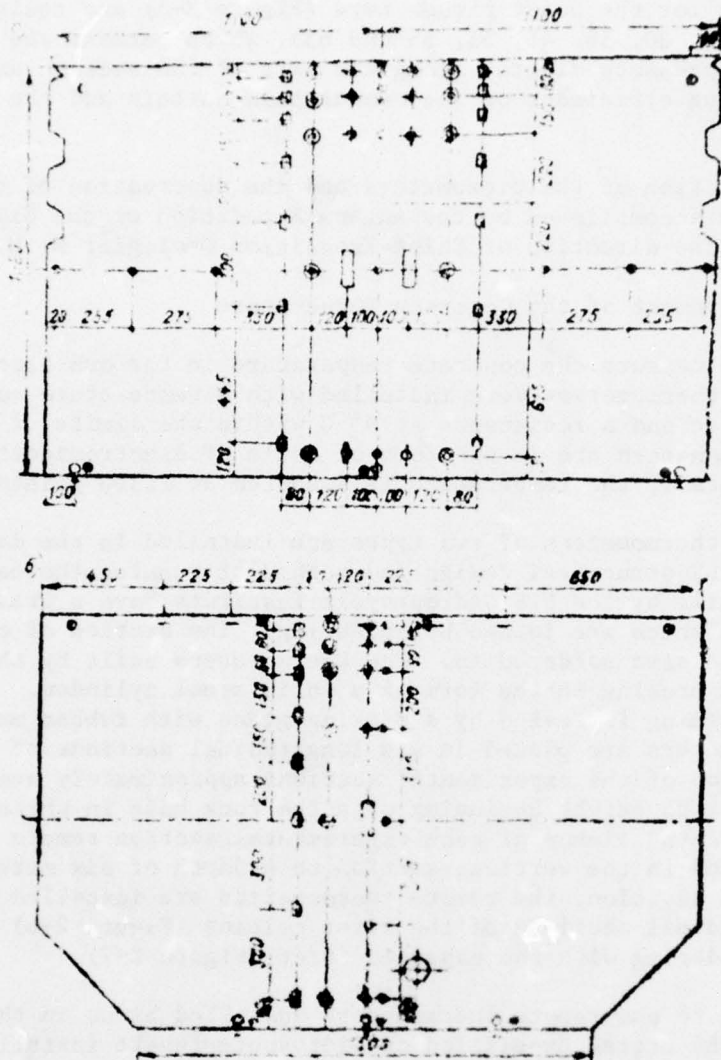


Figure 2-6. Schematic of the placement of the instruments in the first column of section 30 at the following marks: a -- 22 meters; b -- 40 meters. (The provisional notation is the same as for figure 2-1,b).

2-5. Measurement of Strains and Stresses in Concrete

The strains and stresses in the concrete have been investigated using the remote strain gages placed in the two horizontal sections with respect to the axis of each experimental section at 12-15 and 30-33 meters and above the base of the dam. The remote strain gages are installed in groups at the center of each block on the section level, and in the first and sixth columns, also on the pressure and downstream faces respectively. Each

BEST AVAILABLE COPY

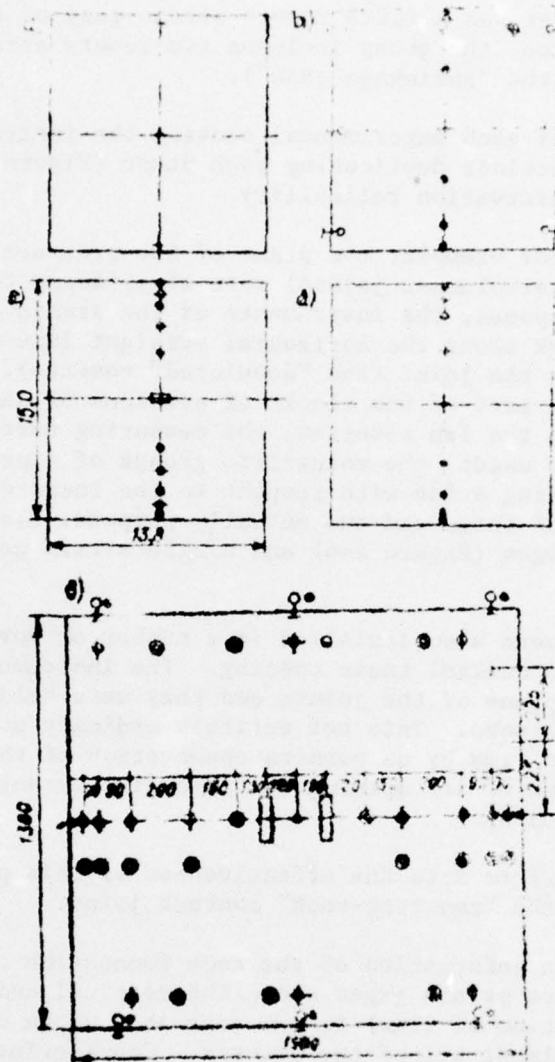


Figure 2-7. Schematic of the placement of the instruments in the longitudinal sections (between the expanded joints) and blocks 30-II-5, 6, 7, 8 and 9: a -- in the rock base to a depth of 0.20 meters under the [illegible] column; b -- in the middle of the block next to the rock 30-III-5; c -- in the middle of the block 30-III-6; d -- at a distance of 20 cm from the lower and upper surfaces of the blocks 5, 6, 7, 8; e -- in the middle of the block 30-III-9. (Provisional notation the same as in Figure 2-1,b)

group (or measuring point) comprises four remote strain gages: vertical, horizontal and two inclined (at 45° and 135°) forming the strain gage "fan" rosette in the plane of the transverse cross section of the section.

Perpendicular to the latter was a fifth remote strain gage of the group (along the dam axis). In addition, the group includes two remote strain gages and the nonstressed samples (the "shrinkage cone").

At the 22-25 meter mark of each experimental section the instruments were placed in two parallel sections duplicating each other (Figure 2-1, b and 2-6,a) to increase the observation reliability.

Near the open surfaces (for example, the plane of the pressure and downstream faces and also at the intercolumnar joints) were significant temperature and stress gradients proposed, the instruments of the strain gage rosette were installed on one mark along the horizontal straight line parallel to the plane of the face or the joint (the "developed" rosette). The rosette fan was also installed in part of the blocks of sections 51 and 30 next to the rock. In addition to the fan rosettes, the measuring parts of a different composition were also used: the volumetric groups of nine remote strain gages were installed forming a fan with respect to the rosette in each coordinate plane. Groups of three and two mutually perpendicular (vertical and horizontal) strain gages (Figure 2-6) and single strain gages (Figure 2-7) were also used.

The single strain gages were also installed in a number of horizontal construction joints so as to control their opening. The instruments were installed normally to the plane of the joints and they were held by their anchors in two adjacent blocks. This not entirely ordinary monitoring procedure used for the first time by us permits observation of the joints and not only catching the time of its opening but also discovering the nature of the growth of this opening.

It is especially necessary to note the effectiveness of this procedure for monitoring the state of the "concrete-rock" contact joint.

In order to determine the deformation of the rock foundation of the dam, we installed groups of remote strain gages along the vertical and horizontal directions (in the direction of flow) in the rock at a depth of 20-40 cm from the footing under almost all of the columns. Considering the jointing of the rock, we did not install the third (inclined) strain gage which in the case of a uniform and isotropic foundation but also the possibility of determining the tangential stresses which in the case of a uniform and isotropic foundation but also the possibility of determining the tangential stresses.

In several cases, so far as we know, remote strain gages were installed in the unstressed rock sample (the rock cone) for the first time.

The string remote strain gages of three types distinguished by the base, the length of the string and the housing rigidity (Figure 2-8) were installed in the Bratsk Hydroelectric Power Plant dam. The remote strain gages (Figure 2-8, 1) designed by the BNIIG [18] were built at the workshops of the Leningrad Agricultural Institute (LSKhI). The instrument base was 200 mm; the

string length was 100 mm, the sensitivity was $(0.7-0.8) \cdot 10^{-6}$ of the relative deformation per unit frequency modulus, the temperature coefficient of the electromagnet coil was from [deleted] to 5 ohm/deg. The housing rigidity is equivalent to the Young's modulus of the concrete $E_b = 1 \cdot 10^5$ kg-force/cm². The instrument was modified by the author in 1958 (21). The instrument base was enlarged from 150 to [deleted] mm, and the cable input was sealed using a packing gland with packing made of a special rubber mass¹, which eliminated the primary defect of the device -- its insufficient seal which we discovered in the Kakhovskiy and Novosibirsk hydroengineering complex structures [22,23].

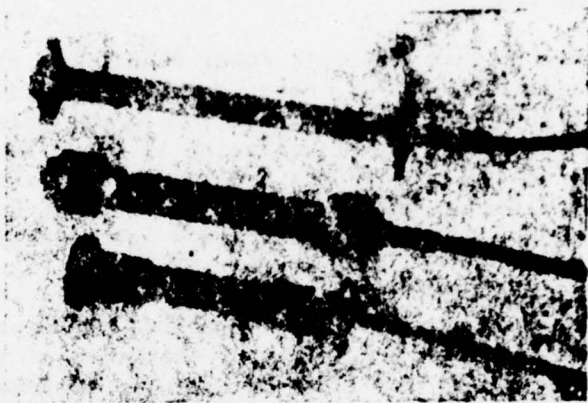


Figure 2-8. String type remote strain gages of different designs. 1 -- VNIIG; 3 -- KVU; 3 -- BT-300.

The KVU remote strain gages designed by I. Petrik and O. Gorn (the Czechoslovakian Academy of Sciences) and built by the Metra plant in Prague [18, 24] are shown in Figure 2-8,2. The length of the device is 270 mm, the string length is 165 mm. The sensitivity is $3 \cdot 10^{-6}$ of the relative deformation per unit frequency modulus. The housing rigidity is equivalent to $E_{\text{concrete}} = 2 \cdot 10^5$ kg-force/cm². The two quadrapolar electromagnets are located at a distance of one third the length of the string from its ends. The structural design of the instrument is reliable; there are only individual cases of its failure (about 3%).

¹This method of sealing the cable lead was applied by the author to all of the VNIIG string devices (the remote thermometers, the reinforcing dynamometers, the [deleted] dynamometers, the piesodynamometers). The experience in the application of these devices at the structures of the [illegible], Brask, Krasnoyarsk and Ust'-Ilinskij Hydroelectric Power Plant demonstrated that with proper quality of packaging, manufacture and installation the instruments are quite reliable.

In Figure 2-8, 3 we have the BT-300 remote strain gage designed and built by the NIS Gidroproyekt Institute. The base of the device is 300 mm, the string length is 120 mm. A characteristic feature of the device is practical absence of longitudinal rigidity as a result of inclusion of silphon insert in the instrument housing. The housing parts located above this insert are soldered with tin which gives the instrument temporary rigidity required to withstand the additional tuning of the string. It is proposed that the first deformation of the instrument with the concrete will shear the tin solder and the instrument will begin to operate in the "string-concrete" system.

2-6. Measuring the Pressure of the Seepage Water in the Horizontal Structural Joints at Monolithic Concrete

On the dam of the Bratsk Hydroelectric Power Plant, the pressure of the water seeping through the concrete of the first columns is measured using the string piezodynamometers placed in the horizontal interblock joints of the three sections at a depth from the normal backwater level of 90 and 75 meters and in one section at a depth of 26 meters. In addition, in three sections the instruments are installed in the monolithic concrete at half the height of the three meter blocks. The piezodynamometers are located in the section from the pressure face to the line of drainage holes or intercolumnar joint I-II along the horizontal sections parallel to the axis of the section with respect to 5-7 of the instruments in the section. The lower level sections are duplicated (Figure 2-1,b). The piezodynamometers of the diaphragm type with the string horizontally stretched on the pegs fastened to the diaphragm are used in the dam. The water pressure is transmitted to the diaphragm through a viscous liquid (grease, vaseline) filling the space between the diaphragm and the protective cover. In the piezodynamometers built by the VNIIG Institute this is a steel, perforated cover; in the piezodynamometers of the NIS Gidroproyekt Institute the cover is made of porous ceramic.

2-7. Study of the Static Operation of the Pressure (Turbine) Conduit

In order to determine the stressed state of the steel conduit under the conditions of its joining operation with reinforced concrete, the stresses are measured in the steel shell, the circular reinforcing and the concrete. The field studies of the stresses are made in section 36 in the lower part of the inclined section of the conduit at its contact with the horizontal section. The instruments are located (Figure 2-9) in two cross sections (a-a and b-b) normal to the axis of the conduit 6 meters away from it, and in each cross section, with respect to two mutually perpendicular diameters, forming four groups (radii).

In each group the following are installed: a) applied string remote strain gages on the shell between the stiffening ribs two each in the longitudinal and tangential directions and one on the webbing of the stiffening ribs; b) three reinforcing dynamometers in the annular reinforcing rods; c) remote strain gages for the concrete with respect to three mutually perpendicular directions (longitudinal, radial and circular) with three shrinkage cones placed on a continuation of the radius at a distance of 0.9, 2 and 2.7 meters from the shell; d) from the piezodynamometer on the wall of the stiffening rib.

BEST AVAILABLE COPY

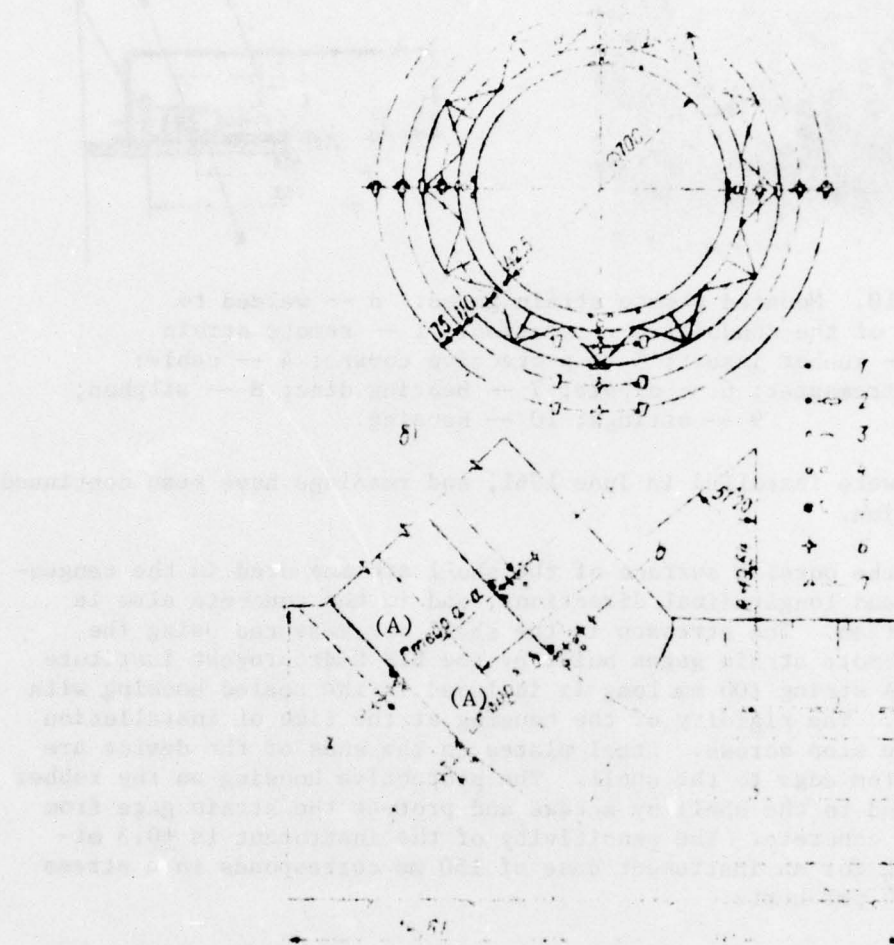


Figure 2-9. Placement of the instruments in the turbine conduit of section 36: a -- transverse section; b -- longitudinal section. 1 -- remote resistance thermometer; 2 -- reinforcing dynamometer; 3 -- mounted remote strain gage; 4 -- pie o-dynamometer; 5 -- remote strain gage in the housing; 6 -- group of radio remote strain gages; 7 -- group of [illegible] remote thermometers.

Key: A. section

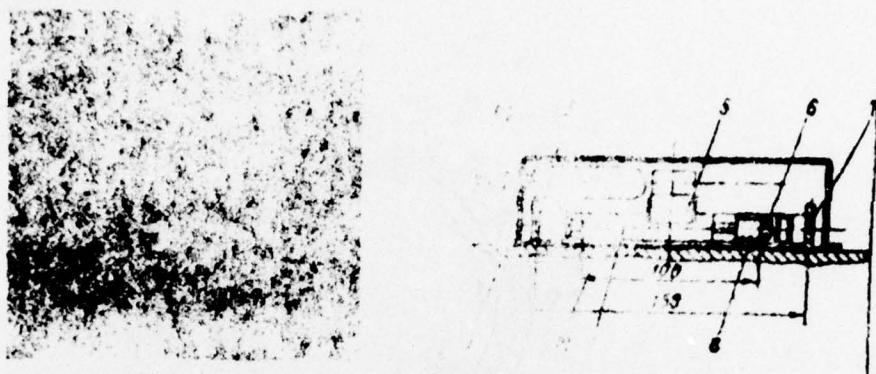


Figure 2-10. Mounted remote strain gages: a -- welded to the shell of the conduit; b -- section. 1 -- remote strain gage, 2 -- rubber insert; 3 -- protective covers; 4 -- cable; 5 -- electromagnet; 6 -- nipple; 7 -- bearing disc; 8 -- silphon; 9 -- strings; 10 -- housing.

The instruments were installed in June 1961, and readings have been continued to the present time.

The stresses on the outside surface of the shell are measured in the tangential (circular) and longitudinal directions, and in the concrete also in the radial direction. The stresses in the shell are measured using the string mounted remote strain gages built by the NIS Gidroprojekt Institute (Figure 2-10). A string 100 mm long is included in the sealed housing with a silphon insert. The rigidity of the housing at the time of installation is insured by the stop screws. Steel plates on the ends of the device are welded by the bottom edge to the shell. The protective housing on the rubber insert is fastened to the shell by screws and protect the strain gage from contact with the concrete. The sensitivity of the instrument is ± 0.3 micros/hertz which for an instrument base of 150 mm corresponds to a stress of 4 kg-force/cm^2 per hertz.

The stresses in the circular reinforcing are measured by string dynamometers for reinforcing 40 mm in diameter built by the NIS Gidroprojekt Institute. The string length is 100 mm, the instrument sensitivity is 5 kg-force/cm^2 per hertz. Before welding the dynamometers in the circular reinforcing, the extension pieces were cut off (Figure 2-11) in order to decrease the length of the rectilinear insert.

In the conduit of section 36 a total of 256 instruments were installed.

By request of the Bratsk Gesstroy trust, the instruments were also installed in the reinforcing and the concrete of the housings of the temporary water intakes in sections 43-45 and also in the shell of the conduit and in the concrete plug between the abutments. The total number of instruments in sections 43 and 45 is 129.



Figure 2-11. Reinforcing dynamometer with extension pieces (1) and without them (2).

2-8. Receiving Instruments

In order to measure the vibration frequency of the string in the electro-acoustic instruments, the TsS-2 tube generator-frequency meters designed by the NIS Gidroprojekt Institute were used which turned out to be quite reliable and stable under the severe construction conditions under the condition of application of frost resistant batteries.

The semiconductor TsS-5 generator-frequency meters of the NIS Gidroprojekt Institute began also to be used in the middle of 1963. With respect to their overall dimensions and weight (2.5 kg) they are highly convenient for use as portable instruments.

The strain gages built by the Metra plant are equipped with a measuring station in which the frequency of the operating string of each instrument is compared with respect to the Lessage patterns on the screen of a cathode ray tube with the frequency of the standard string, the tension of which is varied by the micrometric device [24]. As a result of the heavy weight (14 kg) and the necessity of connecting the instrument to an ac network near each measurement point, we used the same frequency meters for the Czech instruments as for the Soviet instruments, establishing the conversion factor from one station to the next by calibration.

In order to measure the resistance of the remote thermometers and the remote crevice meters, the all-purpose MVU-49 and MO-2 Wheatstone bridges were used which are convenient with respect to size and reliable inoperation.

In addition to the above enumerated instruments for studying the static operation of the dam 50 the IIPD dynamographs were installed. These instruments,

which measure the dynamic effect of waves on the pressure face of the dam are located in sections 30 and 51 between the 99 and 123 meter marks in the vertical sections on one edge of each section along its axis. The spacing between the instruments with respect to height varies from 3 meters in the lower part to 1 meter in the upper part.

2-9. Instrument installation.

The reliable and long-term operation of remote measuring instruments depends to a great extent on the quality of the cable used and the seal of its joint. For the instruments of the Bratsk Hydroelectric Power Plant a cable was used with rubber insulation on the strands and a hose type rubber sheathing ShRPS and ShrPL 0.75 to 1.00 mm² in cross section.

Inasmuch as many of the instruments which we placed in the structures of the Kakhovsiy [22] and the Novosibirsk Hydroelectric Power Plant failed as a result of insufficient reliable seal of the cable joints, at the Bratsh Hydroelectric Power Plant we used hot vulcanization of splices of the connecting cable with a short segment of cable built into the instrument when it was manufactured. The junction box from the segment of gas pipe 25 mm in diameter with packing glands at the ends [25] promoted increased mechanical strength of the joint.

The installation of the remote instruments was accomplished so that before pouring the concrete no sections of unprotected cable were left in the block. For this purpose all of the cables from the instruments were laid in troughs of channel iron; they were pulled upward to the surface of the concreted block through uprights made of pipe 100-150 mm in diameter; they were coiled and stored in iron boxes with covers welded to the uprights (Figure 2-12). As the columns were poured, the uprights were built up, and the boxes were moved to the top of the next concreted level until reaching the monitoring and control equipment tunnel. The troughs were filled with mortar, and the uprights with molten bitumen.

The instruments were installed as follows.

The remote thermometers placed in the concrete were tied to a thin rod welded at a given height to the upright made of reinforcing steel 15-20 mm in diameter or a segment of pipe 20-25 mm in diameter. The remote thermometers placed in the rock foundation were attached at a given distance to the hemp line with a weight on the end and they were lowered in the form of strings into a drilled hole 10 to 12 cm in diameter drilled in the rock after which the hole was filled with mortar.

The remote strain gages designed for placement in the concrete blocks were mounted using a supporting head welded to an upright made of reinforcing steel or a segment of pipe 25 to 38 mm in diameter fastened on the lower end of the concrete or welded to the trough. The ends of the rods (see Figure

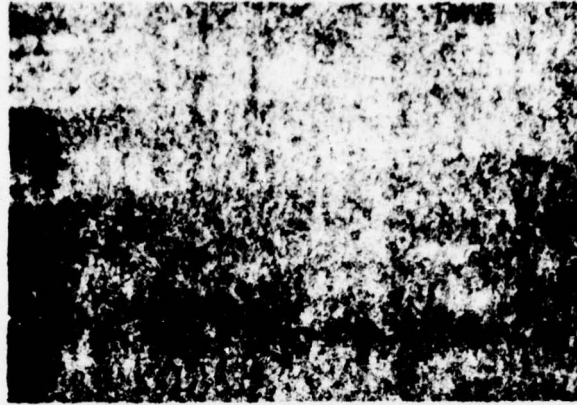


Figure 2-12. Installation of the instruments in the block. 1 -- thermometers; 2 -- group of 5 remote strain gages; 3 -- form of the housing; 4 -- trough; 5 -- uprights; 6 -- cable box.

2-13, a) on which the remote strain gages designed by the VNIIG Institute (see Figure 2-14,a) were screwed or the remote KVU strain gages (Figure 2-14,b) were attached, were inserted in the cylindrical recesses of the supporting head drilled at an angle of 45°.

The structural design of these rods permitted the instrument to move freely along its axis on settling of the concrete, and the supporting head insured fast installation of the instrument with observation of the given orientation.

The cables were stretched from the instruments along the upright to the trough and protected by a segment of angle iron from damage (or they were run inside a tubular upright).

The shrinkage cone (Figure 2-13,b) with a remote strain gage placed inside it was installed on the three-legged support made of thin reinforcing rods at the mark of the middle of the group of remote strain gages (Figure 2-12) 1.2 meters from it, which corresponds approximately to the three largest diameters of the cone. At the edge of the block the cones were installed symmetrically with respect to the group of strain gages at a distance of 1.5 meters in the direction of the headrace and tailrace.

The remote strain gages were fixed in the new rock using mortar: vertical in drilled holes 10 to 12 cm in diameter and 30 to 40 cm deep (Figure 2-15,a) and horizontal in the toothings made in the rock (Figure 2-15,b). In the contact joints the remote strain gages were fixed using anchor discs in the concrete and rock (Figure 2-15,c).

In order to build the rock cone around the hole drilled for the remote strain gage, an annular slit is drilled, insulating the rock cylinder with the

BEST AVAILABLE COPY

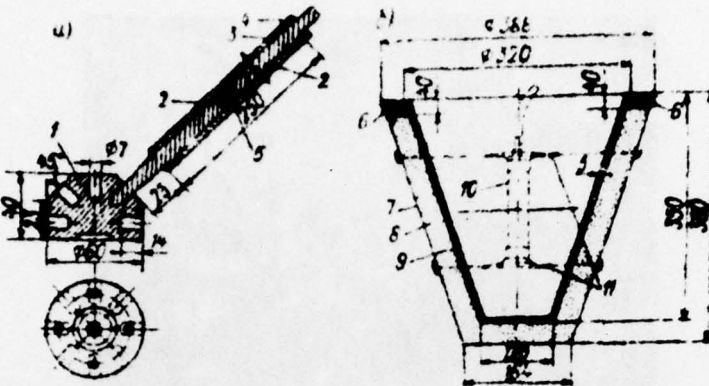


Figure 2-13. Auxiliary devices for installing remote strain gages; a -- supporting head and rod for installing remote strain gages; b -- shrinkage cone. 1 -- supporting heads; 2 -- steel rod; 3 -- guide tube; 4 -- rubber washers; 5 -- rubber plugs; 6 -- plug made of oakum bitumen; 7 -- outside girders; 8 -- sawdust; 9 -- inside girder with bitumen lubrication; 10 -- remote strain gage with 200 mm base; 11 -- wire tension members.

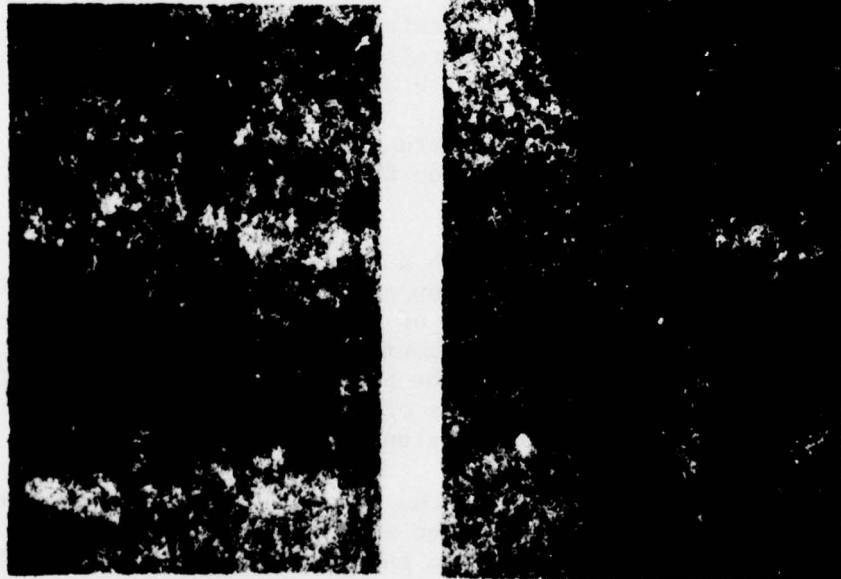


Figure 2-14. Fastening of the remote strain gages: a -- threaded; b -- by clamps.

BEST AVAILABLE COPY

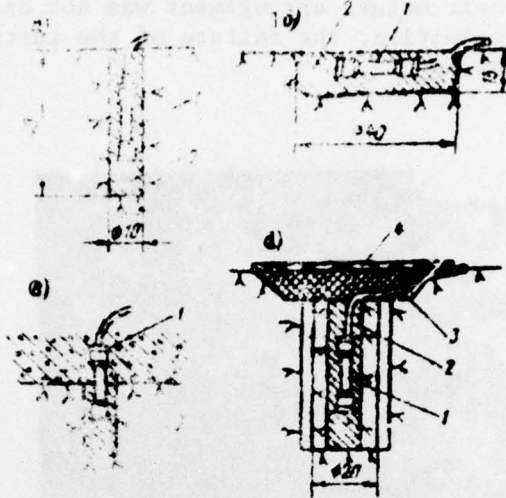


Figure 2-15. Installation of remote strain gages in the rock foundation: a -- vertical; b -- horizontal; c -- in a joint; d -- in the rock "cone." 1 -- remote strain gage; 2 -- mortar; 3 -- bitumen; 4 -- wood panel.

remote strain gage from the environment. The top of the weld was 7 to 10 cm deep from the rock surface and it was covered by the wooden panel, and the space under it was filled with bitumen in order to prevent the grout from getting into the annular slit (see Figure 2-15,d).

It is necessary, however, to note that part of the "rock cones" turned out to be unsuitable for use as a result of cracks in the rock occurring with drilling the annular slit with small (to 400 mm) diameter. It is more proper to build an annular slit 900 to 1000 mm in diameter.

The remote crevice gage was installed on the support made of reinforcing or faceted iron near the joint (Figure 2-16); the stem of the slit meter was wedged into the hole drilled in the concrete and filled with mortar. In the absence of adjacent block, the crevice meter connection was introduced into the wooden panel which was removed before concreting the adjacent block.

The piezodynamometers in the plane of the horizontal joint were fixed in holes 25 × 25 × 10 cm in size and they were filled with gravel. In the monolithic concrete the instrument was installed in a mold forming a cylindrical cavity above the cover of the instrument. This cavity was filled with gravel and was covered with a piece of ruberoid. The gravel created a porous layer above the instrument in which water was accumulated, promoting a fast pressure drop.

The concreting of the block with the instruments was accomplished with mandatory presence of a co-worker from the VNIIG Institute group which saw that

when the concrete was fed to the block or when vibrating it, the instruments were not damaged and their mutual arrangement was not disturbed. As a result of the constant inspection, the failure of the instruments during concreting was a rare phenomenon.



Figure 2-16. Installing the remote crevice gage in the inter-sectional joint.

The failure of the instruments was explained by the following causes: failure of the wire to sound as a result of "sticking"; penetration of water to the instrument; damage to the cables stored in the boxes above the uprights; damage to the cables on the concrete during drilling operations; confused numbering when collecting the instruments to the commutator panels. With respect to the causes which depend on the quality of the instruments and their installation, at the beginning of 1965, 285 instruments or 12.3% of the total number were not operating. On reviewing the commutation in 1968 part of the instruments were repaired.

It is necessary to discuss the organization of operations with respect to field studies of the Bratsk Hydroelectric Power Plant dam. These operations were performed under the direction and with the participation of the author by the group of coworkers of the field studies laboratory of the VNIIG Institute, the number of which reached 18.

The group co-worker I. S. Yeremin was constantly on location, and all of the operations with respect to the preparation and installation of the instruments and readings taken by them were performed under his inspection. The preparation of the instruments was done by 3 to 5 electricians assigned by the Bratskgesstroy trust. For taking readings by the instruments, the Bratskgesstroy trust assigned observers, the number of which increased as the

number of installed instruments increased from 4 to 12. The electricians and observers of the Bratskgesstroy trust dealing with the preparation and installation of instruments and taking readings from them were operationally subordinate to the VNIIG Institute group, and they were not used for other jobs. During the installation operations in each block the construction sections made welders, concrete workers and various laborers available to the VNIIG Institute group.

The schematics for the arrangement of the holes in the block under the upright and the instruments and also the specifications for the necessary troughs, uprights and so on were transmitted to the construction section 10 to 14 days before concreting the corresponding block. If the preparation of the block corresponded to the scheme, then the installation of the instrument took 5 to 8 hours. The information without which the block could not be accepted for concreting was generated on completion of the installation of the instrument by the VNIIG co-workers.

The instrument reading were taken daily for the first month after installation; in the second month they were taken every other day, in the third month they were taken twice a week and then every 5 to 10 days. The readings were taken by three groups of observers (three people each).

The advantage of the adopted organization of operations is that the permanent group of electricians and observers which essentially is the group under the work superintendent of the Bratskgesstroy trust with respect to measuring instruments was operationally subordinate to the field group of the field studies laboratory of the VNIIG Institute in the Braskgesstroy trust. This simultaneously led to centralization of the operations with respect to installation of the instruments at the construction site and insured constant procedural and technical direction of these operations by the VNIIG Institute.

The results of the operations were presented to Bratskgesstroy, the directorate of the Bratsk Hydroelectric Power Plant of the Gidroproyekt Institute in the form of annual reports.

The readings, even preliminary readings, of the 2000 instruments require enormous computational work. Beginning in 1963 the concrete stresses according to the measured deformations were calculated by the computer.

2.10. System of Monitoring and Measuring Instruments of the Operational Inspectorate and Its Organization

During the six years of industrial operation the Bratsk Hydroelectric Power Plant, the correspondence of the system of monitoring and control instruments of the concrete dam to the goals of the operational inspectorate was tested, and work was done to eliminate the detected defects in the system. As a result of insufficient accuracy of the section observations detected during the temporary operation, in 1971 the string-optical section was installed with a wire laid on floats every 44 meters, the position of which with respect to the structure was controlled by an optical alignment device. The

reconstruction of the system of readings with respect to the reverse plumbobs was planned. The mechanical units for the checking devices of the straight plumbobs and the crevice gages in some of the joints on the downstream face [30] and also additional remote strain gages in the rock-concrete joint on the pressure face were installed.

The condition of the remote instruments permits evaluation of their quality and also the organizational and technical level of the operations with respect to their preparation and installation. At the beginning of 1972, 83.3% of the total number of installed instruments (Table 2-2) were still in operation in the dam. In the next four years seven instruments failed, five of them were damaged during drilling operations. This condition of the instruments must be considered good.

Table 2-2

Instruments	Installed, No of pieces		Failed, No of pieces		Operating pieces / %
	of pieces	to 1968	after 1968		
Remote thermometers	640	35	5	540	84.5
Remote strain gages	1209	145	2	1062	88.0
The same mounted	117	72	—	45	38.4
Reinforcing dynamometers	54	6	—	58	90.0
Piezodynamometers	149	35	—	114	76.6
Remote crevice gages	136	24	—	112	82.4
	2315	377	7	1931	83.3

For the needs of the operational inspectorate, constant readings are not required with respect to all of the installed instruments. Therefore only half of the instruments were commuted to the central control panel in the hydroelectric power plant building where the set of semiautomatic devices are installed for remote readings by the instruments in the dam (Figure 2-16).

The first development of this equipment by the initiative of the author and the technical specifications put together by him was accomplished at the beginning of 1959. On the basis of the DShI-100 step-by-step finder and the flat RPN relays, L. Ya. Eydel'man installed an experimental device with one three-wire cable line for 100 sensors and instruments with calling of each of them by means of the remote telephone dial. The device operated well, but with time a small variation in the measured resistance was detected as a result of oxidation of the contacts. Then a set of equipment was developed including the remote switches for 50 sensors each in the form of a sealed step-by-step finder with palladium plated contacts, a control panel, a digital frequency gage (50-2000 hertz), a digital ohmmeter (0-9999 ohms with 0.1% precision), a reader and an alphanumeric printer [26]. The complex was installed at the Bratsk Hydroelectric Power Plant in 1971 and is operating satisfactorily.

Beginning in 1962 the engineer of the hydroengineering shop of Bratsk Hydroelectric Power Plant was assigned to the VNIIG Institute group at the construction site for development of the composition of the observations and the monitoring and measuring systems. This engineer subsequently headed the observation group of the hydroengineering shop of the Bratsk Hydroelectric Power Plant. With respect to the situation in the middle of 1974 the group comprised 25 people divided into three subgroups: geodetic, seepage and remote instruments. The group has a workshop with permanent workers for repairing the measuring instruments [20].

CHAPTER 3. DETERMINATION OF THE PHYSICAL-MECHANICAL AND THERMOPHYSICAL CHARACTERISTICS OF CONCRETE

3-1. Test Composition and Procedure

In the field laboratory organized by the author at the construction site, tests were made on concrete samples to determine the Young's modulus and the creep characteristics of the concrete required when calculating the stresses by the deformations measured in the dam blocks. In addition, the limiting extensibility of the concrete was determined. For the tested samples the compressive and tensile strengths were also determined.

The samples for these tests, with the exception of one series, were prepared from concrete taken directly in the block or from the concrete carriers sent to the corresponding block (Table 3-1). In all, eight series of type 100, V-2 and 200, V-8 and V-4 samples were tested.

The compressive strength of the concrete was determined on cubic samples $20 \times 20 \times 20$ cm, 1, 3, 7, 14, 28, 90, 180 and 360 days old using three samples in each age group. The tensile strength of the concrete was determined by rupture of figure-eight samples with a transverse cross sectional area of $7.06 \times 7.06 = 50$ cm^2 . In each age group three samples were tested on the lever-type press with an arm ratio of 1:100.

The relation between the strains and stresses by which the deformation modulus of the concrete and also the quick characteristics were established, was determined on prismatic samples $10 \times 10 \times 40$ cm in moistureproof insulation. The string remote strain gage was installed along the axis of each sample. The tests performed on the lever-press with an arm ratio of 1:100 consisted in the application of a step-by-step increasing compressive axial force of up to 2.5-3.0 ton-force with a stress interval of 5 kg-force/ cm^2 to three samples coaxially installed one above the other. For each test three loading and unloading cycles of the samples were used. The deformations obtained were averaged.

During creep testing the load is kept constant, and the readings by the instruments in the samples were taken daily during the first month, every other day in the second month and then once a week. The readings were taken by instruments in three of the same type unloaded samples during the same periods of time.

Table 3-1

Series No	Block	Concrete pouring dates	Type of concrete	Cement ¹	Composition, kg per m ² in dry state			Water, kg/m ²	
					Cement Sand	Coarse filler, mm	Plasti- cizer		
					5-20	20-40	40-80		
I	65-IV-9a	1959 17/VII	200, V-8 Mra-100	PTs-500 PUTs-400	230 196	680 632	700 658	690 --	SSB-5 134
II	65-III-9	6/VIII	100, V-2	PUTs-400	160	544	773	590	SSB-4 135
III	63-D-4	20/X	100, V-2	PUTs-400	190	669	498	--	SNV-3, 2 110
IV	51-U-9	21/XI	100, V-2	PUTs-400	180	659	583	928	SNV-5, 6 135
V	45-P-14	1960 9/VIII	100, V-2	ShPTs-400	180	450	418	SSB-3, 6 122	
VI	38-U-6	1961 28/III	200, con- duit	ShPTs-400	240	450	530	430	615 SSB-8 120
VII	--	20/VII	200, V-8	ShPTs-400	242	700	480	400	670 SSB-5, 3 105
VIII	6-D-4	12/IX	100, V-2 with ice	ShPTs-400	160	668	549	416 SSB-4 123	

¹ PTs -- portland cement; PUTs -- pozzuolianic cement; ShPTs -- slag portland cement.

All of the lever presses were built on site by our specifications [19].

It was most difficult of all from the procedural point of view to determine the limiting extensibility of the concrete. There is no generally accepted method of determining this highly important characteristic of concrete. During the tests various instruments are used to measure the deformations of the concrete; usually it is rarely possible to take the reading at the very time of rupture of the concrete. In addition, the use of mechanical and also mounted string-type remote strain gages to measure the deformation of the concrete unavoidably leads to errors caused by chipping of the concrete, especially the young concrete, by the points of the supporting prisms of the instruments.

The deformations when testing the figure eights of concrete at the Bratsk Hydroelectric Power Plant were measured using wire strain gages 20 and 160 mm long. Initially the deformations were reckoned by the ISD-2 device and then, in order to obtain a picture of the deformation tube rupture, the pin recording instruments were used [19].

3-2. Compressive and Tensile Strength of Concrete

The dam concrete is characterized by fast buildup of compressive strength (R), reaching the designed value at an age of 10 to 30 days. By the time it is a half year old, the cubic strength of the concrete exceeded the norm by 1.5-2.6 times (see Table 3-2) [8]. The nonuniformity of the concrete of the laboratory sample types 100, V-2 and 200, V-8 with respect to compressive strength R_{160} is characterized by the variation coefficient equal to 0.28 and 0.18 respectively [10].

Table 3-2

Type of concrete	Cubic strength of concrete poured in 1958-1962. R_{160} kg-force/cm ²		
	Average	Minimum	96% guaranteed
100, V-2	233	130	
200, V-8	326	211	
200, V-8 Mrz-250	324	252	
400, V-12	450	322	

The tests run on 148 cores drilled from the dam indicates still greater non-uniformity. The variation coefficients for the indicated types are 0.32 and 0.34 [8], and the strength guarantee is 100% and 90%.

The buildup with time of the compressive strength of the concrete (Figure 3-1) is satisfactorily approximated by the formula of the logarithmic type:

$$R = a + b \lg (t + 1), \quad (3-1)$$

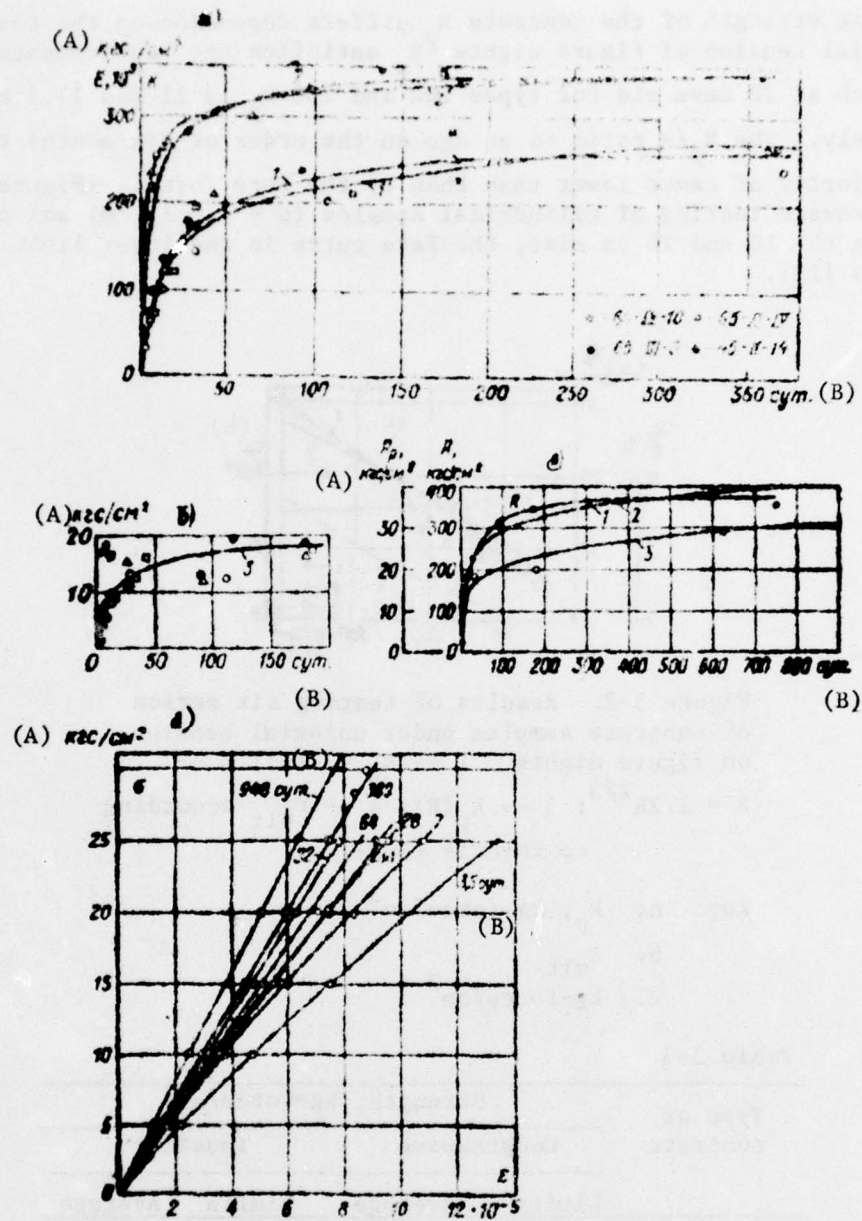


Figure 3-1. Results of testing concrete samples: a, b -- types 100, V-2; c -- types 200, V-2. 1 -- cubic strength; 1' -- the same by formula (3-1); 2 -- Young's modulus; 2' -- the same by the Graf formula; 3 -- tensile strength.

Key: A. $kg\text{-force}/cm^2$ B. days

where t is the age of the concrete in days; a and b are coefficients.

The tensile strength of the concrete R_p differs depending on the test method. For uniaxial tension of figure eights R_p satisfies the requirements of SN55-59 by which at 28 days old for types 100 and 200 R_p is 11 and 17.5 kg-force/cm² respectively. The R_p/R ratio to an age on the order of six months remains in the majority of cases lower than by the Fere formula (Figure 3-1, 3-2). During cleavage testing of cylindrical samples ($d = l = 15$ cm) and cubic samples on the 10 and 20 cm side, the Fere curve is the lower limit of the R_p/R ratio [13].

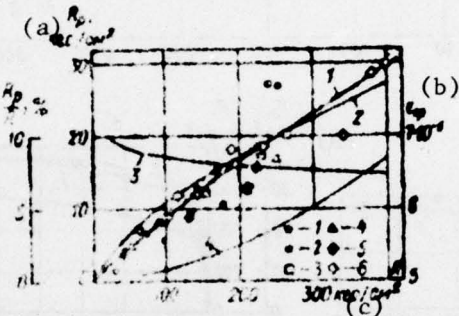


Figure 3-2. Results of testing six series of concrete samples under uniaxial tension on figure eights. 1 -- $R_p = F(R)$; 2 -- $R = 1/2R_p^{2/3}$; 3 -- $R_p (R)$; 4 -- ϵ_{ult} according to formula (3-2).

Key: a. R_p , kg-force/cm²
 b. ϵ_{ult}
 c. kg-force/cm²

Table 3-3

Type of concrete	Strength, kg-force/cm ²			
	Compressive		Tensile	
	Limits	Average	Limits	Average
100, V-2	124-371	263	11-37	13
200, V-8	144-456	292	16-45	31

The tests of the same samples made of type 200, V-8 concrete specially prepared by us for strength comparisons obtained by the methods of uniaxial tension and cleavage confirmed the divergence of the strengths determined by the methods after reaching an age of 28 days. The test results for the samples 10 × 10 × 10 cm differ especially sharply from each other.

The divergence in the values of R_p with respect to both methods is explained to some degree by the difference in moisture of the samples [27] and the measurement errors, the basic cause is the provisionalness of the cleavage method with the application of the elasticity theory formulas for concrete in the destruction stage [19, 28-31].

The compression and tensile testing (cleavage testing) for 150 cores drilled from the dam ages 2 to 3 years gave good scattering of the values of the strength characterizing the significant nonuniformity of the concrete (Table 3-3) [31].

3-3. Young's Modulus of Concrete

Between the stresses σ and the relative deformations ε a linear function is established in the 7-14 day age group (Figure 3-1, d).

The sharp buildup of the Young's modulus in the early age (Figure 3-1) is characteristic of the concrete of the Bratsk Hydroelectric Power Plant dam. In the three day age group the Young's modulus reaches values on the order of $E = (1.8-2) \cdot 10^5$ kg-force/cm², and in the seven day group $E = (2.3-2.8) \cdot 10^5$ kg-force/cm². In the one month age group the Young's modulus of the concrete reaches 75-90% of the maximum value pertaining approximately to the year age. It is necessary to note that this nature of growth of the Young's modulus is typical of the hydroengineering concrete in general (Figure 3-3).

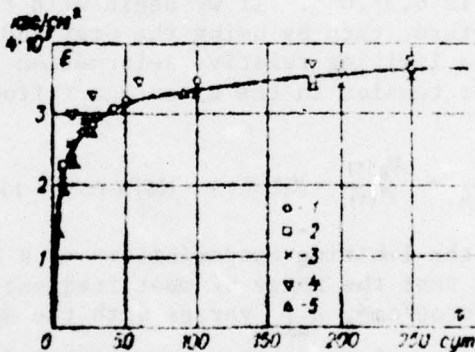


Figure 3-3. The buildup of the Young's modulus with respect to the laboratory test data for the concrete of five dams is as follows: 1 -- Kakhovskiy; 2 -- Novosibirsk; 3 -- Bratsk; 4 -- Ust'-Ilimskiy; 5 -- Krasnoyarsk.

Key: a. kg-force/cm² b. days

The Young's modulus for concrete type 100, V-2 reaches approximately $3.5 \cdot 10^5$ kg-force/cm², and for type 200, V-8 10% more. These values of the Young's modulus are retained to stresses on the order of 50-60 kg-force/cm². The

Table 3-4

Type of concrete	E_* , 10 kg-force/cm ²		E_{st}	* [illegible]
	limits	mean	mean	
200, V-8	3.62-4.51	4.18	3.35	
100, V-2	3.66-4.34	3.93	3.14	

buildup of the Young's modulus is approximated satisfactorily by the Graf formula (3-1).

The ultrasonic tests of the concrete samples in all of the cores drilled from the dam agree with the results of testing under static loads with respect to magnitude for $E_{st}/E_* \approx 0.8$ (Table 3-4) and with respect to nature of buildup in time.

3-4. Limiting Extensibility of Concrete

The figure eight tests under uniaxial tension demonstrated that the linear relation between the deformations and the stresses is retained without any significant section of plastic deformation to the rupture time which thus is brittle (Figure 3-4).

The limiting extensibility is within the range from $4.2 \cdot 10^{-5}$ to $10.1 \cdot 10^{-5}$ and on the average it is $6.3 \cdot 10^{-5}$. If we begin with the elastic operation on the concrete to rupture, then by using the Graf and Fere formulas it is possible to calculate a limiting relative deformation corresponding to the concrete strength under tension in the given age τ from the expression

$$\epsilon_{ult} = \frac{R_p(\tau)}{E(\tau)} \approx 10K_R(\tau) - 150K(\tau)^{-1.5} \cdot 10^{-6} \quad (3-2)$$

In Figure 3-2 we have the limiting extensibility as a function of R (3-2). It is possible to note that the range of most frequently encountered values R from 100 to 400 kg-force/cm², ϵ_{ult} varies with the small limits from $5.1 \cdot 10^{-5}$ to $6.7 \cdot 10^{-5}$ which is quite close to the experimental data.

The limiting extensibility $\epsilon_{ult}(\tau)$ increases with the concrete age, but in the framework of each age significant scattering of the measured values of ϵ_{ult} is observed (see Figure 3-4, b).

The Young's modulus of the concrete under tension calculated as the ratio of R_p/ϵ_{ult} is within broad limits from 2.6 to $4.2 \cdot 10^5$ kg-force/cm². The ratio of E_p/E_{comp} for the tested samples is $0.74-1.09$.

3-5. Measure of Creep

The samples tested for determining the creep characteristics were loaded at the given ages under a step compressive load to 25-30 kg-force/cm², and they remained under this load for 2 to 4 years. During loading the elastic-instantaneous part of the total deformation $\sigma_0/E(\tau)$ and the Young's modulus at the time of loading $E(\tau)$ were determined. For the measures at each subsequent point in time t , the total deformation was determined comprising the elastic deformation $\epsilon_e(\tau)$, the creep deformation $\epsilon_c(t, \tau)$ and the thermal shrinkage deformation $\epsilon_{t.s.}(t - \tau)$.

$$\epsilon(t, \tau) = \sigma_0/E(\tau) + \sigma_0 C(t, \tau) + \epsilon_{t.s.}(t - \tau). \quad (3-3)$$

From complete deformation with respect to (3-3) at each point in time the temperature-shrinkage deformation was calculated and measured in the unloaded samples.

The total unit deformation was

$$\delta(t, \tau) = 1/E(\tau) + C(t, \tau) \quad (3-4)$$

where C is the measure of creep.

Each value of $\epsilon(t, \tau)$ and $\epsilon_{t.s.}(t - \tau)$ was defined as the mean deformation measured in three samples.

For load ages (τ) from 10 to 512 days the average measure of creep with a duration of effect of the load ($t - \tau$) equal to six months is within the limits from 0.43 to $0.10 \cdot 10^{-6}$, and the limiting measure of creep is from $0.47 \cdot 10^{-5}$ to $0.11 \cdot 10^{-5}$. The corresponding values of the limiting creep characteristic $\phi_{t-\tau} = \epsilon_c(t, \tau)/\epsilon_0(\tau)$ vary within the limits from 1 to 0.4 (Table 3-5).

The nature of the buildup of the measured creep is shown in Figure 3-5.

3-6. Calculation and Measurements of the Relaxation Stress Coefficients

There are a number of methods of calculating the concrete stresses considering the creep [18, 32, 33]. We used the method of stress relaxation coefficients [34]. The relaxation coefficient is the ratio of the unit stress at the time t to the unit stress applied at the time τ .

In order to construct the relaxation curves we have the following initial data available: 1) the function of the Young's modulus $E(\tau)$; 2) the function of the measure of creep $C(t, \tau)$.

It is convenient to represent the function $C(t, \tau)$ in the form

$$C(t, \tau) = \phi(\tau) F(t - \tau).$$

(3-5)

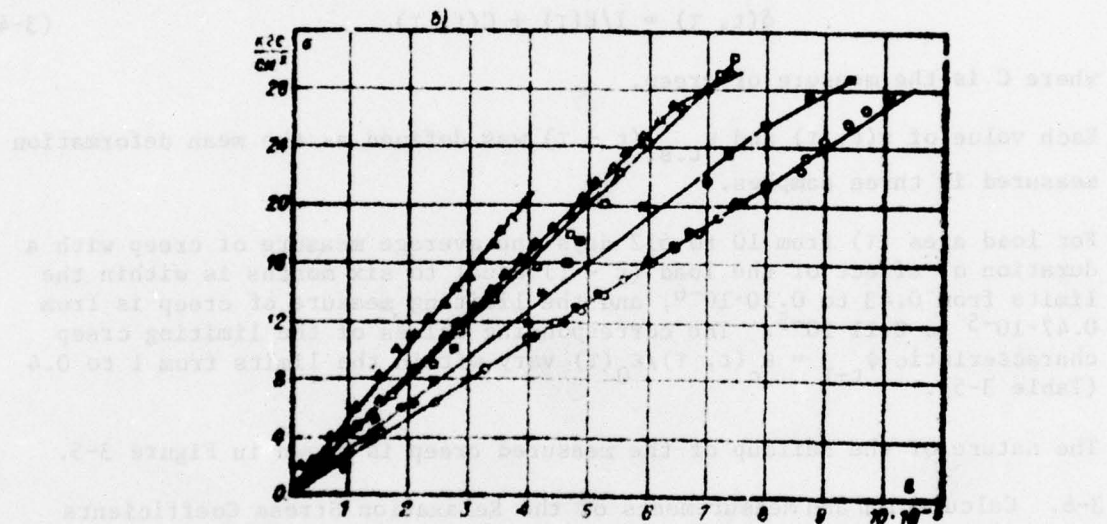
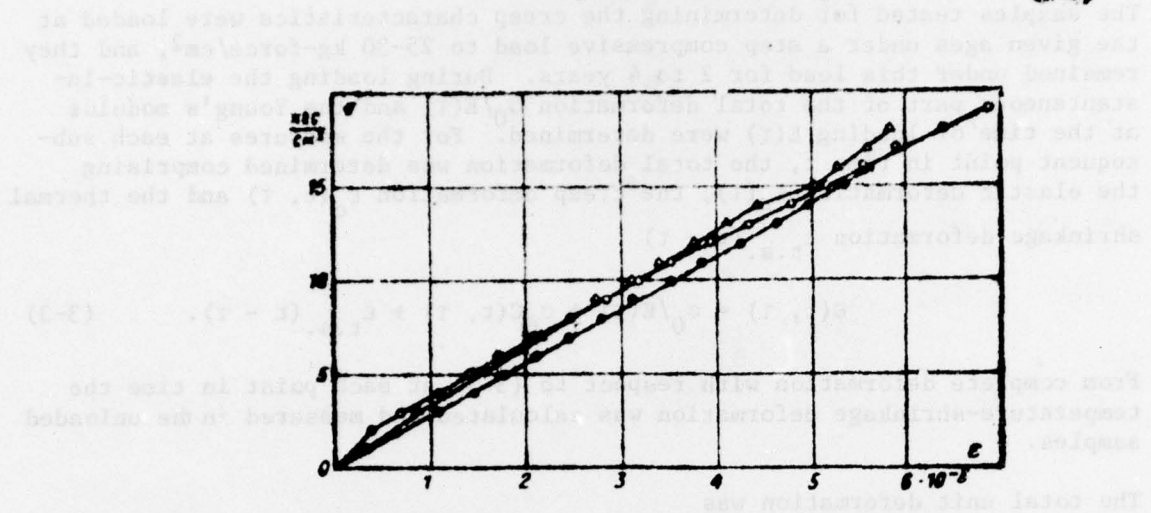


Figure 3-4. Creep compliances to be fitted to reduce a few small differences between the curves obtained by different methods of aging. The curves have been fitted to obtain the creep function $F(t - \tau)$ and the aging function $\phi(\tau)$.

where $\phi(\tau)$ is the aging function which is constructed by the limiting values of the measuring creep for different τ (see the curve ϕ in Figure 3-5; $F(t - \tau)$ is the creep function used by dividing the ordinates of the curve for the creep measure by the corresponding ordinates of the aging function

$$F(t - \tau) = \frac{C(t, \tau)}{\phi(\tau)} \quad (3.6)$$

Table 3-5

Series	Measure of creep $C(t, \tau), 10^{-5}$				
	Age on loading, days				
	10-15	27-86	90-112	203-240	512
I	0.56	0.42	—	—	—
II	—	0.24	—	—	—
III	0.45	0.54	0.20	0.11	—
IV	0.29	0.24	0.17	0.14	0.10
Mean	0.43	0.28	0.18	0.12	0.10
$E(\tau), \text{kg-force/cm}^2$	2.20	2.90	3.30	3.50	3.80
$C(\tau, t) 10^{-5}$	0.47	0.32	0.21	0.19	0.11
$\phi(\tau, t)$	1.04	0.93	0.70	0.46	0.40

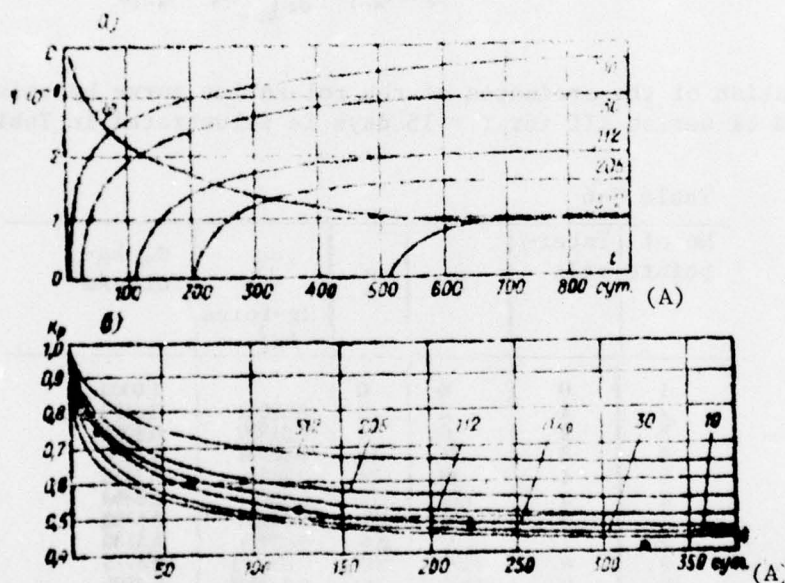


Figure 3-5. Creep curves (a) and relaxation curves (b) with respect to tests of the concrete samples type 100, V-2.

Key: A. days

In order to construct the relaxation curves two methods were used.

The method of the average rate of variation of stresses begins with the creep equation written in the following form:

$$\sigma_0 C(t, \tau) + \int_{\tau_0}^t \frac{ds}{E(s)} \left[\frac{1}{E(s)} + C(s, \tau) \right] ds = 0. \quad (3-7)$$

Dividing the investigated time period ($t - \tau$) by the number of intervals and assuming that within the limits of each interval the rate of variation of the stress is $\frac{\partial \sigma}{\partial \tau}$ remains constant and equal to some mean rate $\frac{\partial \sigma}{\partial \tau} \Big|_{\text{mean}}$, for the nth interval we have

$$\frac{\sigma_n}{\sigma_0} \Big|_{\text{cpn}} = \frac{\sigma_0 C(t_n, \tau_0) + \sum_{i=1}^{n-1} \frac{\partial \sigma}{\partial \tau} \Big|_{\text{cpn}} \int_{\tau_{i-1}}^{\tau_i} \left[\frac{1}{E(\tau)} + C(\tau, \tau_0) \right] d\tau}{\int_{\tau_{n-1}}^t \left[\frac{1}{E(\tau)} + C(\tau, \tau_0) \right] d\tau}. \quad (3-8)$$

The integrals in (3-8) are found by the graphical integration method.

The magnitude of the stress at the end of each interval is

$$\sigma_n = \sigma_{n-1} - \frac{\Delta \sigma}{\Delta \tau} \Big|_{\text{cpn}} (\tau_n - \tau_{n-1}). \quad (3-9)$$

The calculation of the ordinates of the relaxation curve by this method for the samples of series III for $\tau = 15$ days is illustrated in Table 3-6.

Table 3-6

No of points	Inter-	τ	$\frac{\Delta \sigma}{\Delta \tau}$	σ , kg-force/m ²
	vals			kg-force/m ²
1	0	0	0	1.0000
2	1	2	0.0000	0.9900
3	2	4	0.0100	0.9800
4	3	24	0.00005	0.9799
5	4	48	0.00044	0.7616
6	5	120	0.00143	0.6263
7	6	240	0.00069	0.5700
8	7	360	0.00275	0.3180
9	8	480	0.002071	0.1775
10	9	500	0.00035	0.1666

The purely graphical method presupposes that within the limits of each time interval the stress remains constant, varying discontinuously on the length from one interval to the next (stepwise) where the initial creep curve is corrected in accordance with the decrease in the stress for each interval.

This method was used to calculate the relaxation curve for the samples of series V for five values of τ and $(t - \tau)$ to one year.

The highly tedious process of constructing the stress relaxation curves by the experimental creep curves can give exact results only in the case where there are a sufficiently large number of points by which the aging curve is constructed, that is, a sufficient number of loading ages and duration of effect of the load. The results of calculating the relaxation coefficients by the data from the numerous and short term tests have a highly approximate nature.

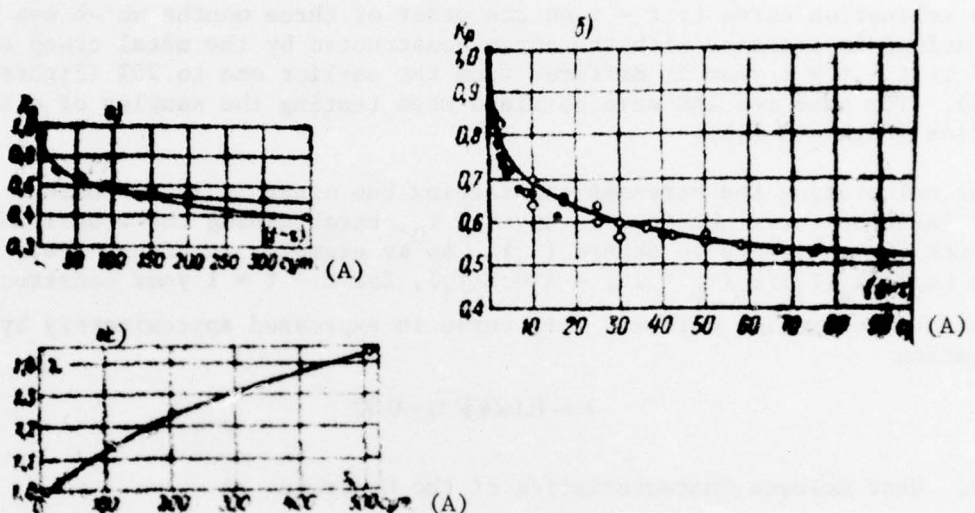


Figure 3-6. Relaxation curves with experimental points (black dots) and points calculated by the curves (light dots): a -- series V -- $\tau = 112$ days; b -- series I, III, V -- $\tau = 15-36$ days; c -- curve $\lambda = F(\tau)$.

Key: A. days

The author performed tests to determine the stress relaxation coefficient by direct measurement. For this purpose the stress in the sample $\sigma(\tau_i)$ was decreased so that the measurements in them of the deformations $\varepsilon(\tau_i)$ after subtraction of the temperature-shrinkage deformation increment $\Delta\tau_{t.s.}$ remained constant

(3-10)

Three samples of age τ were loaded in steps of [illegible] kg-force/cm² to stresses of $\sigma_0 = 25-30$ kg-force/cm² and the average elastic deformations $\varepsilon_{mean}(\tau)$ were calculated. Then after defined, gradually increasing time intervals at ages t_i the deformation was measured in the loaded and

the three samples, and the deformation $\epsilon_{\text{average}}(t_i)$ and $\epsilon_{\text{ave.t.s.}}(t - \tau)$ was calculated. The compressive load on the samples was decreased (by removing the weights from the lever press) to a value of $\sigma(t_i)$ at which

$$\epsilon_{\text{average}}(t_i) - \sigma_{\text{ave.t.s.}}(t - \tau) = \epsilon_{\text{ave}}(\tau_0)(1+0.05).$$

The ratio $\sigma(t_i)/\sigma(t_0) = k_p(t_i)$ corresponded to the relaxation coefficient for age t_i . The tests were performed for a year [19].

The relaxation curve to $t - \tau$ on the order of three months which was obtained coincided in practice with the curve constructed by the metal creep curves, and at $t - \tau = 1$ year it differed from the earlier one to 20% (Figure 3-5 and 3-6). The same results were obtained when testing the samples of other series (Figure 3-6,b).

When calculating the stresses considering the creep it is convenient to use a relaxation curve obtained in any age τ_0 , establishing the transition coefficients from this age to others (τ). As an example, in Figure 3-6,c we have the curve $k_p(\tau_i)/k_p(\tau_0) = 10 = \lambda = F(\tau_i)$, for $t - \tau = 1$ year constructed by the five relaxation curves. This curve is expressed approximately by the equation

$$\lambda = 0.024 \sqrt{\tau_i} + 0.92 \quad (3-11)$$

3-7. Heat Release Characteristics of the Concrete

The specific heat release in the concrete of the cement of the Krasnoyarsk plant according to the determination in the adiabatic calorimeter [35] was 69.3 kcal/kg for the slag portland cement and 83.6 kcal/kg for portland cement.

The actual heat release of the cement in the concrete was determined with respect to the temperature buildup in the characteristic blocks of the dam.

With respect to the initial section of the temperature curve in the center of the blocks 3-6 meters high the initial branch of the adiabatic heat release curve (Figure 3-7) was determined considering that the heat release depends only on the cement consumption

$$q = \frac{c\gamma(T_{ad} - T_{c.mix})}{C}, \text{ kcal/kg,} \quad (3-12)$$

where c is the specific heat capacity of the concrete; γ is the specific weight; T_{ad} is the temperature under adiabatic conditions; $T_{c.mix}$ is the temperature of the concrete mix; C is cement consumption.

For the points on the heat release curve lying beyond the limits of the adiabatic periods, the hardening temperature is excluded by going from the adiabatic process to the isothermal process.

Beginning with the heat release theory developed by I. D. Zaporozhets [36], all the data are reduced to one temperature equal to 20° C, and the heat release values were calculated by the formula

$$Q = Q_{\max} [1 - (1 + A_{20}\tau)^{-0.893}], \quad (3-13)$$

where Q is the release of the concrete to the age τ ; Q_{\max} is the maximum possible heat release of the concrete; A_{20} is the coefficient of the heat release rate.



Figure 3-7. Exothermal heating of the concrete modules: a -- module 30-II-[illegible] from 21 August 1962 to 18 September 1962; b -- the module 65-I-16 from 1 June 1960 to 27 June 1960. 1 -- calculated by the isothermal heat release characteristics; 2 -- measured.

Key: A. days

By recalculation for the isothermal regime, the times are established at which for a hardening temperature of 20° C the concrete demonstrates the same heat release as for the adiabatic regime

$$\tau_s = \int_0^{\infty} \frac{t_{is}(t) - 20}{10} dt. \quad (3-14)$$

The heat release characteristics were determined for 25 modules at which the hardening temperature is above 20° C [19, 37].

As is obvious from the summary data (Table 3-7), by the maximum specific heat release of the cement in the concrete $q_{\max} = 60-100$ kcal/kg the concrete

can be classified as moderately thermal. The gradual increase in q_{\max} with time is explained by the increase in the activity of the cements of the Krasnoyarsk plant [13]. The somewhat greater q_{\max} in the concrete with a smaller content of slag portland cement ($170-200 \text{ kg/m}^3$) is obviously connected with the active water reserve per kg of cement. The broad range of values of A_{20} within the limits from 0.2 to 1.0 basically dependent on the nonuniformity of the activity of the cement caused the generation in the center of the blocks of from 30 to 80% of Q_{\max} for the first three days.

Table 3-7

Year	Type of cement	Cement		Additive	Heat release characteristic		
		Type	Consumption, kg/cm^2		Q_{\max} , thousands of kcal/cm^2	[illegal] q_{\max} , kcal/kg	A
1959	150, V-8 Mrz-100	PTs	250	SNV	14-16	50-65	0.4-0.8
1960	200, V-5	ShPTs	230-260	SSV	15-20	60-50	0.1-1.0
1961	100, V-2		170-200		12-15	70-85	
1962	200, V-8 Mrz-100	PTs	230-260	SSB	17-25	75-100	0.2-0.5

The characteristic of thermicity of the cement in the concrete is usually considered to be the specific heat release under adiabatic conditions in 7 days (q_7). The actual value of q_7 for portland cement reached 70-80 kcal/kg, and for slag portland cement to 68 kcal/kg. In individual blocks for which q_7 cannot be determined, q_3 reached 65-70 kcal/kg and it is possible to assume that q_7 under adiabatic conditions reached 90-100 kcal/kg.

3-8. Thermophysical Characteristics of Concrete

In 1960 field and laboratory studies were made on experimental long blocks of sections 4 and 6 of the dam [38] to determine the thermal conductivity and thermal diffusivity of the type 100 and 200 concrete [39].

The studies demonstrated that the coefficients of thermal conductivity λ and the thermal diffusivity a have the largest value for the concrete mix $\lambda = 2-2.4 \text{ kcal}/(\text{m}\cdot\text{hr}\cdot\text{deg})$ and $a = 0.0036-0.0048 \text{ m}^2/\text{hr}$. As the concrete hardens with gravometric moisture of 4-7%, a gradual decrease in the coefficients λ and a takes place where the sharpest decrease occurs in the first two months: $\lambda = 1.8-2.1 \text{ kcal}/(\text{m}\cdot\text{hr}\cdot\text{deg})$ and a to $0.0034-0.0043 \text{ m}^2/\text{hr}$. By the age of the concrete of 20 months, $\lambda = 1.7-1.9 \text{ kcal}/(\text{m}\cdot\text{hr}\cdot\text{deg})$ and $a = 0.0031-0.0037 \text{ m}^2/\text{hr}$.

The coefficient of thermal conductivity increases with an increase in the moisture of the concrete w , remaining constant for moisture greater than 6%. For dry concrete it is $1.5 \text{ kcal}/(\text{m}\cdot\text{hr}\cdot\text{deg})$ and for moisture of 5% it is $2 \text{ kcal}/(\text{m}\cdot\text{hr}\cdot\text{deg})$.

As a result of the studies for concrete with a volumetric mass of gamma = 2450 kg/m², moisture w = 4-7% and to a temperature of T = 5-20° C, the following values of λ and a are recommended (see Table 3-8).

3-9. Coefficient of Linear Expansion of Concrete

This coefficient was determined by the deformations of the concrete and the so-called shrinkage cones (see Chapter 2). Inasmuch as the concrete in them was isolated from the existing stresses, the measured deformations are free and are caused by changes in temperature and moisture and also the volumetric variations as a function of the cement hydration.

Table 3-8

	λ , kcal/(m-hr-deg)	a, m ² /hr
0.5	2.1	0.0040
2.0	2.0	0.0040
12	1.9	0.0037
20	1.4	0.0036

The role of the last factor is small and is limited by the initial hardening period. The moisture of the concrete at a distance of 30-40 cm from the open surfaces remains constant [18] and thus for sometime after the concrete is poured the deformations measured in the cones are temperature deformations which are connected to the variation of the temperature by a linear function.

With respect to deformations and temperature measured in 170 cones in 41 blocks of dam, the mean value of the coefficient of linear expansion is established for a positive temperature $\alpha = 0.24 \times 10^{-5} \text{ }^{\circ}\text{C}^{-1}$. The variation coefficient of this function $C_e = 0.15$.

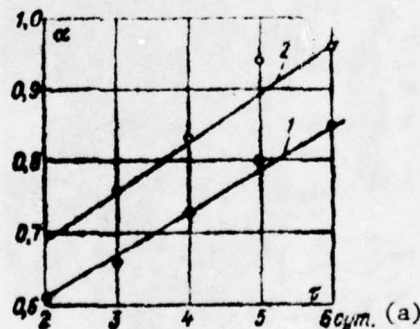


Figure 3-8. Buildup of the coefficient of linear expansion in the early age of concrete. 1 -- gravel + rubble, OK = 3 cm; 2 -- gravel, OK = 2 cm.

Key: a. days

In accordance with the method of determining α , the values obtained for α did not pertain to the early age of the concrete. The special studies by V. I. Dubnitskiy [39] demonstrated that for type 200, V-4 concrete with a volumetric mass of 2.4 tons/m³ at a temperature of 12° C, α for ages from 2 to 6 days increases intensely (Figure 3-8).

3-10. Effect of the Negative Temperature on the Physical-Mechanical Properties of Concrete

The series of laboratory studies [40-43] were used to establish significant variations of the physical-mechanical properties of concrete at negative temperature. The results of these studies give, however, only a qualitative picture, and they did not reflect the changes taking place in the massive hydroengineering concrete at negative temperature. This is explained first of all by the small sizes of the tested samples (2.5 × 2.5 cm; 5 × 5 cm) causing a concrete composition without coarse filler and secondly, great intensity of freezing (10-20 deg/hour) not occurring in the concrete structures.

The first field studies of the temperature variations in the frozen massive concrete were executed on the Bratsk Hydroelectric Power Plant dam [44]. For periodic freezing of the dam sections (see Chapter 4) the concrete temperature was reduced to -(1-4)° C in the axial cross sections and to -(10-20)° C at the edges of the section. The duration of the effect of the negative temperature is from 1 to 9 months.



Figure 3-9, Loaded samples under the direct effect of outside air.

There were 120 cones located in the frozen areas of the dam. The analysis of the deformations and temperature measured in them made it possible to establish the variation of the coefficient of linear expansion of the frozen concrete in the structure.

In order to establish the effect of the negative temperature on the Young's modulus and creep of the concrete and also the effect on these properties of the concrete composition, age, thermal regime and moisture content, the laboratory tests of samples in series I-VIII (Table 3-1) and specially prepared new samples were organized. The tests were performed in a refrigeration chamber [45] built at the OISM laboratory of Bratsktesstroy trust, and in individual cases under the direct effect of the outside air (Figure 3-9). We used samples $10 \times 10 \times 40$, $15 \times 15 \times 50$, $15 \times 15 \times 70$ (tension) and $30 \times 30 \times 60$ cm. The concrete deformations were measured by the string remote strain gages built into each sample.

These studies and also the analysis of the data from the field observations performed over a number of years by V. N. Durcheva gave the following results.

In the massive hydroengineering concrete free of moisture exchange with the outside air at a temperature below -2°C , an increase in the coefficient of linear expansion is always observed directly proportional to the moisture content of the concrete and inversely proportional to its type strength.

In the temperature range from -2 to -12°C the temperature deformations are linearly connected with the temperature $\epsilon = \alpha'(T - 2) \cdot 10^{-5}$. For deeper freezing ($T < -12^{\circ}\text{C}$) the coefficient of linear expansion decreases (Figure 3-10):

$$\alpha' = n_a \alpha - m(T - 12), \quad (3-15)$$

where T is the value of the temperature.

For the hydroengineering concrete free of moisture exchange with the outside air, n_a 1.1-2.

The effect of the negative temperature and the type strength of the concrete in the coefficient of linear expansion is described empirically by the equation.

For $T \geq -12^{\circ}\text{C}$:

For all types of concrete

$$\alpha' = [1.25 + 0.07(20 - V_R)] \cdot 10^{-5} \quad (3-16)$$

For $T = -(12-40)^{\circ}\text{C}$;

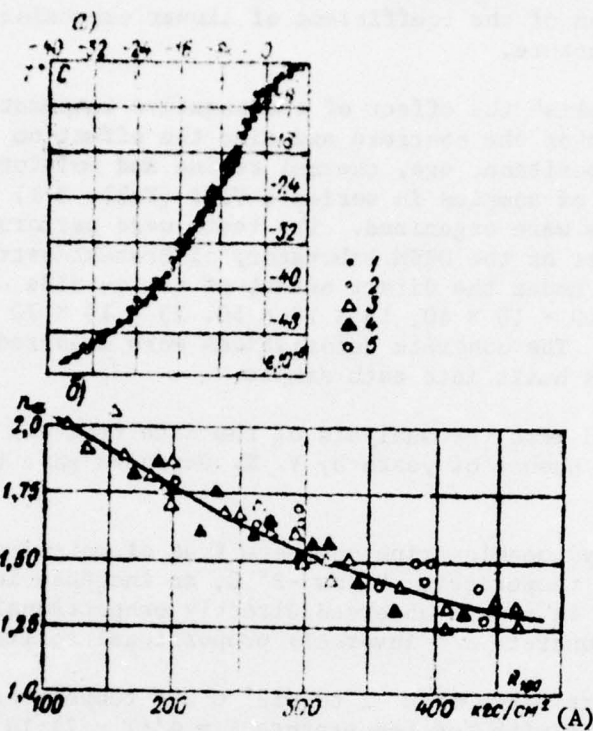


Figure 3-10. Deformation of the concrete at negative temperature: a -- function $\epsilon = P(T)$; b -- function $n_\alpha = f(R_{180})$. 1 -- in the structure; 2 -- in the sample; 3 -- concrete of the Bratsk dam; 4 -- concrete of the Ust'-Ilim dam; 5 -- laboratory tests.

Key: A. kg-force/cm²

For types 100-200

$$\epsilon = [1.25 + 0.07(20 - \sqrt{R}) - 0.02(T - 12)] \cdot 10^{-5} \quad (3-17)$$

for types 250-300

$$\epsilon = [1.25 + 0.07(20 - \sqrt{R}) - 0.018(T - 12)] \cdot 10^{-5} \quad (3-17')$$

These relations occur for the strength of the concrete at the time of freezing exceeding 40-60 kg-force/cm². The freezing of the concrete in the early age, when the strength is on the order of 20-30 kg-force/cm², is accompanied by expansion deformations indicating the stress relief of the concrete structure.

In the concrete of the surface layers of the structure which has moisture exchange with the outside air and loses part of the water of hardening, the

coefficient of linear expansion does not depend on the sign of the temperature [44].

The crystallization of the water in the frozen concrete eliminates the defects in its structure, increasing its uniformity. A consequence of this is the increase in strength of the concrete under compression and tension by 1.5-2 times and its limiting extensibility to 2-[illegible] times. The Young's modulus of the concrete (E_{-T}) increases directly proportionally to the magnitude of the negative temperature:

$$E_{-T} = E_0 + n_E (T - -1), \text{ kg-force/cm}^2, \quad (3-18)$$

where E_0 is the Young's modulus before freezing; n_E is the coefficient of deformability of the concrete. The value of n_E is proportional to the amount of free water in the concrete at the time of freezing. It is within the limits of (2,000 to 9,000) kg-force/cm²-deg), and it depends on the strength of the concrete, the type of filler and the load.

The increase in the adhesive strength of the coarse filler with the concrete solution at negative temperature causes a larger value of n_E under tension than under compression. Here $n_E^{\text{tens}}/n_E^{\text{comp}}$ depends on the state of the contact zone basically limited to the type of filler. Thus, for M250 concrete on gravel $n_E = 8870$ kg-force/(cm²-deg) is 1.5 times larger than for M300 concrete on rubble.

Between the Young's modulus of the frozen concrete under compression and the coefficient of linear expansion there is a function approximately expressed by the formula [45]

$$n_E = (n_0 - 1) \cdot 10^4, \text{ kg-force}/(\text{cm}^2\text{-deg}). \quad (3-19)$$

The creep of the frozen massive concrete (with the exception of the concrete of early age) is curtailed. It is renewed with variations of the negative temperature and with thawing of the concrete [47].

The thawing of the massive concrete is accompanied by the residual deformations of expansion (on the order of $1 \cdot 10^{-5}$) a temporary reduction in the negative Young's modulus and renewal of the creep deformations, which is a consequence of some stress relief of its structure. At positive temperature after thawing, an increase in the strength and Young's modulus is observed which indicates not only the self-healing of the concrete but also its hardening. In the concrete frozen in the ice stage the residual expansion deformations reach $4 \cdot 10^{-5}$; in the case of short term freezing cycles replaced by long-term hardening of the concrete at positive temperature, the residual deformations are reversible. The long-term freezing (10-15 days) leads to irreversible destructive processes.

CHAPTER 4. TEMPERATURE REGIME OF THE DAM

4-1. Air and Water Temperatures

The stressed and strained state of a high concrete dam is to a significant degree caused by the temperature effects. In the construction period these effects are determined by the climatic conditions and the set of measures taken to control the concrete temperature; during operation of the structure the thermal state depends on the ambient temperature -- the outside air and the reservoir water.

For the dam at the Bratsk Hydroelectric Power Plant built in a location with a severe, sharply continental climate, the role of the temperature effects is especially great.

Air Temperature. The perennial variation of the mean monthly temperature within the limits of a year is approximated by the equation

$$T = -21.3 \cos \frac{2\pi t}{365} - 4 \sin \frac{2\pi t}{365} - 2.6. \quad (4-1)$$

where t is the time in days.

In 15 years that have passed since the beginning of the pouring of the concrete in the channel dam, the mean annual air temperature has been 1.7° C which is 0.9° C lower than the mean over many years. The annual amplitude of the mean monthly air temperature during this period is within the limits from 35 to 48.3° C and on the average it is 39.3° C, which is 3.7° C below the mean amplitude of 42° C over many years (see Table 4-1).

The open surfaces of the concrete massif are under the effect of large air temperature variations within the limits of the month, ten day period and 24-hour period characteristic of the sharply continental climate. Thus, for example, the amplitude of the temperature fluctuations during the day reaches 27° C.

The solar radiation has a noticeable effect on the temperature of the concrete on the pressure face oriented to the south in the summer construction period.

Table 4-1

Years	Months												Mean
	I	II	III	IV	V	VI	VII	VIII	IX	X	XI	XII	
1958	-22.1	-21.2	-14.1	-32	-4.5	18.3	15.4	6.2	6.0	-6.7	-16.5	-1.7	-1.7
1959	-22.9	-18.6	-6.9	-0.2	6.5	16.7	17.6	15.6	9.0	-1.4	-14.8	-2.8	-1.7
1960	-24.8	-13.7	-14.0	-0.2	6.9	15.6	18.4	15.0	9.2	-0.6	-11.5	-21.8	-1.7
1961	-19.4	-17.7	-9.5	1.3	9.5	12.5	21.8	15.6	8.9	-3.6	-10.9	-21.7	-1.7
1962	-15.7	-13.4	-8.0	-0.8	8.6	14.8	19.3	16.7	8.6	-1.2	-15.3	-1.7	-1.7
1963	-20.2	-10.7	-7.5	-2.6	6.8	12.4	18.7	16.3	7.5	0.8	-8.0	-1.7	-1.7
1964	-14.9	-21.4	-11.4	-3.5	7.7	14.2	18.8	17.1	9.1	-2.6	-7.3	-17.7	-1.7
1965	-21.3	-20.5	-8.5	-1.0	8.3	15.2	18.2	16.9	7.5	2.3	-13.3	-2.1	-1.7
1966	-23.3	-23.1	-12.7	-5.1	6.2	14.0	18.6	15.3	11.3	1.1	-12.4	-2.1	-1.7
1967	-20.4	-17.6	-7.5	0.3	6.7	14.1	18.3	12.7	6.0	2.8	-15.0	-17.1	-1.7
1968	-22.8	-19.7	-4.4	0.9	7.5	13.6	19.2	15.8	4.4	0.2	-13.5	-25.9	-1.7
1969	-28.6	-28.9	-12.0	-2.0	4.9	13.8	19.7	15.3	7.0	-0.4	-5.6	20.4	-1.7
1970	-20.0	-26.2	-14.4	-6.2	5.7	13.8	17.8	13.9	7.1	-1.7	-9.8	-17.2	-1.7
1971	-16.9	-24.9	-13.1	-0.5	7.1	18.4	16.0	15.7	8.3	4.0	-4.9	-18.2	-1.7
1972	-20.8	-16.5	-10.0	1.2	4.3	14.8	16.3	13.3	6.9	-2.3	-11.9	-17.4	-1.7
Mean for 15 years	-21.0	-18.1	-10.2	-1.0	5.8	14.4	18.3	15.3	7.8	-0.2	-10.9	-19.4	-1.7
Mean over many years	-28.6	-27.4	-11.6	-1.9	7.2	15.9	18.2	15.8	7.8	-1.4	-13.0	-22.2	-2.6

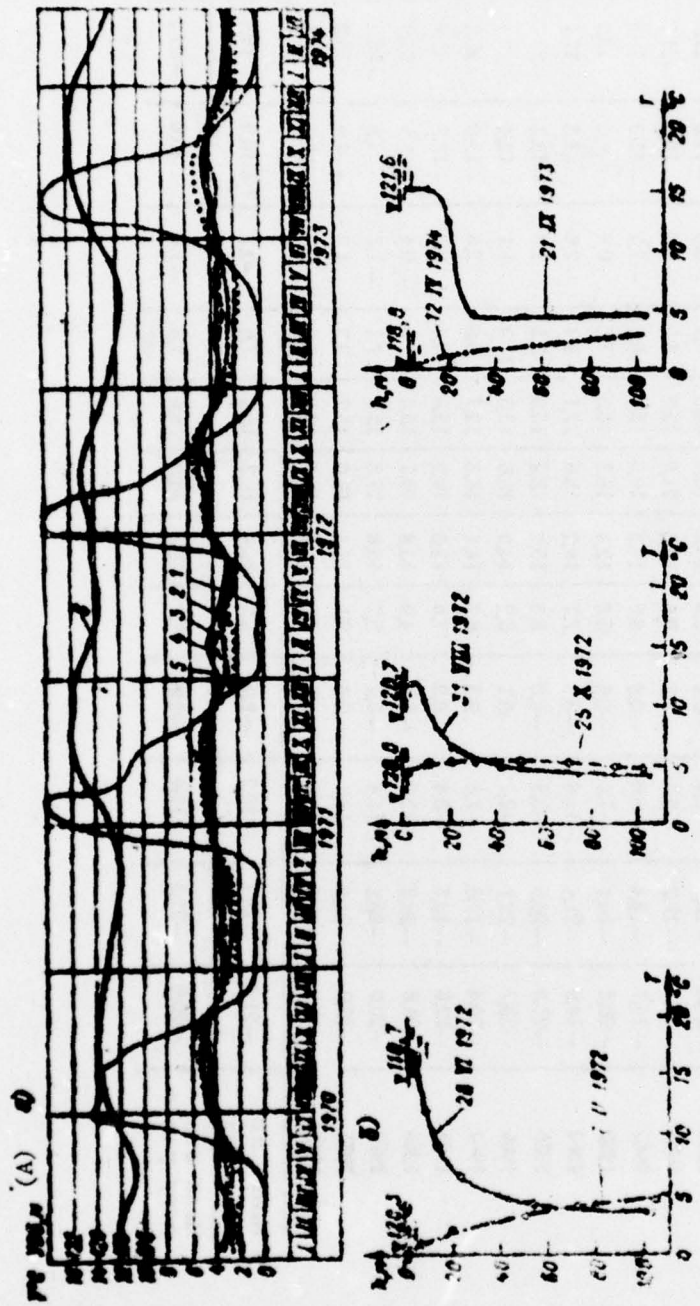


Figure 4-1. Reservoir of water temperature under the normal operating conditions of the hydroelectric power plant: a — annual temperature fluctuations at different marks; b — temperature distribution with respect to depth. 1 — at the surface; 2 — 63 meters; 3 — 81 meters; 4 — 45 meters; 5 — at the bottom; 6 — headwater level.

Key: A. $T^{\circ} C$, headwater level, meters

According to the data from the Bratsk Meteorological Observatory, the radiation influx of heat during the daylight hours of the most sunny days in July reaches $9,500 \text{ kcal/m}^2$. On these days the surface temperature of the concrete exceeded the outside air temperature by 10 to 15° C . At a depth of 18-20 cm from the surface the increase in the concrete temperature reached 8° C .

Reservoir Water Temperature. As the reservoir filled, the water temperature, the amplitude of its annual fluctuations and the distribution vertically changed gradually. The latter became uniform in May to June and November (Figure 4-1). During the summer the heating of the surface layers of the water is gradually extended to a depth of about 25 meters. In the section from the surface to this depth, a sharp decrease in the temperature by 10 to 15° is observed. In the winter the temperature varies from the surface zero to 30° C at the bottom.

This nature of the temperature distribution observed during the first years after the beginning of the filling of the reservoir is retained also in the constant operating regime. During the periods of uniform temperature distribution with respect to the vertical, its values remain $2.5\text{--}3^\circ \text{ C}$ in the spring and $4.5\text{--}5^\circ \text{ C}$ in the fall. The water temperature in the bottom layers varies within the limits of $3\text{--}5^\circ \text{ C}$ within the year (Figure 4-1).

4-2. Air Temperature Regime in the Cavities of the Expanded Joints

The thermal state of the columns of the inside region of the dam during the construction period was caused by the air temperature in the expanded joint. It basically determines the thermal state of these columns also during permanent operation.

In the cavities of the expanded joints only partially overlapped on the bottom side with great depth (in 1962, more than 50 meters) there was no air circulation; therefore the temperature in the cavities in the winter was close to the outside air temperature, and in the summer appreciably below it. The mean annual air temperature in the part of the joints next to the rock remained below the mean annual outside air temperature (see Table 4-2).

In the fall of 1963 the expanded joints were covered with wooden shields at the locations where there was no permanent overlap. This increased the temperature in the joints somewhat and decreased the amplitude of the temperature variations. The winter temperature of the joints remained, however, negative.

By the winter of 1964 to 1965 the greater part of the joints without the pylons of the concrete scaffolding was covered with a permanent cover provided for by the plant. A significant difference occurred between the air temperature on the two sides of the sections. In the zone next to the rock of all of the joints the temperature was about the same and equal to $-(14\text{--}16)^\circ \text{ C}$ inasmuch as the joints communicate with each other by drainage tunnels.

Table 4-2

Temperature	Air temperature in °C in 1962						
	VIII	IX	X	XI	Dec	Jan	Feb
Outside air	17.7	13.4	8.6	-0.8	8.6	14.8	19.1
At the 63 meter mark	-15.9	-13.0	-9.0	-0.8	8.6	15.6	18.7
At the 45 meter mark	-15.0	-13.5	-9.0	-0.8	4.6	9.6	15.0
At the 27 meter mark	-15.0	-13.5	-9.0	-1.7	1.7	6.4	11.5
Next to the rock	-15.0	-13.5	-9.0	-2.8	0.1	3.4	6.5

(table continued)

Temperature	Air temperature in °C in 1962						
	VIII	IX	X	XI	Dec	Mean annual	
Outside air	16.7	8.6	-1.2	-15.3	-12.1	0.0	
At the 63 meter mark	16.6	8.9	-1.1	-15.4	-12.1	0.01	
At the 45 meter mark	16.6	8.9	-1.1	-15.4	-12.1	-1.10	
At the 27 meter mark	11.7	6.5	-1.1	-15.4	-12.1	-2.55	
Next to the rock	8.5	5.0	-2.0	-15.4	-12.1	-3.9	

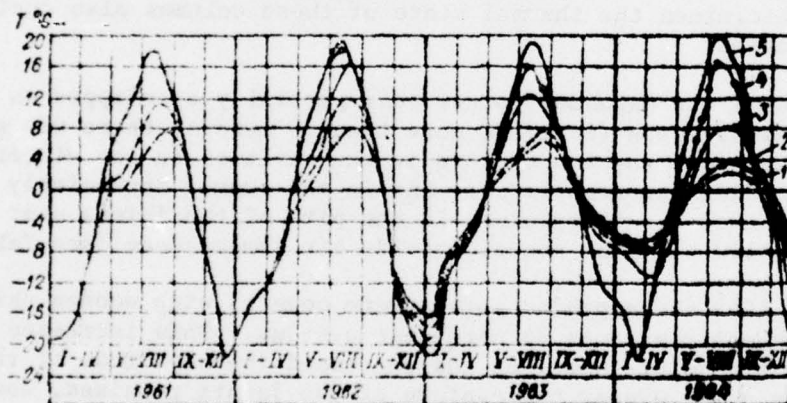


Figure 4-2. Mean monthly air temperature in the expanded joints of the channel part of the dam at different marks.
 1 -- zone next to the rocks; 2 -- 27 meters; 3 -- 45 meters;
 4 -- 63 meters; 5 -- outside air (Orgenergostroy data).

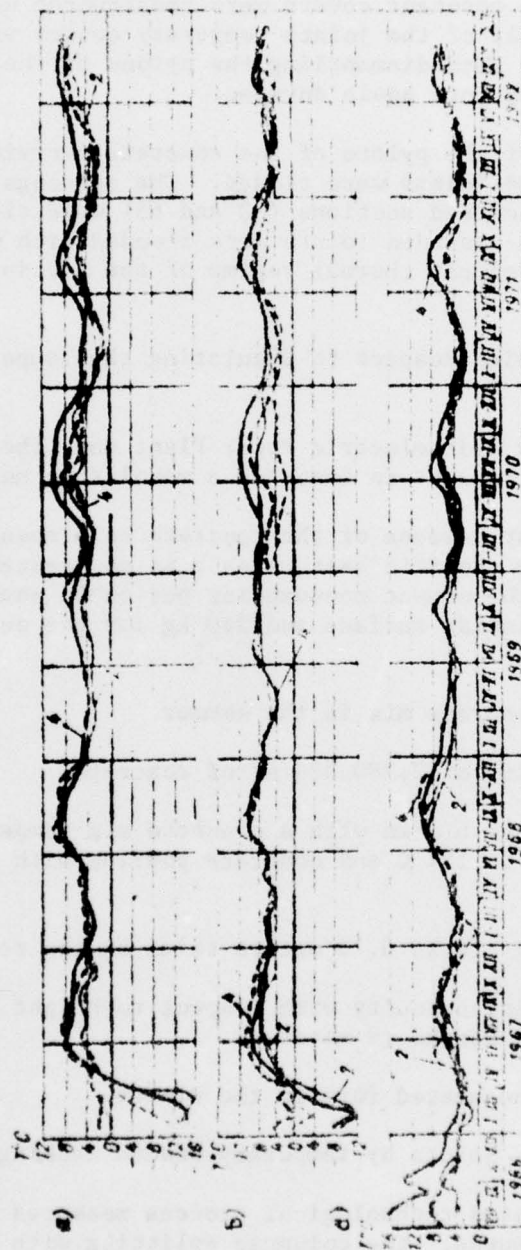


Figure 4-3. Air temperature in the expanded joints measured in the sections: a -- 65; b -- 30, c - 51. The curves 2 -- at V 27 meters, curves 4 -- at V 63 meters.

The approximate mean monthly values of the air temperature in the joints with the pylons are presented in Figure 4-2,

In 1965 and 1966 in the expanded joints of the dam there was a highly unstable temperature regime. On half of the joints without pylons of the concrete carrying trestle constant covers were constructed according to the plan; on the other half of the joints temporary covers were subsequently uncovered in connection with dismantling the pylons of the concrete carrying trestles and then they were again covered.

In 1967 the dismantling of the pylons of the concrete carrying trestle was completed and the expanded joints were closed. The openings that remained in the coverings of the two closed sections (30 and 65) were closed in June 1967, and in September 1967 the expanded joints were flooded with water to the tailrace level. The subsequent thermal regime of the air in the joints is shown in Figure 4-3.

4-3. Planning Measures with Respect to Regulating the Temperature of the Concrete

When designing the Bratsk Hydroelectric Power Plant dam, the following measures were developed with respect to insuring a monolithic nature of the dam.

1. A decrease in the heat release of the concrete as a result of the application of the cement with specific heat release is no greater than 60 kcal/kg, and the restrictions on the cement consumption per cubic meter of concrete weighing 160 kg for the inside surface and 240 kg for the outside regions of the dam.
2. The cooling of the concrete mix in the summer.
3. Artificial pipe cooling of 2,780,000 m³ of concrete.
4. Pouring the three meter blocks with a concrete mix temperature in the summer no higher than 10 to 12° C and concrete pouring with no more than 5 to 6.5 meters/month.
5. In the summer pouring blocks 0.75 meters thick on the rock base.
6. Restriction of the discontinuity with respect to height between adjacent columns to no more than 3 blocks (9 meters).
7. The application of the heated form in the winter.
8. Covering the expanded joints by temporary wooden decking.

In addition to the indicated technological process measures the plans provided for structural measures: the columnar splitting with spacing between the longitudinal joints of 13.8 meters and the construction of auxiliary notch joints in the channel section of the dam from the base to the 19 meter

mark at the depth of the first column. In the deep sections on the downstream face side provision was made for the notch joints to a depth of 4.5 meters [48, 49].

4-4. Exothermal Heating of the Concrete

In Table 4-3 the mean monthly concrete mix temperatures in the covered layer are presented for 1960-1962 during which 3,278,000,000 cubic meters of concrete were poured. The temperature of the concrete mix in the covered layer during the October to April period exceeded the normative 5° C by 1-3° C, and in the summer months, it exceeded the mean monthly outside air temperature by about the same amount. The winter concrete temperature on the average exceeded the fall concrete temperature or was equal to it as a result of superheating of the mix at the concrete plant.

Table 4-3

Year	Mean monthly concrete temperature in the covered layer, ° C											
	I	II	III	IV	V	VI	VII	VIII	IX	X	XI	XII
1960	7.4	7.4	7.8	5.4	8.7	17.6	20.6	18.6	13.9	6.8	7.3	8.1
1961	8.2	7.8	6.7	6.2	9.9	15.8	19.9	16.3	13.0	7.2	8.9	7.6
1962	7.2	7.9	7.8	6.2	10	16.8	21.0	19.6	14.2	8.9	13.1	9.6
Mean	7.6	7.7	7.4	5.9	9.5	16.7	20.5	17.8	13.7	7.3	9.8	8.4

As is obvious from (3-7), the heat release of the cements used q amounted to 70 to 80 kcal/kg for 7 days for portland cement and 48-60 kcal/kg for slag portland cement. Higher values were also observed. The heat release rate A_{20} (under isothermal conditions) was within broad limits from 0.2 to 1.0.

The planned cement consumption was sharply raised [7].

In addition to the 3 meter block, 6 meter blocks were also poured, the number of which at the end of 1961 was 34% of the total number of blocks (in the 3 meter execution).

The mean rate of pouring the concrete in the dam sections was 1.4-6.4 m/month in 1960-1961, that is, it was close to the design value; the maximum concrete pouring rates for the individual columns were within the limits from 6 to 24 m/month, amounting to 14.9 m/month on the average for 148 columns.

The indicated conditions determined the maximum temperature level in the concreting blocks.

Under the design conditions: for a height of the blocks of 3 meters, a concrete pouring rate of 5 m/month and a concrete mix temperature of 10° C the maximum temperature (t_{max}) calculated by formula (3-12) for $C = 0.25$ kcal/kg and $\gamma = 2400 \text{ kg/m}^3$ without considering the effect of the temperature on the heat release is about 22° C for $C = 160 \text{ kg/m}^3$ and it is 28.5° C at

$C = 240 \text{ kg/m}^3$. Under other conditions occurring in the construction, the calculated value reached $38\text{--}47^\circ \text{C}$ for the three meter blocks and $43\text{--}51^\circ \text{C}$ for the six meter blocks.

In Table 4-4 we have the measured values of the temperature of the concrete mix $T_{c,\text{mix}}$ and the maximum temperature T_{max} at the center of the 87 blocks of a number of sections poured during the 1959-1962 period.

The exothermal rise in temperature at the center of the block was 20 to 30°C and on the average for 87 blocks it was 24°C . The lower limit of the maximum summer temperature (32°C) presented in Table 4-4 pertains to the block with a concrete mix cooled by adding ice to 7°C .

Table 4-4

Block	No.	$T_{c,\text{mix}}, {}^\circ \text{C}$			T_{max} of the concrete, ${}^\circ \text{C}$		
		from	to	average	from	to	average
Summer	23	11	21	18.5	32	52	15
Fall	10	5	10	16	23	47	32
Winter	14	5	14	9	25	43	32
Spring	9	5	15	9	27	42	37

The maximum temperature of the fall-winter and spring blocks was within the limits from 20 to 47°C . The high maximum temperature pertains predominately to the six-meter blocks pured in the massifs with a high concrete pouring rate. The mean temperatures which are 32 to 37°C , that is, 11-16° C less than the mean maximum summer blocks are more indicative. This is basically explained by the low temperature of the concrete mix.

The duration of the exothermal heating period of the concrete depending on the heat release rate and the time of covering the block was within the limits from 3-7 days to 1-1.5 months. The lower limit is characteristic of the uncovered blocks and the high heat release rate (A_{20}) such as for example the 30-II-22 block¹, $A_{20} = 0.868$ (Figure 4-4,a). The upper limit usually occurs for a low value A_{20} , for example, the 30-III-15 block, $A_{20} = 0.292$ (Figure 4-4,a) and the high rate of pouring concrete in the adjacent blocks with respect to height, for example, in the 45-II-14, 47-II-14 (Figure 4-5) and 30-III-7 blocks (Figure 4-4,b).

The experiment in the cooling of the concrete mix by adding crushed ice to the mix demonstrated that the effect of cooling the concrete mix in this way can reach 10 to 12°C [50].

¹Here and hereafter in the block index the first number is the section number, the second number is the column number and the third number is the concrete pouring level.

The determination of the maximum temperature in the blocks of low height is provided by pouring experimental long blocks at the construction site in the fall and winter period of 1959 to 1960 and in the summer of 1961.

For $T_{mix} = 6$ to $11^\circ C$, the rise in temperature in the blocks of sections 63 and 4 which is 1.5 meters high was 12.7 - $16^\circ C$ and 9.5 - $10^\circ C$ respectively, and the maximum temperature in these fall and winter blocks did not exceed $23^\circ C$. In the summer blocks (section 6) the concrete mix was poured with a temperature of 10 to $12^\circ C$ cooled with ice added, and the surface of the blocks after setting of the concrete was flooded with water. The maximum temperature reached $25.3^\circ C$, that is, it exceeded the given temperature by $4^\circ C$.

The decrease in the maximum temperature for the applied discontinuous flooding was $3^\circ C$.

According to the calculation, the effect of continuous flooding can be about $5^\circ C$ [38].

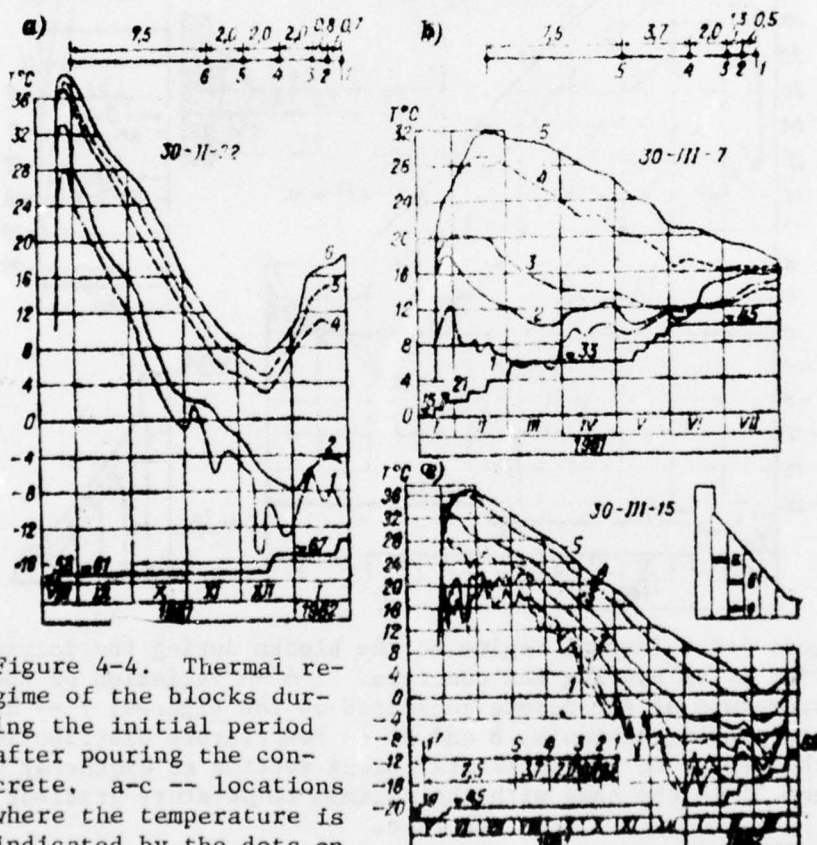


Figure 4-4. Thermal regime of the blocks during the initial period after pouring the concrete. a-c -- locations where the temperature is indicated by the dots on the diagrams were measured.

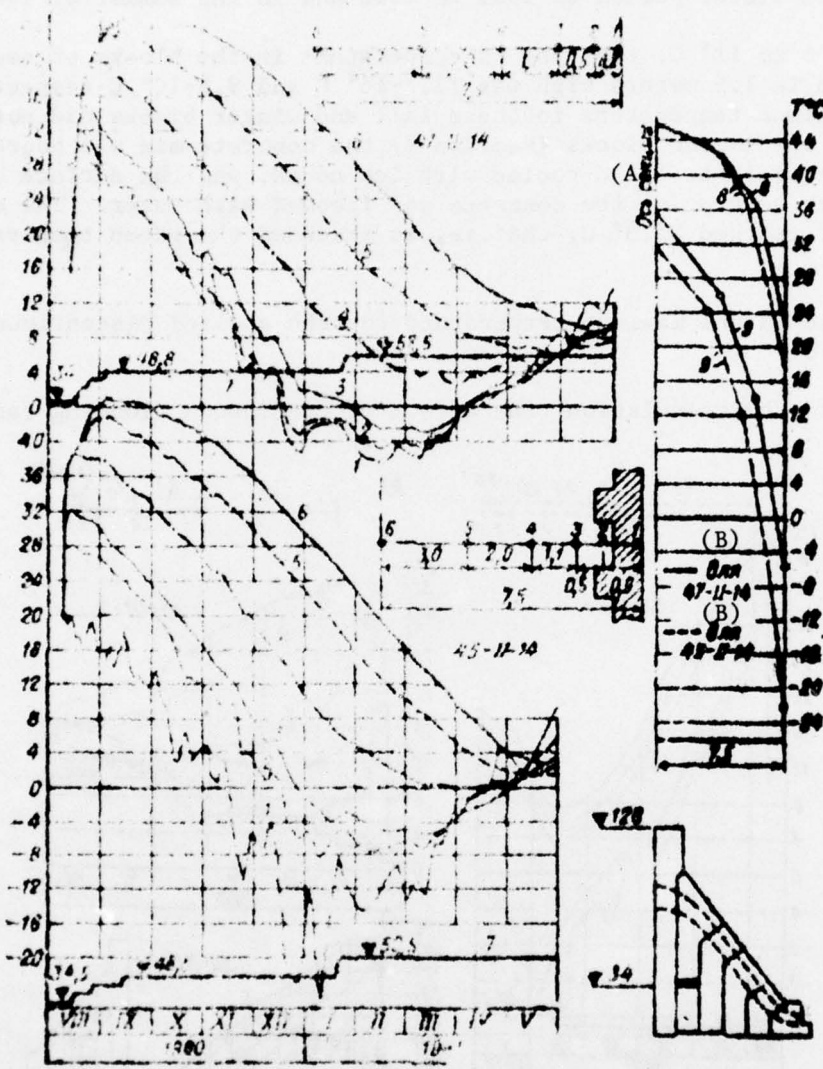


Figure 4-5. Thermal regime of the blocks during the initial period after pouring the concrete. 1-6 -- variation of the temperature at the points indicated on the figures; 7 -- concrete pouring schedule; 8 and 8' -- temperature distribution with respect to the horizontal cross section at exothermy peak; 9 and 9' -- the same with the maximum temperature gradient center to face.

Key: A. axis of the cross section B. for

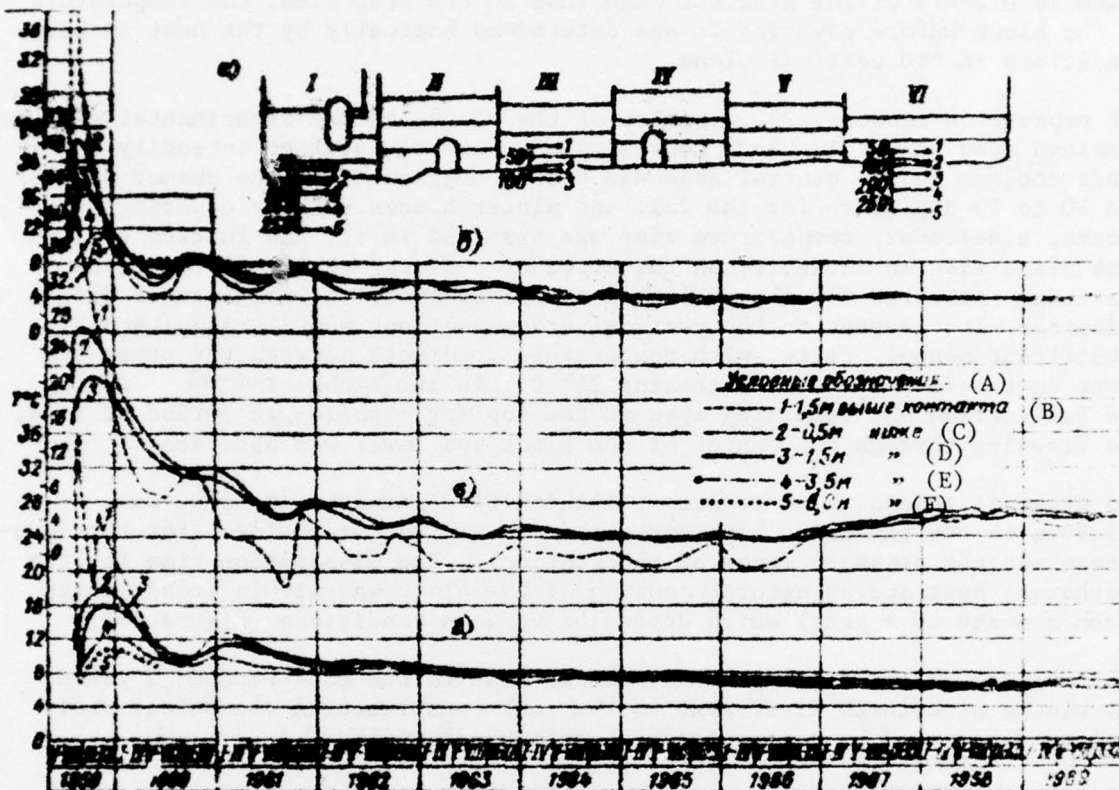


Figure 4-6. 1 -- in the center of the block next to the rock;
 I -- at the contact with the rock; 2 -- at a depth from the
 footing of 0.5 meters; 3 -- the same 1.5 meters; 4 -- the same
 3.5 meters; 5 -- the same 6 meters.

Key:

- A. provisional notation:
- B. 1-1.5 m above contact
- C. 0.5 m below the contact
- D. 1.5 meters below the contact
- E. 3.5 meters below the contact
- F. 5-6.0 meters below the contact.

The nature of heating of the rock foundation of section 51 is illustrated in Figure 4-6. The rise in temperature in the rock as the temperature rises in the center of the block next to the rock was 60 to 70% at a depth of 10-20 cm from the contact plane and 15-20% at a depth of 6 meters from it. The

shift in time from the exothermy peak in the center of the block next to the rock was 10-15 days and 4-6 months respectively.

4-5. Dissipation of Exothermal Heat

For the blocks of the Bratsk Hydroelectric Power Plant dam, the height of which is 0.2-0.4 of the greatest magnitude in the plan view, the temperature in the block before covering it was determined basically by the heat exchange conditions in the vertical plane.

For production reasons [7], a number of the blocks of the experimental sections remained open at the top to 6 months or more and the average intensity of their cooling in the central zone was 6 to 8 deg/month for the summer blocks and 10 to 15 deg/month for the fall and winter blocks. After covering the blocks, a secondary temperature rise was observed in it, and further cooling took place with an intensity on the order of 3-5 deg/month. In the blocks remaining uncovered for the prolonged period of time, the temperature distribution with respect to the vertical cross sections was distinguished by significant nonuniformity, with temperature gradients between the upper and lower surfaces of the block reaching 25° C. In the blocks poured during the fall period and remaining open at the top for a prolonged period of time, the freezing through the center of the block and lower was observed.

The greatest intensity of cooling, reaching 24 deg/month and more, was observed in the blocks at high marks open on two to three sides (for the downstream and the pressure faces of the section). The dissipation time for the exothermal heat during natural cooling of the block was within broad limits (from a month to a year) which depend on various conditions (Figure 4-7).

The duration of the cooling of the blocks next to the rock reached 2 years. The blocks of columns II-IV next to the rock constitute an exception; their cooling was caused by the presence of drainage tunnels.

It is necessary especially to discover the cooling times of the concrete to the temperature at the center of the blocks of 10° C for which in the extra-contact zone cementation of the intercolumnar joints was permitted. The concrete poured in November inclusively, reached a temperature of 10° C and lower by the beginning of the summer under the conditions of natural cooling. In the blocks poured from December to May, the concrete temperature by the beginning of the summer was within the limits 11 to 30° C and the temperature drop in them to 10° C in the summer was impossible without artificial cooling.

The pipe cooling of the concrete of the channel dam was started in the fall of 1961 and it was done predominately with river water or by cooling the brine by circulating in the pipes laid in the open air. The refrigeration unit (see §1-4) operated in 1962 and 1963 a total of 4,400 compressor hours [51].

The pipe cooling was accomplished in all sections of the dam and encompassed 1,4750,000 m³ of concrete. Before April 1962, the old concrete poured in

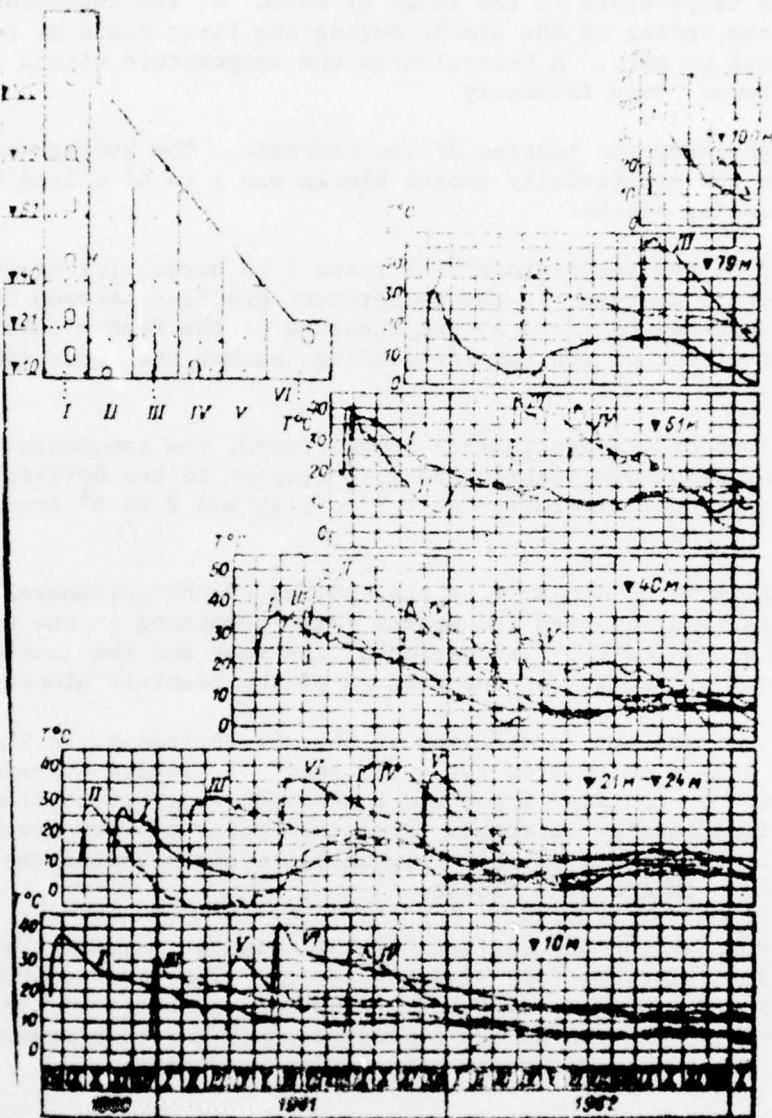


Figure 4-7. Temperature at the center of the blocks of section 30 with various marks (I-VI -- column numbers)

1960 to 1961 had cooled, and during the April-June period for 1962, the concrete one to four months old. Beginning in June 1962, the cooling was connected to the freshly poured concrete from two to three days after pouring the concrete. The massifs 30 to 40 meters high were cooled simultaneously. In the upper part of the cooled massif there were recently poured blocks with high temperature and in the lower parts, already partially cooled blocks.

The tube cooling gave the greatest effect when it was included during the period preceding the exothermy peak. The intensity of the cooling was increased with an increase in the concrete temperature with which cooling was started. At the temperature in the range of 40-50° C, the reduction in temperature at the center of the blocks during the first month of cooling was 15 to 20 deg/month or more. A reduction in the temperature within the subsequent period takes place intensely.

During the summer there was heating of the concrete. The average magnitude of the latter in the artificially cooled blocks was 1 to 4° C less than in the naturally cooling blocks.

The equalization of the temperature with respect to horizontal cross sections of the blocks with a decrease in the temperature gradient between their center and the edges established by the readings of the remote thermometers is a significant effect of the tubular cooling, except the reduction in maximum temperature.

As the observations of Gidrospetsstroy demonstrated, the temperature of the blocks with tube cooling was distributed with respect to the horizontal and vertical cross sections uniformly. At the coil it was 2 to 5° lower than between them.

In order to decrease the intensity of the cooling of the peripheral columnar massifs the Bratskgesstroy used the winter forms remaining on the surfaces of the concrete blocks to the warm period of the year and the concrete form blocks as the heat protection of the surface of the concrete blocks.

The basic effect of the heat protection is that it decreases the thermal gradient at the same time retards the development of tensile stresses during the initial period of cooling of the block when the concrete still has not acquired sufficient tensile strength. From this point of view leaving the wooden form until spring had positive significance and promoted the decrease in cracks on the surface of the blocks.

The concrete forms used on the surfaces of the columnar massifs which reach the expanded joints have the following advantages. They are constant heat protection; they decrease the total heat release as a result of their heat capacity and decrease an area of the concreted block and they remove the edge 70 cm from the region of lowest temperature gradients.

The field studies of the thermal and the thermally stressed state of the summer blocks in the warm wooden and concrete block forms were made by the author and also the Scientific Research Institute of the Orgenergostroy [19] under approximately analogous conditions ($T_{c.mix} = 20-22^\circ \text{C}$; $C = 180-250 \text{ kg/m}^3$, $q = 70-80 \text{ kcal/kg}$; the concrete pouring rate 19 meters/month). These studies demonstrated that the thermal protective properties of both types of forms are approximately identical [$k = 1.5 \text{ kcal/m}^2\text{-deg-hr}$] and are insufficient for preventing the inadmissibly large (to 35-40° C) thermal gradients from the center to the face.

Simultaneously with an increase in the temperature in the central part of the block there was dissipation of the heat from their open surfaces. Therefore, already by the peak of exothermal heating the temperature with respect to horizontal cross sections was distributed nonuniformly with the center-face thermal gradients reaching 25° C and more (Figure 4-4).

The maximum thermal gradients were usually found in the first winter after pouring the concrete; their magnitude under other equal conditions depended on the season in which the concrete was poured.

The greatest center-face thermal gradients were observed in the naturally cooled blocks from summer concrete pouring in which by December the temperature at the center was high (25-30° C), and the temperature of the surface of the block drops to -15 to 25° C (Figure 4-5).

The temperature gradients in the blocks poured in the fall and winter had lower magnitude than in the summer blocks as a result of lower temperature peak of exothermy and less heat loss through the warm form (Figure 4-4,b).

The blocks poured in the spring (April to May) were under the most favorable conditions. Along with cooling of the central region of the blocks there was heating of its edges which limited the development of the temperature gradient in the early age of the concrete (4-4,c).

In accordance with the thermal regime of the blocks, the lowest value of the center-face thermal gradient usually occurred in the August to September period, and the highest in the December to January, in the first winter after pouring the blocks. Then the temperature gradient varied periodically with amplitude, decreasing as the columnar massifs cooled. In the columns of the inside region, the thermal gradients decreased sharply after covering the expanded joints (Figure 4-8).

4-6. Variation in Time and Temperature Distribution in Concrete Massifs

During the process of building up the columnar massif with respect to height, the temperature fields of the block had a three dimensional nature caused by pouring the blocks lying above and adjacent in the plan view and also dissipation of the heat through the open surfaces. As the blocks cooled, the temperature of them was equalized; the thermal fields of the columns were transformed into two-dimensional, and within the limits of several adjacent blocks with respect to height, into one dimensional.

After completion of the period of dissipation of the exothermal heat, further variation of the temperature in the concrete massif acquired a quasistationary nature caused by the fluctuations of the ambient temperature. It is possible to calculate the temperature deviations from the mean annual value if the temperature fluctuations of the surface of the concrete massif are expressed by the function

$$T = T_{\text{mean}} + T_a \cos 2\pi t/\theta, \quad (4-2)$$

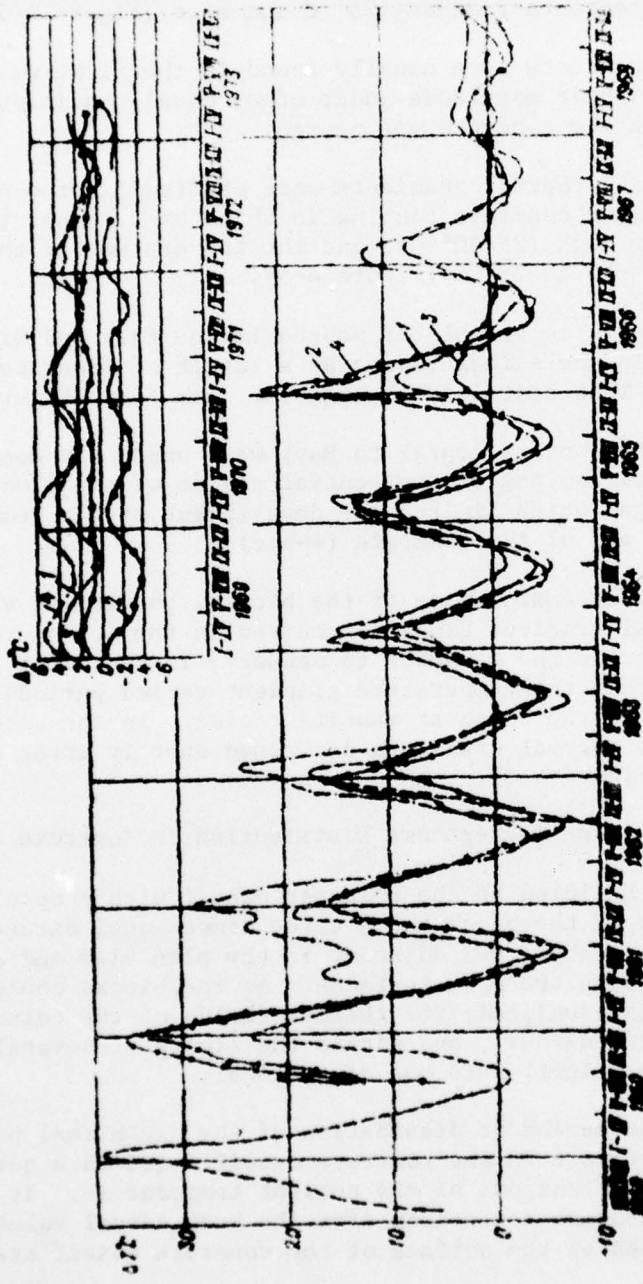


Figure 4-8. Center-face temperature gradients in the blocks. 1 -- 65-III-9;
2 -- 47-III-14; 3 -- 30-III-15; 4 -- 45-III-14.

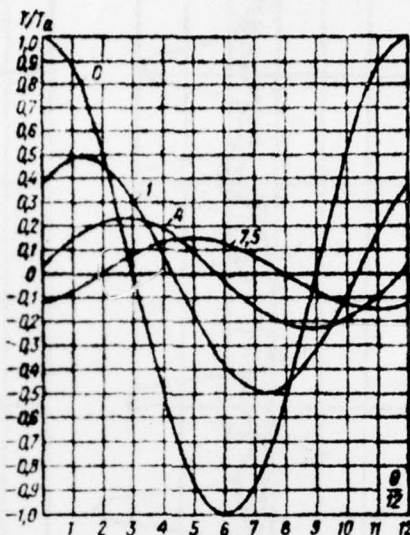


Figure 4-9. Variations of the temperature in the plate at various distances from its surface during harmonic variations in the temperature of the annual cycle environment.

where T_{mean} is the mean annual temperature; T_a is the amplitude of the annual fluctuations; θ is the temperature fluctuation period, years; t is the time, months.

For harmonic variations in the annual cycle temperature on one side of the concrete slab with thickness l under the conditions of the one-dimensional problem and first type boundary conditions, the temperature at a point a distance x from the surface at any point in time t will be determined [52] from the function:

$$T(x, t) = T_a \frac{1}{A^2 + B^2} \left[(AC_x + BD_x) \cos \frac{2\pi t}{\theta} - (AD_x - BC_x) \sin \frac{2\pi t}{\theta} \right]. \quad (4-3)$$

where $A = \sinh kl \cos kl$; $C_x = \sinh k(l-x) \cos k(l-x)$;
 $B = \cosh kl \cos kl$; $D_x = \cosh k(l-x) \sinh k(l-x)$;

$$k = \sqrt{\frac{\pi^2}{\alpha \theta}}. \quad (4-4)$$

Setting the coefficient of thermal conductivity $\alpha = 0.003 \text{ m}^2/\text{hr}$, $\theta = 8760 \text{ hours}$, we obtain $k = 0.346$.

The relative values of $T(x, t)$ for $T_a = 1$ and $l = 15 \text{ meters}$, for harmonic variations of the temperature of the environment on both sides of the slab [19] shown in Figure 4-9.

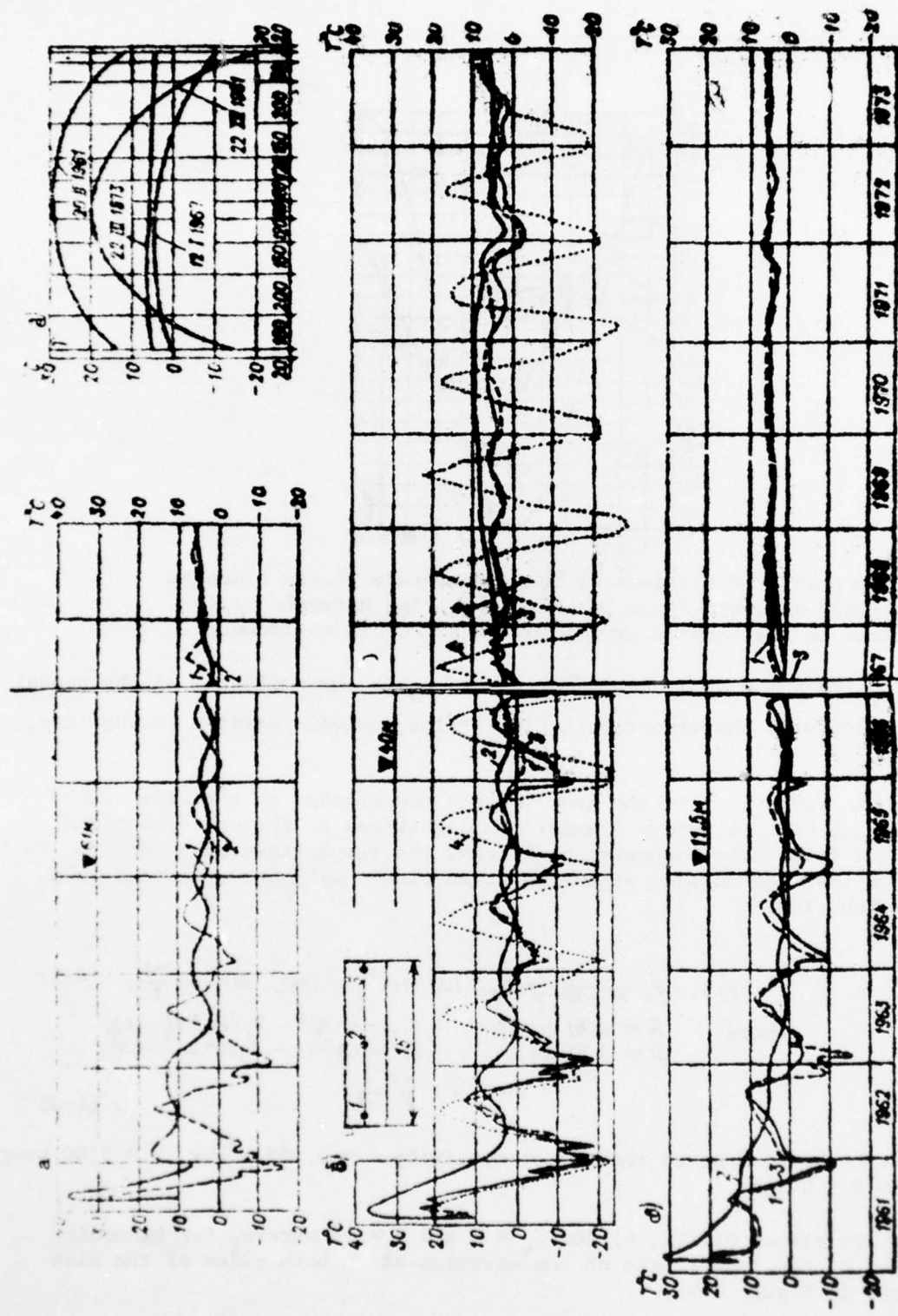


Figure 4-10. Thermal regime of the blocks of III column of section 30: a, b — [deleted] marks; c — temperature distribution along the horizontal axis of the block [illegible] 22 meters. 1 and 3 — edges; 2 — center of the bloc; 4 — mean annual air temperature.

The actual temperature variation in the columnar massifs were determined by the different temperature of the environment and its stratification at the massif boundaries.

The temperature of the first column in the construction period was caused by the effect of the air temperature on the open pressure face, the water temperature of the reservoir, the level of which rose to the normal backwater level in 6 years and also the air temperature in the expanded joints. As a result of the heat exchange with the reservoir water, the heat flux was directed in the winter in the direction of the water and in the summer in the direction of the dam. During the periods of uniform temperature distribution of the water with respect to depth of the reservoir, the lower part of the pressure face was heated by the water and its upper part was cooled. Accordingly, the thermal regime of the first columns remained for a number of years nonsteady state, and the temperature distribution remained nonuniform. Thus, for example, the annual difference in the temperature variations of the concrete on the pressure face of section 30 in 1964 varied with respect to the height of the first column from 1.9° C in the block next to the rock to 38° C at the base of the head. The temperature fluctuations at the center of the blocks and in the intercolumnar joint I-II were insignificant in the lower part of the profile and they reached to $10-12^{\circ}\text{ C}$ in the upper part.

At the temperature of the blocks of the first column at the intercolumnar joint I-II was influenced by the openings in communication with outside air (the sections with the elevator shafts and the stairwells) and also the inspection tunnels. In the latter, as a result of the numerous exit to the expanded joints, the vertical drain pipes, the indicated vertical shafts, intensive ventilation occurred during the construction period. In combination with the steam heating of the tunnels during the winter, this created a nonuniform thermal regime in them with respect to length and variable in time with large seasonal fluctuations of the temperature and negative values to $-(10-15)^{\circ}\text{ C}$.

The thermal regime of the columns of the inside region was connected with the variation of the air temperature in the expanded joints.

During the construction period in the blocks there were periodic temperature fluctuations with gradually decreasing amplitude (see Figure 4-10,a,b,c). The maximum and minimum temperature on the lateral surface of the columns was observed respectively at the end of the summer (August-September) and at the end of the winter (January to March). In the central part of the column the maximum temperature was observed in the winter (November to January), and the minimum in the summer (June to August). The temperature distribution in the longitudinal direction was close to uniform in May to June and September to October, and in the remaining times of the year it had a parabolic nature (Figure 4-10,d).

From the end of 1964, as a result of the presence of more or less open expanded joint along the one side of each section and the expanded joint covered by the plan on the other side, in the columnar massifs of the inside region of the dam the highly characteristic temperature regime was created

with asymmetric temperature distribution. On the edges of the columns of both sides of the sections, in the winter a temperature difference to 10-12°C was observed.

The annual difference in the maximum and minimum temperatures of the surface of the columnar massifs reaching 30 to 35° in 1962 decreased significantly; however in 1964 and 1965 at the edges of the columns which exit to the partially open expanded joints, this difference reached 20 to 25° C.

4-7. Freezing of the Dam Sections

A characteristic feature of the thermal state of the dam sections during construction and temporary operation was the mass freezing of the columnar massifs caused by the propagation of the heated temperature from their surfaces emerging in the expanded joint.

From the end of 1961 the thermal condition of the sections was determined by the variable temperature regime of the reservoir water during the process of filling it, the air temperature in the cavities of the joints and the build-up of height of the columns.

The thermal field of the sections was made up of two zones. In the lower zone the process of the dissipation of the exothermal heat basically ended, and the temperature variations in it were determined by the seasonal fluctuations of the ambient temperature. The local temperature fields formed around the recently poured blocks were adjacent to the formed temperature field of this zone.

The small freezing regions formed during the first years of construction at the surfaces of the columns emerging in the standard joints spread deeper as the average column temperature dropped, and in the winter of 1961 to 1962 in the lower part of the column (to a height on the order of 17-20 meters) they reached the axial cross section of the sections. As the exothermal heat dissipates in the upper part of the columns of the concrete zone frozen to the entire thickness of the section, it rose higher with each year (Figure 4-11,b) encompassing up to 35% of the area of the axial transverse cross section of the sections.

The negative temperature began to spread from the edge of the blocks in November and reached the axial cross section of the sections after five to seven months. The spread of the positive temperature began at the edge of the sections from May to June and reached the axis of the cross sections after 3 to 4 months (see Figure 4-12).

The concrete in the peripheral region of the section remained in the frozen state with a minimum temperature to -(20-26)° C to 8 months. The negative temperature in the axial region of the section remained for 3 to 6 months and in the majority of cases it did not drop below -(1-2)° C (Figure 4-12).

AD-A039 541 COLD REGIONS RESEARCH AND ENGINEERING LAB HANOVER N H F/G 13/13
FIELD STUDIES OF THE CONCRETE DAM AT THE BRATSK HYDROELECTRIC P--ETC(U)
APR 77 S Y EIDELMAN

UNCLASSIFIED

CRREL-TL-621

NL

2 of 4
AD
A039541



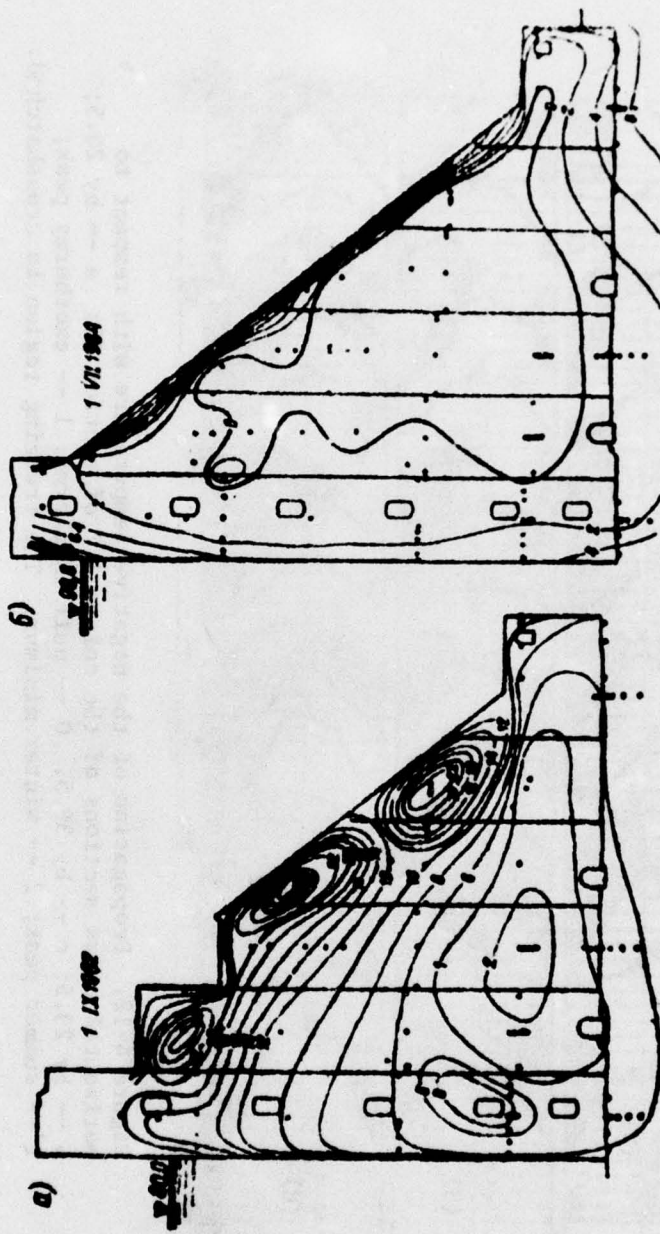


Figure 4-11. Isotherms with respect to the axial transverse cross section of section 63.

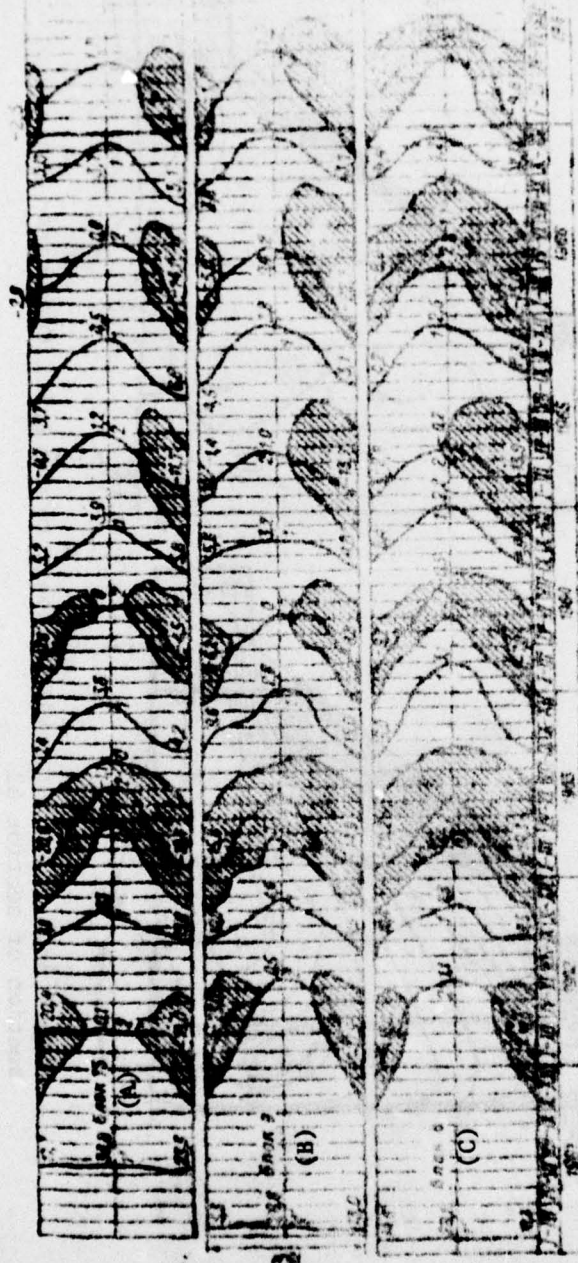


Figure 4-12. Propagation of the negative temperature with respect to horizontal cross sections of the column III of section 30: a -- by 20.5; b -- by 23.5; c -- by 38.5. 0 -- null isotherms; 1 -- exothermy peak; 1' -- summer peak; 2 -- winter minimum. The freezing region is crosshatched.

Key: A. block 15 B. block 9 C. block 8

The propagation picture of the regions of the frozen concrete with respect to the horizontal cross sections of the section presented in Figure 4-12 is quite general for all sections of the channel concrete.

After the temporary covering of the expanded joints by the winter of 1963 to 1964, the minimum temperature on the lateral surfaces of the columns rose (Figure 4-10, 4-11), but it still remained low (to -10° C) and by the end of this winter the volume of frozen concrete in the dam was about 1,300,000 m^3 [51].

As was noted above, in 1965 and 1966 the temperature regime of the air in the cavities of the expanded joints was very unstable; the regions of freezing in the sections increased, and in others they decreased. On one May 1966 these regions encompassed columns I, III and IV of all sections of the channel part of the dam to the height from the base to 40 meters. During the seasonal maximum the concrete temperature in the axial cross sections of the sections was 2 to 4° C in the lower part of the dam and $4\text{-}6^{\circ}\text{ C}$ in the upper part.

4-8. Thermal Regime of the Dam During Permanent Operation of the Hydroelectric Power Plant

After covering the expanded joints and filling them with water to the tailrace level, the air temperature regime in the cavities of the joint is determined by the heat transfer through the covering slab (2.5 meters thick) and the water temperature in the lower part of the cavities.

As is obvious from Figure 4-13,a, the temperature on the inside surface of the slab fluctuates during the year within the limits from $7\text{-}8^{\circ}\text{ C}$ to $-(2\text{-}4)^{\circ}\text{ C}$. The water temperature changes little and is $3\text{-}5^{\circ}\text{ C}$.

The effect of the covering of the expanded joints was felt during the first winter even to flooding of the joints. Thus, for example, the joint 50-55 was covered in the fall of 1966 and in the winter of 1966 to 1967 the temperature in it was positive and was compared with the temperature in the previously covered (in the cover of 1965) joint 51-52. This was felt in the temperature of the concrete of section 51. The asymmetric distribution of the temperature with respect to longitudinal cross section with significant negative temperature on the side of the partially covered joint occurring in the winter of 1965-1966 was not observed in the winter of 1966 to 1967. In section 30 with the depression in the cover, the nature of the temperature distribution in the winter of 1966 to 1967 did not change by comparison with the preceding winter and only after covering the opening (in May 1967) did the temperature become positive on both sides of the section (see Figure 4-3).

The covering of the expanded joints of the summer and their flooding increased the temperature in the columns of the internal region of the dam and eliminated the freezing phenomena in them. In the period from April to December 1968, the expanded joints were dried out; however in this year in the axial transverse cross sections of the sections, the temperature of 4° C predominated at the end of the winter and 6° C at the end of the summer. In the

contact zone of the rock base a temperature of 3.5-4° C was established. Under the sixth columns of the station part of the dam the temperature was 2 to 3° C higher than the corresponding temperature at the remaining part of the dam (see Figure 4-6).

The phenomenon of the freezing of the concrete is observed annually in a region 8 to 10 meters wide adjacent to the lower face of the section (Figure 4-13, b).

It is appropriate to note that the establishment of the joints of a positive operating temperature of 2-3° C turned out to have low probability. Inasmuch as the thickness of the covering (2.5 meters) is less than the depth of freezing of the concrete it was proposed that in the expanded joints a one-way convection regime was established where the air cools by the lower surface of the covering will drop down in the winter with the formation of the stagnant negative temperature zone as result of which the flooded of the expanded joints becomes impossible. The Bratskgesstroy has proposed the establishment within the expanded joints of a permanent operating heating of 2,000 kilowatts [51]. These proposals turned out to be unfounded inasmuch as the great effect of the presence of ice in the lower part of the joint cavities on the air temperature in them was not taken into account.

In accordance with the calculation considering the main values of the outside air temperature over many years, the main integral temperature of the latter in the closed cavities of the expanded joints remains negative for 10 months per year. However, in the presence of water with a temperature of 5° C in the lower part of these cavities the main integral air temperature in them varies periodically (Table 4-5) within the limits from 2.7° C (February) to 5.2° C (August).

Table 4-5

Calculation conditions	Mean integral air temperature in joints, °C												Mean annual
	V	VI	VII	VIII	IX	X	XI	XII	I	II	III	IV	
Without water	-2.3	-1.3	-0.4	0.1	0.2	-0.2	-1.0	-1.0	-2.0	-4.5	-4.0	-4.0	-1.0
During first year after flooding													
With water at T=5°C	4.4	4.0	3.3	2.1	1.3	0.8	0.3	0.0	0.0	0.0	0.0	0.0	4.4
Steady state													
The same	3.8	4.1	4.0	3.2	2.1	1.0	0.1	-0.1	-0.5	-0.5	-0.5	-0.5	3.8

The 32 electric heating units with a total power of 49 kilowatts installed in the longitudinal and transverse tunnels of the dam during the period from 1968 to the middle of 1970 had some effect on the air temperature in the expanded joints. The purpose of them was to improve the conditions of taking readings by the instruments and prevent corrosion of the contacts of the commutation panels. After connecting the instruments to the central remote

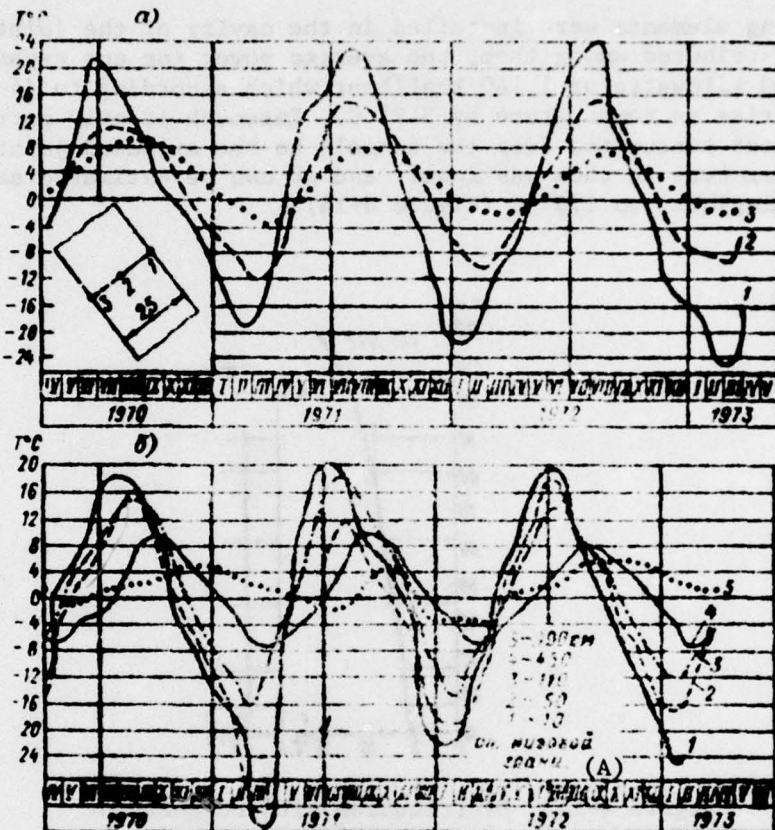


Figure 4-13. Concrete temperature on the downstream face of the section: a -- in the covering of the expanded joints; b -- in the monolithic concrete.

Key: A. from the downstream face

panel these devices were disconnected for the period from March to October 1972, and they remained only in the tunnels at the upper marks. The electric heating of the individual tunnels and the elevator shaft continued also thereafter.

In accordance with the calculation of [53], the mean annual steady state temperature in the joints in the presence of heating elements in them will be

$$T_{\text{mean}} = (-1.6 + 0.00323S), ^\circ \text{C}, \quad (4-5)$$

where -1.6°C is the mean annual air temperature in the joints in the absence of water in them; S is the power of the heating units in kcal/hour.

If the heating elements were installed in the cavity of the joints and are uniformly distributed among them, the average power for one expanded joint would be 1.33 kilowatts or 1,140 kcal/hour which according to (4-5) corresponds to a rise in temperature by 3.7°C . Inasmuch as only part of the additional heat penetrated from the tunnels to the expanded joints, the rise in temperature in them was lower, and it can be estimated as on the order of [illegible] to 1.5°C (Figure 4-14).

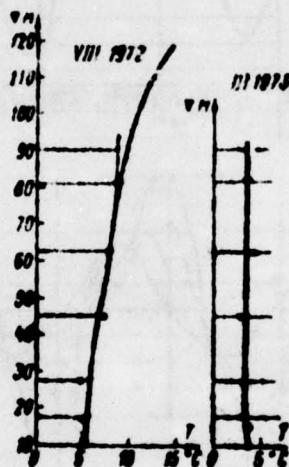


Figure 4-14. Distribution with respect to height of the expanded joint of the mean (for 6 cavities) air temperature. The light dots are the temperature in the section tunnel.

It must be noted that according to (4-5) in order to prevent the freezing of the columns of the inside region it is necessary to place the heating elements with a total power of about 2.0 kilowatts in the cavity of each expanded joint (in the absence of water in it).

During the period of permanent operation of the hydroelectric power plant, the air temperature in the expanded joints varies seasonally with variable amplitude with respect to height. During the summer maximum of 1972, the mean temperature for the cavities of the 6 expanded joints increases from bottom to top, and in the period of the winter minimum, it is distributed approximately uniformly, amounting to 3.2°C which is 0.5°C greater than the above indicated minimum mean integral temperature. As is obvious from Figure 4-14, the air temperature in the longitudinal tunnels of the dam is close to the air temperature in the expanded joints.

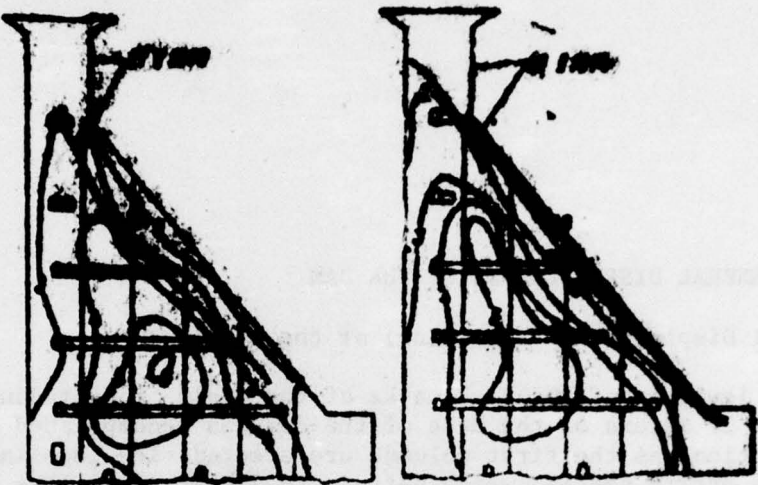


Figure 4-15. Isotherms with respect to the axial transverse cross section of section 65.

The constant heating of the longitudinal tunnels in the first columns of all sections and also a number of transverse tunnels increased the temperature of the concrete in the dam blocks bordering with these tunnels by 2 to 4° C by comparison with the blocks of the unheated sections. The heating of the tunnels was felt also on the temperature in the blocks of the first columns in which, in spite of the gradual cooling of the reservoir water, the increase in temperature was observed (Table 4-6). The thermal condition of one of the sections (65) closest to the steady state condition, is shown in Figure 4-15.

Table 4-6

Cross section mark, meters	Mean annual temperature at center of cross section, ° C										
	1963	1964	1965	1966	1967	1968	1969	1970	1971	1972	1973
11.5	4.7	4.6	4.1	3.4	3.6	4.0	—	—	—	—	3.9
25.5	5.2	3.4	3.6	2.9	3.7	4.2	5.7	5.3	4.3	4.8	4.9
40.5	4.7	3.6	3.1	3.3	4.0	4.9	5.7	5.7	5.2	5.2	5.5
61.5	6.1	4.3	3.5	3.5	4.7	5.8	6.0	5.9	5.7	5.7	6.2
79.5	5.6	5.4	5.0	4.7	5.3	6.8	7.2	7.8	6.8	6.8	6.2
100	8.8	6.1	5.6	5.1	5.1	6.3	6.2	6.5	5.8	6.1	6.7

CHAPTER 5. GENERAL DISPLACEMENTS OF THE DAM

5-1. Vertical Displacements (Settling) of the Sections

The precision leveling of the high marks of the basic longitudinal sections at a height of 17 meters of the base of the dam was accomplished by the successive sections as the first columns are erected. The leveling data with respect to the entire section which pertain to January 1961 were taken as the provisional beginning of the height observations.

At the beginning of filling of the reservoir with a specific vertical load of the base of about 6 kg-force/cm^2 the settling of the first columns was 7 to 8 mm and it increased sharply as the headwater level rose (Figure 5-1).

The calculation of the settling was made beginning with the solution of the Boussinesque problem for a layered halfspace [54]. The base was assumed two-layer with the following elasticity characteristics: for the diabases $E = 9 \cdot 10^5 \text{ kg-force/cm}^2$; $v = 0.28-0.3$, and for the sandstones $E = 9 \cdot 10^4 \text{ kg-force/cm}^2$, $v = 0.35$. The distribution of the normal and the central stresses with respect to the footing of the dam was assumed linear. The mass of the reservoir water was not taken into account inasmuch as by assignment, the layers of the base were considered in the suspended state. The settling of the dam for a normal backwater level was calculated as 37 mm.

The measured settling increases from the banks of the channel to its middle, reaching a maximum under the 53 located above the zone of increased water permeability of the diabases and sandstones. The difference in the settling of the adjacent sections does not exceed 1-2 mm; the nonuniformity of the settling of the sections in the direction of the longitudinal axis of the dam has the greatest value, approximately 2 mm for the extreme shore sections. The left bank sections are inclined in the direction of the right bank, and the right bank sections, in the direction of the left bank [55, 56] (Figure 5-2).

The most intensive growth of the settling occurred during the first month of the filling of the reservoir (Figure 5-3, a); later the intensity of the settling diminished. The settling of the sections in the middle part of the channel built up more rapidly than the shore part. The actual settling

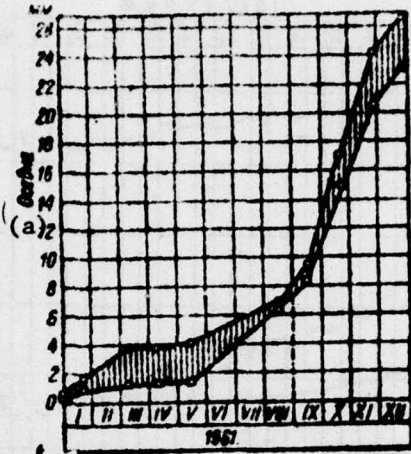


Figure 5-1. Limiting values of the settling (bending) of the sections 41, 46-49 and 51.

Key: a. settling

exceeded the calculated value in 1962 when the first columns were erected only to 75% of their full height, and the headwater level was 40 meters below the normal backwater level. This basically is explained by the settling of the bed of the reservoir under the effect of the mass of water filling it not taken into account in the calculation [19]. The settling of the bed of the reservoir and surrounding territory was fixed by natural observations and a series of dams [57-59].

In the vicinity of the part of the reservoir of the Bratsk Hydroelectric Power Plant next to the dam, 62 ground reference markers were installed. By the Class II leveling performed since May 1962 twice a year, it was established that the settling funnel extends 2-3 km in the direction away from the reservoir.

Already in the early stage of the observations (1963) we established the clear relation between the settling increment and the buildup of the water level [61, 62]. Beginning with the water level mark of 57 meters, between the settling of the increase in level (pressure) there is a relation which is close to linear ($2'.3''$) giving the increase in the settling by 1 meter increments of the headwater level within the limits approximately from 0.5 mm for the shore section to 0.85 mm for the channel sections (see Figure 5-3,a) [63].

For section 53 under which the maximum settling is observed, the magnitude of the latter is expressed by the formula

$$\Delta v = 17 + 0.85(H - 57),$$

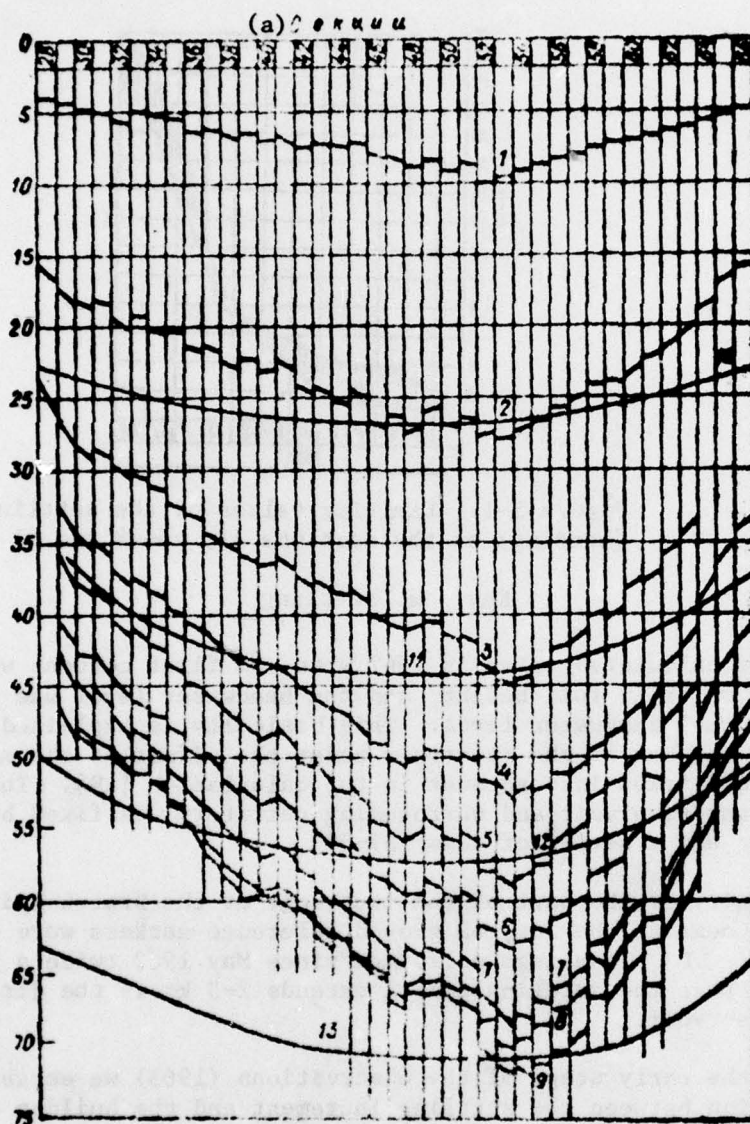


Figure 5-2. Settling diagrams for the channel dam. 1 -- September 1964; 2, 3, 4, 5, 6, -- January 1962, 1963, 1964, 1965 and 1966; 7 -- December 1966; 8 -- January 1968; 9 -- July 1968; 10 -- calculated diagram for January 1962; 11 -- the same for September 1963; 12 -- the same for September 1965; 13 -- the same for the normal backwater level.

Key: a. sections

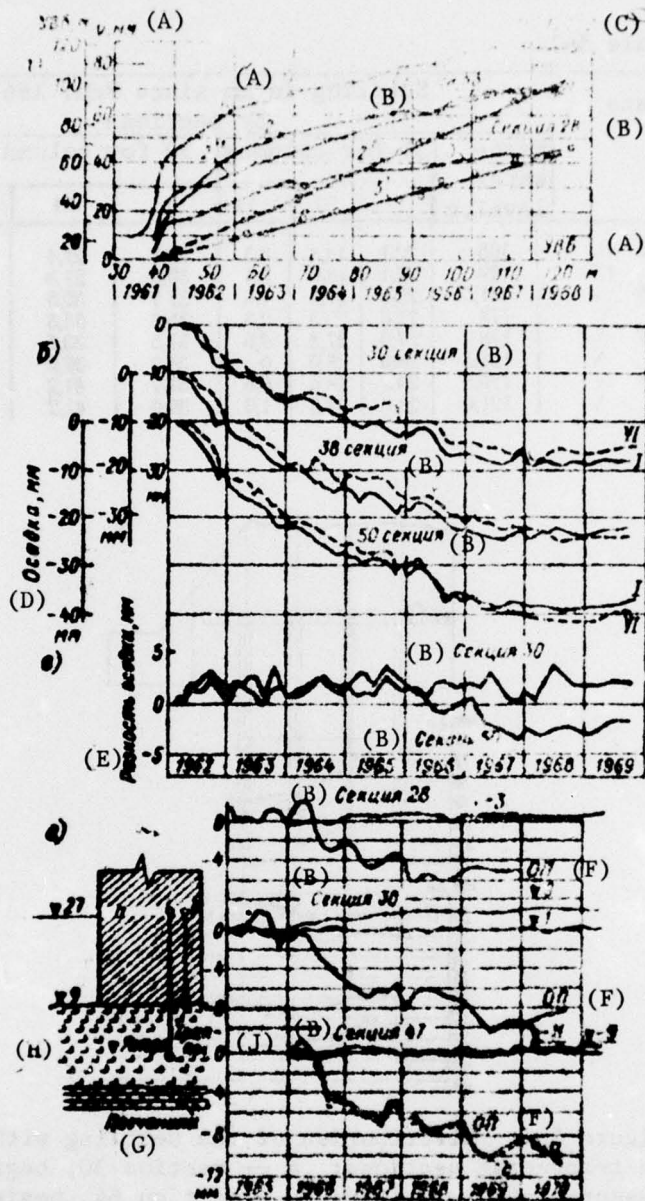


Figure 5-3. Settling of the channel dam; a -- buildup of the settling (2 and 3) and its dependence (2' and 3') on the headwater level (λ); 2' -- calculated settling of the section 53; b -- settling of the first (I) and sixth (VI) columns; c -- difference in settling of the first and sixth columns; d -- settling of the base of the dam and vertical deformation of the diabases to the mark indicated on the charts (a and b) -- altitude marks).

Key: A. headwater level, m B. section C. normal backwater level
 D. settling, mm E. difference in settling, mm F. dam base
 G. sandstones H. anchors J. traprock

Table 5-1

Date	Head-water level, m	Settling in mm since Feb. 1962 by sections					
		31 for columns			50 for columns		
		I	VI	I-VI	I	VI	I-VI
1965	105	22.1	18.8	3.3	29.5	28.4	1.1
	109	22.1	18.0	3.4	30.2	27.3	2.9
1966	111.5	22.6	21.0	1.6	31.1	30.6	0.5
	118	27.6	25.3	2.3	35.3	35.8	-0.5
1967	118	27.9	27.3	0.6	37.5	39.6	-2.1
	121.5	28.0	24.0	0	38.9	39.6	-2.7
1968	120.5	29.2	28.6	0.6	37.7	41.2	-3.5
	121.0	28.8	27.8	1.0	39.0	41.2	-2.2

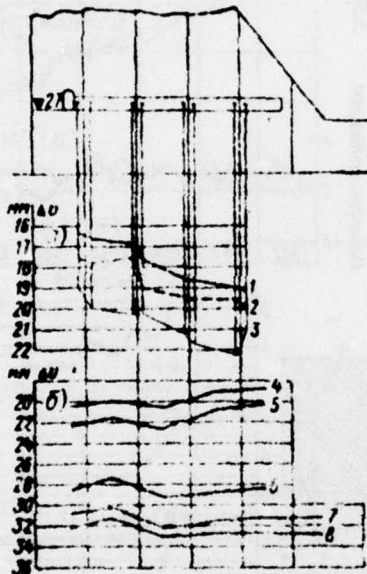


Figure 5-4. Distribution of the settling with respect to transverse sections: a -- section 30, beginning of measurements July 1963; b -- section 64, beginning of measurements [illegible] 1962. 1 -- December 1967; 2 -- October 1968; 3 -- January 1970; 4 -- August 1964; 5 -- November 1964; 6 -- November 1966; 7 -- October 1967; 8 -- October 1968.

which for normal backwater level ($H = 133$ m) gives settling on the order of 72 mm.

Inasmuch as the settling was primarily caused by the mass of water in the reservoir, a gradual slope of the sections in the headwater direction was

observed, the magnitude of which varied with time with some similarity to the surface (Figure 5-3,h,c). The slope in the direction of the headwater increased in the warm part of the year and decreased in the cold part. The difference in the settling in the first and sixth columns at the end of 1964 on the average for sections 28-5 [deleted, may be anything from 50 to 59] was about 5 mm. After 1966 intensive buildup of the settling of the sixth columns was observed (see table 5-1) as a result of the effect of the bending moment from the hydrostatic load with high headwater level. This is confirmed by the data from leveling the marks in the transverse tunnels of dam which, in addition, also indicate that the settling of the adjacent columns of the section is different. The difference in settling reaches 1 to 1.5 (Figure 5-4).

Table 5-2

Date	Head-water level	Settling of the sections, mm								
		28	36	46	47	51	52	61	65	
1962		67.4	17.1	18.5	23.1	26.2	26.4	27.7	21.9	16.5
1963		87.3	26.3	28.7	36.4	40.8	42.6	44.7	37.1	32.0
1964		95.6	32.5	35.1	43.9	50.1	49.9	53.2	45.9	35.5
1965		102.9	36.0	38.2	48.5	55.5	55.5	58.7	51.1	40.9
1966		110.0	40.1	42.6	53.0	59.4	59.8	65.2	56.6	43.0
1967		117.9	43.5	43.5	57.5	64.3	64.8	68.8	62.0	48.1
1968	VII	120.7	46.0	48.4	59.6	67.3	67.4	71.8	66.7	52.7
1969		119.5	45.1	47.1	58.2	65.4	65.8	69.7	63.1	49.6

Increasing proportionally to the headwater level, settling of the dam had reached a maximum for normal backwater level. The measured maximum settling was observed in the summer of 1968 for the headwater level of 121.5 meters (see Table 5-2) and for the channel sections it was 71.8 mm (section 53), and for the shore sections 46 mm (section 28) and 51.1 mm (section 66).

In all up to September 1973, 95 precise leveling cycles have been executed. During the last 10 cycles (from July 1968) the settling varied by 1-3 mm both in the direction of a decrease and an increase. These variations, which correspond to the magnitude of the use of the reservoir are explained by the errors from the measurement and calculation of the altitude position of the marks.

For a length of the basic leveling stroke between the foundation reference marks $\Phi 3$ and $\Phi 6$ (Figure 2-2) equal to 4.6 km, the admissible error in the forward and return courses is about ± 3.5 mm. Although the actual error was lower than the admissible error, the mean square error in determining the mark reached $\pm (0.75 \text{ to } 1.75)$ mm, and the error in calculating the settling reached $\pm (1.1 \text{ to } 2.5)$ mm [20]. It is also necessary to note the variation in the excess of the reference marks $\Phi 3$ and $\Phi 6$ in 1969.

Beginning in 1972, the leveling procedure was adopted which significantly raises its precision (the permanent spikes for the reference marks, two independent operating brigades, the readings for two levels of the instrument

with respect the basic and auxiliary scales, and so on). However, under these conditions the variations in the settling between observation cycles were commensurate with the errors in the latter and in this way the settling of the dam can be considered stabilized within the limits of the measurement precision.

The settling of the hydroelectric power plant building during the entire observation period is less than the settling of the dam in the corresponding time intervals coinciding with it with respect to nature.

Interesting results are obtained from comparing the settling measured by the first columns in the tunnel at a height of 17 meters above the base with the vertical variations with respect to an invar thread of the return plumbs in the first level. The anchors for the return plumbs are buried to 20 meters in the diabases, and the head is located in the same tunnel. The settling increments reached 10 to 12 mm, and the increments of the vertical deformations are insignificant and are obviously connected with the variations in temperature of the concrete column 17 meters high (Figure 3-3, d). From this it follows that the settling of the dam is caused by compression of the sandstones underlying the diabases.

The calculation of the settling of the dam was also performed considering the mass of water in the reservoir with a modulus of deformation of the dia-base variable with respect to depth [see (1-1) and (1-1')] and the deforma-tion modulus of the sandstones determined beginning with the actual settling. The magnitude and distribution, of the settling calculated under these con-ditions [64] are illustrated in Figure 5-2.

5-2. Horizontal Displacements of the Dam Sections

The basic factors determining the horizontal displacements of the high con-crete gravity dam are, as is known, variations of its temperature, hydro-static pressure of the water in the dam, nonuniform settling of the base and irreversible deformations of the body of the dam and its base which are a function of time.

The first of these factors causes many of the sections, the magnitude in the direction of which depends on the nature of distribution of the temperature with respect to the horizontal cross sections. The second factor causes dis-placement of the shift and also bending in the direction of the tailrace, increasing with an increase in the head. The second factor, which depends on the deformability of the base causes rotation of them in the direction of the greater shift. The fourth factor causes rotation in the direction of the tailrace caused by the cooling of the body of the dam, creep of the concrete, closure of the joints and cracks, and so on.

The measurements performed for establishing the picture of the plan-view shifts of the dam at the Bratsk Hydroelectric Power Plant are enumerated in the second chapter. A set of these measurements had to offer the possibility of establishing the plan view shifts of the dam at the 27 meter mark and with

respect to the shores and base and also the nature bending of the profile from this mark to the crest. The measurements by the return plumbs of the first stage permits determination of the joint operation of the dam with the base had to be especially significant.

After a number of years of observations it is necessary to recognize the section-optical method of measuring the absolute horizontal displacements turned out to be unsuitable for the Bratsk dam. The steam heating of the tunnels during the winter and the poorly closed exits to be expanded joints in each section created a sharply nonuniform temperature distribution in the tunnel with large gradients in the longitudinal and transverse directions, a consequence of which was the significant convective air currents. The refraction phenomena when working on the section and the poor visibility were the cause of large systematic errors commensurate with the displacements determined during the construction period.

The picture of the horizontal displacements of the dam sections obtained by the results of the section-optical observations is represented in qualitative respects as quite justifiable. Along with the small periodic displacements in the direction of the tailrace and headwater, the presence of irreversible¹ displacements in the direction of the tailrace was established. The mean magnitude of these displacements in 1968 (considering from the beginning of the section observations in July 1962) increased from 1 mm in sections 28 and 66 to 8 mm in sections 47, 48.

During the normal operation of the hydroelectric power plant, the dimensions in the tunnel by comparison with the construction period were favorable. According to the reckoning of the Irkutsk Polytechnical Institute, for two measurement cycles in April 1972, the air temperature in the tunnel was 5.6°C with deviations along the length of the section (850 meters) of no more than 1° C. However, in the tunnel air flows were noted with a velocity on the order of 0.1 m/sec which created unfavorable conditions for the optical observations. The images were oscillatory and constantly changed shape. The results of the section observations turned out to be an order greater and with a different sign by comparison with the corresponding displacement with respect to the return plumbs.

The string-optical observations were started in March 1971, and to March 1974 seven cycles of these observations were performed.

The dam sections are displaced from string section in the direction of tailrace during the cold part of the year and the opposite direction in the warm part of the year. The magnitude of the seasonal displacements does not exceed 0.5 mm. The observations on the return plumbs of the first stage indicate that the end signs of the section also are shifted with respect to

¹Here and below we shall call the displacements irreversible which are caused by a rise in the headwater level to the mark of maximum drawdown of the reservoir -- 116 meters.

the anchors of the return plumbs. The displacements of the sections with respect to these anchors in the direction of the tailrace for March 1971 are approximately 1.5 mm.

From a comparison of the horizontal displacements in the period from March to November 1971 measured by three methods (Table 5-3) it is obvious that the results of the observations on the string-optical section are commensurate with the readings of the return plumbs and differ somewhat from the displacements measured by the section-optical method. The corrections as a result of the displacement of the end signs of the string section exceed the deviations of the sections from the section. The results of the creative observations depend on the observation precision on the return plumbs.

The optical and string observations are performed on the same wall signs. Therefore the difference in the deviations from the section and by the simultaneously performed observations using both methods, can be adopted as the correction to the displacements measured by the optical method from the beginning of the measurements. For the sections 37, 47 and 57, this difference in 47 cycles (March 1971) was 4.9, 5.1 and 5.2 m respectively. The greatest absolute horizontal displacements in the direction of the tailrace at a height of 17 meters above the base of the dam calculated considering this correction for 9 years of observations were about 4 mm (see Table 5-3).

Table 5-3

Cycle	Measure- ment me- thod	Displacement of the sections, mm				
		28	37	47	57	66
46-47	Optical	0.0	1.1+(0.2)	-2.1+(0.5)	-0.9+(0.7)	0.9
	String	0.0	0.4+(0.2)	0.2+(0.5)	0.1+(0.7)	0.9
	Return plumbs	0.0	0.5	0.4	0.4	0.9
47-1	Optical	1.5	6+(0.6)	9.2-(0.2)	4.9-(1)	-1.9
	String	1.5	1.1+(0.6)	4.1-(0.2)	0.3-(1)	-1.9

Note. In parentheses we see the corrections for the displacement of the ends of the section.

The observations on the return (floating) plumbs (just as the section-optical observations) were performed to 1970 by the Angara Expedition of the Gidroprojekt Institute. The installation, mastery and adjustment of the return plumbs performed under the conditions of Bratsk for 5 years (1962 to 1966) were connected with significant difficulties, and a set of discontinuities lasting from 1 to 5 months were observed in their observation. For the plumbs in the first stage the majority of these difficulties were caused by penetration of the water into the protective tube (which must be dry) and condensation of moisture in the float pools above the unfrozen liquid. The freezing of the water interfered with the operation of the plumb and caused discontinuous variations in the measured displacement. Therefore, it was not possible to establish a continuous picture of the variations from the beginning of the observations.

During the years of normal operation of the dam the displacements measured on the return plumbs of the first stage became more stable, especially after revision and repair of the plumbs performed by the hydraulic shop in 1970-1971. The actual precision of the readings obviously remains below the rated value (0.05 mm), and it can be estimated as on the order of \pm (0.1-0.2) mm.

It is possible to note the seasonal nature of the displacements of the heads of the return plumbs at the 27 meter mark with respect to their anchors. The annual scale of the fluctuations is about 0.5 to 1.0 mm with maximum displacement in the direction of the tailrace at the end of the winter and minimum at the end of the summer. In the buildup of the measured displacements the effects of the seasonal variations of the headwater level are felt with some shift in time. The displacements in the direction of the dam access were stabilized. The best defined determination regarding the relative horizontal displacements (sags) of the dam sections are provided by the observations on the straight plumbs. They were performed under the direction of the VNIIG Institute, and in section 51 they were started on 4 September 1961 simultaneously with the beginning of filling of the reservoir, and in sections 65 and 30, in October 1961. In each of these sections the measurements were performed at five points with respect to altitude. During the first three years the readings with respect to the coordinate gages located at the 27 meter mark were performed every three days; then with an interval of 5-10 days, and during operation, twice a month.

The measured displacements have static nature caused by the annual temperature fluctuations. During the warm part of the year the displacements are in the direction of the headrace, and in the cold part of the year, in the direction of the tailrace (Figure 5-5,a). The periodic fluctuations of the displacements during the period of filling of the reservoir occurred with respect to the mean displacement gradually increasing in the direction of the tailrace which is for the most part an irreversible sag from the hydrostatic load (see Table 5-4). These irreversible displacements are calculated as the sliding mean annual values of the displacements measured at each mark (see Figure 5-5,b).

When the reservoir was filled to the normal backwater level, the increase in the deflection in the direction of the tailrace ceased, and then insignificant changes were observed which were caused by the drawdowns of the reservoir. The maximum magnitude of the measured displacements occurred in 1968 with a reservoir water level close to the normal backwater level (see Table 5-5).

The displacements of the crest of the dam measured by the return plumbs of the second and fourth stages (Figure 5-6) gives the same picture of the variation in time and the direct plumbs with some divergence with respect to magnitude of the seasonal fluctuations for different sections (see Table 5-5).

The horizontal displacements in the direction of the dam axis are measured both by the direct and the return plumbs. The magnitude of these displacements of the level of the dam crest is small (2 to 3 mm) (see Figure 5-6).

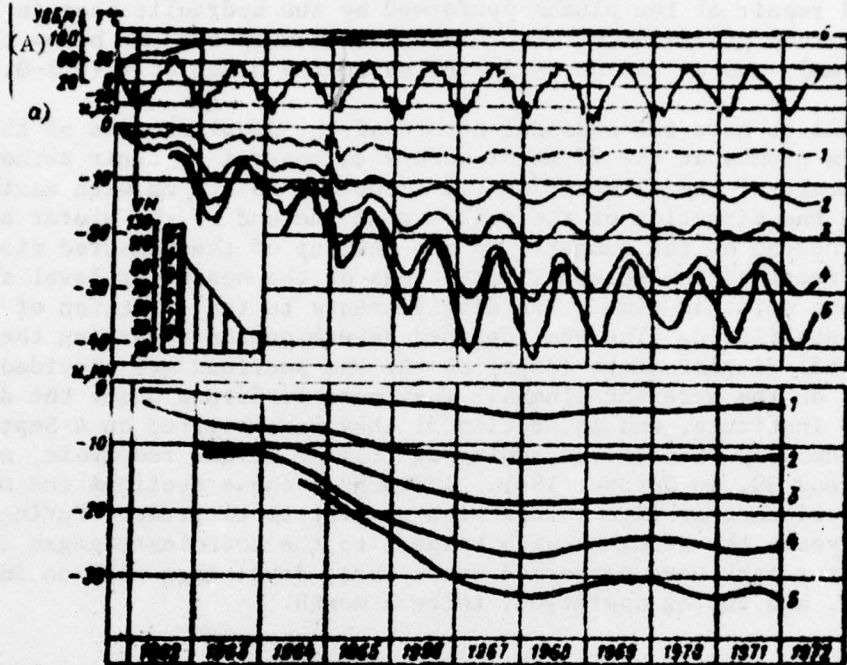


Figure 5-5. Relative horizontal displacements of section 30 measured by the direct plumb: a -- measured; b -- calculated sliding mean annual values at the marks (0 -- measurement location): 1 -- 45 meters; 2 -- 63 meters; 3 -- 81 meters; 4 -- 102 meters; 5 -- 123 meters; 6 -- backwater level; T -- average 10 day air temperature.

Key: A. headwater level

The vertical displacements measured on the return plumbs in stages II and III are proportional to the length of the latter and reflect the thermal deformations of the corresponding column of concrete.

5-3. Thermal Displacements of the Sections of the Dam

The variation of the thermal state has significant effect on the horizontal displacements of the dams. The nonuniform distribution with respect to the horizontal cross sections of the temperature increments increasing from one edge of the cross section to the causes rotation of the cross section in the direction of the colder edge. In accordance with the distribution of the temperature variations with respect to height of the dam, bending deformations occur in it, and the initial rectilinear vertical axis of the dam is distorted.

During the period of the scattering of the exothermal heat the temperature distribution with respect to the horizontal cross sections is caused to a

Table 5-4

Sections	Sags (mm) at the marks				
	6	61	81	102	103
Direct plumbs					
Maximal					
30	5.7	14.0	21.8	32.2	43.2
51	7.7	16.5	22.6	29.4	38.0
65	4.4	9.1	16.2	22.0	29.2
Irreversible					
30	4.8	12.5	19.3	27.6	34.0
51	6.9	15.6	20.7	28.0	31.5
65	5.9	8.1	14.4	18.8	22.2
Seasonal					
30	1.3	2.8	4.8	8.5	17.3
51	1.2	2.0	4.5	6.5	15.5
65	1.5	1.6	3.3	6.0	14.5

Table 5-5

Sections	Beginning of observation	Measured deflections, mm		
		Maximum	March-July 1973	August 1973 to March 1974
30	II. 1964	20.0	12.0	14.8
35	III. 1964	31.0	1.6	16.5
41	IV. 1965	21.9	22.1	16.5
47	IV. 1964	21.5	12.3	16.5
54	II. 1967	11.9	11.9	17.5
64	IV. 1963	22.5	10.7	14.5

significant degree by the thermal state of the internal region. For dams with expanded joints this state depends on the degree of their insulation from the surrounding air and also the presence in the power of the heating elements in the cavity of the joints.

The horizontal displacements of the columns of the dam are observed during its construction when a sharp nonuniform temperature distribution occurs with respect to the horizontal cross sections. Thus, when erecting the dam of the Bratsk Hydroelectric Power Plant, it was observed that the intense pouring of the blocks of the columnar mass with one open face causes its rotation in the direction of this face with opening of the anticolumnar joint. The heating of the adjacent part of the previously poured and cooled column, if it also has an open face, also causes its rotation which increases the opening of the joint [19, 61]. The periodic temperature fluctuations of the environment (air, water) differ on the pressure and downstream sides

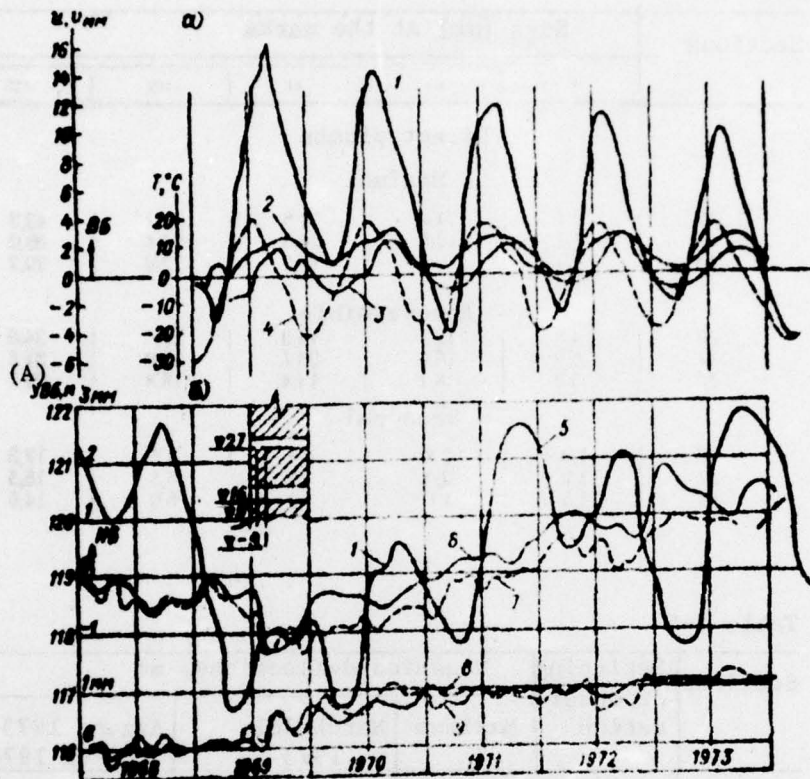


Figure 5-6. Displacements measured by the return plumbs of section 30: a -- with respect to the 27 meter mark; b -- the 27 meter mark with respect to the base. 1 -- crest with respect to the flow; 2 -- the same along the axis of the dam; 3 -- vertical; 4 -- mean monthly air temperature; 5 -- headwater level; 6, 7 -- displacements with respect to the anchor in the rock at 119 meters and with respect to the flow; 8, 9 -- the same along the axis of the dam.

Key: A. headwater level

are accompanied by the horizontal displacements of the dam usually in the direction of the headwaters during the warm part of the year and in the direction of the tailrace in the cold part of the year. During the construction period and during the filling of the dam the annual amplitude of the temperature displacements varied with time. For normal operation, the process of the variation in time of the temperature displacements assumed a steady state nature.

Considering the temperature field one dimensional and beginning with the hypothesis of the flat cross sections, it is possible with some approximation to adopt temperature shifts corresponding to the linear-average temperature

distribution. In drawing the closing curvilinear temperature diagram so that the algebraic sum of the areas in the total static moment with respect to a vertical axis will be equal to zero, we obtain

$$e_y = \frac{a}{1 - v} \left[T_2 + \frac{T_2 - T_1}{l} s \right] \quad (5-1)$$

This displacement can be divided into two components: the translational displacement

$$e_y = \frac{a}{1 - v} \cdot \frac{l}{l} = \frac{a}{1 - v} T_0 \quad (a) \quad (5-2)$$

Key: a. T_{mean}

and rotation of the cross section

$$\varphi(y) = \frac{a}{1 - v} \frac{T_2 - T_1}{l} = \frac{a}{1 - v} \Gamma(y), \quad (5-3)$$

where a is the coefficient of linear expansion of the concrete; v is the Poisson coefficient; Ω_T is the area of the temperature diagram; T_1 and T_2 are the temperatures at the edges of the cross section; $\Gamma(y)$ is the tangent of the angle of the closing or the mean temperature gradient.

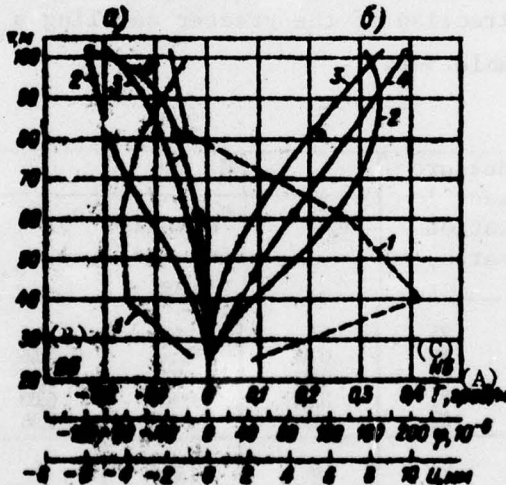


Figure 5-7. Calculated and measured seasonal variations of the deflections of section I.
 1 -- temperature gradients (Γ); 2 -- angles of inclination (ϕ); 3 -- calculated deflections (u); 4 -- measured deflections.

Key: A. , deg/meter B. headrace C. tailrace

Constructing the diagram of the temperature gradients and the mean temperatures with respect to height of the section it is possible by numerical integration to determine the angles of rotation ϕ , the horizontal u and vertical v displacements at the given marks y

$$\Gamma = \frac{d}{dy} \int T dy \quad (5-4)$$

$$u = \int pdy \quad (5-5)$$

$$v = \frac{d}{dy} \int T_{\phi} dy \quad (5-6)$$

In Figure 5-7 we have the diagrams for Γ , ϕ and u calculated for the annual period from September 1963 to September 1964 broken down into two seasonal intervals between the maximum displacements in the direction of the headrace and the tailrace. The temperature gradients (Γ) are the tangent of the angle of slope of the closing temperature diagrams with respect to horizontal cross sections from the pressure face to the downstream face of section 51 at the levels of the remote thermometer sections. The measured deflections coincide with the calculated temperatures with respect to direction, and are shifted somewhat with respect to them in the direction of the tailrace. This displacement can be a consequence of the nonuniform settling of the base and the hydrostatic pressure of the reservoir water. In Table 5-6 the sums of the temperature displacements u and the displacements from rigid rotation of the section in the direction of the greater settling $u_{\text{nonuniform settling}}$ were calculated in Table 5-6.

Table 5-6

Time interval	Measure- ment lo- cation marks, m	U, mm			u_{measured} , mm
		u_T	$u_{\text{nonuni-}}form set-tling}$	$u_T +$ $+ u_{\text{n.u.s.}}$	
IX 63 - III 64 $\Delta H = 1.5 \text{ m}$	25	0	0	0	0
	40	0.34	0.22	0.56	2.20
	61	2.21	0.52	2.76	4.30
	81	5.22	0.81	6.03	5.60
	102	8.54	1.12	9.66	9.80
III 64 - IX 64 $\Delta H = 7 \text{ m}$	25	0	0	0	0
	40	0.13	-0.49	-0.62	-0.4
	61	0.94	-1.18	-2.12	-0.5
	81	2.50	-1.85	-4.35	-1.50
	102	4.73	-2.53	-7.30	-5.80

During the first interval the water level in the reservoir rose by 1.5 meters, and the total $u_T + u_{\text{nonuniform settling}}$ coincides with u_{measured} better, the

higher the investigated cross section. In the second interval the water level increased by six meters and u_{measure} was shifted more in the direction of the tailrace than the total $u_T + u_{\text{nonuniform settling}}$.

As the experience of natural investigations in a number of the dams indicates [59, 65], the calculation of the thermal displacements with respect to the linearly averaged temperature diagrams gives satisfactory results of the structures with uniform temperature distribution with respect to the longitudinal cross sections. For the dam with open expanded joints this calculation can give only highly approximate results.

5.4. Calculation of the Deflection of the Dam from the Hydrostatic Pressure of the Reservoir Water

The effect of the hydrostatic load on the horizontal displacements of the dams is determined by the usual means of measurements during the process of fast drawdowns and filling of the reservoir. For the slowly varying headwater level, the periods are used where the temperature in the corresponding cross sections remains approximately constant. With a gradually increasing headwater level and nonsteady state thermal regime the deflection of the dam from the hydrostatic pressure can be determined with some approximation without using the results of the static calculation of the dam, the calculated temperature displacements and the measured total displacements.

Under the effect of the hydrostatic pressure of the water on the pressure face of the dam bending of its body takes place with horizontal displacements in the direction of the tail race determined by the negative and nature of distribution of the normal and tangential stresses in the cross sections of the dam. The nonuniform distribution of the stresses with respect to the plane of the footing causes deformation of the base with rotation of the contact plane in the direction of the tail race which is greater the more pliable the base. Simultaneously, settling occurs and rotation of the base in the direction of the headwater. The horizontal displacement of the dam also takes place as a result of elastic compression of the contact zone under the effect of the horizontal load.

For a gravity dam with triangular profile with vertical pressure face and a reservoir filled to the level of the top of the profile, the components of the horizontal displacements from the effect of the normal (σ_x, σ_y) and tangential (τ_{xy}) stresses can be calculated by the following formulas from elasticity theory [65, 66].

From the vertical stresses σ_y (Figure 5-8,a)

$$Ea = \gamma h^2 \left(\frac{1}{m^2} - \frac{v}{2m} \right) : \gamma h \left(\frac{v}{2m} - \frac{2}{m^2} \right) y + \frac{V^2}{m^2} x^2 - \frac{Vv}{m^2} yx. \quad (5-7)$$

From the horizontal stresses σ_x (Figure 5-8,b)

$$\Delta u = \pm \frac{\gamma m h}{2} + \frac{\gamma m h}{2} y - \gamma y x. \quad (5-8)$$

Depending on the ratio of the Young's moduli of the dam and the base, various cases of deformation distribution with respect to length of the footing can be observed:

- a) The deformations decrease from $\Delta u = \gamma m h^2$ under the pressure face to $\Delta u = 0$ under the downstream face -- the plus sign in (5-8);
- b) The deformations buildup from $\Delta u = 0$ under the pressure face to $\Delta u = -\gamma m h^2$ under the downstream face -- the minus sign in (5-8);
- c) The deformations decrease from the edges of the footing to its middle. then

$$\Delta u = \frac{\gamma m h}{2} y - \gamma y x. \quad (5-8')$$

Under the pressure face $\Delta u = \gamma m h^2/2$, and under the downstream face $\Delta u = -\gamma m h^2/2$.

From the tangential stresses τ_{yx} (Figure 5-8,c)

$$\Delta u = \frac{\gamma h^2}{m} (1 + v) - \frac{\gamma h}{m} (1 + v) y. \quad (5-9)$$

The total horizontal displacement is defined as the sum of its components with respect to (5-7)-(5-9):

$$\begin{aligned} \Delta u &= \gamma m h \left(\frac{1}{m^2} + \frac{2+v}{2m} \pm \frac{v}{2} \right) + \gamma h \left(\frac{m}{2} - \frac{2+v}{2m} - \frac{v}{m^2} \right) y + \\ &\quad + \frac{\gamma y^2}{m^2} + \frac{\gamma' x^2}{m^2} - \gamma \left(1 + \frac{v}{m^2} \right) xy \end{aligned} \quad (5-10)$$

The horizontal displacement of the crest from (5-10) will be

$$\Delta u_0 = \gamma m h \left(\frac{1}{m^2} + \frac{2+v}{2m} \pm \frac{v}{2} \right). \quad (5-11)$$

In (5-11) the third term corresponds to cases a and c of the equation (5-8). For case c this term will be zero and (5-11) assumes the form

$$\Delta u_0 = \gamma m h \left(\frac{1}{m^2} + \frac{2+v}{2m} \right). \quad (5-11')$$

Total vertical displacement can be calculated by the equation

$$\begin{aligned} \frac{\gamma h^2}{2} \left(\frac{1}{m^2} + \cdot \right) - \gamma h \left(\frac{m}{2} - \frac{2+v}{2m} - \frac{v}{m^2} \right) x + \frac{\gamma}{2} \left(1 - \frac{2+v}{2m} \right) x^2 + \\ + \frac{\gamma}{2} \left(v + \frac{1}{m^2} \right) y^2 - \frac{2\gamma}{m^2} xy. \end{aligned} \quad (5-12)$$

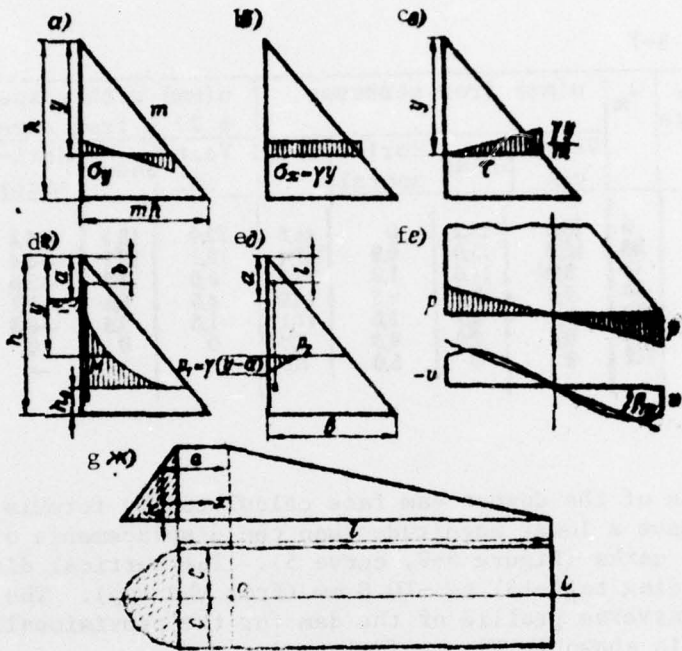


Figure 5-8. Calculation of the horizontal displacement of the dam from the hydrostatic load.

For $x = y = 0$ the vertical displacement of the crest

$$F = \frac{1}{E} \int_{-h}^0 \frac{1}{1 - \nu^2} \sigma_y dy \quad (5-13)$$

In the above presented formulas: E is the Young's modulus of the dam; γ is the specific weight of the water; h is the height of the triangular profile; m is the laying of the downstream face; ν is the Poisson coefficient; x, y are the coordinates reckoned from the top of the profile.

For the Bratsk dam at $h = 112$ m, $m = 0.8$ and $\nu = 0.16$ the expressions (5-7)-(5-12) for the components of the horizontal displacements assumes the form:

$$\begin{aligned} Eu_x &= 23250 - 427y + 1.95y^2 + 0.31x^2 - 0.25xy; \\ Eu_y &= 18200 - 162y; \\ Eu_{rep}^{(a)} &= 45y - xy; \\ \Sigma Eu &= 41495 - 544y + 1.95y^2 + 0.31x^2 - 1.25yx. \end{aligned} \quad (5-14)$$

Key: a, hor

Considering the condition $E = 1 \cdot 10^6$ ton-force/m², we obtain the distributions of the horizontal displacements with respect to height of the pressure face of the dam and the normal backwater level presented in Table 5-7 and in Figure 5-9.

Table 5-7

Mark, meters	u m	u(mm) from stresses				u(mm) with respect to $\phi 27$ m from stresses			
		Verti- cal	Shear	Hori- zontal	Total	Verti- cal	Shear	Hori- zontal	Total
[deleted]	0	18.3	18.2	0	41.5	22.9	15.3	-4.2	24.0
	12	14.5	15.0	0.9	31.4	15.1	12.1	-3.4	22.6
	24	11.6	11.6	1.8	22.4	8.6	8.7	-0.5	14.9
	36	8.7	8.7	2.6	16.2	4.5	5.5	-1.7	12.3
	48	6.8	6.8	3.8	11.1	1.5	2.8	-0.4	1.5
	60	5.0	5.0	4.3	7.6	0	0	-	-
	72				5.0	-	-	-	-

The displacements of the downstream face calculated by formula (5-10) and $x = my = 0.8 y$ have a lower magnitude than the displacements of the pressure face at the same marks (Figure 5-9, curve 5). The vertical displacement of the crest according to (5-13) is -10.8 mm (from the top). The deformed state of the transverse profile of the dam for the provisionally adopted Young's modulus is shown in Figure [deleted].

The formula (5-10) permits calculation of u and its distribution with respect to height for the reservoir fills to the normal backwater level. For the approximate determination of u for partial filling of the reservoir water it is convenient to use the well-known Mohr formula

$$\frac{1}{E} \int_{y_1}^{y_2} \frac{M y}{J} dy \quad (5-15)$$

where M is the bending moment from the hydrostatic load on the pressure face of the dam; J is the moment of inertia of the transverse cross section (Figure 5-8).

Considering the general case of measuring the deflections by the plumbob attached at a distance b (meters) from the top of the triangular profile, on partial filling of the reservoir to the level a meters below the top (Figure 5-8,d), for the vertical stresses we have

$$M = \frac{1}{6} \frac{(y-a)^3}{b}, \quad J = \frac{\pi b^3}{12},$$

$$s_1 = \frac{2}{3} \frac{1}{\pi b^2} \int_0^b \frac{(y-a)^3}{b} (y-b) dy. \quad (5-16)$$

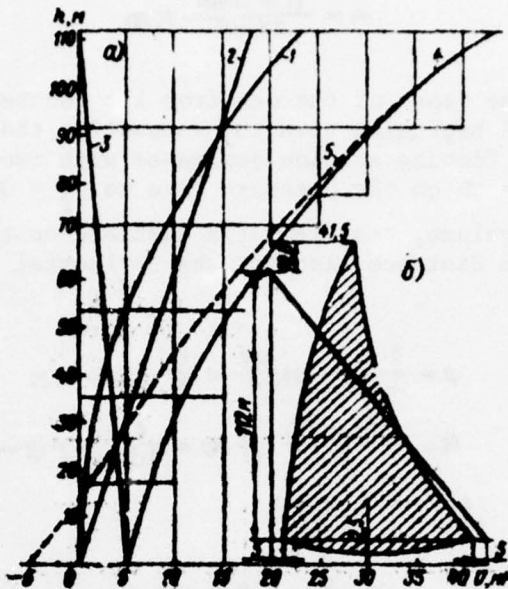


Figure 5-9. Horizontal displacements of the crest of the dam at normal backwater level and $E = 1 \cdot 10^6$ tons-force/m²; a -- components; b -- deformed state from the stresses.
 1 -- from the vertical; 2 -- from shear; 3 -- from horizontal; 4 -- total displacements of the pressure face;
 5 -- the same for the downstream face.

The integration of expression (5-16) for the notation $\xi = [deleted]$ gives

$$\int \left(F_1 + F_2 + F_3 + F_4 + F_5 \right) \frac{dy}{y} = \left(\frac{1}{1} u_1 + u_2 + u_3 + u_4 + u_5 \right) \frac{h^2}{2} = u_1 h^2 \quad (5-17)$$

or

$$u_1 = \frac{1}{3} \frac{h^2}{E} \left[F_1 (y) - \frac{h}{A} F_5 (y) \right] \quad (5-18)$$

The deflection of the crest of the dam of the shearing forces, considering the distribution of the tangential stresses with respect to the horizontal cross sections uniform can be calculated from the expression

$$u_2 = \frac{1}{E} \int_a^b \tau dy \quad (5-19)$$

$$u_2 = \frac{1(1+\nu)}{S_y E M} \int_a^b \frac{(y-a)^2}{y} dy = \frac{1(1+\nu)M}{2S_y E C} \left(1 - 4\zeta + 2\zeta^2 + 2\zeta^3 \ln \frac{1}{\zeta} \right) \quad (5-20)$$

or

$$u_1 = \frac{(1+\gamma) \gamma h^3}{2S_1 m E} F_1(\xi). \quad (5-21)$$

The deflection of the crest of the dam from the counter pressure (see Figure 5-8,e) is calculated beginning with the assumption that the counterpressure with respect to the footing section decreases with respect to a linear law from a value of $p_1 = \gamma h$ on the pressure face to $p_2 = 0$ on the drainage tunnel in the same column, that is, at a distance on the order of $(1/4)B$. Let us take the same distance also for the horizontal interblock joints; then

$$\begin{aligned} P &= \frac{1}{2} \gamma (y-a) \frac{m y}{4} = \frac{1}{8} \gamma m (y-a) y; \\ M &= \frac{\gamma m y (y-a)}{8} \frac{5}{12} m y = \frac{5}{96} \gamma m^2 y^3 (y-a); \\ \frac{M}{J} &= \frac{5}{6} \frac{1(y-a)}{m y}; \\ u_2 &= -\frac{5}{384 \beta} \int_0^a \frac{1 - \frac{a}{y}}{y} dy; \\ u &= \frac{5}{96} \frac{\gamma h^3}{S_1 m E} \left[(1-\beta)^2 - 2\beta + 2\beta \left(1 + \ln \frac{1}{\beta} \right) \right]; \end{aligned} \quad (5-22)$$

$$u = \frac{b}{96} \frac{\gamma h^3}{S_1 m E} \left[F_2(0) - 2\beta + 2\beta \left(1 + \ln \frac{1}{\beta} \right) \right]. \quad (5-23)$$

where $\beta = b/h$.

In formulas (5-15) to (5-23) S_1 and S_2 are the ratios of the moment of inertia and the area of the horizontal cross section of the section with expanded joints to the corresponding values for the rectangular cross section.

The total deflection

$$\begin{aligned} u &= \frac{\gamma h^3}{S_1 m^2 E} \left\{ F_1(\xi) - \frac{5}{6} F_1(0) + \frac{(1-\beta)^2 m^2}{2S_1} F_2(0) + \right. \\ &\quad \left. + \frac{5}{16} m^2 \left[F_2(0) - 2\beta + 2\beta \left(1 + \ln \frac{1}{\beta} \right) \right] \right\}. \end{aligned} \quad (5-24)$$

The graphs $F_1(\xi)$, $F_2(\xi)$, $F_3(\xi)$ and $F_4(\xi)$ are presented in Figure 5-10.

For the normal backwater level and attachment of the plumb at the level of the top of the triangular profile $a = 0$, $\xi = 0$, $F_1(\xi) = F_2(\xi) = F_3(\xi)$; $\beta = 0$.

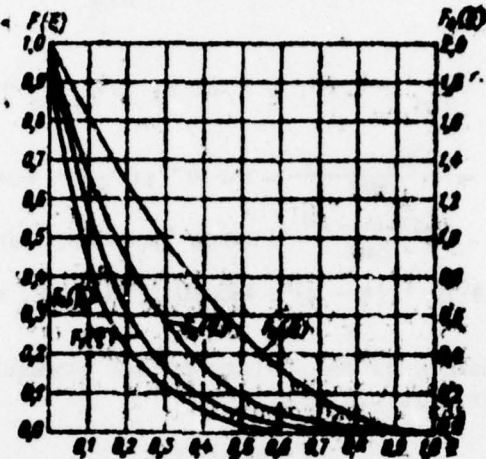


Figure 5-10. Calculation of the horizontal displacements of the dam from the hydrostatic load.

Considering $\gamma = 1 \text{ ton-force/m}^3$, $v = 0.15$, $S_1 = 0.9$, $S_2 = 0.81$, $m = 0.8$, we obtain

$$\theta = \frac{\gamma h}{B} \left(\frac{1 + 0.412 + 0.289}{0.312} \right) = \frac{3.14}{B}. \quad (5-25)$$

The bending of the crest of the dam for normal backwater level according to formula (5-11) is

$$\theta = \frac{\gamma h}{B_{\text{mean}}} \left(\frac{1}{2} + \frac{v}{2} + 1 \right) = \frac{3.14}{B_{\text{mean}}}. \quad (5-26)$$

5-5. Horizontal Displacement of the Dam from Rotation of the Base

Under the effect of the load on the base transferred by the dam and the reservoir water, deformations of the base occur with rotation of the contact cross section (the fitting of the section). The mean angle of rotation (Figure 5-8,c) can be calculated with the following formula:

$$\theta_m = (1 - v_m) \frac{3p}{B_{\text{mean}}} + \frac{(1 + v)(1 - 2m)}{B_{\text{mean}}} \tau. \quad (5-27)$$

where $p = M/W$ is the maximum value of normal stress on the faces of the dam in the contact plane; τ is the mean intensity of the tangential stresses, $M = \gamma(h - a)^3 l/6$ is the bending moment from the hydrostatic load on the pressure; $W = B^2 l_{\text{mean}}/6 = m^2 h^2 l_{\text{mean}}/6$ is the moment of resistance of the contact cross section; B is the width of the footing along the flow; l is the length of the section with respect to pressure face; l_{mean} is the mean length of the section -- the side of the rectangle with an area equal to

the error F of the T-foothing cross section, $\ell_{\text{mean}} = F/B = 1589 \text{ m}^2 / 88.8 = 17.9 \text{ m}$; E_r is the deformation modulus of the base; ν_{dis} is the Poisson coefficient of the base.

For $\gamma = 1 \text{ ton-force/m}^3$; $\nu_{\text{dis}} = 0.20$; $\ell = 22 \text{ m}$; $\ell/\ell_{\text{mean}} = 1.23$, we obtain

$$p = \frac{1.23\gamma(h-a)^3}{m^3h^2} = 153 \cdot 10^{-6} \gamma(h-a)^3, \text{ ton/m}^2 \quad (5-27')$$

$$\tau = \frac{1.23\gamma(h-a)^2}{2m^2} = 686 \cdot 10^{-5} \gamma(h-a)^2, \text{ ton/m}^2 \quad (5-27'')$$

$$E_r p = 14 \cdot 10^{-5} \gamma(h-a)^3 + 495 \cdot 10^{-5} \gamma(h-a)^2, \text{ ton/m}^2. \quad (5-28)$$

The horizontal displacements of the points on the pressure face $(0, y)$ with rigid rotation on the contact plane will be

$$u_x = p(h-y).$$

The horizontal displacement of the crest for $h = 112 \text{ meters}$.

$$E_r p = 15.7 \cdot 10^{-3} \gamma(h-a)^3 \cdot 555 \cdot 10^{-3} \gamma(h-a)^2, \text{ ton-force/m}, \quad (5-29)$$

for $a = 0$, $E_r u_x = 28.95 \cdot 10^3 \text{ ton-force/meter}$.

The rotation of the contact plane of the base from the effect of the bending moment is accompanied by horizontal displacement which for the middle of the footing will be

$$u_m = \frac{(1-2\nu)(1+\nu)}{E_r} \frac{pB}{6}. \quad (5-30)$$

Substituting the value of p calculated by (5-27') and τ (5-27''), we have

$$E_r u_m = 1.63 \cdot 10^{-3} \gamma(h-a)^3. \quad (5-31)$$

The horizontal displacement of the contact zone from the shearing stresses in the middle of the footing

$$u_x = \frac{2}{E_r} \tau B \ln 2 \quad (5-32)$$

Substituting the value of τ from (5-27''), we obtain

$$E_r u_x = 27.2 \cdot 10^{-3} \gamma(h-a)^2. \quad (5-32)$$

For $a = 0$, $E_r = 1 \cdot 10^6$ the total horizontal displacements with respect to (5-32) and (5-32') will be $2.3 + 3.4 = 5.5 \text{ mm}$. These displacements are not measured by the direct plumbbs.

The angle of rotation of the base from the variation of the mass of the reservoir water with respect to the solution for the three-dimensional problem with trapezoidal triangular shape with respect to the bottom of the water surface and constant width can be expressed as follows: (the formula is proposed by A. A. Khrapkov)

$$\rho_{\phi} = \frac{2(1 - v^2) p(x_0)}{\pi E_r} \left[\ln \frac{C_0 + \sqrt{C_0^2 + 1}}{C_L + \sqrt{C_L^2 + 1}} + \frac{C_L}{C_0 - C_L} \left[\ln \frac{C_0 + \sqrt{C_0^2 + 1}}{C_L + \sqrt{C_L^2 + 1}} + \right. \right. \\ \left. \left. + C_0 \left(\ln \frac{1 + \sqrt{C_0^2 + 1}}{1 + \sqrt{C_L^2 + 1}} - \ln \frac{C_0}{C_L} \right) \right] \right]. \quad (5-33)$$

where x_0 is the point for which ρ is calculated; a is the point at which the ordinants of the backwater curve begin to decrease; L is the point at which the backwater curve bridges out (the end of the reservoir); C is the half-width of the reservoir (Figure 5-8,g). $C_0 = C/x_0$ in this case; $C = C/a$; $C_L = C/L$. For $x_0 = a$; $C_0 = C_a$

$$\rho_{\phi} = \frac{2(1 - v^2)}{\pi E_r} p(x_0) \frac{C_0}{C_0 - C_L} \left[\ln \frac{C_0 + \sqrt{C_0^2 + 1}}{C_L + \sqrt{C_L^2 + 1}} + \right. \\ \left. + C_L \left(\ln \frac{1 + \sqrt{C_0^2 + 1}}{1 + \sqrt{C_L^2 + 1}} - \ln \frac{C_0}{C_L} \right) \right]. \quad (5-33')$$

For $L \rightarrow \infty$; $C_L \rightarrow 0$

$$\rho_{\phi} = \frac{2(1 - v^2)}{\pi E_r} p(x_0) \ln(C_0 + \sqrt{C_0^2 + 1}). \quad (5-34)$$

As is known, the rock base is water permeable and the force effect of the seepage water is realized by volumetric forces applied at the inside points of the base and by the surface forces applied in the contract cross section (the back pressure). The latter is taken into account in the loads applied on the footing of the dam to the rock base.

The correction factor for the approximate value of the angle of rotation in the middle of the footing from the effect of the volumetric forces of the seepage in terms of the value of the corresponding magnitude from the effect of the water on the water permeable bed of the reservoir, the ratio of the curvature from the effect of the volumetric seepage forces and the external load on the bed of the reservoir is obtained.

This ratio $k_{\phi,n} = \frac{1+v}{2(1-v)} = \frac{1+v}{1-v}$, for $v = [deleted]$, $k_{\phi,n} = 0.624$.

The displacement of the crack from the mass of the water in the headrace

$$E_{H,n} = 1.79(A - a) H_{H,n} = 1.79(A - a) \quad (5-35)$$

5-6. Deflection of the Dam in the Normal Operating Regime

As is obvious from Figures 5-5, 5-6, the deflections of the dam in the normal operating regime have the periodic nature caused by seasonal fluctuations of the air temperature. A comparison of the mean annual sliding values of the headwater level and the measured deflections of the crest of the dam in five years indicates (Figure 5-11) that with the exception of the temperature fluctuations the deflections of the dam are a function of the variations of the headwater level during the drawdown and filling process of the reservoir. The buildup of the deflections with time which would have to be considered the result of irreversible processes (creep, pliability of the base, and so on) is not noticeable.



Figure 5-11. Comparison of the fluctuations of the headwater level and deflections. 1 -- headwater level; 2 -- section 51; 3 -- section 30; 4 -- sections 65.

Key: a. headwater level.

Thus, the seasonal variations of the deflections of the dam can be considered to depend basically only on two factors: the temperature fluctuations and the fluctuations of the hydrostatic loads: $u = F(T, H)$.

During the system of equations with the constant coefficient expressing the effect of the temperature and force parameters on the measured deflections (the method of "coefficients of effect" [68-71]), it is possible with known approximation to divide the measured deflections into the components from the temperature and the static load. For a large number of measured displacements the number of equations for determining the "influence coefficients" greatly exceeds the number of coefficients subject to determination. The most probable value of these coefficients is given by the [deleted] by balancing calculations by the least squares method.

The first efforts to determine the components from the temperature of the hydrostatic mode were made by us at the beginning of the [deleted] using the deflection of the crest of the dam for three years of normal operation of the hydroelectric power plant [1967-1969].

A study was made of various versions of the temperature parameter, including:

a) The sliding mean for 30 days preceding the given deflection, the air temperature measured during the investigated period and also the mean values over many years.

b) The trigonometric series approximating the air temperature fluctuations with an annual period.

The dependence of the displacement on the hydrostatic load is given by the third degree function from the increase in the headwater level.

The solution to 60 to 70 equations (two points [deleted]) each type demonstrated that the best comparison with the measurements of the displacements is provided by the equation with a time function in the trigonometric series.

When using the sliding mean for 30 days as the temperature parameter, the linear dependence of the displacement on the temperature was obtained for constant headwater level with a proportionality coefficient $\Delta u_T = 0.4$ mm [deleted]. However, the difference $\Delta u_u = \Delta u_{meas} - \Delta u_T$ was not obtained uniquely.

Hereafter, as the temperature parameter, the temperature of the concrete of the downstream face of the sections is taken in which the direct plumbs are located. The equations for the deflections assume the following form:

$$u(\tau) = aT(\tau) + bH(\tau) + c[\Delta u_u] \quad (5-36)$$

where $u(\tau)$ is the deflection of the crest at the time $H(\tau)$ -- the rise of the headwater level above the level of maximum drawdown of the reservoir (116 meters); $T(\tau)$ is the measured temperature of the concrete; a , b , c are the influence coefficients. The systems of 90 to 100 equations (two points per month) for 5 years beginning in 1967 were solved [deleted]: with a correction with respect to the given leveling for rotation of the footing as a result of nonuniform settling and without this correction. The influence coefficients in the first case are presented in Table 5-8.

Table 5-8

Sections	Coefficients			
	a	b	c	[deleted column]
51	-0.003	-0.001	-0.002	
52	-0.002	-0.001	-0.002	
63	-0.003	-0.001	-0.002	

The free term d is the [deleted] mean value around which the fluctuations of the measured values of the deflections take place. The components of the measured deflections for section 51 are shown in Figure 5-12.

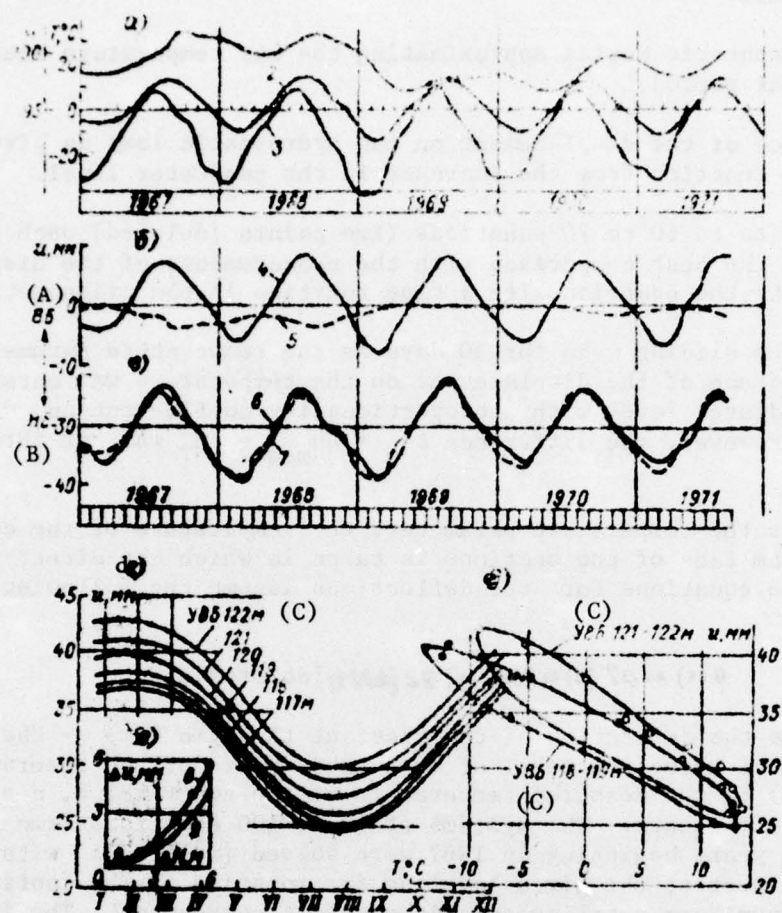


Figure 5-12. Horizontal displacements of the crest of section 51 during the first years of normal operation of the hydroelectric power plant; a -- initial data; b -- component displacement; c -- total displacement; d -- annual displacement cycle for constant headwater level; e -- relation between the displacements and the temperature of the concrete of the downstream face for constant headwater level; f -- $\Delta U = F(\Delta H)$. 1 -- headwater level; 2 -- concrete temperature on the downstream face; 3 -- air temperature; 4 -- from the temperature fluctuations; 5 -- from the fluctuations of the headwater level; 6 -- calculated; 7 -- measured; 8 -- considering the nonuniform settling; 9 -- the same without considering it.

Key: A. headrace

B. tailrace C. headwater level

It is possible to note the significantly greater influence on the deflection of the crest of the dam from the temperature than the hydrostatic load. The above noted nonuniformity of the dependence of the deflection on the temperature for the given headwater level is illustrated in Figure 5-12,e). In the cold part of the year when the dam sags in the direction of the tailrace, the temperature component coincides with respect to direction with the component from the hydrostatic load. During the warm part of the year the dam deflects in the direction of the headwaters, and the directions of the deflection components are positive. For this reason, for the given headwater level and the same temperature, for example, in the spring and fall, the magnitude of the deflections were different.

The use of the influence coefficients, for example, according to Table 5-7, offers the possibility of approximating and predicting the picture of the effective deflections of the crest of the dam from both components.

In the range of fluctuations of the headwater level between the 116 and 122 meter marks, the increments of $\Delta F(\xi)$ and Δu respectively are approximately linearly dependent on $(\Delta H)^2$. This offers the possibility of adopting a simple function for $u = F(T, H)$

$$u(t) = aT(t) + b[H(t)]^2 + d. \quad (5-37)$$

5-7. Determination of the Young's Modulus of the Dam and the Rock Base

The formulas for calculating the deflections of the dam from the hydrostatic pressure of the water on the pressure face include the Young's modulus E of the dam and the rock base E_r . As a result of the large number of horizontal interblock joints and vertical longitudinal joints (and cracks) the Young's modulus of the dam as a structural element E_k usually differs from the Young's modulus of the concrete of the material E_b . The deformation modulus of the rock base is determined by testing by dies in individual points also can differ significantly from the modulus of deformation considered as the integral characteristic of the pliability of the base under the entire area of the footing of the structure.

The Young's modulus of the dam can be determined with some approximation with respect to the measured deflections in the following way. Let in the formulas for calculating the deflection of the dam from the hydrostatic pressure (5-10) to (5-35) the Young's modulus $E = 1$; then the right-hand side of these formulas will be the "elasticity coefficient" (K , ton-force/meter); and the expression for the deflection assumes the form

$$u = \frac{K}{E}; \quad u_r = \frac{K_r}{E_r}. \quad (5-38)$$

The deflection from hydrostatic load on the pressure face of the dam can be expressed as follows:

$$u = \frac{K}{E} + \frac{K_r - K_{r0}}{E_r} = \frac{K}{E} + \frac{K_r}{E_r}. \quad (5-39)$$

Let

$$\frac{E_r}{E} = \gamma. \quad (5-40)$$

$$L_u = \frac{K}{u} = \frac{K_r}{\gamma u}. \quad (5-41)$$

The precision with which E_k is calculated will be determined by the correctness of the representation of the uniformity of the deformed properties of the dam used as the basis for calculating K and the reliability of the available data of the deformative properties of the base. In the best case these data are known for individual points. As is noted in §1-1, the values of E_r according to the experimental data are within a broad range from 130,000 to 440,000 kg-force/cm². The data in Table 5-4 indicate that both the total and seasonal deflections of the section are different.

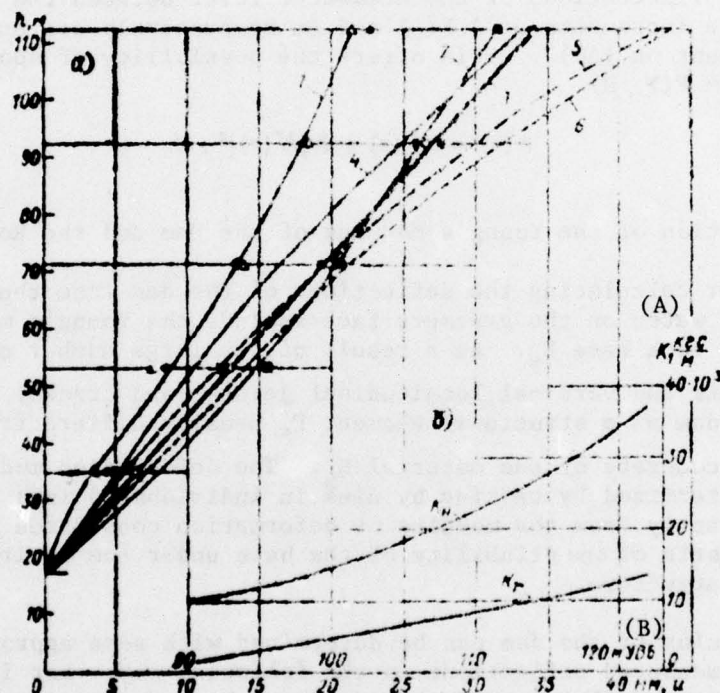


Figure 5-13. Calculation of the Young's modulus of the sections; a -- distribution of the deflections (u) with respect to height of the sections; b -- elasticity coefficients. 1, 2, 3 -- measured u in the sections 65, 51, 30; 4 -- calculated MKE; 5 -- the same considering the seasonal temperature minimum; 6 -- measured seasonal maximum u in section 30; $\Delta, *$ -- measured.

Key: A. K_1 , kg-force/m B. headwater level

In Figure 5-13 for the three sections the distribution is shown with respect to altitude of the deflections measured at five marks where the reservoir level close to the normal backwater level. The deflections are different both with respect to magnitude and with respect to nature of distribution. In section 50 the deflections increase with respect to the height of the sections by a linear law. In the other two sections the increase in the deflection decreases with respect to height.

Beginning with the elasticity coefficient K calculated by (5-27), (5-32) and (5-35), the measured deflections and the deformation moduli of the rock known for the sections [19, Table 6-1], the following values of E_k and E_r were obtained for which the distribution of u is approximated with sufficient approximation: for the section 30 $E_k = 1.6 \cdot 10^5$ kg-force/cm²; $E_r = 1.2 \cdot 10^5$ kg-force/cm² (o -- in Figure 5-13, a); for section 65, $E_k = 1.9 \cdot 10^5$ kg-force/cm²; $E_r = 3.8 \cdot 10^5$ kg-force/cm² (● -- in Figure 5-13,a).

The calculated values of K and K_p for all sections are identical, and the deformed state is different. This is explained by the peculiarities of the sections (ste of the joint and cracks) and also the nonidentical and non-uniform pliability of their bases.

The deflection of the crest calculated by the method of finite elements for $E = 2 \cdot 10^5$ kg-force/cm² and $E_r = 1.5 \cdot 10^5$ kg-force/cm² is 33.6 mm.

The mean deflection of the cross sections 30 and 51 is about 33 meters. The component from rotation of the base with respect to (5-29) and (5-3 [deleted]) $u_r = 10.7$ mm. The differences of 22.3 mm by formulas (5-11) and (5-11)' with the coefficient $S_1 = 0.9$ corresponds to $E_k = 2.06 \cdot 10^5$ kg-force/cm² to $2.3 \cdot 10^5$ kg-force/cm², and by formula (5-25), $1.98 \cdot 10^5$ kg-force/cm².

From the presented data it is possible to consider that the probable value of E_k is within the limits of $(1.5-2.0) \cdot 10^5$ kg-force/cm².

The Young's modulus E_k can be considered as the characteristic of the rigidity of the dam. Considering the large number of horizontal construction joints and by comparison with E_k on other dams [72] it is possible to consider the order of E_k for the Bratsk dam satisfactory.

CHAPTER 6. STRESSED STATES OF CONCRETE MASSIFS

6-1. Calculation of the Stresses with Respect to the Deformations Measured in Concrete

As was indicated in § 2.5, the remote strain gages in the blocks are located in the majority of cases in a group forming a sand rosette in the plane of the transverse cross section of the dam. This group includes also the remote strain gage oriented with respect to the normal to this plane, that is, in the direction of the longitudinal axis of the dam. In addition to these five instruments, the group includes two remote strain gages in the unstressed (free) samples.

Having the tensometric rosette in the plane of the transverse cross section of the structure, usually we begin with the proposition that the structure operates under the conditions of the planar stressed state or the planar deformation and the stress state of it is determined by three components σ_x , σ_y and τ_{xy} . In order to determine their components it is sufficient to measure three relative linear deformations with respect to three arbitrary directions passing through a given point. In our case, as the directions we have taken the horizontal direction ϵ_x , the vertical direction ϵ_y and ϵ_{45} which is at an angle of 45° to them. The fourth remote strain gage of the fan rosette is located at an angle of 135° to ϵ_x and offers the possibility of observing the conditions of invariance of the sum of the deformations with respect to the perpendicular directions

$$\epsilon_x + \epsilon_y = \epsilon_{45} + \epsilon_{135}. \quad (6-1)$$

The observation of this condition indicates that the concrete at the investigated point is quite uniform and isotropic. The fifth remote strain gage of the rosette measured the deformation ϵ_z in the direction of the dam axis and permits judgment of the correctness of the proposition that the structure operates under the conditions of the two-dimensional problem.

The center of the two modules (65-III-9 and 51-III-9) there are object rosettes of 9 remote strain gages which form a fan with respect to the rosette in each of three mutually perpendicular planes. In Figure 6-1 we have the relative

deformations unmeasured by 9 remote strain gages of the volumetric rosette of block III-9 in years. When investigating the graphs in Figure 1 attention is given to the following:

The condition of invariance of the total deformation (6-1) is observed with sufficient accuracy in all three coordinate planes for the entire observation period. From this it follows under normal conditions the concrete can be considered as a uniform and isotropic body.

Sometimes the condition (6-1) was not observed from the very beginning of the observations which is explained best of all by a disturbance of the orientation of the instrument when pouring the block. The cases were observed where the observation of conditions (6-1) ceased some time after pouring the block was basically explained by the [deleted] crack intersecting the axis of one of the instruments. In individual cases this could be explained by the nonuniformity of the concrete or the nonuniformity of the state in which the instruments of the strain gage rosette turned out to be at the [deleted] stressed points, for example, in the strain gage blocks that are uncovered for a prolonged period of time.

During the construction period of the relative deformation of the concrete in the direction of the dam axis ϵ_x is commensurate with respect to magnitude with the deformations ϵ_y and ϵ_z , and in the number of cases it exceeds them.

From this it follows that the structure operates under the conditions of the volumetric stressed state. Accordingly, in the cases where the direction of the principal stresses could be considered known, groups of three mutually perpendicular remote strain gages were installed in the modules of the group (Figures 2-5, 2-6) and the normal stresses were calculated: with respect to three mutually perpendicular areas σ -- with respect to the vertical area, parallel to the dam axis, σ_z along the vertical area parallel to the section axis (along the flow); σ_y with respect to the horizontal area.

In the measured deformations ϵ_x , ϵ_y and ϵ_z , in the process of their development in time, the joint effect of the external forces, the Poisson effect and the temperature stresses were summed. The latter, as is known, occurs in cases where the inside or outside relations limit the temperature deformations of the investigated concrete element, and therefore the magnitude of the temperature stresses is proportional to the difference between the actual and the free temperature deformations.

The free temperature deformations occur in the body which can expand freely; for variations of the temperature that are uniform or are linear coordinate functions. The magnitude of the free temperature deformations for these cases will be respectively

$$\begin{aligned}\epsilon_0 &= \epsilon_{0x} = \epsilon_{0y} = \epsilon_{0z} = \alpha \Delta T; \\ \epsilon_0 &= \epsilon_{0x} = \epsilon_{0y} = \epsilon_{0z} = \alpha(C_1x + C_2y + C_3z),\end{aligned}\tag{6-2}$$

where α is the coefficient of linear expansion,

The relation between the measured deformations and the effective stresses in the presence in the latter of the temperature component is expressed by the following formulas [73, 74];

$$\left. \begin{aligned} \epsilon_{xx} &= \frac{1}{E} [\sigma_x - \nu(\sigma_y + \sigma_z) + \alpha \Delta T], \\ \epsilon_{yy} &= \frac{1}{E} [\sigma_y - \nu(\sigma_x + \sigma_z) + \alpha \Delta T], \\ \epsilon_{zz} &= \frac{1}{E} [\sigma_z - \nu(\sigma_x + \sigma_y) + \alpha \Delta T]. \end{aligned} \right\} \quad (6-3)$$

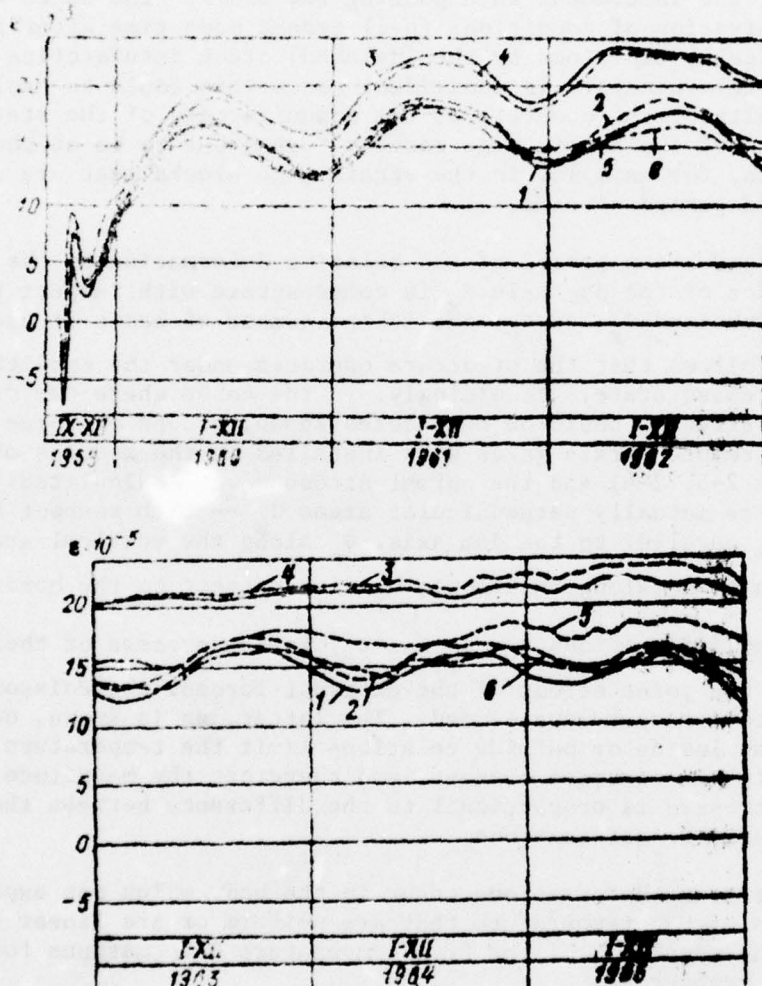


Figure 6-1. Sum of the deformations with respect to two mutually perpendicular directions in the 51-III-9 block.
1-2--in the xy plane; 3,4--in the xz plane; 5,6--in the yz plane.

The magnitude of the free temperature deformation $\alpha\Delta T$ at each given point in time is the basic component of the free linear deformation ϵ_0 measured by the remote strain gage and the stressed sample (the "shrinkage cone") entering into the composition of each tensometric point.

The calculation of the stresses by the measured deformations ϵ_{mx} , ϵ_{my} , ϵ_{mz} is performed by the formulas:

$$\sigma_x = E \frac{\epsilon_x' (1 - \nu) + \nu (\epsilon_y' + \epsilon_z')}{(1 + \nu)(1 - 2\nu)}, \quad (6-4)$$

$$\sigma_y = E \frac{\epsilon_y' (1 - \nu) + \nu (\epsilon_x' + \epsilon_z')}{(1 + \nu)(1 - 2\nu)},$$

$$\sigma_z = E \frac{\epsilon_z' (1 - \nu) + \nu (\epsilon_x' + \epsilon_y')}{(1 + \nu)(1 - 2\nu)},$$

$$\epsilon_x' = \epsilon_{nx} - \epsilon_0; \quad \epsilon_y' = \epsilon_{ny} - \epsilon_0; \quad \epsilon_z' = \epsilon_{nz} - \epsilon_0. \quad (6-5)$$

Substituting the value of $\epsilon'(x, y, z)$ with respect to (6-5 in (6-4), we obtain the known Duamel'-Neuman formulas following directly from (6-3).

As was noted in § 2-5, the calculation of the stresses by the measured deformations was made beginning with 1963 using a computer by two programs: the group of instruments comprising the fan rosette with the remote strain gage with respect to the normal to its plane and for the group of three mutually perpendicular remote strain gages. Successive calculations of the frequency modulus of the vibrations of the string of each instrument were introduced as the initial information ($M = f^2 \cdot 10^{-3}$, where f is the frequency in hertz), the coefficient $k = \Delta\epsilon/\Delta M$, the ordinates of the curve of the variation in time of the Young's modulus of the concrete and the stress relaxation.

By the first program the stresses were calculated in the following order. The corrections as the result of failure to observe the invariant conditions were introduced into the measured deformations ϵ_{mx} , ϵ_{my} and ϵ_{mz} (6-1)

$$C = \pm \frac{(\epsilon_{nx} + \epsilon_{ny}) - (\epsilon_{nz} + \epsilon_{nz})}{\epsilon_{nx} + \epsilon_{ny} + \epsilon_{nz} + \epsilon_{nz}}. \quad (6-6)$$

From the relative deformation with respect to each direction for each date the free deformation $\epsilon_0(\tau)$ is calculated for the same date

$$\epsilon_i'(\tau) = \epsilon_i(\tau) - \epsilon_0(\tau), \quad (6-7)$$

where $\epsilon_i(\tau) = \epsilon_{mi} \pm C$,

The corrections as the result of the Poisson effect are introduced into the relation deformations ϵ_i' with respect to (6-7)

$$\left. \begin{aligned} \epsilon_x' &= \frac{\theta'}{1+\nu} + \frac{\epsilon_0'}{(1+\nu)(1-\nu)} \\ \epsilon_y' &= \frac{\theta'}{1+\nu} + \frac{\epsilon_0'}{(1+\nu)(1-\nu)} \\ \epsilon_z' &= \frac{\theta'}{1+\nu} + \frac{\epsilon_0'}{(1+\nu)(1-\nu)} \end{aligned} \right\} \quad (6-8)$$

where $\theta = \epsilon_x' + \epsilon_y' + \epsilon_z'$.

For calculation of the variable Young's modulus of the concrete in time, the calculation of the normal stresses with respect to (6-4) is performed by the "step" method for which the following are calculated:

1) The increments of the relative deformation between the readings on two successive dates are $\Delta \epsilon(\tau_i) = \epsilon(\tau_i) - \epsilon(\tau_{i-1})$

$$\Delta \epsilon(\tau_i) = \epsilon(\tau_i) - \epsilon(\tau_{i-1}); \quad (6-9)$$

2) The stress increments in the same time intervals were

$$\Delta \sigma(\tau_i) = E(\tau_i) \Delta \epsilon(\tau_i), \quad (6-10)$$

where $E(\tau_i)$ is the average Young's modulus of the concrete for the time interval $\tau_i - \tau_{i-1}$;

3) The normal stresses for the given point in time

$$\sigma(t) = \sum_{i=1}^{n+1} \Delta \sigma(\tau_i). \quad (6-11)$$

The stresses considering the creep of the concrete for the given time intervals are calculated by the formula

$$\sigma^*(t) = \sum_{i=0}^{n+1} \Delta \sigma(\tau_i) k_p(t - \tau_i) \lambda(\tau_i), \quad (6-12)$$

where $\Delta \sigma$ is the increment of the stresses with respect to (6-10); k_p is the stress relaxation coefficient with respect to the relaxation curve for the age τ_0 ; λ is the empirical coefficient which considers the age at the time of application of each stress increment $\Delta \sigma(\tau_i)$ (see § 3-6).

The main deformations of the two-dimensional problem and their directions are calculated by the known formulas

$$\epsilon_r = \frac{1}{2} (\epsilon_x' + \epsilon_y' + \epsilon_{xy}' + \epsilon_{yz}') \pm \frac{1}{2} \sqrt{(\epsilon_x' - \epsilon_y')^2 + (\epsilon_{xy}' - \epsilon_{yz}')^2}. \quad (6-13)$$

$$\varphi = \frac{1}{2} \arctg \frac{\epsilon_{xy}' - \epsilon_{yz}'}{\epsilon_x' - \epsilon_y'}. \quad (6-14)$$

The principal stresses cannot be calculated by the measured deformations by the method of "steps," inasmuch as it is impossible to sum the stress increments with respect to different areas. Therefore they were calculated by the stress components calculated by the "step" method for each direction σ_x , σ_y , σ_{45} and σ_{135} with respect to (6-10) to (6-11). The principal stresses σ_1 and σ_2 and their directions ϕ are calculated with respect to (6-13) and (6-14) by substituting the corresponding values of σ_1 in place of ϵ_1 .

The maximum tangential stresses are calculated by substituting σ_1 and σ_2 in the formula

$$\sigma_{\max} \quad (6-15)$$

The stresses with respect to the second program were calculated by formulas (6-7)-(6-12).

When calculating the stresses, the Young's modulus and the stress relaxation coefficients which are variable in time but the same for all points of the investigated blocks determined by testing laboratory samples were used. As is known, the elasticity and creep characteristics of the concrete depend on the temperature of its hardening, and they are thus a function of not only time but also coordinates.

The effect of the variable temperature T on the intensity of growth of the Young's modulus under isothermal conditions can be determined from the curve $E = F(T)$ obtained experimentally for the constant temperature T_0 :

Let $T_0 = 20^\circ C$; then [75]

$$T_f = \frac{1}{F_E(T)} t_n \quad (6-16)$$

$$F_E(T) = \left(\frac{30+T}{50} \right)^{1.3} \quad (6-17)$$

The effect of the hardening temperature on the magnitude of the Young's modulus in the early age of the concrete is illustrated in Figure 6-2,a. With respect to the temperature buildup curves in the center of the summer blocks 65-III-9 (curve 2) and the fall block 61-II-10 (curve 3) and the experimental curve $E = F(T)$ (curve 1), the growth curves (2 and 3) of the Young's modulus to an age of 28 days were constructed. The smooth variation of the temperature is replaced by step variation with the duration of the constant temperature E in each i -th step Δt_i . The measured value of T for each age of the concrete is reduced to the reduced time t_{red} calculated by the formula

$$t_{red} = \sum_{i=1}^n \Delta t_i F_E(T_i) \quad (6-18)$$

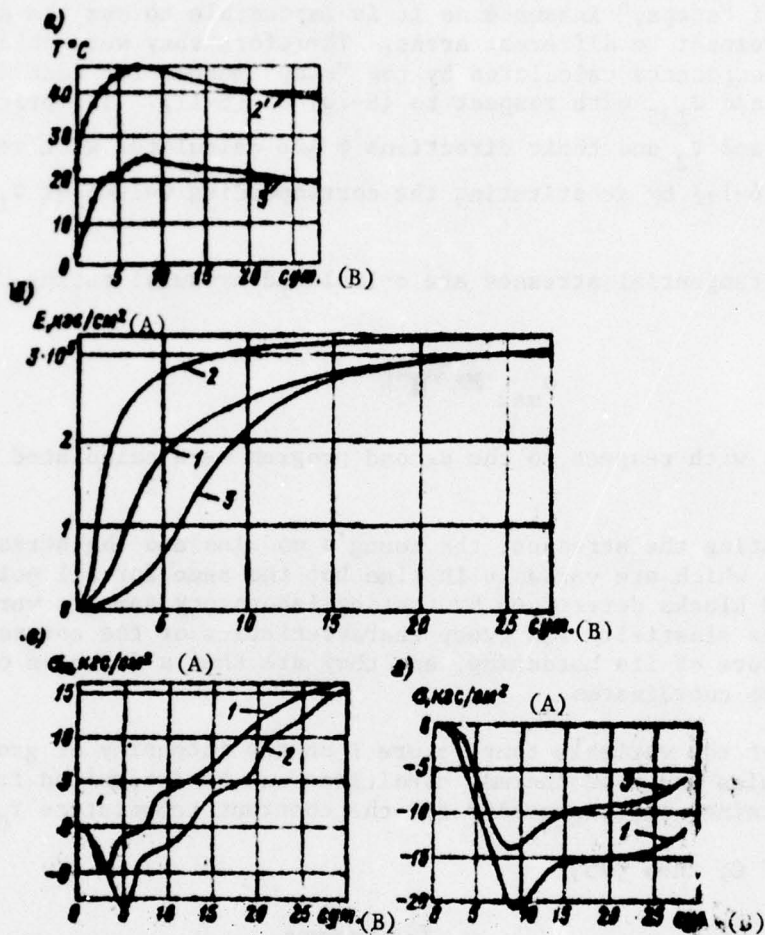


Figure 6-2. Young's modulus and stresses of the concrete as a function of its hardening temperature: a -- temperature at the center of the blocks; b -- Young's modulus; c, d -- stresses. 1 -- samples at 20° C ; 2 -- at the center of the summer blocks; 3 -- at the center of the fall block.

Key: A. kg-force/cm² B. days

As is obvious from Figure 6-2, consideration of the effect of the hardening temperature on the Young's modulus of the concrete has noticeable significance when calculating the stresses in the early age of the concrete.

For the nonstationary temperature fields of the poured blocks and great nonuniformity of the distribution of the temperature with respect to their cross section, the consideration of the effect of the hardening temperature on the Young's modulus of the concrete of each block presents significant

difficulties. The consideration of this effect on the creep characteristics of the concrete in general is impossible in the absence of theoretical and experimental data.

The insufficiently reliable values of the Young's modulus of the concrete used when calculating the stresses are the most significant source of error in the strain gage measurements in the massive concrete. These errors can be used somewhat by determining the elasticity and creep characteristics of the concrete directly in the concrete near the strain gaging rosette. However, for a number of organizational reasons, this method which is proposed by the author in 1962 [76] was not used at the Bratsk Hydroelectric Power Plant dam.

During the strain gage measurements in a massive block of concrete a number of errors are presented which are caused by the type of receiving equipment used (unstable frequency meters) and the location of the usual strain gage rosettes at the plants with naturally nonuniform stressed state [77]. The errors of this type did not occur in the Bratsk Hydroelectric Power Plant dam.

The distortion produced by the instrument having constant rigidity in the deformation (stress) field of the concrete, the rigidity of which increases gradually in time is an unavoidable source of error. Depending on the ratios of the rigidity of the concrete E_b and the strain gage meter E_T the deformations ϵ_T which are larger or smaller than the effective deformations of the concrete ϵ_b will be measured last. The distortion of the measured deformation can be estimated [78] by the formula

$$\delta = \frac{\epsilon_b}{E_T} - 1$$

$$1 + \frac{E_b}{E_T} \frac{d_T}{l_T} (1 - \nu^2)$$
(6-19)

where l_T and d_T are the length and diameter of the remote strain gage.

The actual deformation is as follows

$$\epsilon = \frac{\epsilon_b}{E_T} + \delta$$
(6-20)

The measured deformations will be less than the actual ones to values of $E_b = E_T$ and higher than them for $E_b > E_T$. The deviations of ϵ_b from ϵ_T for the ratio $l_T/d_T = 200/27 = 7.5$ are presented in Table 6-1.

The equivalent Young's modulus of the remote strain gages used is $1 \cdot 10^5$ kg-force/cm² and $2 \cdot 10^5$ kg-force/cm² (see § 2-5) which corresponds to the Young's modulus of the concrete at an age of 1 to 3 days. Inasmuch as the initial reading by the instruments is usually taken at an age of about 1 day, the reduced deformations were measured in the first 1 to 2 days of observations, and then as the concrete hardens, the measured deformations gradually exceeded their real values by an amount up to 10-15%.

Table 6-1

$E_0 : E_y$	0.2	0.4	0.6	1.0	1.5	2.0	3.0	4.0	8.0	100
k_s	-0.415	-0.210	-0.140	0	0.063	0.098	0.135	0.155	0.166	0.174
$1+k_s$	0.585	0.790	0.860	1.00	1.063	1.098	1.125	1.155	1.166	1.174

The defined measurement error occurs as a result of lack of correspondence of the base of the strain gage L to the size of the large filler of the concrete d. This error will be of insignificant for $L/d \geq 4-5$ [79-81]. Inasmuch as the majority of the remote strain gages at the Bratsk Hydroelectric Power Plant dam were installed in the concrete with $d \leq 40$ mm, the effect of the base of the strain gages on the measurement precision obviously is small. The fillers which are more than 40 mm in size in direct proximity to the strain gages were not permitted.

On the basis of the indicated errors, the surface of the concrete calculated by the measured deformations in it must be considered as approximate.

The formation of the stress fields of the high concrete dam poured in individual blocks is a complex process of the development of which depends on a set of factors. The concrete blocks which are laid at different times are distinguished by their temperature fields and deformative properties. In addition to the "natural" stresses which depend on the temperature field of the block itself, the "forced" stresses from the forces of interaction with the base and between adjacent blocks occur in it. For various combinations of the technological factors in the concrete blocks, different temperature fields and thermal stress fields are formed with which the stresses from the force factors are summed: the natural weight of the concrete and the hydrostatic load. The magnitude and the distribution of the total stresses are influenced by the opening of the constructed joints and the cracks which occur.

The modern methods of calculation permit us to determine with sufficient reliability temperature fields and the stress fields in a number of schemes which taken into account the basic factors influencing the formation of these fields [82-85]. However these schemes cannot consider all of the variety of the factors occurring in the construction process. Therefore, in spite of the nearness of the results of the tensometric measurements, their value is difficult to overestimate. They are the most reliable means of studying the process of occurrence and development of stresses in concrete massifs and its relation to the temperature, technological process and force factors.

Below we have the nature of formation of the stresses in the standard units with respect to location of the dam, the variation of these stresses and the course of the construction period of the stress state of the blocks during the constant operating time.

In connection with the nearness of the results of the tensometric measurements it is necessary to express the regrets that we were not able to use in this experiment instruments which measure the compressive stresses directly (of the type of the Karlson dynamometer [18, 86]). The comparison of the compressive forces calculated by the measured deformations of the stresses measured directly would offer the possibility of establishing the actual precision of the tensometric measurements and also the effect of the creep of the concrete on the stressed state of the concrete massifs.

6-2. Stresses in the Blocks next to the Rock

In calculation practice when considering the thermally stressed state of the structural elements it is divided into two zones: the contact zone in which the clamping effect of the base is felt and the extracontact or free zone, where the base has no effect on the temperature deformations.

For the columnar sections of the height of the contact zone of the bases usually taken as $0.5 l$, where l is the greatest size of the column in the plan view.

When calculating the thermal stresses the structural elements, depending on their configuration size, belong to the type of slabs or walls. The elements are called long in which the thermally stressed state of the central cross section is influenced by the conditions of attachment at the ends, and they are called short with the elements for which the effect of the ends must be considered. Both the long and short plates and walls are considered to operate in the state of planar deformation with a uniform temperature field.

The general expression for the increment of the thermal stresses at the time t in the clamped long plate on the distance y from the base when considering the variable Young's modulus of the concrete has the following form:

$$\Delta\sigma_x(y) = \sum_{i=1}^n E(\tau_i) \Delta T(\tau_i) k_{\text{clamp}} k_p(t - \tau_i), \quad (6-21)$$

where $\Delta T(\tau)$ is the temperature variation in the time interval $\tau_i - \tau_{i-1}$; $E(\tau)$ is the Young's modulus of the concrete which is averaged for the same time interval; α is the coefficient of linear expansion of the concrete; ν is the Poisson coefficient; k_{clamp} is the clamping coefficient; $k_p(t - \tau)$ is the stress relaxation coefficient for the time interval $t - \tau$.

In the middle cross section of the short plate clamp with respect to the base with the ratio $h/l = 0.1-0.5$

$$\Delta\sigma_x(y) = \left[\Delta\sigma_x(y) - \frac{8}{h} \sum P_i n_{x/h}(\xi_i) \right] k_{\text{clamp}}, \quad (6-22)$$

where $\Delta\sigma_x(y)$ is the stress in the long plate with respect to (6-21) for the same thermal state; P_i is the resultant of the stress $\Delta\sigma_x(y)_i$ in some section

of the vertical cross section of the plate; ξ_i is the relative coordinate of the plate (a_i) of application of the force P_i , $\xi_i = a_i/h$; $\eta_{xih}(\varepsilon_i)$ is the ordinate of the line of effect of the normal stresses at the point where the coordinate $x:h$ of application of the force P_i to the points of the plate at the points removed from the base to the height [deleted]; h is the height of the plate.

As is obvious from (6-21), the maximum normal stresses on the concrete block caused by the variation in the temperature are proportional to the clamping coefficient k_{clamp} . By the term usually we mean the ratio of the normal stress σ_x in the center of the concrete cross section of the block uniformly heated (cooling) with respect to the face to the stress of total clamping of $\sigma = E\alpha\Delta T$.

According to [87], in order to insure a monolithic nature of the structure during the construction and operating period it is necessary that in accordance with the contact zone ($0-0.2l$) the difference between the highest temperature of the concrete during its heating and the lowest temperature at the same point after its cooling not exceed the provisional ultimate tensile strength of the concrete. The mean steady state (operating) temperature is taken as the lowest temperature. Thus, the crack resistance of the block is defined by the temperature difference $\Delta T = T_{\max} - [deLETED]$ which for the columnar section is limited to a value of 18^{\max} to 20°C .

As experience shows, the crack formation in the clamped blocks usually occurs soon after the concrete is poured and is current for the difference in temperature occurring between the block and its base. The effort of the block to expand counters an obstacle on the part of the colder base as a result of which the tension arises in the contact zone of the latter, and compression in the concrete. As the concrete cools, the tension builds up in it, and compression builds up in the base until the temperature of the block in the base are comparable and they will decrease identically to the steady state temperature. The monolithic nature of the block, consequently, depends on the temperature difference $\Delta T = T_{\max} - T_{\text{cool}}$ which is limited to a value within the limits of 20 to 25°C .

Any rock base is pliable to one degree or another; the clamping of the block is elastic, and the value of k_{clamp} depends on the relative height of the block h/l and on the ratio of the Young's modulus of the concrete E_c and the base E_t . The solutions to the thermal elasticity theory obtained in recent times offer the possibility of establishing, depending on these parameters, the relative values of the normal stresses for different temperature distribution with respect to height of the block.

Thus, A. A. Khrapkov found the solution for the rectangular block in the halfplane. With uniform temperature fields, contact stresses, the main stresses on the outline and also the stresses in the middle of the vertical

cross section and a number of inside points of the dam and the rock for the cases of uniform heating and heating with respect to the linear law are defined [88].

The rock base always has vertical cracks and can not take the significant tensile stress. Therefore in a number of cases it is more correct to consider the rock base in the form of the halfband.

L. P. Trapeznikov and L. A. Ugol'nikov gave a solution for the "rectangular halfband-block" system. A study was made of three cases of the uniform temperature field: uniform heating with the ordinate T_0 , heating by the linear law $T = T_0 y/h$ and heating with respect to some curve $T = T_0 (y/h)^2$.

The temperature at the point located at a distance of y from the base can be written as follows:

$$T(y) = T_0 + T_0 \frac{y}{h} + T_0 \left(\frac{y}{h}\right)^2 \quad (6-23)$$

The stresses can be calculated by the formula

$$\sigma_x(y) = \frac{E_a T_0}{1 - \nu} k_{sym} + \frac{E_a}{1 - \nu} \frac{y}{h} k_{sym} + \frac{E_a}{1 + \nu} \left(\frac{y}{h}\right)^2 k_{sym} \quad (6-24)$$

Key: A. clamp

In Table 6-2 for the three values of h/l the relative stresses σ_x are presented in the proportions of $E_a T$ for the block in the halfplane with uniform cooling. The clamping coefficient decreases from the base to the upper surface of the block and also with an increase with respect to relative height of y/l . On the upper surface of the block k_{clamp} decreases with an increase in the ratio h/l and, beginning with the values of [deleted] = 0.3-0.4 has a negative sign. In practice the distribution of the contact stresses with respect to length of the block investigated in [88] is important. All of the stress components have the concentration near the angular points which is exhibited most of all in the stress distribution with respect to the horizontal area σ_y . In the rest of the contact cross section, stresses of opposite sign occur which are distributed in saddle shape with maximum at about $l/4$ (see Table 6-3). By this it is possible to explain the opening of the contact joints in the midsection of the cross section when heating the block and its edges when cooling observed at the Bratsk Hydroelectric Power Plant (see Chapter 7), the Ust'-Ilimsk Hydroelectric Power Plant and other dams [90]. This opening is more probable the smaller the ratio $E_{concrete}/E_t$. The distribution σ_x is in practice uniform.

The value of k_{clamp} is influenced for the relative height of the transition zone from the base temperature at the contact to the temperature of the concrete foundation.

Table 6-2

$\frac{h}{\ell}$	$\frac{x}{\ell}$	For $\frac{h_0}{\ell} = \frac{h}{\ell}$		
		1/3	1	2
0.10	0.0	0.89	0.71	0.54
	0.5	0.85	0.68	0.51
	1.0	0.55	0.67	0.50
0.2	0.0	0.72	0.57	0.46
	0.5	0.60	0.39	0.25
	1.0	0.53	0.29	0.13
0.4	0.0	0.72	0.57	0.46
	0.25	0.52	0.39	0.29
	0.5	0.30	0.19	0.13
	1.0	-0.11	-0.18	-0.19

Table 6-3

Cross section x/ℓ	$\sigma_y/E\alpha T$ in a block with $h/\ell = 0.20$ for different $E_{concrete}/E_r$			
	0	1/3	1	2
0.025	0.062	0.470	0.361	0.191
0.25	-0.193	-0.140	-0.099	-0.053
0.50	-0.116	-0.101	-0.074	-0.039

With an increase in the ratio h_{ter}/ℓ the value of k_{clamp} decreases:

$$\frac{h_{ter}/\ell}{k_{clamp}} : \dots : 0.15 \quad 0.25 \quad 0.5 \quad 1.0$$

The clamping coefficient k_{clamp} with respect to the data from the natural measurements can be defined as the ratio of the variable stress in the block variable to the stress $\sigma_T(\tau) = E\alpha\Delta T(\tau)$ calculated by the temperature variation. When calculating the stress considering the variable Young's modulus in time of the concrete

$$k = \frac{\int_0^1 \sigma_{measured}(t) dt}{\sigma_T(t)} = \frac{\sum \Delta \sigma(t) E(t)}{\sum \Delta T(t) E(t)}. \quad (6-25)$$

Key: 1. $\sigma_{measured}$

¹Here and hereafter, if it is not specially stipulated, the stresses are given without considering creep. The plus sign is the attention and the minus sign is compression.

In contrast to the block which cools uniformly with respect to the base, in the actual base simultaneously with the exothermal cooling there is also heat dissipation through the upper open surface and also to the base, and the temperature distribution with respect to the vertical section passing through the center of the block turns out to be nonuniform at the end of the exothermy peak. The stress state of the block is determined by this nonuniformity of the temperature diagram and its variations during the process of the cooling of the block. The covering of the block causes the distribution of the temperature and the stresses.

As the results of the natural observations indicate, the nonuniformity of the temperature distribution with respect to the horizontal direction has also a significant effect of the stressed state of the blocks in the contact zone similarly to how this occurs in the blocks in the extracontact zone. If we characterize this nonuniformity by the magnitude of the center-face temperature gradient, then for the blocks with open side faces the increase in the gradient at the center of the clamped block causes additional compression, and its decrease, tension. These additional stresses are summed with the stresses from the temperature distribution vertically.

The stresses σ_{measured} calculated by the deformations measured at the same point of the block next to the rock reflect the actual stressed state of the block caused by its joint operation with the base as a result of the temperature changes from the beginning of the measurements. If the stresses calculated by the measured temperature also reflect the actual thermal state of the block, then they will coincide with σ_{measured} .

In Figure 6-3 we have σ_{measured} and σ_T for nine points of the vertical section passing through the centers of the four blocks of column III of section 30 adjacent with respect to height beginning with the block next to the rock. The stresses σ_T are calculated by (6-24) beginning with the distribution of the measured temperature with respect to height of the blocks [91]. It is possible to note satisfactory agreement of σ_T with σ_{measured} in general.

In the absence of thermometers in the vertical section block and when calculating T with respect to the temperature increments at one point, for example, the center of the block, the calculated values of the coefficient will be variable until the ratio E_{concrete}/E_r stops varying, and the temperature distribution vertically will become uniform. From this time a nonlinear relation is established between σ_T and σ_{measured} of the type

$$\sigma_{\text{measured}} = \sigma_0 + \beta E_{\text{concrete}}, \quad (6-26)$$

where σ_0 is the stress caused by the nonuniformity of the temperature distribution, with respect to the cross sections of the block where the

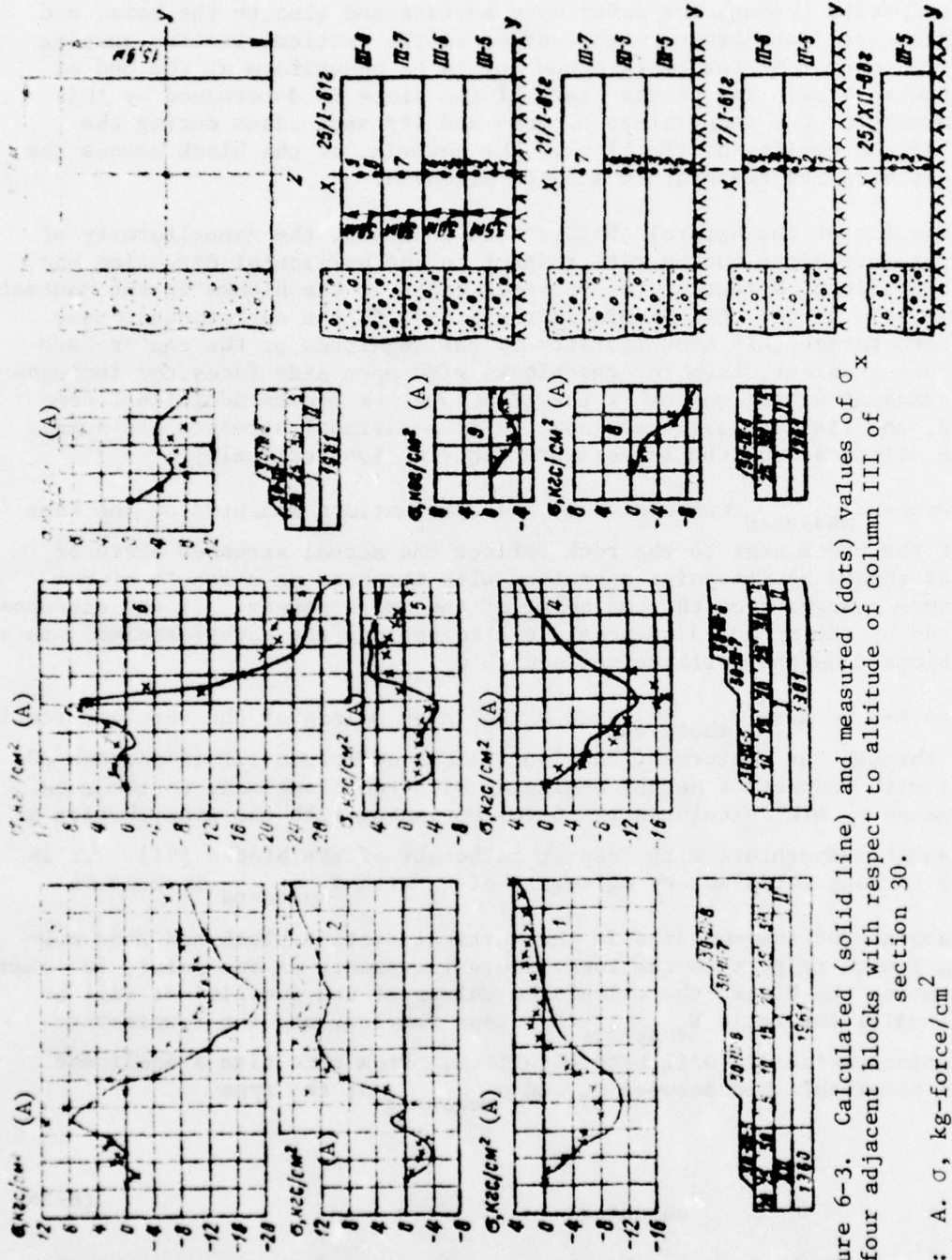


Figure 6-3. Calculated (solid line) and measured (dots) values of σ_x in four adjacent blocks with respect to altitude of column III of section 30.

Key: A. σ , kg-force/cm²

external relations, ΔT is the temperature variation at the investigated point. After covering the block, the function (6-26) is disturbed, and a new linear relation is established with the other angular coefficient k (see Figure 6-4).

The graphs of Figure 6-4 constructed by σ_{meas} and σ_T calculated as uniaxial with respect to deformations and temperature measured in the center of the block without considering the variable ratio $E_{\text{concrete}}/E_{\text{base}}$ on hardening of the concrete.

For the block 30-III-5 (Figure 6-3, 6-4) before covering, the coefficients are obtained at the lower point (0.2 m from the rock) $k = 0.8$, and for the center of the block $k = 0.33$, σ_T was calculated by various methods: considering the ends of the block with respect to (6-22), with respect to [88], considering the effective Young's modulus $E_{\text{eff}} = E_{\text{concrete}}/(1 + 0.1E_{\text{concrete}}/E_{\text{base}})$ [92]. Here values of k were obtained which are equal to 0.33, 0.36 and 0.42 respectively. At the upper point of the block the coefficient k , decreasing gradually, passed through negative values and after a year was 0.05-0.01.

It is possible to assume that the steady state values of the coefficient k calculated by the deformations measured at the center of the blocks and the temperature are close to k_{clamp} . These values of k usually differ from the theoretical values of k_{clamp} in the direction of a decrease as a result of the effect of the actual nature of the temperature distribution and the relative height of the transition zone. For example, for the four noncovered blocks on the rock k is within the limits of 0.22-0.33.

Let us consider the nature of development of the stresses in the blocks of the contact zone. At the center of the blocks during the process of the exothermal heating, the triaxial compressive stresses develop more the greater the magnitude and the longer the period of the temperature rise. The compression reaches a maximum at the exothermy peak, and then as the block cools it begins to decrease and becomes tension. The influx of heat from above after covering the block decreases the tensile stresses in its central region sharply, the minimum value of which compares with the second peak exothermy (Figure 6-5, a). The continuing cooling of the block is accompanied by a further increase in the tensile stresses. The greatest values of the latter occur with respect to the vertical areas (σ_x , σ_z) and the least, with respect to the horizontal areas (σ_y).

As a result of the seasonally variable temperature distribution with respect to the horizontal direction the stresses in the centers of the blocks acquire a periodic nature with maximum tension in the summer and minimum in the winter. The stresses σ_y are the most sensitive with respect to seasonal changes.

The development of the tensile stress in the concrete is caused by a combination of the temperature gradient between the block in its base, and the

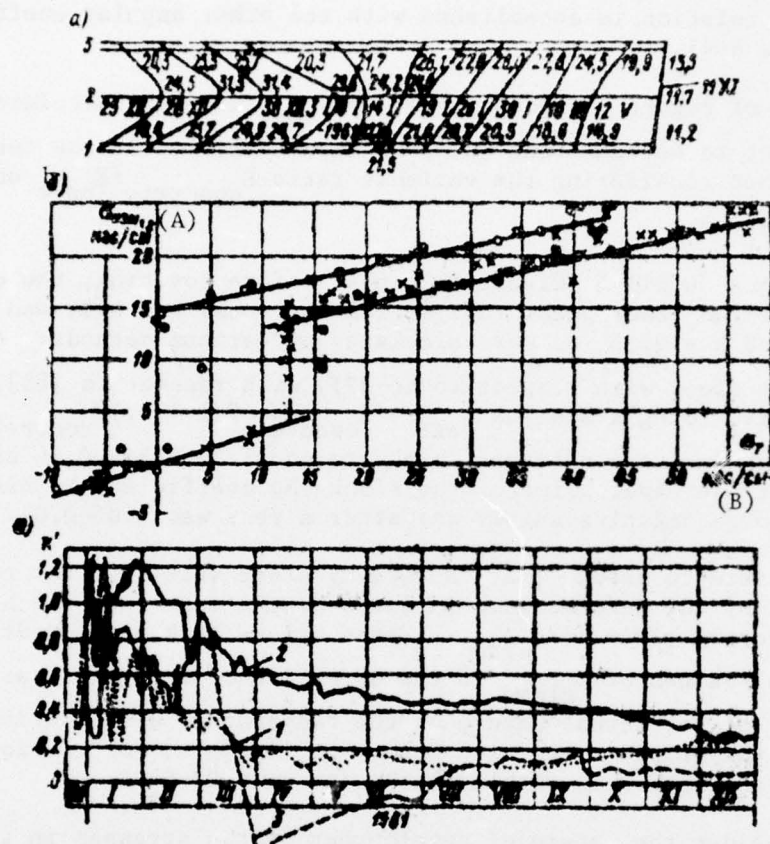


Figure 6-4. The stresses σ in the block 30-III-5 next to the rocks: a -- the temperature distribution with respect to the vertical cross section of the block; b -- the relation between the measured σ and $\sigma_T = E\alpha\Delta T$ calculated by the measured temperature ($\bar{\sigma}$ -- mean with respect to the vertical axis, \bullet -- mean with respect to the horizontal axis, \times -- at the center of the blocks); c -- the variation in time of the ratio of $\sigma : \sigma_T$ at the points of the vertical axis of the block (1 -- at the contact with the rock; 2 -- at the center of the block, 3 -- at the upper surface).

Key: A. σ_{meas} , kg-force/cm² B. kg-force/cm²

intensity of the cooling of the concrete, the times of covering of the block and the stacking of adjacent blocks in the plan view. The three blocks next to the rock of section 51 were poured in the summer of 1959 above the blocks 0.75-1 meter in thickness laid directly on the rock. The maximum temperature gradients of the center of the block-base were 25 to 30° C, that is, they exceeded the admissible values. In two blocks with high maximum temperature the intensive cooling (Table 6-4) led to an increase in

the tensile stresses faster than the increase in the tensile strength of the concrete (R_0^*). The relief of the stress σ_x in the block in the inside region

Table 6-4

Date (a)	Type (b)	Date (c)	(d) (e) (f)			Diameter, g) mm	Measure- (i)	Covered (j)	Cooling (k)	Center- (l)	σ_b (m)	σ_{max} (n)
			(d)	(e)	(f)							
III-4						15	0	4.5	-	11.7	11.7	11.7
IV-III-4						15	0	4.5	11	11.4	11.4	11.4
IV-IV-4						15	0	4.5	11	11.4	11.4	11.4
IV-III-4						15	0	4.5	11	11.4	11.4	11.4
IV-IV-4						15	0	4.5	11	11.4	11.4	11.4
V-5.0						15	0	4.5	-	11.5	11.5	11.5
IV-V-5						15	0	4.5	-	11.5	11.5	11.5
IV-IV-5						15	0	4.5	-	11.5	11.5	11.5
IV-IV-6						15	0	4.5	-	11.5	11.5	11.5
IV-IV-7						15	0	4.5	-	11.5	11.5	11.5
IV-IV-8						15	0	4.5	-	11.5	11.5	11.5
IV-IV-9						15	0	4.5	-	11.5	11.5	11.5
IV-IV-10						15	0	4.5	-	11.5	11.5	11.5
IV-IV-11						15	0	4.5	-	11.5	11.5	11.5
IV-IV-12						15	0	4.5	-	11.5	11.5	11.5
IV-IV-13						15	0	4.5	-	11.5	11.5	11.5
IV-IV-14						15	0	4.5	-	11.5	11.5	11.5
IV-IV-15						15	0	4.5	-	11.5	11.5	11.5
IV-IV-16						15	0	4.5	-	11.5	11.5	11.5
IV-IV-17						15	0	4.5	-	11.5	11.5	11.5
IV-IV-18						15	0	4.5	-	11.5	11.5	11.5
IV-IV-19						15	0	4.5	-	11.5	11.5	11.5
IV-IV-20						15	0	4.5	-	11.5	11.5	11.5
IV-IV-21						15	0	4.5	-	11.5	11.5	11.5
IV-IV-22						15	0	4.5	-	11.5	11.5	11.5
IV-IV-23						15	0	4.5	-	11.5	11.5	11.5
IV-IV-24						15	0	4.5	-	11.5	11.5	11.5
IV-IV-25						15	0	4.5	-	11.5	11.5	11.5
IV-IV-26						15	0	4.5	-	11.5	11.5	11.5
IV-IV-27						15	0	4.5	-	11.5	11.5	11.5
IV-IV-28						15	0	4.5	-	11.5	11.5	11.5
IV-IV-29						15	0	4.5	-	11.5	11.5	11.5
IV-IV-30						15	0	4.5	-	11.5	11.5	11.5
IV-IV-31						15	0	4.5	-	11.5	11.5	11.5
IV-IV-32						15	0	4.5	-	11.5	11.5	11.5
IV-IV-33						15	0	4.5	-	11.5	11.5	11.5
IV-IV-34						15	0	4.5	-	11.5	11.5	11.5
IV-IV-35						15	0	4.5	-	11.5	11.5	11.5
IV-IV-36						15	0	4.5	-	11.5	11.5	11.5
IV-IV-37						15	0	4.5	-	11.5	11.5	11.5
IV-IV-38						15	0	4.5	-	11.5	11.5	11.5
IV-IV-39						15	0	4.5	-	11.5	11.5	11.5
IV-IV-40						15	0	4.5	-	11.5	11.5	11.5
IV-IV-41						15	0	4.5	-	11.5	11.5	11.5
IV-IV-42						15	0	4.5	-	11.5	11.5	11.5
IV-IV-43						15	0	4.5	-	11.5	11.5	11.5
IV-IV-44						15	0	4.5	-	11.5	11.5	11.5
IV-IV-45						15	0	4.5	-	11.5	11.5	11.5
IV-IV-46						15	0	4.5	-	11.5	11.5	11.5
IV-IV-47						15	0	4.5	-	11.5	11.5	11.5
IV-IV-48						15	0	4.5	-	11.5	11.5	11.5
IV-IV-49						15	0	4.5	-	11.5	11.5	11.5
IV-IV-50						15	0	4.5	-	11.5	11.5	11.5
IV-IV-51						15	0	4.5	-	11.5	11.5	11.5
IV-IV-52						15	0	4.5	-	11.5	11.5	11.5
IV-IV-53						15	0	4.5	-	11.5	11.5	11.5
IV-IV-54						15	0	4.5	-	11.5	11.5	11.5
IV-IV-55						15	0	4.5	-	11.5	11.5	11.5
IV-IV-56						15	0	4.5	-	11.5	11.5	11.5
IV-IV-57						15	0	4.5	-	11.5	11.5	11.5
IV-IV-58						15	0	4.5	-	11.5	11.5	11.5
IV-IV-59						15	0	4.5	-	11.5	11.5	11.5
IV-IV-60						15	0	4.5	-	11.5	11.5	11.5
IV-IV-61						15	0	4.5	-	11.5	11.5	11.5
IV-IV-62						15	0	4.5	-	11.5	11.5	11.5
IV-IV-63						15	0	4.5	-	11.5	11.5	11.5
IV-IV-64						15	0	4.5	-	11.5	11.5	11.5
IV-IV-65						15	0	4.5	-	11.5	11.5	11.5
IV-IV-66						15	0	4.5	-	11.5	11.5	11.5
IV-IV-67						15	0	4.5	-	11.5	11.5	11.5
IV-IV-68						15	0	4.5	-	11.5	11.5	11.5
IV-IV-69						15	0	4.5	-	11.5	11.5	11.5
IV-IV-70						15	0	4.5	-	11.5	11.5	11.5
IV-IV-71						15	0	4.5	-	11.5	11.5	11.5
IV-IV-72						15	0	4.5	-	11.5	11.5	11.5
IV-IV-73						15	0	4.5	-	11.5	11.5	11.5
IV-IV-74						15	0	4.5	-	11.5	11.5	11.5
IV-IV-75						15	0	4.5	-	11.5	11.5	11.5
IV-IV-76						15	0	4.5	-	11.5	11.5	11.5
IV-IV-77						15	0	4.5	-	11.5	11.5	11.5
IV-IV-78						15	0	4.5	-	11.5	11.5	11.5
IV-IV-79						15	0	4.5	-	11.5	11.5	11.5
IV-IV-80						15	0	4.5	-	11.5	11.5	11.5
IV-IV-81						15	0	4.5	-	11.5	11.5	11.5
IV-IV-82						15	0	4.5	-	11.5	11.5	11.5
IV-IV-83						15	0	4.5	-	11.5	11.5	11.5
IV-IV-84						15	0	4.5	-	11.5	11.5	11.5
IV-IV-85						15	0	4.5	-	11.5	11.5	11.5
IV-IV-86						15	0	4.5	-	11.5	11.5	11.5
IV-IV-87						15	0	4.5	-	11.5	11.5	11.5
IV-IV-88						15	0	4.5	-	11.5	11.5	11.5
IV-IV-89						15	0	4.5	-	11.5	11.5	11.5
IV-IV-90						15	0	4.5	-	11.5	11.5	11.5
IV-IV-91						15	0	4.5	-	11.5	11.5	11.5
IV-IV-92						15	0	4.5	-	11.5	11.5	11.5
IV-IV-93						15	0	4.5	-	11.5	11.5	11.5
IV-IV-94						15	0	4.5	-	11.5	11.5	11.5
IV-IV-95						15	0	4.5	-	11.5	11.5	11.5
IV-IV-96						15	0	4.5	-	11.5	11.5	11.5
IV-IV-97						15	0	4.5	-	11.5	11.5	11.5
IV-IV-98						15	0	4.5	-	11.5	11.5	11.5
IV-IV-99						15	0	4.5	-	11.5	11.5	11.5
IV-IV-100						15	0	4.5	-	11.5	11.5	11.5
IV-IV-101						15	0	4.5	-	11.5	11.5	11.5
IV-IV-102						15	0	4.5	-	11.5	11.5	11.5
IV-IV-103						15	0	4.5	-	11.5	11.5	11.5
IV-IV-104						15	0	4.5	-	11.5	11.5	11.5
IV-IV-105						15	0	4.5	-	11.5	11.5	11.5
IV-IV-106						15	0	4.5	-	11.5	11.5	11.5
IV-IV-107						15	0	4.5	-	11.5	11.5	11.5
IV-IV-108						15	0	4.5	-	11.5	11.5	11.5
IV-IV-109						15	0	4.5	-	11.5	11.5	11.5
IV-IV-110						15	0	4.5	-	11.5	11.5	11.5
IV-IV-111						15	0	4.5	-	11.5	11.5	11.5
IV-IV-112						15	0	4.5	-	11.5	11.5	11.5
IV-IV-113						15	0	4.5	-	11.5	11.5	11.5
IV-IV-114						15	0	4.5	-	11.5	11.5	11.5
IV-IV-115						15	0	4.5	-	11.5	11.5	11.5
IV-IV-116						15	0	4.5	-	11.5	11.5	

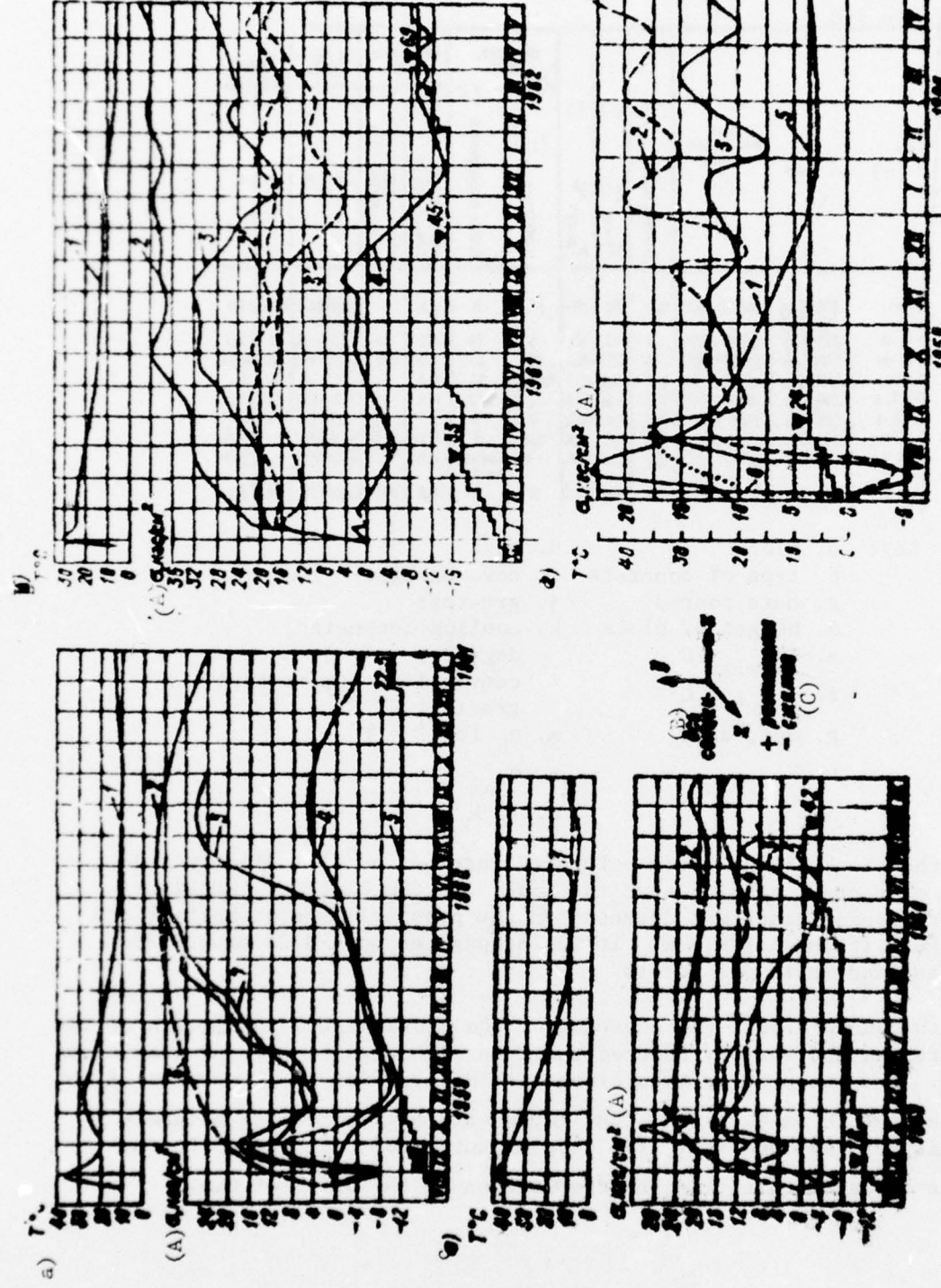


Figure 6-5. Development of stresses in the center of blocks near to the core. 1 - temperature T ; 2 - σ_x^* ; 3 - σ_z^* ; 4 - σ_1 [deleted]; 5 - R^* ; 6 - $kE\Delta T$.
Key: A. σ , kg-force/cm² B. section axis C. + tension, - pressure

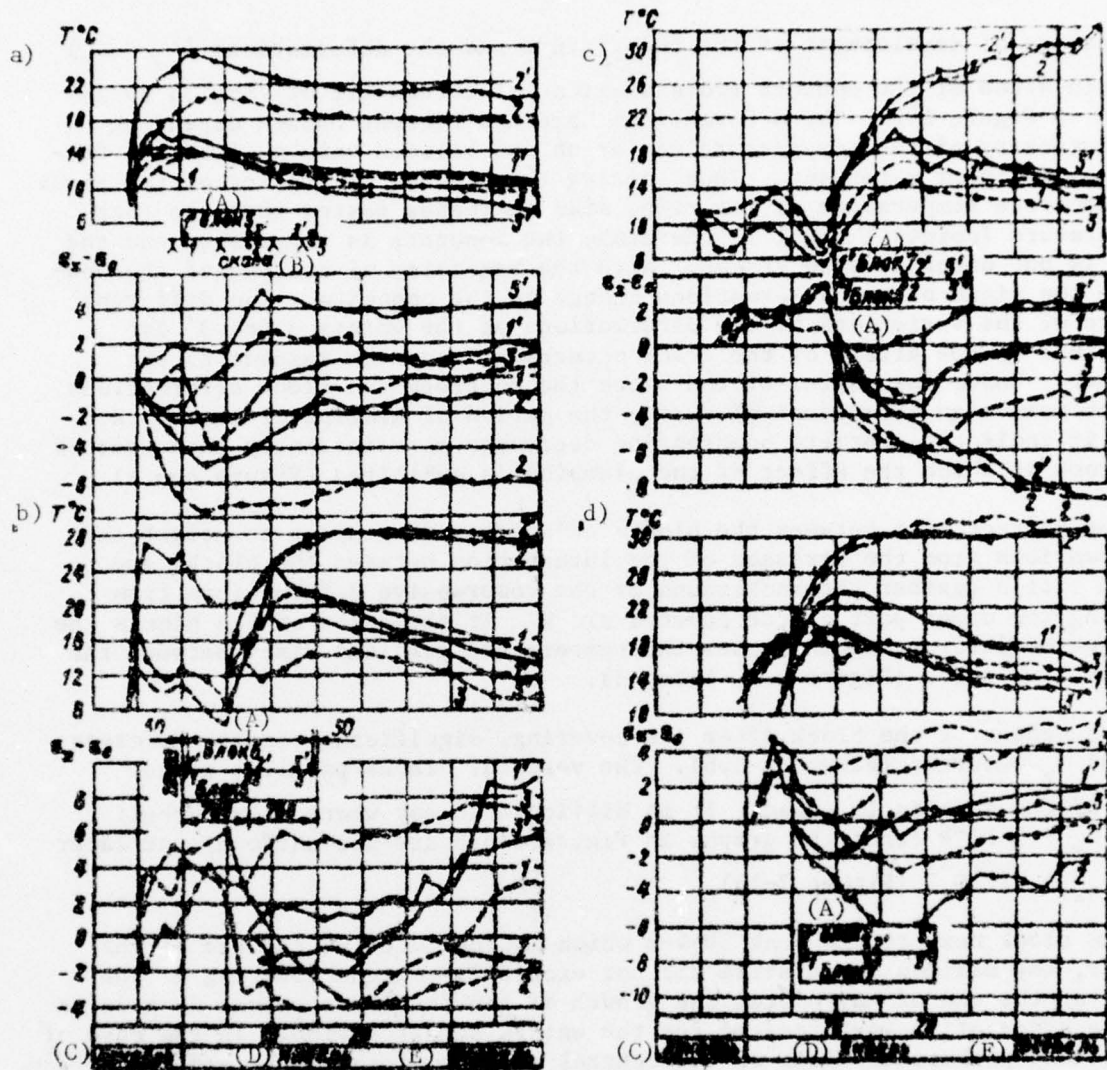


Figure 6-6. Development of the temperature and deformations of the side of the compact cross section of the adjacent blocks with respect to height (the curve numbers correspond to the [deleted] points on the schematics of the block).

Key:	A, block	C, December	E. February
	B, rock	D, January	

In Figure 6-5,a,c, the simultaneous [deleted] increase in the stress σ_z 8 to 9 months after pouring the blocks attracts attention. This is explained obviously by the opening of the construction joint between the halfblocks

a and c after the tensile stresses compensated for the compression occurring in the joint during heating of the halfblocks.

The nature of development of the temperature and the deformations ($\varepsilon_x - \varepsilon_0$) on both sides of the contact cross sections of column III of section 30 is shown in Figure 6-6. The deformations have a different nature depending on the intensity of the temperature variation and various values of the coefficients of linear expansion. Thus, during the process of heating of the block the concrete temperature on its right side increases faster than the rock temperature (points 1 and 1'); therefore the concrete is compressed and the rock is put under tensile stress. With the beginning of cooling of the concrete the signs of the deformations change to the opposite. The different nature of the variations of the deformations at the points 3 and 3' is explained by the effect of the crack occurring here with respect to the contact. Under the center of the block the concrete and block deformations of the same sign (compression) during the period of heating of the block. When it cools the concrete compression decreases more intensely than that of the rock in which the effect of the clamping is exhibited (Figure 6-6,a).

In the contact zone between the blocks adjacent with respect to height the deformations from the stresses of the interaction between the blocks are noted little against the background of the compressive deformations from heating the upper part of the covered block. At the edges of the blocks the elongation deformations increase the temperature gradient rises between the blocks 1, 3 and 2 (Figure 6-6, b, c, d).

At the center of the block after its covering, significant tensile stresses σ_x and σ_z occurred (Figure 6-5,b). The vertical cracks parallel to the axis of the section is fixed. It is difficult to say where it occurred: for $\sigma_z = 5 \cdot 10^{-5}$ (then the graphs in Figure 6-5,b are not uniform) or later for $\sigma_z = 12 \cdot 10^{-5}$ (Figure 7-14).

In the block next to the rock 30-V-5 which is concreted at the end of the winter, the maximum temperature did not exceed $31^\circ C$; the covering of the block at the end of May halted the growth of the tensile stresses at a value on the order of 14 kg-force/cm^2 for the entire summer period. In the case of slow cooling characteristic of the central regions of the fifth and sixth blocks, the tensile stresses reached a value on the order of 26 kg-force/cm^2 in the aging of the concrete above [deleted] and then they decreased slowly. The growth of the normal stresses σ_y under the effect of the hydrostatic load on the dam and their seasonal variations as a result of the changes in the center-face temperature gradient and also the seasonal horizontal displacements of the dam is characteristic. Obviously the latter are caused by the continuing periodic variations of σ_y after covering the expanded joints (Figure 6-7).

6-3. Stresses in the Blocks in the Extracontact Zone

The dam blocks in which the remote strain gages are placed are at a height from the base of 12 to 15 meters and 29-30 meters, that is, they belong to the extracontact zone.

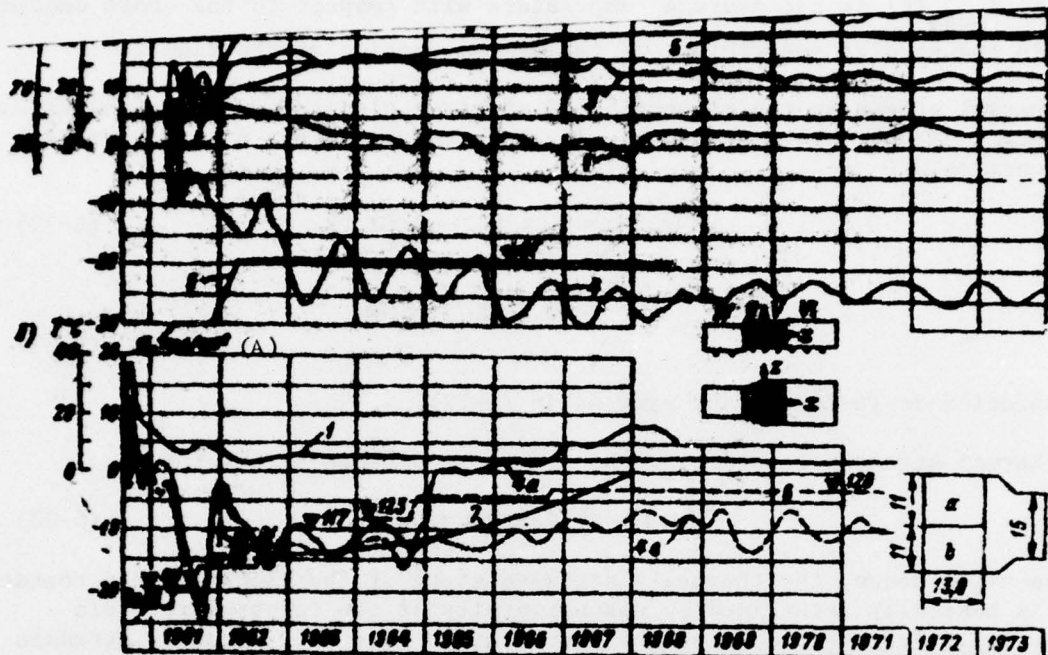


Figure 6-7. Normal stresses in the blocks next to the rock: a -- at the center of the block 30-V-5; b -- at the pressure face of the block 30-L-5. 1 -- temperature; 2 -- σ_x ; 3 -- σ_z ; 4 -- σ_y ; 4a and 4b -- σ_y in the half-blocks a and b; 5 -- headwater level; 6 -- concrete pouring schedule; 7 -- model σ_y considering the counterpressure.

Key: A. σ , kg-force/cm²

With a distance between the longitudinal joints of 13.8 meters the effect of the base can be considered in practice imperceptible even at a height on the order of 7 meters and with uniform temperature field of the block in the higher lying part of the section it is possible to consider it as a free plate.

The thermal stresses $\sigma(x, t)$ at the point with the coordinate of the free long plate at the time t when considering the variable Young's modulus of the concrete in time is determined by the expression:

$$\sigma(x, t) = \sum_{i=1}^n \Delta \sigma_i = \frac{E}{1 - \nu} \sum_{i=1}^n E(t_i) \Delta [T(x, t) - T_{cp}(t) - k(t)x], \quad (6-27)$$

where $\Delta \sigma_i$ is the stress increment in the time interval (deleted), Δt_i is the calculated time interval, $t = \sum_{i=1}^n \Delta t_i$, n is the number of different intervals

Δt_i ; $E(t_i)$ is the mean value of the Young's modulus with the time interval Δt_i ; $T(x, t)$ is the ordinate of the temperature curve at the point x at the time t ; $T_{\text{mean}}(t)$ is the average temperature with respect to the cross section; $k(t)$ is the angular coefficient of the closing section at the time t .

The thermal stress in the midsection of the free plate considering the unloading effect of the joints at the spacing between the joints d is determined by the function:

$$\sigma(x, t)_d = \sigma(x, t) - \Delta \sigma(x, t)_d, \quad (6-28)$$

where

$$\Delta \sigma(x, t)_d = \frac{1}{d} \sum P_l \eta_{xd}(t_l). \quad (6-29)$$

The notation in (6-29) is the same as in (6-22).

The thermal stresses considering the creep are defined by the formula:

$$\sigma^*(x, t) = \sum \Delta \sigma(x_i) k_p(t - t_i). \quad (6-30)$$

As was noted above, the thermally stressed state of the blocks of the contact zone is basically determined by the uniformity of the temperature field vertically. For the blocks of the extracontact zone the thermally stressed state is caused by the nonuniformity of the temperature field with respect to the horizontal direction.

During the isothermal heating of the block the greatest rise in temperature occurs in the middle and lower sections of it in which the compressive stresses developed, and in the [deleted] cooling lateral surfaces, tensile stresses. The system of stresses in the block for uniform temperature field is self-equalized and therefore the increase in the stress in its edges is accompanied by an increase in the compression central region and vice versa. Accordingly, for seasonal variations in the ambient temperature, periodic stress variations take place in the block. In the central region the compression increases in the cold part of the year or decreases in the warm part of the year. On the lateral surfaces the seasonal variations of the stresses have a reversible nature. In the steady state after equalization of the temperature with respect to cross section on the edges of the block the compressive stresses remain, and in the central region small tensile stresses.

Under the conditions of a one-dimensional temperature field the seasonal variations of the temperature distribution with respect to the horizontal cross section caused the greatest effect on the stresses with respect to areas parallel to the plane of the temperature field. For the blocks of the first columns this is σ_z , and for the blocks of the inside region σ_x . In all cases the stresses σ_y turn out to be most sensitive to the seasonal temperature variations [19].

In the uncovered blocks the cooling of the concrete on the upper surface is accompanied by the development of the tensile stresses here which, as a result of the inflow of heat from above after covering the block, become compressive. For regular stacking of the blocks with small time intervals the magnitude of these stresses usually exceeds the tension caused by the interaction with respect to the contact of the two blocks (Figure 6-6). If the block remains uncovered for a long time, the tensile stresses in its upper part reach a significant amount, [deleted] of these stresses is propagated downward, and a vertical crack can occur in the block. The crack can occur soon after covering of the block when the tensile stresses accompanying the heating of the upper block, summing with the attention occurring in the block exceed the compression, the inflow of heat from above (see Table 7). When laying a block of the extracontact zone on the all base [deleted] the stressed state of the block in the initial period will [deleted] by the temperature gradient vertically between the [deleted] and the block and the stresses of the latter will develop just as in the elastic clamp block. They are satisfactorily approximated by calculations of the elastically clamped block [deleted] the clamping coefficient [deleted] 9.4. Only after some long period of time [deleted] the stresses begin to [deleted] by the nature of variation in time with the thermal stresses calculated by (6-27).

Then the block operates as free plate, the comparison of the measured calculated stresses is better the greater the detail of the temperature diagrams of the more correctly the boundary conditions are taken into account and, in particular, the unloading effect of the vertical joints. For spacing between the latter of 13.8 meters, this influence highly noticeably (Figure 6-8) decreases the thermal stresses from the seasonal fluctuations of the air temperature [93].

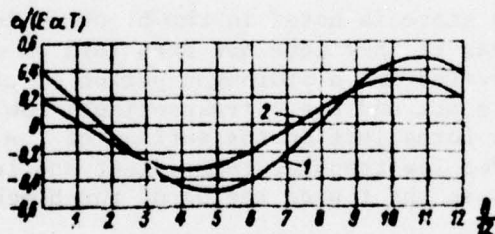


Figure 6-8. Calculated stress on the surface of the block when considering the stress relieving effect of the joints located every 13.8 meters. 1 -- stresses of the elastic problem; 2 -- the same considering the creep of the concrete.

As is obvious from what has been discussed, the basic condition of the favorable development of the stresses in the blocks of the extracontact zone is their regular stacking for which with respect to vertical areas in the center of the blocks over a prolonged period of time the compressive stresses developed. For deviations from the regular stacking occurring in many cases

tensile stresses arise with respect to these areas immediately after [deleted] exothermy.

The nature of the development of the stresses of the center of the blocks of the extracontact zone caused by aging of the base and the covering times (Table 6-4) is illustrated by Figure 6-9 and 6-10. In each of the summer blocks, judging by the measured deformations, cracks occur. In the block 51-I-10,a (Figure 6-9,a) the relief of σ_z indicates the spread downward of the crack which was mentioned earlier (Figure 6-5,d). In block 65-III-9 (Figure 6-9,b), a crack occurred parallel to the axis of the section when σ_x exceeded σ_p^* . Then in block 30-IV-9 with favorable development of the stresses at the end of winter, a horizontal crack arose (Figure 6-9,c) causing stress relief at the location of the leveling rosette.

In Figure 6-10 we have the stress development for the period of 12[deleted] in the fall block 51-III-9 laid in the base three weeks old and covered at 17 days. The average intensity of cooling of the concrete in the uncovered block between this time at a point at the distance from the open surface of 10, 150, 225 and 290 cm was correspondingly 0.8, 0.5, 0.4 and 0.13 deg/day.

In connection with the nonuniform temperature distribution vertically the tensile stress at the center of the block occur from the time of the exothermy peak. After only a year the measured σ_z began to coincide with the calculated values with respect to (6-27) with respect to nature of variation time differing significantly from them with respect to magnitude. The main stresses of the planar problem have a periodic nature in accordance with the nature of thermal stresses. The average vertical stresses σ_z were stabilized at the ~22 kg-force/cm² level, which is 7-8 kg-force/cm² greater than the mean compression [deleted] of the concrete of column III.

A satisfactory stressed state is noted in the blocks which are poured during the cold part of the year if they have not been laid on old concrete and they were not left uncovered for a prolonged period of time. The low temperature of the concrete mix and the correspondingly low maximum concrete temperature, the winter forms left on the surface of the blocks to the warm part of the year, insured low temperature gradient and less intense buildup of the tensile stresses in the inside region of the blocks than in the summer blocks.

As an example let us consider the stress state of the blocks of the adjacent concrete pouring levels subsequently laid with small time intervals in the lower part of column III of the section.

The stresses in the adjacent blocks of the columnar mass with respect to altitude. [deleted] 8 blocks (stages 5 to 12) were poured during the period from the end of December 1960 to the beginning of March 1961. After a 2.5-month break, four more blocks were poured over a period of 3 weeks (stages 13-16).

The columnar massif erected to a height of 36 meters was left open for 9 months in the lower section on three sides and in the upper section on 4 sides.

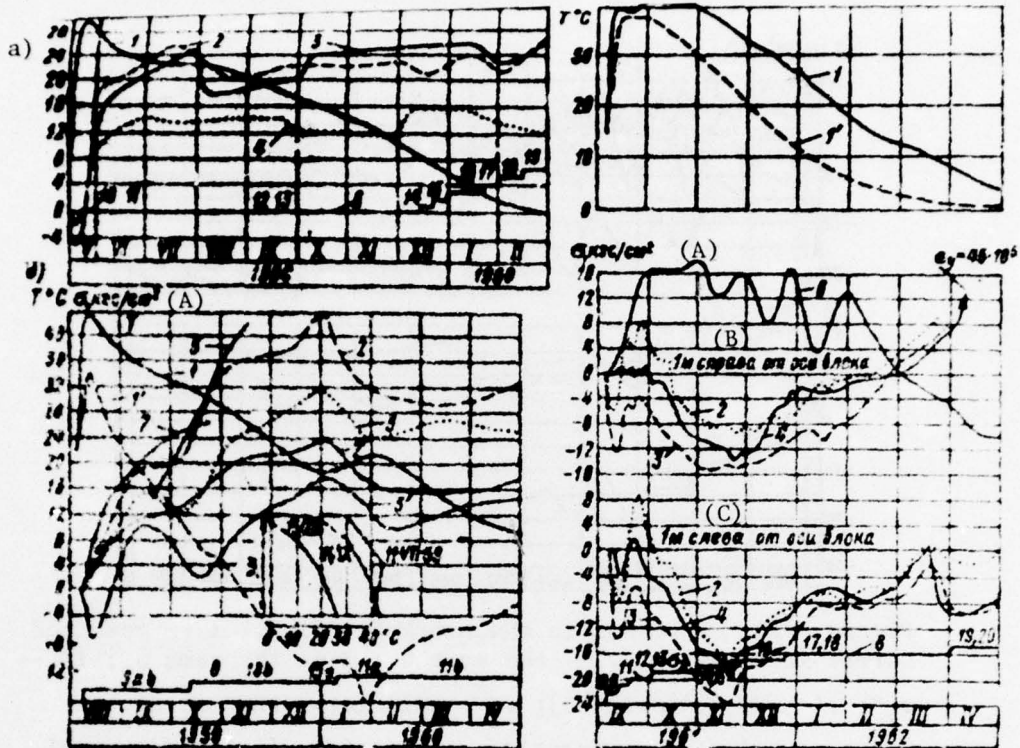


Figure 6-9. Nature of development of the normal stresses in the extracontact zone blocks during the period of exothermal heating and subsequent cooling of the block: a -- 51-I-10a, b -- 65-III-9, c -- 30-IV-9. 1 -- T; 1' -- T_{surf} ; 2 -- σ_x ; 3 -- σ_z ; 4 -- σ_y ; 2' -- σ_x^* ; 3' -- σ_z^* ; 5 -- σ_T ; 6 -- $\sigma_{x,surf}$; 7 -- R_p^* ; 8 -- concrete pouring schedule.

Key: A. kg-force/cm²

B. 1 meter to the right of the block axis

C. 1 meter to the left of the block axis

The maximum temperature in the winter blocks did not exceed 30-32° C, and in the upper summer blocks, 37° C. The average cooling rate in the central part of the lower blocks was 2 deg/month, and in the upper ones, about 4.5 deg/month. The concrete temperature at the edges of the blocks reached -20° C in the first winter with an average cooling rate of 6 to 7 deg/month.

The comparatively regular laying of the blocks with an average rate of 10 to 12 m/month insured the development in the most stresses with respect to the free plate scheme. The normal compressive stresses occurring in the central region of the blocks with respect to the vertical areas (σ_x , σ_z)

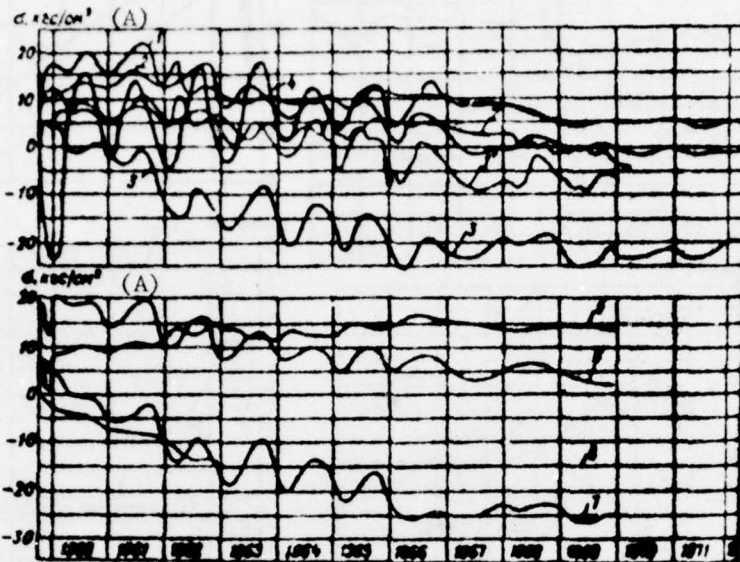


Figure 6-10. Stresses in the block 51-III-9. 1 -- measured normal stresses σ_x ; 2 -- the same σ_z ; 3 -- the same σ_y ; 1' -- σ_x^* ; 2' -- σ_z^* ; [deleted]; 4 -- calculated thermal stress σ_T ; 5 -- principal tangential stress; 6 -- [deleted] normal stress σ_1 ; 7 -- the same σ_z ; 8 -- average mass of the concrete of the column III.

Key: A. σ , kg-force/cm²

after 2 or 3 months turned into small tensile stresses or remained compressive (Figure 6-10). The periodic nature of the oscillations of σ_z and σ_y varied in accordance with the variation of the nature of the fluctuations of the center-face temperature gradients and stabilized after covering the expanded joints in May 1967 (Figure 6-11). The average value of σ after stabilization of the seasonal fluctuations exceeds the average stress from the weight of the concrete of the third column. The mean compression with respect to the vertical areas (σ_z) also increased gradually. The stress of σ_z depends on the temperature distribution with respect to the transverse stress, it is insignificant and varies little with time.

The effective nature of the temperature fields of the column opened on three sides for a long period of time differs from the uniform one, and calculation of the stresses by (6-28) and (6-29) can only give an approximate coincidence with the measured stresses. The results of this calculation for block 30-III-[illegible] using the P. M. Varvak lines of influence for the square plate

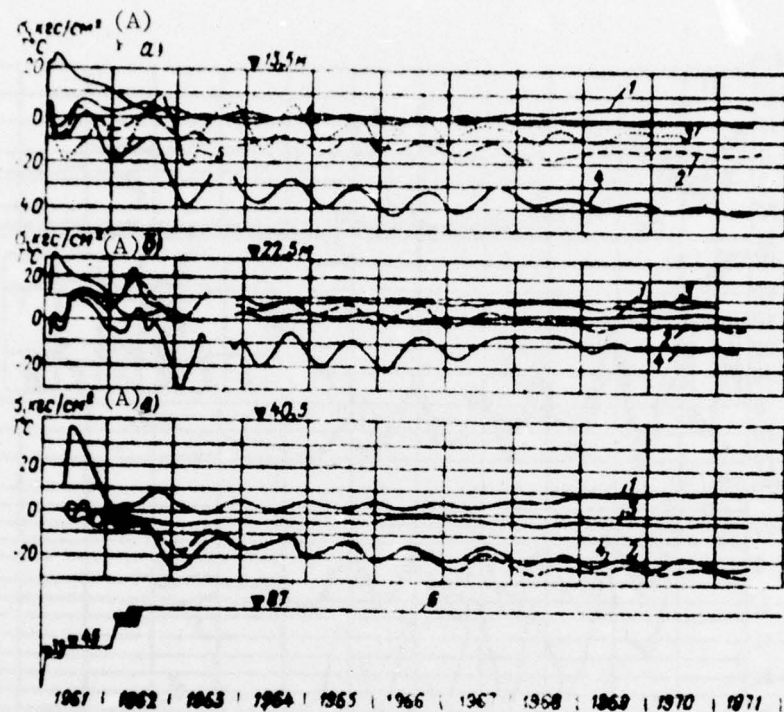


Figure 6-11. Normal stresses in the centers of the blocks of column III of section 30: a -- 30-III-6; b -- 30-III-9; c -- 30-III-15. 1 -- temperature; 2 -- σ_x , 3 -- σ_z ; 4 -- σ_y ; 5 -- σ_x calculated by the temperature diagram; 6 -- concrete pouring schedule.

Key: A. σ , kg-force/cm²

are presented in Figure 6-12,b. The calculated σ_T confirms the temperature origin of the measured σ_x . In the stabilized state the latter exceeds σ_T with respect to the magnitude of compression, and the defect of the hydrostatic load is felt possibly in this.

The effect of the significant compressive stresses on the vertical areas and at the open surfaces of the column is significant. The magnitude of σ_x at a distance of 0.5-0.9 m from the surfaces is 15-20 kg-force/cm² (Figure 6-12). The effect of the temperature state of the expanded joints on the stresses at the edges of the blocks is illustrated highly clearly by the graphs of the strains $\sigma_x - \sigma_0$ and $\sigma_y - \sigma_0$ measured on both sides of blocks 30-III-9 (see Figure 6-12,a).

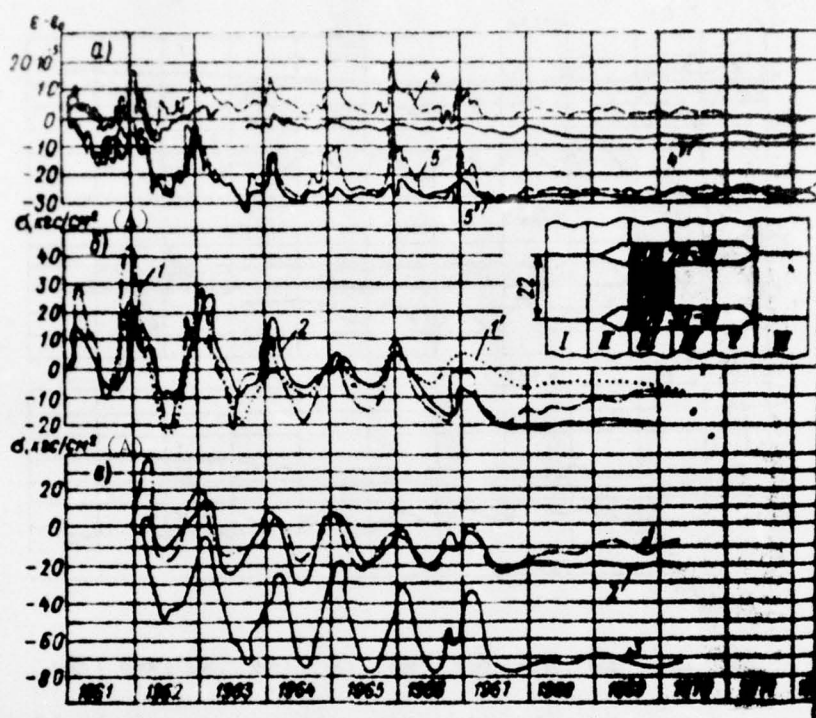


Figure 6-12. Stresses (strains) of concrete in the lateral surfaces of the blocks: a - 30-III-9; b -- 30-III-6; c -- 65-IV-16. 1 -- σ_T ; 1' -- the same considering the stress relieving effect of the longitudinal joints; 2 -- measured [deleted]; 3 -- measured σ_y ; 4 -- σ_x on the right side; 4' -- σ_x on the left side; 5 -- σ_y on the right side; 5' -- σ_y on the left side.

Key: A. kg-force/cm²

In connection with the different temperature regime of the air in the expanded joints on both sides of the section the deformations from the edges of the block are different. On the left side at the block temperature of up to -14°C the elongation deformation reaches values of $\epsilon_x = 19 \cdot 10^{-9}$ twice as great as the limiting extensibility of the concrete. It was assumed that a vertical joint occurred here. The presence of the latter becomes doubtful if we consider the doubling of the coefficient of linear expansion and the limiting extensibility of the frozen concrete (see § 3-10). The dependence of the measured stresses on temperature is illustrated in Figure 6-13.

On the side of the section with covered expanded joint, the hardening deformations are basically measured.

The same nature of the variation in time also is obtained for the deformations $\sigma_y - \sigma_0$ on both sides of the section. The stresses σ_y calculated by these deformations (the uniaxial stresses) reach values on the order of 100 kg-force/cm². The large compressive stresses with respect to the horizontal areas, on the lateral surfaces of the column, [illegible], their seasonal fluctuations with stabilization after covering the expanded joints are measured also in the blocks of the other columns (Figure 6-12,c).

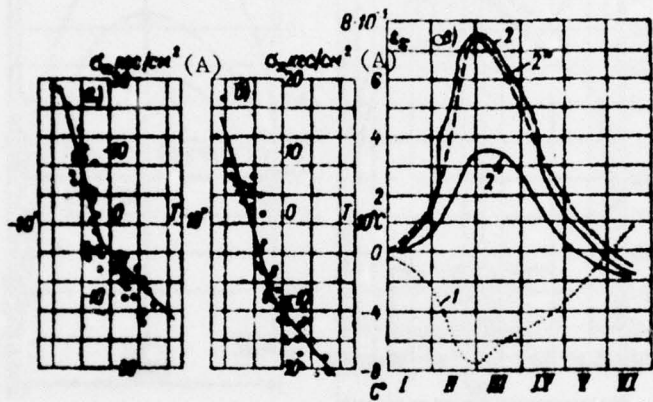


Figure 6-13. Effect of negative temperatures on the stresses and deformations measured on the lateral surface of the blocks; a -- dependence of the measured stress on temperature in blocks 30-III-6; b -- the same in block 30-III-15; c -- measured and calculated formations in block 30-III-9. 1 -- concrete temperature; 2 -- measured deformation σ_y ; 2' -- deformation calculated for $\alpha = \text{const}$; 2'' -- same for $\alpha = F(-T)$. The black dots (●) is the reduction in the temperature, and the light dots (○) is the increase in temperature.

Key: A. kg-force/cm²

The distribution of σ_y and σ_z with respect to the longitudinal cross sections of the columns has the parabolic nature with a large thermal reduction at the open surfaces. For the axial transverse cross section of the columns, the stress concentration at the intercolumnar joints through the toothed couplings of which the load is transferred from one column to the other is characteristic. The distribution of the stresses with respect to the vertical passing through the centers of the blocks has a sawtooth nature with [deleted] stress variation at the block boundary. This nature of the analysis occurring during the process of erection of the blocks [19] remained also later (Figure 6-14).

Thus, in the columnar massif of three meter blocks regularly poured in the winter and spring under the effect of external forces and thermal effects compressive stresses arose and remained with respect to the horizontal (σ_y) and vertical (σ_x) areas, in the central region of the blocks and greater temperature reduction (σ_z) in the lateral surface. All of the above presented examples pertain to the blocks in the columnar section. Let us consider the stresses in the long blocks.

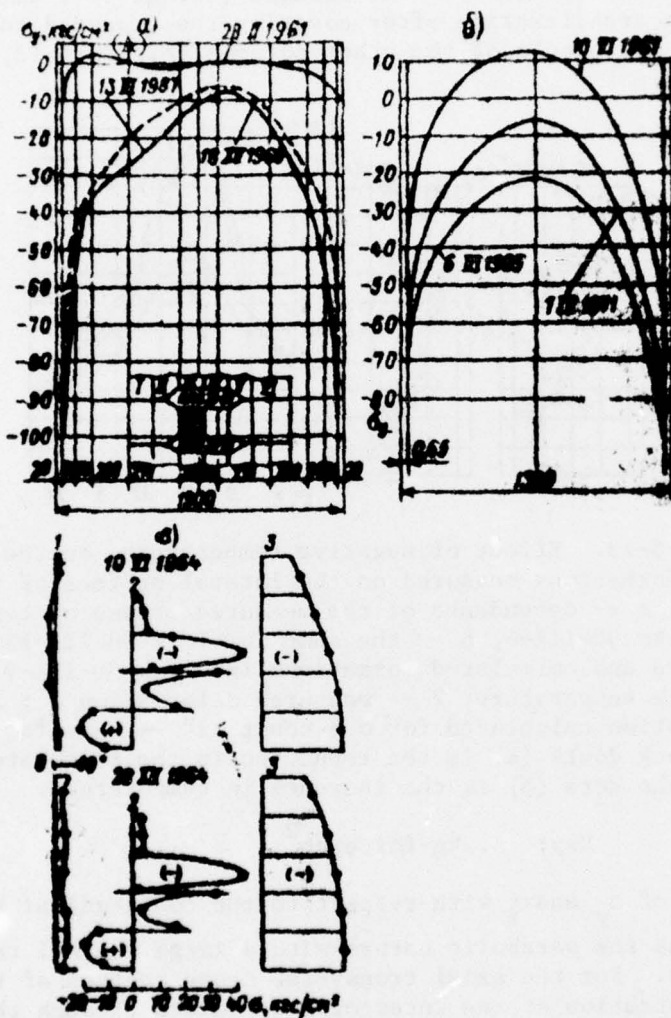


Figure 6-14. Stress distribution with respect to the axes of the block 30-III-9: a -- longitudinal; b -- transverse; c -- vertical. (1 -- T; 2 -- σ_x ; 3 -- σ_y).

Key: A. kg-force/cm²

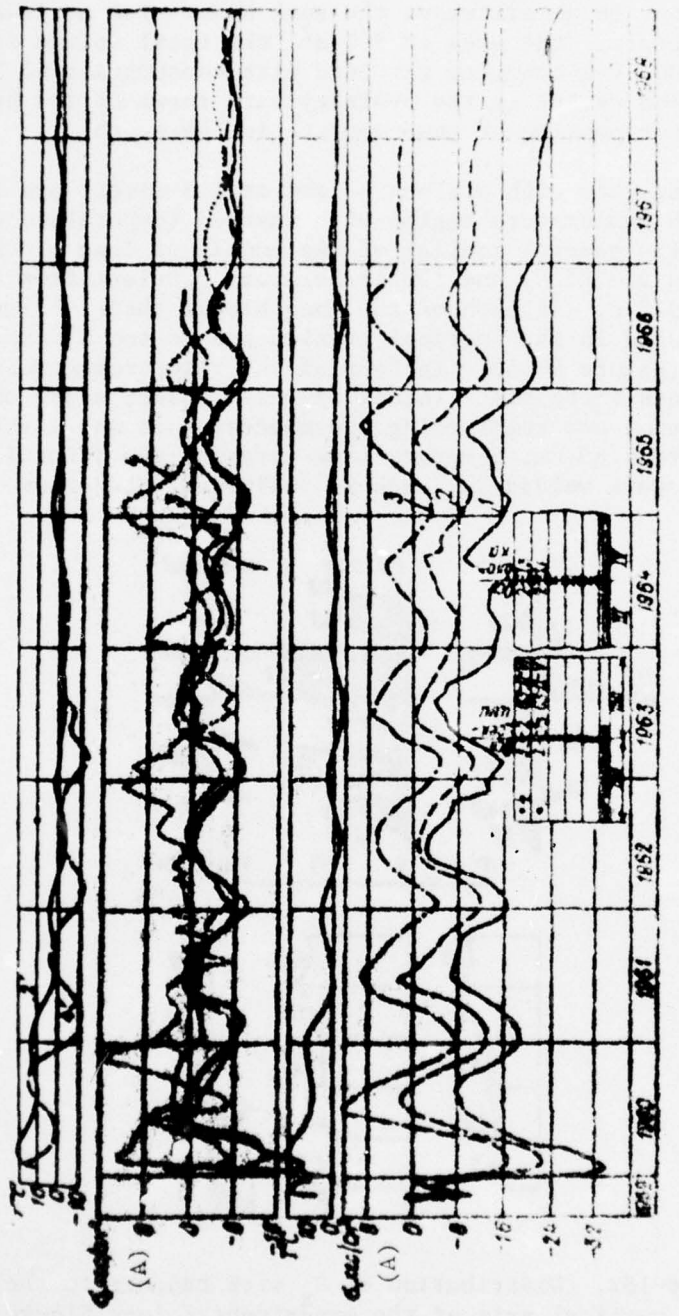


Figure 6-15A. Normal stresses σ_x measured in the concrete of experimental long blocks of section 63 and the temperature T . 1 -- 15 cm from the upper surface of the block; 2 -- average height of the block; 3 -- 15 cm from the lower surface; 4 -- 0.75 m of the block surface; 2' and 4' -- temperature at points 2 and 4.

Key: A. $\text{kg-force}/\text{cm}^2$

Stresses in the long block. In section 63 of the dam in the fall and winter of 1959/60, nine long blocks were poured which cover four columns (II-IV) at a height of about 16 meters above the rock base. The maximum length of the block is 55 meters, the area is 900 m^2 , the total volume is $11,000 \text{ m}^3$ [38]. The type 100, V-2 concrete was used with consumption of 170 kg/m^3 of the slag portland cement in the ordinary warm forms of the Bratskgesstroy Institute for winter pouring of the concrete in the teeth.

The regular pouring rate with a block height of 1.5 meters and low temperature insured the design temperature regime with maximum temperature no higher than 24° C . However, the general cooling of the massif of long blocks in the central region was $21-32^\circ \text{ C}$, and the temperature gradient from the center to the face reached 32° C . In each of the long blocks three measuring points each were established in the vertical section and in two blocks, one point on the left face (Figure 6-15). In four of the reinforcing rods 50 mm in diameter of the equalizing plate (block 63-D-1) located along the entire length of the section one reinforcing dynamometer each was installed. Under them between the rods 60 mm, 5 meters long covering the joint II-IV another four dynamometers were welded in, each in individual rod 45 mm in diameter.

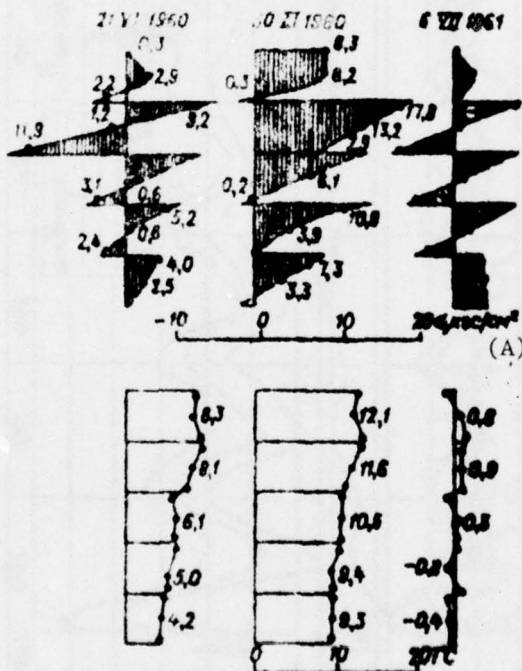


Figure 6-15B. Distribution of σ_x with respect to the vertical axis of the experimental long blocks.

Key: A. kg-force/cm²

The normal stresses σ_x^* calculated considering the stress relaxation are shown in Figure 6-15A. The process of exothermal heating of the blocks extended for 1.5 months as a result of laying them after short time intervals [38] caused the occurrence of large compressive stresses on the axis of the sections which went into the tensile stresses 10 kg-force/cm^2 in magnitude on the lower face of the blocks. In addition, the tensile stresses on the lateral surface led to the formation of a vertical crack which runs along the device which demonstrated the stress relief.

The maximum tensile stresses in the rods of the lower temperature grid on the lateral surface of the block reached $2270 \text{ kg-force/cm}^2$ in the first winter. On the axis of the section the maximum tension was observed in the summer and was $1,000 \text{ kg-force/cm}^2$. The stresses in the reinforcing rods covering the joint exceeded by 1.6-2 times the stresses in the reinforcing of the upper grid. After covering the expanded joints the stresses in the reinforcing along the entire width of the sections was stabilized at the $200-400 \text{ kg-force/cm}^2$ level (Figure 6-16).

According to the calculation by (6-27), (6-30), beginning with the actual temperature diagrams, the stresses in the reinforcing even when considering the properties of the frozen concrete did not have to exceed $500 \text{ kg-force/cm}^2$. It is obvious that the measured stresses $\sigma_\alpha = 2270 \text{ kg-force/cm}^2$ were caused by opening of the intercolumnar joint III-[deleted] with an average reduction in temperature in the columns covered by the block 63-D-1 by 21° C . The opening of this joint measured in January 1960 amounted to 2.6 mm, and on continuation of it in blocks 63-D-1 a visible crack 60 cm long appeared.

In the fall-winter period of 1960 to 1961 and the summer of 1961, the field study of the experimental long blocks 0.75-1.5 meters high and in the shore sections No. 4 and 6 was performed. In spite of the very warm forms in the interblocks [illegible] = $0.5-0.6 \text{ kgal}/(\text{m}^2\text{-deg-hr})$ which was not removed for more than a year, in spite of the cooling of the concrete mix, adding ice and the surface flooding of the poured concrete, crack resistance of these blocks was not insured, and in the first winter, cracks of great extent and opening appeared on their surface [38, 94].

Thus, the experimental [deleted] of long blocks large with respect to volume and carefully executed confirmed that for ordinary methods of performing the concrete laying operations surface conformation cannot be prevented in the long blocks.

6-4. Stresses on the Downstream Face

These stresses are measured at the 40 meter mark in sections 30, 51 and 65 using the strain gage fan rosette arranged parallel to the face at a distance of 0.4-0.5 meters from it. The fifth strain gage measured the deformations perpendicular to the face.

The nature of the variation in time of the stresses measured in three sections is identical. In accordance with the temperature variation of the concrete

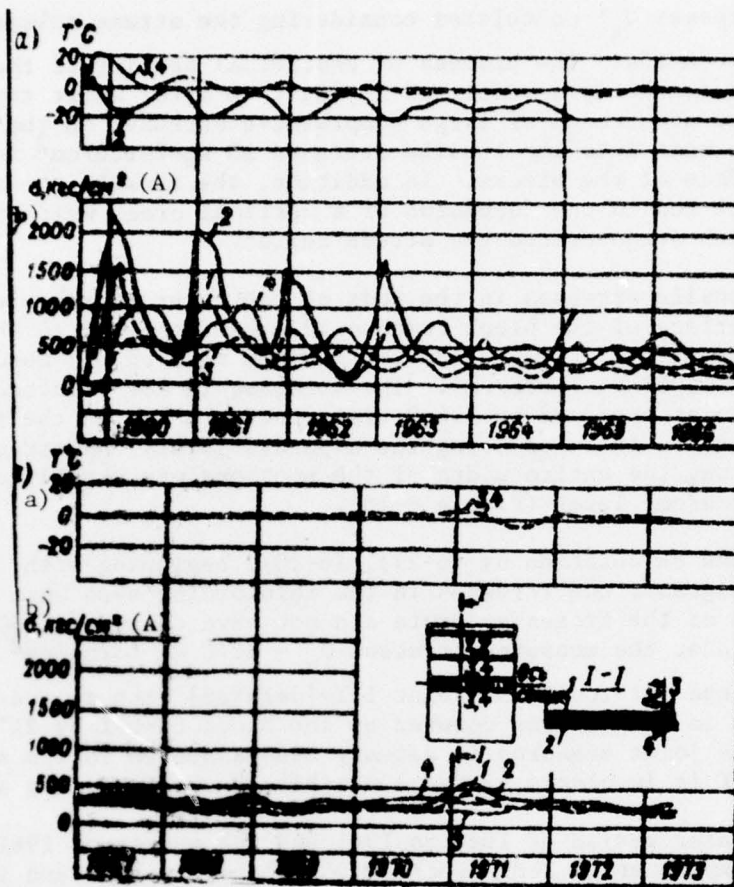


Figure 6-16. Stresses in the reinforcing and equalizing slabs: a -- temperature; b -- stresses.

Key: A. $\text{kg-force}/\text{cm}^2$

temperature on the downstream face the stresses with respect to three mutually perpendicular areas vary seasonally with large amplitude. The smooth stresses with respect to the area perpendicular to the face (σ_2) have the greatest magnitude. In the summer large compressive stresses are observed which decrease sharply in the winter. The mean compression with respect to which the cyclic fluctuations of σ_2 take place gradually increases and remains close to the calculated main stresses from the natural weight and the hydrostatic pressure of the water on the dam (Figure 6-17).

The main stress σ_2 in the winter remains impressive in spite of the low negative temperature of the concrete in the investigated point during the first winter minimum. In accordance with the calculation with respect to the temperature diagram during this period large tensile deformations (distresses)

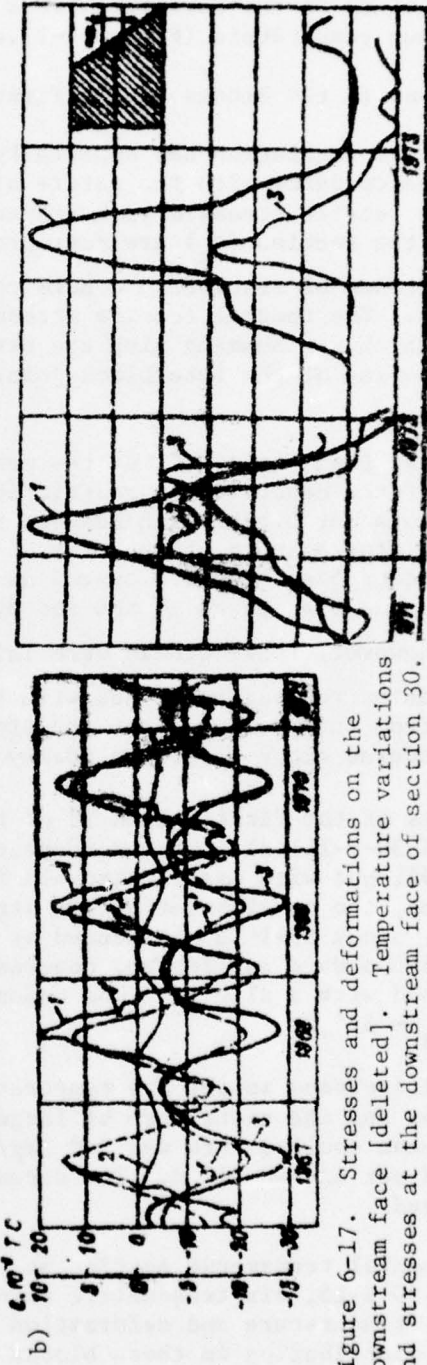
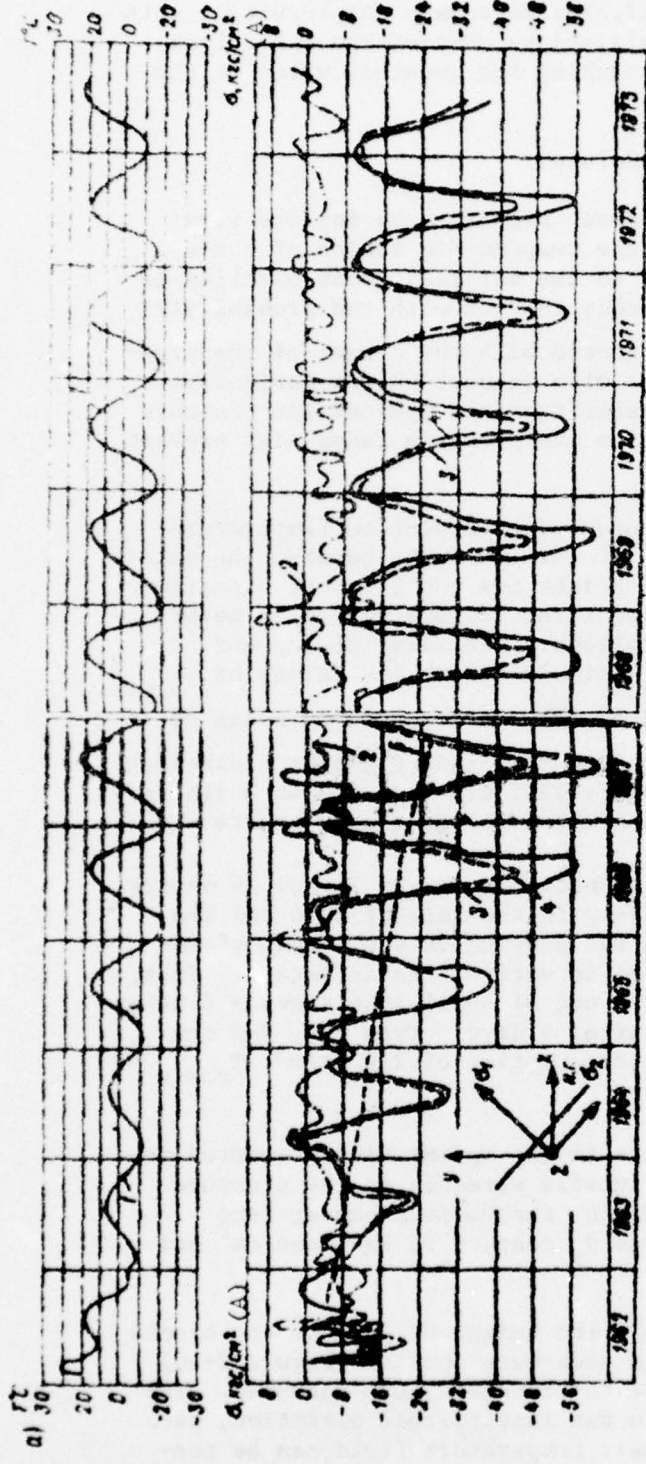


Figure 6-17. Stresses and deformations on the downstream face [deleted]. Temperature variations and stresses at the downstream face of section 30.
 1 -- concrete temperatures; 2 -- main stresses and strains on the downstream face, a -- [deleted]; b -- temperature increment [deleted]; 1, 1' -- temperature in cross sections 30 and 31; 3, 3' -- the same for the main deformations [joints] c -- measured openings [joints]
 Key: A. kg-force/cm²

had to occur. The deformations in the center of the block at a distance 6 meters from the downstream face (Figure 6-17,b) also remain compressive. This nature of variation of the stresses is explained by opening the interblock horizontal joints on the downstream face reaching the greatest value at the winter minimum temperature (Figure 6-17,c).

6-5. Stresses in the Blocks of the First Columns

The temperature regulation has especially great significance for the first column. In accordance with the nature of the temperature fields of these columns, the tensile stresses with respect to the vertical areas parallel to the axis of the section (σ_x) are most probable in them with the probability of the occurrence of transverse cracks connected with the danger of the pressure seepage. The thermal tensile stresses with respect to the horizontal areas (σ_i) which, on summing with the stresses from the hydrostatic pressure can imply opening of the interblock joints on the pressure faces also present a threat.

As has already been noted, out of the measures with respect to temperature regulation of the concrete the restriction of the intervals between the dates of pouring adjacent blocks with respect to height has the greatest significance. Thus, for example, the blocks of the first columns at the 24 meter mark of section 65 and 51 were poured as follows: the first at the end of October 1959 and the second at the end of April 1960 with low values of $T_{c.mix}$ and T_{max} . However, these blocks were laid on the old concrete with age of 5 and 8.5 months respectively, and with the remote strain gages at a distance of 1 meter from the pressure face the stress relief was recorded as a result of the transverse crack occurring nearby 1 month after pouring concrete.

In the blocks of the first column 30 of the section at marks 24 and 39 meters (30-I-10 and 30-I-15) also poured respectively in the fall of 1960 and the spring of 1961 but with small intervals in the pouring of the blocks of adjacent stages, the development of the stress is entirely satisfactory. Thus, for example, block 30-I-15 was poured at the end of April 1968 above a 6 meter block poured two days earlier and covered after 9 days. Type 200, V-8 concrete was used with a slag portland cement consumption of 240 kg/m^3 , $T_{c.mix} = 8^\circ \text{ C}$, $T_{max} = 37^\circ \text{ C}$.

The seasonal increase in the air temperature in the spring time prevented intense cooling and the occurrence of large tensile stresses on the pressure face. The mean cooling rate was 3.0 deg/month ; the maximum center-face gradient did not exceed 24° C . The stresses σ_x reached 16 kg-force/cm^2 and then decreased.

In the horizontal transverse section at half the height of each of the blocks 30-I-10 and 30-I-15, six tensometric points each were located (Figure 2-10) in which the temperature and deformation of the concrete were measured. The temperature distribution in these blocks in the longitudinal direction, beginning with some time, is uniform, and their temperature field can be considered uniform.

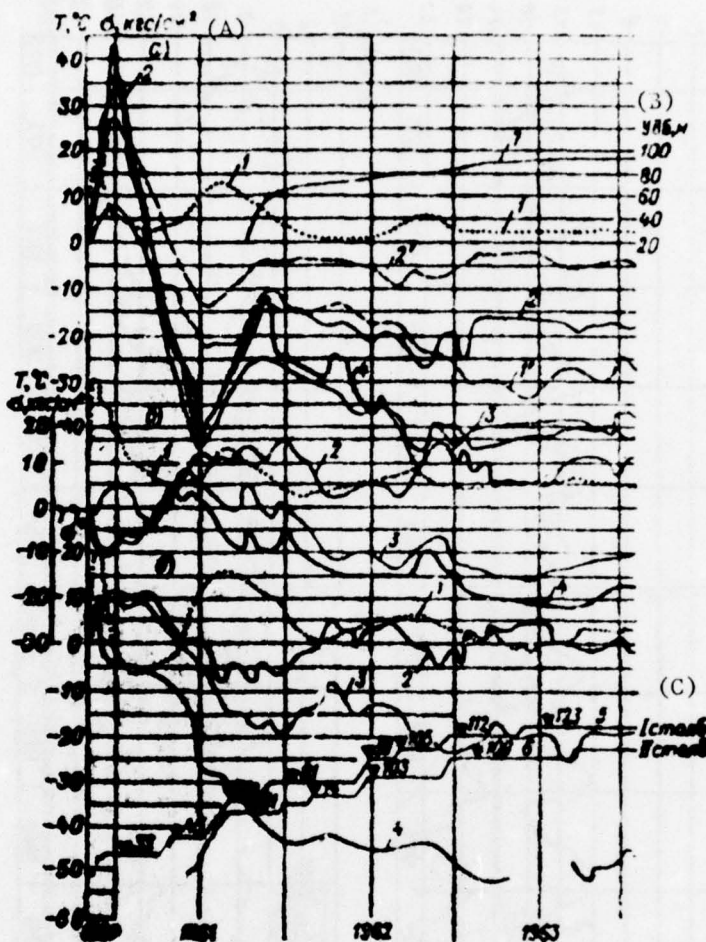


Figure 6-18. Normal stresses σ_y in block I of column 30-I-10: a -- the pressure face 6.2 meters; b -- at the center of the block; c -- on the intercolumnar joint. 1 -- temperature; 2 -- stress σ_T ; 3 -- $\sigma_T + \sigma_x$; 4 -- measured σ_y ; 5 -- graph of the concreted column I; 6 -- the same for column II; 3', 4' -- at the point 1 m from the pressure face; 7 -- headwater levels.

Key: A. kg-force/cm² C. column I, column II
B. headwater level

The planned sizes of the first columns and the temperature conditions on their pressure face give a somewhat autonomous nature to the temperature fields of the investigated blocks during the construction period differing

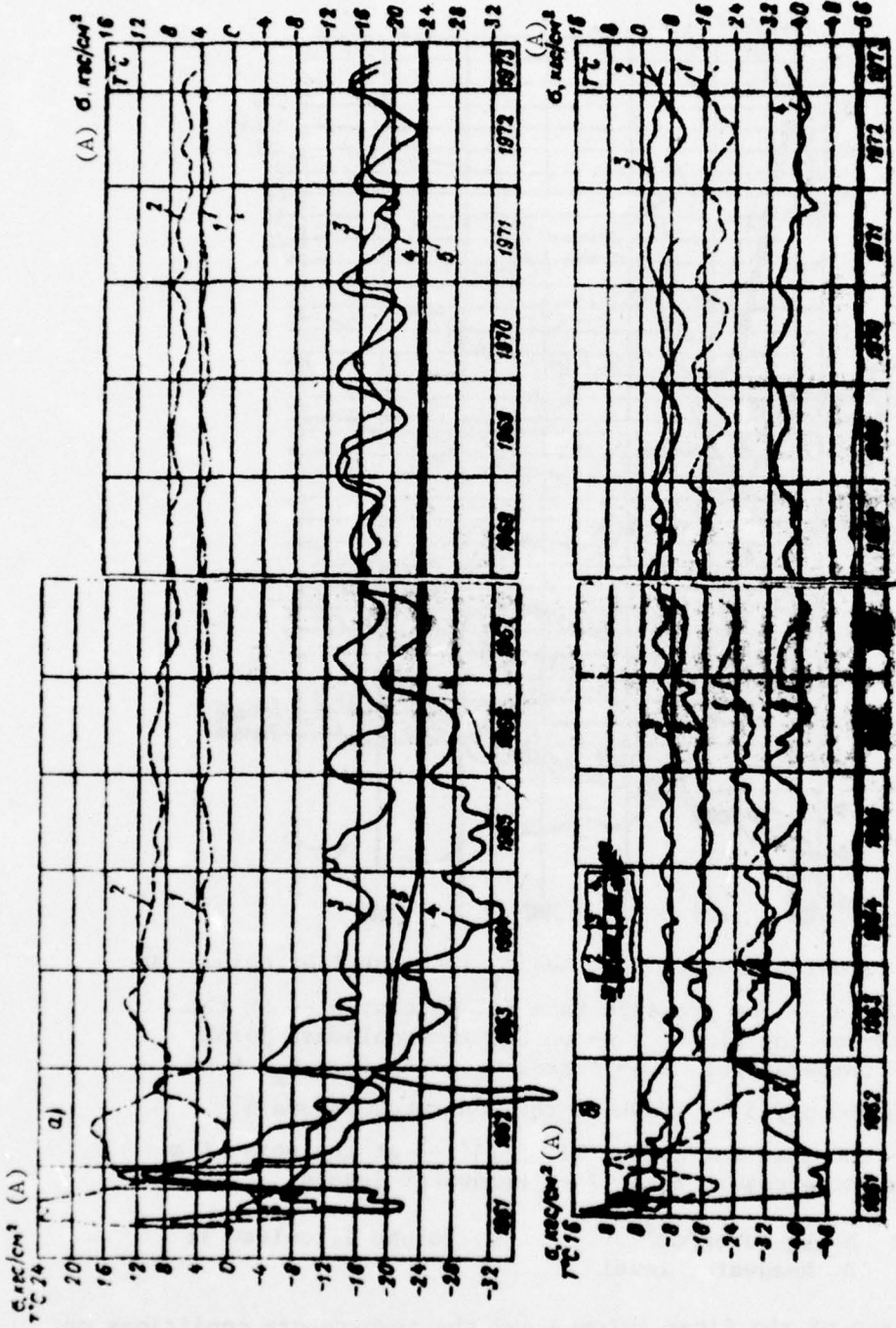


Figure 6-19. Normal stresses in column 30-I-15; a --- σ_y at four points 0.2 meters distance from the pressure base; b --- σ_x ; c --- σ_z ; 1 --- temperature; 2 --- σ_y ; 3 --- σ_x ; 4 --- mean stress from the concrete mass.

Key: A. kg-force/cm²

from the temperature fields of the adjacent blocks of the second columns. Therefore the calculation of the temperature stresses at the indicated 6 points of the horizontal sections was carried out beginning with the assumption that the temperature diagram in the transverse direction was self-equalized within the limits of the first column.

In the formation of the stresses in blocks 30-I-10, 30-I-15 and analogous blocks of other experimental sections it is possible to note the following peculiarities.

With respect to the horizontal areas on the pressure face, tensile stresses arose during the first exothermal heating which during the process of cooling of the blocks became compressive. The beginning of the filling of the reservoir (September 1961) coincided with the maximum compression caused by the summer increase in air temperature. Further cooling of the pressure face occurred under the conditions of heat exchange with the water which limited the development of the tensile stresses and created a compression reserve on the pressure face.

The magnitude of σ_y on the pressure face coincides satisfactory with the sum of the thermal stresses (σ_T) and the mean stress from the weight of the concrete (σ_b) both at the points at a distance of 0.2 meters and 1 meter from the pressure face and in the center of the block. As is obvious from Figure 6-18, on the pressure face there are large gradients of σ_y . The sharp fluctuations of σ_y are caused by the thermal component.

The normal compressive stresses σ_y measured on the intercolumnar joint I-I reached 50 kg-force/cm^2 and more which significantly exceeds the temperature stresses calculated for this point considering the weight of the concrete. The greater part of this compression occurred during the period of heating of part of the blocks and the joints after laying the blocks of the adjacent column (Figure 6-18). Further variations of compression on the intercolumnar joint were caused by forced stresses in the contact region between the columns on their interaction through the toothed couplings. The interaction occurs as a result of the effort of adjacent columns for linear and angular displacement of different magnitude and sometimes different sign and also for seasonal deflections of the dam. Simultaneously with the fluctuations of σ_y in certain cases opening of the horizontal interblock joints at the contact between the columns was observed. These openings were detected by the remote strain gages and the 30-II-15, 16 (see Figure 7-14) and 65-II-15 blocks.

The nature of development of the normal stresses σ_y and σ_z caused by non-uniformity of the temperature field and the transverse cross section is identical. The magnitude of σ_y is greater than σ_z as a result of the vertical stress component from the natural weight of the concrete. The nature of development of σ_x differs from σ_z and σ_y inasmuch as it depends on the temperature distribution in the direction of the longitudinal axis of the dam (Figure 6-19).

6-6. Stresses in the Blocks
Effect of the Hydrostatic Load

During the Filling of the Reservoir.

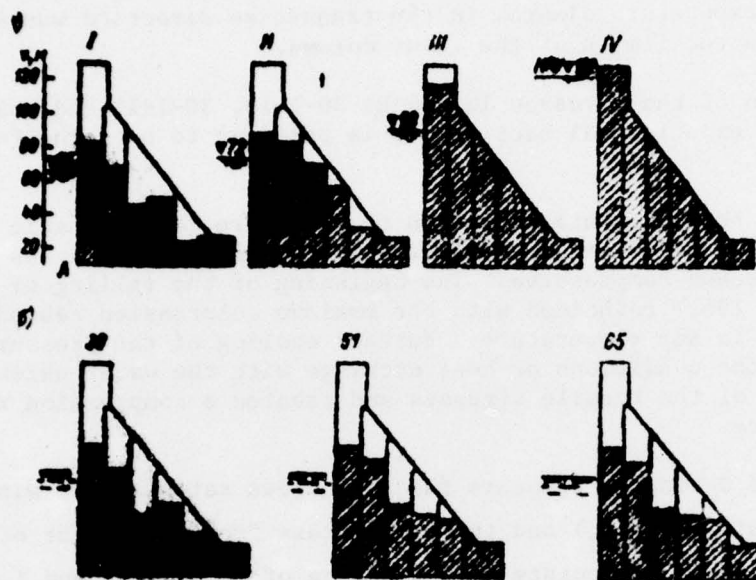


Figure 6-20. Stages in the erection of the dam; a -- by the plan; b -- profile of the section state of cementation of the intercolumnar joints at the end of January 1962.

By the static calculation of the technical design the stresses at the point A, depending on the height of the sections, amount to 2.4 to 3 kg-force/cm² for the normal backwater level, and the principal stress of the base of the downstream face are 29 to 33 kg-force/cm². The calculation provides for a load from the water pressure of the dam built to its complete height.

The effect of the magnitude and distribution of the stresses are caused by the step-by-step erection of the dam in four stages (Figure 6-20,a), the filling of the reservoir with incomplete (toothed) profile of the dam, the magnitude of the openings and order of cementation of the intercolumnar joints and also in its thermal state.

The experimental (model) studies performed by the laboratory of the OMIN VNIIG Institute [95-96] demonstrated that for the monolithic dam before the rise in water level in all stages of construction at the base of the pressure face significant compressive stresses are retained exceeding the requirements of the norms and for normal backwater level considering counterpressure amounting to 2 kg-force/cm² (compression) (Table 6-5).

Under the pressure of the water, bending of the columns takes place with partial covering of the intercolumnar joints and the occurrence of tensile stresses on the upper face of the columns. The greatest increase in the tensile stresses is caused by the hydrostatic pressure per stage. Thus, for

Table 6-5

Item No	Type of load	Head- water level, m	σ , kg-force/cm ²		
			Joints made mo- nolithic for rise headwater level	Joints open by 5 mm	2 mm
1	Natural weight of the first stage		17.0	-15.7	-15.
2	(1) + hydrostatics of the first stage	65	-11.4	2.3	- 2.
3	(2) + natural weight of stage II		-15.6	-2.1	-7.
4	(3) + hydrostatics of stage II	72	-14.8	0.7	-1.
5	(4) + natural weight of stage III		-19.8	-3.5	-3.
6	(5) + hydrostatics of stage III	90	-15.6	4.4	-0.
7	(6) + natural weight of stage IV		-22.2	-2.8	-7.
8	(7) + hydrostatics of stage IV	122	- 7.8	14.2	9.
Total natural weight			-32.8	-31.5	-31.
Total from hydrostatic pressure		25	45.7	40.	

example, for the joints opening by 2 mm, in the dam of the stage the compressive stress of the base of the pressure face considering the counterpressures dropped to 0.5-1 kg-force/cm². At normal backwater level at this point tensile stresses on the order of 14 to 15 kg-force/cm² occur [96].

The studies of the VNIIG Institute, the results of which are presented in Table 6-5, were performed without considering the effect of the toothed couplings between the columns. As the studies of the MISI Institute have demonstrated, the presence of the toothed coupling lowers the tensile stresses on the pressure face by about 5 kg-force/cm² by comparison with the joints without couplings.

By the beginning of filling of the reservoir, the intercolumnar joints of the dam were not all cemented and not to the full height (Figure 6-20, b). After cementation of all of the joints it turned out that its quality was different. Along with the well-cemented charts, there are charts with low quality cementation, after which the joints opened in places. This monolithic of the dam can be considered discontinuous (spotty).

The investigated laboratories of the laboratory OMIN VNIIG Institute and the MISI Institute [97] established that the discontinuous cementation essentially improves the stressed state of the structure by comparison with the uncoupled joints. Under the condition that the length of the open sections of the joint does not exceed one card (9 meters), the stress σ_y in the base of the pressure face differs in the worst direction from the stresses in the monolithic profile by only 2-3 kg-force/cm².

This is confirmed by two subsequent tests in the laboratory model of section 30 with schematized actual openings of the intercolumnar joints. Stresses σ_y on the base of the pressure face (point A) from the hydrostatic loading of the fourth stage (the headwater level equals 110-122 meters) and on the final stage of filling of the reservoir (of the headwater level equals 177-122 meters) it turned out to differ little from the stresses for the monolithic profile [19].

Thus, judging by the results of the model investigations, the discontinuous cementation insignificantly worsens the stressed state of the dam by comparison with the monolithic profiles. From this it follows that the discontinuous cementation (through the cards) insuring the given interval between the rising level of the reservoir and the level of the upper face of the monolithic part of the dam is more expedient than the continuous cementation of the joints, but lagging significantly behind the headwater level.

The thermal effects were not considering during the calculations and the model investigations of the stressed state of the dam. The material from the field studies of the Bratsk Hydroelectric Power Plant dam [19] and also the other responsible [98, 99] and the set of foreign studies [68, 100] of high concrete dams convincingly indicate that the role of the temperature effects is very great in the construction period and in the temporary operating period when the stress state of the dam is formed as a result of the simultaneous effect of the variations of the temperature fields, the increase in height of the structure and the gradually increasing hydrostatic pressure on its pressure face. The thermal effects noticeably influence the stressed state of the dam also during its permanent operation.

The nature of the development of the stresses σ_y on the pressure face of the three sections basically is the same (Figure 6-19, 6-21, 6-22). The tensile stresses of the initial period become compressive stresses gradually with large seasonal fluctions increasing an exceedingly average stress from the weight of the higher lying column of concrete. The maximum seasonal compression reaches 33-[deleted] kg-force/cm² with an average stress from the natural weight on the order of 24 kg-force/cm². During the period from 1964 (headwater level 95-100 meters) to the end of 1967 the average compression with respect to which the seasonal variations take place decreases under the effect of the hydrostatic load and at normal backwater level it is within the limits of 8-20 kg-force/cm². Attention is attracted to the seasonal fluctuations of σ_y with scales on the order of 5-9 kg-force/cm² during the permanent operation of the structure.

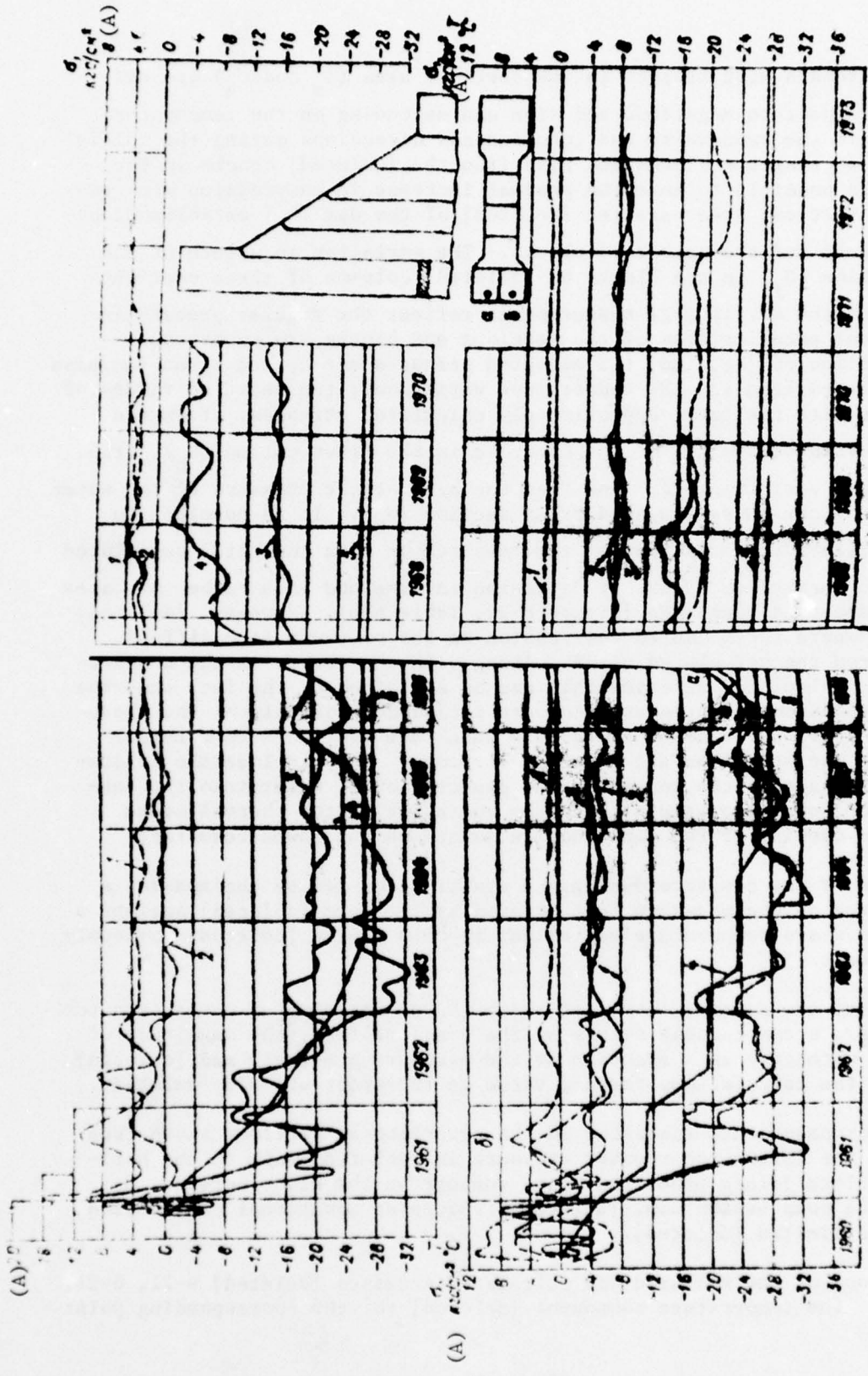


Figure 6-21. Normal stresses on the pressure face (1 meter) at mark 25 meters; a -- block 30-I-10;
 b -- block 51-I-10. 1 -- temperature; 2 -- σ_x ; 3 -- σ_y ; 4 -- σ_z ; 5 -- natural weight of the column
 (a, b) -- halfblocks).

Key: A. kg-force/cm²

The normal stresses with respect to the vertical area (σ_x and σ_z) are different with respect to magnitude and sign and depending on the temperature distribution in the transverse and longitudinal directions during the initial period after pouring the blocks and also from the [deleted] cracks in the blocks. It is possible to note the gradual increase in compression with respect to the vertical area parallel [deleted] of the dam (σ_x) established by the measurements and the number of blocks. The variation in nature of the stress variation (σ_y) in the blocks of [deleted] columns of three sections indicates that the strain gage measurements reflect the regular process in which the local peculiarities of the sections and blocks are superposed. For determination of [deleted] the measured stresses are caused by an increase in the calculated load and the temperature variations; the measured values of σ_y are summed with the total approximately calculated stresses: from the uniformly distributed weight of the concrete in the first column (σ_b), from the temperature variations (σ_T) and from the hydrostatic pressure of the water at the level of the investigagated cross section (σ_H). It is possible to note the satisfactory comparison of the measured σ_y with the total calculated stresses with respect to nature of variation in time and in a number of cases also with respect to magnitude (Figure 6-22, Table 6-6). However, [deleted] are observed where the measured compression on the pressure face differs noticeably from the calculated value. Along with the errors in the measurements and the calculated stresses this can be explained by the fact that the measured stresses on the pressure face are influenced not only by the above-enumerated factors but also other factors which are difficult to consider and cannot be isolated from the measured stresses. They include the following: the shrinkage of the concrete, the penetration of water into the concrete [deleted] of the pressure face, the variation of the thermal state [deleted] and opening of the construction joints on the downstream face.

The shrinkage of the concrete during the construction period encompasses a very large area on the pressure face covered by the form [deleted] against a background of sharp temperature variations in this region [deleted] obviously is insignificant.

The swelling of the concrete connected with the penetration of water into the concrete causes a compressive stress on the pressure face, the magnitude of which varies with time as a function of the pressure gradients and [deleted] according to the calculations reach a value on the order of (0.5-[deleted]).

As the piesodynamometers installed in the experimental sections shown (see Chapter 10), the filtration counter pressure is [deleted] only in the horizontal interblock joints under the block support on the old concrete. By decreasing the compression dam, [deleted] creates an additional compression in the blocks limited [deleted].

The comparisons of the measured and calculated stresses [deleted] 6-21, 6-24, and Table 6-6 the temperature component [deleted] for the corresponding point

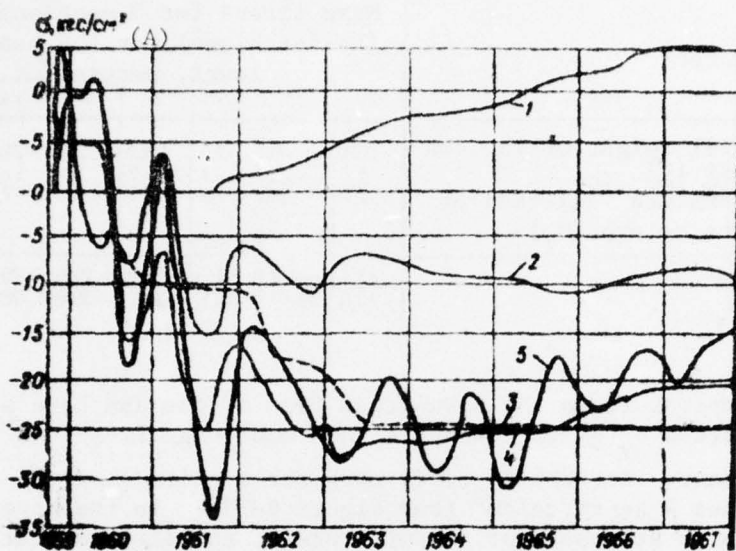


Figure 6-22. Measured and calculated normal stresses on the downstream face (0.9 meters) of section 65 at the 25 meter mark. 1 -- calculated σ_H ; 2 -- the same σ_T ; σ_b ; 4 -- $\sigma_H + \sigma_T + \sigma_b$; 5 -- measured σ_y .

Key: A. kg-force/cm²

on the pressure face by the equation [deleted] within the limits of the first column of the temperature diagram. It was possible with some approximation to estimate the magnitude of the thermal stresses on the pressure face, in particular, its thermal reduction which is the positive effect of the thermal effects. It is obvious from Figure 6-22, the thermal reduction of the pressure face for several years fixes the tensile stresses from hydrostaic load and in the operating dam creates a reserve compression with respect to [deleted] with a normal value of $\sigma_y = 0.25\gamma H$. However, the [deleted] the indicated procedure σ_T cannot explain the large [deleted] fluctuations of σ_y on

the pressure face after reaching the normal backwater level. Inasmuch as the average temperature of the concrete in column I at the investigated marks T_{ave} and the ordinate of the temperature curve $T_{mean} - T_x$ [deleted].

[deleted] the stress state of the concrete at the pressure face of the dam causes a noticeable effect of variation of temperature of the internal region caused by the air temperature regime in the expanded joints and also the seasonal variations in the concrete temperature on the downstream face.

With respect to the data from the experimental studies the MISI Institute and V. V. Kuybyshev [101] with an increase in temperature in the cavities of the expanded joints of the dam on the pressure base, the tensile stresses occur with maximum magnitude of $1.9 \text{ kg-force}/(\text{cm}^2 \cdot \text{deg})$ at a height of 0.1 h which approximately corresponds to the 22 meter mark. The fluctuations of

Table 6-5

Effect	Mean stress for 3 sections (kg-force/cm ²) for the head water level, meters						
	68	40	30	100	110	118	
Natural weight of the concrete (σ_0)	10.4	-1.9	17.5	20.7	-23.8	-24.5	-24.5
Static load (σ_s)	1.7	2.4	3.1	5.2	8.2	11.5	14.2
Temperature [deleted] of of the column (σ_T)	-2.7	2.6	-7.5	-4.5	6.6	-7.5	-8.2
Total	-11.4	-16.1	21.4	-20.0	-22.0	-20.5	-18.5
σ_y	-15.5	-19.1	20.5	-25.2	-30.0	-20.0	-17.7

the concrete temperature on the downstream face of the dam have a noticeable effect on the stress σ_y of the pressure face most significant at a height of 1/2-2/3 of the base. For the 40 meter mark the amplitude of the seasonal variations reaches 4 kg-force/cm² (see Figure 6-23). In the upper part of the dam the tensile stresses for an amplitude of the air temperature fluctuations of $\pm 20^\circ \text{C}$ reach 8-9 kg-force/cm².

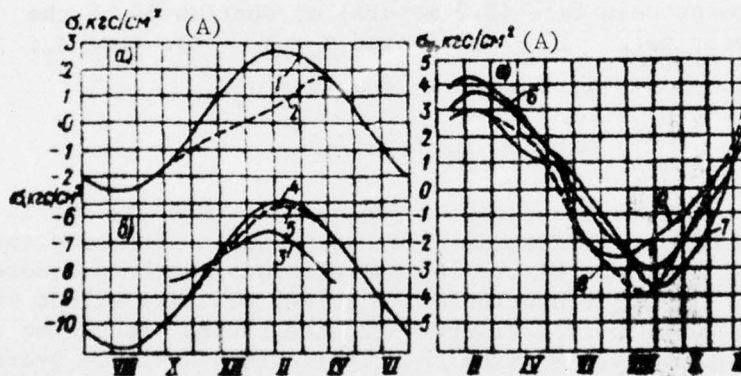


Figure 6-23. Effect of the temperature regime and the opening of the horizontal joints of the downstream face on the stressed state of the upper [deleted]: a -- thermal stresses on the pressure face for the calculated temperature field; b -- total stresses on the pressure face; c -- thermal stresses on the pressure face for the actual temperature distribution. 1 -- without considering the opening of the joints; 2 -- considering the opening of the joint; 3 -- from the natural weight of the dam and the hydrostatic pressure considering the opening of the joints; 4 -- total without considering the opening of the joints; 5 -- the same considering the opening of the joints; 6 -- according to the MISI work; 7 -- according to the VNIIG calculations; 8 -- measured in block 20-I-15 (0.2 m and from the upper boundary); 9 -- the same 1 m from the upper boundary.

Key: A. kg-force/cm²

As was noted in § 6-4, during the winter minimum temperature, the horizontal interblock joints of the downstream face of the dam open up. These openings cause redistribution of the stresses in its body having an effect on the stresses of the concrete in the pressure face. The stresses σ_y from the hydrostatic load increase as a result of a decrease in the operating [deleted] sections. The thermal stresses decrease as a result of a reduction in the amplitude of the temperature fluctuations at the mouths of the [deleted] joints by comparison with the amplitude of these fluctuations on the [deleted] face. The effect of the open joints is more significantly greater their length.

The length of the open part of the joints is determined by calculation¹ on the basis of the brittle fracture theory from the condition that on the continuation of the open joint of the coefficient of intensity of normal stresses from the basic effects is zero. The basic effects are the natural weight of the concrete, the hydrostatic load and the seasonal temperature fluctuations.

In the calculations the following was assumed: the coefficient of thermal diffusivity [deleted] = $0.004 \text{ m}^2/\text{hour}$; the Young's modulus of the concrete $E = 3.6 \cdot 10^5 \text{ kg-force/cm}^2$; the coefficient of linear expansion $\alpha = 1 \cdot 10^{-5} \text{ }^\circ\text{C}^{-1}$, The amplitude of the temperature fluctuations $A = 19.5^\circ \text{ C}$.

In Table 6-7 for the cross section at the 40 meter mark the length of the open part of the joints ℓ and the stresses on the pressure face from the [deleted] temperature fluctuations σ_{yT} , the natural weight and the hydrostatic pressure σ_{yzH} and σ_y tot are presented.

Table 6-7

Head-water level, m	Month	ℓ, m	$\sigma_{yT}, \text{kg-force/cm}^2$	$\sigma_{yzH}, \text{kg-force/cm}^2$	σ_y tot
122	October	0	-1.7	-8.5	-10.2
	November	1.1	-0.95	-8.1	-9.0
	December	2.3	-0.4	-7.5	-7.9
	January	3.3	0.1	-6.8	-6.7
	February	3.5	0.6	-6.6	-6.0
	March	2.7	1.3	-7.3	-6.9
	April	0	1.7	-8.5	-8.8
116	October	0	-1.7	-12.1	-14.7
	November	1.5	-1.0	-11.0	-12.0
	December	3.0	-0.5	-10.4	-10.9
	January	3.3	-0.1	-9.8	-9.9
	February	4.2	0.6	-9.6	-9.3
	March	3.9	0.9	-9.8	-9.9
	April	0	1.7	-12.0	-10.3

¹ The calculation was performed at the laboratory of the OMIN VNIIG Institute by G. S. Geiman under the direction of A. A. Khrapkov. The calculations of the two-dimensional temperature field were performed by A. M. Tsibin using a digital computer.

For the closed interblock joint the stress component for the natural weight of the concrete and the hydrostatic load for the headwater level equal to 116 meters and 122 meters is -12 and [deleted] kg-force/cm² respectively (compression). The amplitude of the temperature component is 2.7 kg-force/cm².

As the length of the open part of the joint (or crack) increases, the compression on the pressure base decreases both from the force factors and from the variations of temperature. The total decrease occurring at the end of the winter (March) is 4.2 to 4.8 kg-force/cm² and the amplitude of the annual fluctuations of σ_y remains equal to 2.7 kg-force/cm² for the calculated temperature field and 3.6 kg-force/cm² for the actual temperature distribution (Figure 6-23,a,c).

The opening of the horizontal joints on the downstream face has little effect on the amplitude of the seasonal fluctuations of σ_y of the concrete on the pressure face (Figure 6-23,b). The magnitude of this amplitude, both by the experimental data of the MISI Institute and by the calculations of the VNIIG Institute can be estimated at 3.5-4 kg-force/cm² which is close to the given field measurements.

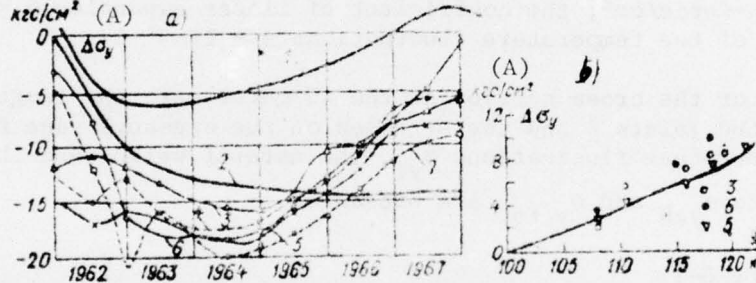


Figure 6-24. Increments of the normal stresses σ_y on the pressure face (1 m). a -- measured on the model and in the field of the 25 meter mark; b -- the function $\Delta\sigma_y = F(\Delta H)$

by calculation and field measurements. 1 -- from the natural weight and hydrostatic load according to the model investigation data; 2 -- the same for the natural weight; 3 -- measured in the field in the section 65; 4 -- in the section [deleted] (form a); 5 -- the same (form b); 6 -- the same in sections 30; 7 -- the same in section 30 at [deleted] 0.2 meters from the pressure face.

Key: A. kg-force/cm²

The component of the measured σ_y from the hydrostatic load on the pressure face can be established only approximately. A comparison of the increments of σ_y by the measurement data and the model studies and also calculation indicates satisfactory comparison in certain cases and noticeable deviations

in others (Figure 6-24). This is explained primarily by the fact that [deleted] during periods when the growth of the hydrostatic load begins [deleted] it acts simultaneous within the series of above enumerated temperature effects reflected differently in the measured σ_y as a result of the local peculiarities of the concrete, including the presence of a crack running through the measurement point or near it.

In order to estimate the relative effect of the fact of determining the magnitude of the measured σ_y and the nature of their seasonal fluctuations during the period of noticeable effect of their hydrostatic load, we used the statistical methods of analysis. By using a digital computer for block 30-I-10 by the field data for 6 years with respect to one point per month the system of 77 equations of the following type was solved:

$$\Delta\sigma_y = a_1 T_{av} + a_2 T' + a_3 T_{p,s} + a_4 T_{n,g} - a_5 H - a_6 H^2 + a_7 H^3 + a_8 \quad (6-31)$$

where the symbol σ_y , T and H designate the increments from January 1964:

σ_y are the stresses at a distance of 1 meter from the pressure face and T is the average temperature with respect to the block and the ordinate to the closing temperature curve at the measured point, $T_{r.sh}$ is the average temperature in the cavity of the banded joints on both sides of the section, $T_{n,g}$ is the concrete temperature at the point [deleted] meters from the downstream face, H is the increment in the headwater level, a_i is the free [deleted].

The hydrostatic has the greatest effect on $\Delta\sigma_y$. The significant seasonal fluctuation caused by the component from the variation of the air temperature in the cavities of the expanded joints decreased sharply after of the covering of the expanded joint 30-31 in 1967. The seasonal fluctuations from the variations of the temperature of the downstream face are shifted with respect to phase by the halfperiod with respect to the effect of the temperature in the expanded joints and during the temporary operation basically determine the seasonal fluctuations of the measured σ_y (Figure 6-25 and Table 6-8).

A comparison of the measured σ_y with calculated values (Figure 6-25) gives a divergence between them, especially noticeable for the summer maximum temperature and exceeding the mean square error in the calculations of $\Delta\sigma_y$ equal to 1.3 mm. It is obvious that in equation (6-31) it would be necessary to include a factor such as, for example, the opening in the inter-columnar joints [deleted] on the downstream page. According to the data from the laboratory of the OMIN [deleted] the opening of these joints to a depth of 5 and 10 meters decreases [deleted] at the point A by two and six kg-force/cm² respectively and is felt to some degree in the stresses and the higher lying points of the pressure face.

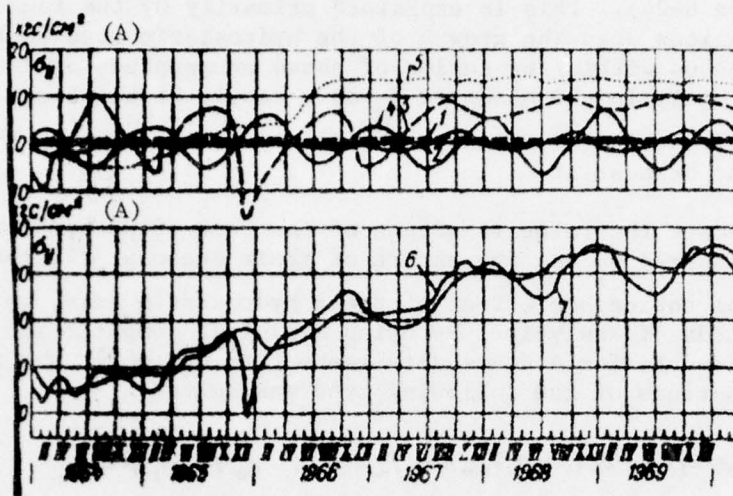


Figure 6-25. Components of the increment of the compressive stress on the pressure fields of section 30 at the 25 meter mark: 1 -- T_{average} , 2 -- T' , 3 -- $T_{\text{expanded joint}}$, 4 -- $T_{\text{downstream face}}$; 5 -- hydrostatic load; 6 -- calculated by digital computer; 7 -- measured.

Key: A. kg-force/cm²

Table 6-8

Date	Increments of the head water level of $\nabla 96.5$	Components $\Delta\sigma_y$ from					a_0	[deleted]
		T_{mean}	T'	$T_{\text{e.j.}}$	$T_{\text{d.f.}}$	H		
III 1966	14	1.1	-0.4	-3.8	5.0	3.7	-0.7	
VII	19	0.9	-1.1	4.4	-4.3	10.9	-0.7	
III 1967	22	0.8	-1.9	-4.1	3.6	13.2	-0.7	
VII	23	1.0	-1.1	4.7	-4.7	13.5	-0.7	
III 1968	25	0.8	-1.9	5.6	5.3	13.1	-0.7	
VII	21	1.0	-1.1	7.3	-4.6	13.4	-0.7	
III 1969	22	0.8	-1.9	7.5	7.1	13.2	-0.7	
VII	21	1.0	-1.1	7.9	-3.7	12.6	-0.7	
III 1970	21	0.8	-1.9	8.5	5.0	12.6	-0.7	

As is obvious from the results of the field observations presented above, the failing force components of the normal stresses measured on the pressure face with respect to the horizontal area σ_y are the natural weight of the concrete and the hydrostatic load, that is, the calculated load. From the

temperature effects the most significant must be considered to be the thermal shrinkage of the pressure face naturally occurring and having the positive effect on the stress state of the dam and also the fluctuations of σ_y from the seasonal fluctuations of the temperature of the downstream face (the outside air). The magnitude of the thermal reduction depends on the technological factors and can be regulated. The minimum value of this shrinkage can be approximately established by calculation, and obviously it must be considered when designing the dams.

Under the conditions of permanent operation the stresses with respect to the horizontal areas of σ_y at a distance of 1 meter from the pressure face during the period of their seasonal minimum are within the limits from [deleted] to 14 kg-force/cm² at the 22-24 meter marks and 5-6 kg-force/cm² at the 40 meter mark. Here at 0.2 meters from the pressure face $\sigma_y = 13-15$ kg-force/cm². [deleted] gives the stress gradient on the order of 10 kg-force/(cm²-deg) with consideration of which σ_y at the face itself will be 1.5-2 times larger than at a distance of 1 meter from it.

Thus, in the lower part of the extracontact zone on the pressure face the compressive stresses exceeding the requirements of the norms were maintained. The horizontal interblock joints of the pressure face were compressed, which is confirmed by the readings of the instruments [deleted] several joints. This, combined with the above presented [deleted] stresses in the central and peripheral regions of the third, fourth and fifth columns indicates the satisfactory stress state of the indicated zone of the [deleted] sections of the dam.

The stress state of the contact zone of the dam is less favorable in the vicinity of the pressure face. The first evidence of a deviation of this state from the normative was the relief of the compressive stress σ_y on the pressure face of the halfblock 30-I-5,a (Figure 6-7, b) fixed by the remote strain gage at the beginning of 1965 for a headwater level of 103 meters. Then at this point tensile stresses arose reaching a kg-force/cm² at the normal slackwater level. Simultaneously with relief of the compression the instrument at the contact zone on the axis of the halfblock 30-I-5c recorded a sharp elongation deformation to $\epsilon = 50 \cdot 10^{-5}$, that is, opening of the contact zone. At another point of the halfblock 30-I-5a the stresses σ_y remain [deleted] with minimum seasonal value on the order of [deleted]. The σ_y at a distance of 3.5 meters from the pressure face of section 51 have the same nature.

The normal stresses of the blocks next to the rock are different. The hydrostatic load decreases the compression in the first columns and increases it in the fifth and sixth. In the block of column IV σ_y [deleted] by the thermal variations in the drainage tunnel. The average value of the compression (in kg-force/cm²) with respect to which the seasonal fluctuations of σ_y took place during the first year of the permanent operation was -5.6 in block 51-I-4a, -7.6 in 30-I-5a, -17.5 in [deleted]-III-5; -26.5 in 30-V-5, -9.5 in 51-VI-5, -12.0 in block 30-VI-5 and +2.5 in block 30-IV-7.

6-7. Deformations in the Contact Zone of the Rock Base

The phenomenon of opening of the contact joint on the pressure face noted above has received further development. After a year [deleted] the joint in the neighboring halfblock and the crack under them in the rock. Simultaneously the joint opened in section 65, the adhesion in which [deleted] was disturbed immediately after the block next to the rock. At the beginning of 1966, the elongation deformation began to show at a distance of 10 meters from the pressure base. The openings of the contacts [deleted] of the joint increased in the winter and decreased in the summer (Figure 6-26).

The reliability of the operation of the instruments subjected primarily to [deleted] was confirmed by the results of the control drilling done by the Bratskgesstroy in several sections and above all by the high counter pressure in a number of sections. [deleted] on the cementation curtain side detected in [deleted]. Further studies are required.

According to the program compiled by the author by resolution of the expert commission of the technical council of the Ministry of Power, in a number of sections of the dam three [deleted] control holes 219 mm in diameter were drilled from the cementation tunnel; two of them were at an angle of 65° in the direction of the headrace and the tailrace and one vertically downward into the cementation curtain. The walls of the hole were examined using the RVP-451 periscope; the contact core was examined, and specific water absorption and the flow from the holes were measured.

The work with respect to the control drilling starting in 1967 was performed in 25 sections by the beginning of 1970. The results are presented in the following form.

In the majority of holes drilled in the direction of the pressure face, at the contact of the concrete with the rock there were cracks that intersect the entire core or part of it. In the diabase cracks made by the chloride and calcite, the cement rock was not detected with the exception of one hole.

The specific water absorption in the contact zone of the rock base not exceeding 0.01 to 0.02 meters per minute per meter after cementing in 1960 to 1963 increased by 1 to 2 orders, reaching 3 to 5 meters per minute in several sections (Table 6-9). The largest values of the specific water absorption were observed in the holes drilled in the direction of the pressure face; on going away from the latter the large specific water absorptions were more rarely encountered, just as going away from the contact surface into the rock base (Figure 6-27, Table 6-9).

The flow rates from the hole located in the direction of the pressure face in a number of cases reached large values, on the order of 200 liters per minute.

The mean specific water absorption (q_{mean}) according to table 6-9 has dimensionality of liters per minute per meter of hole and per meter of head,

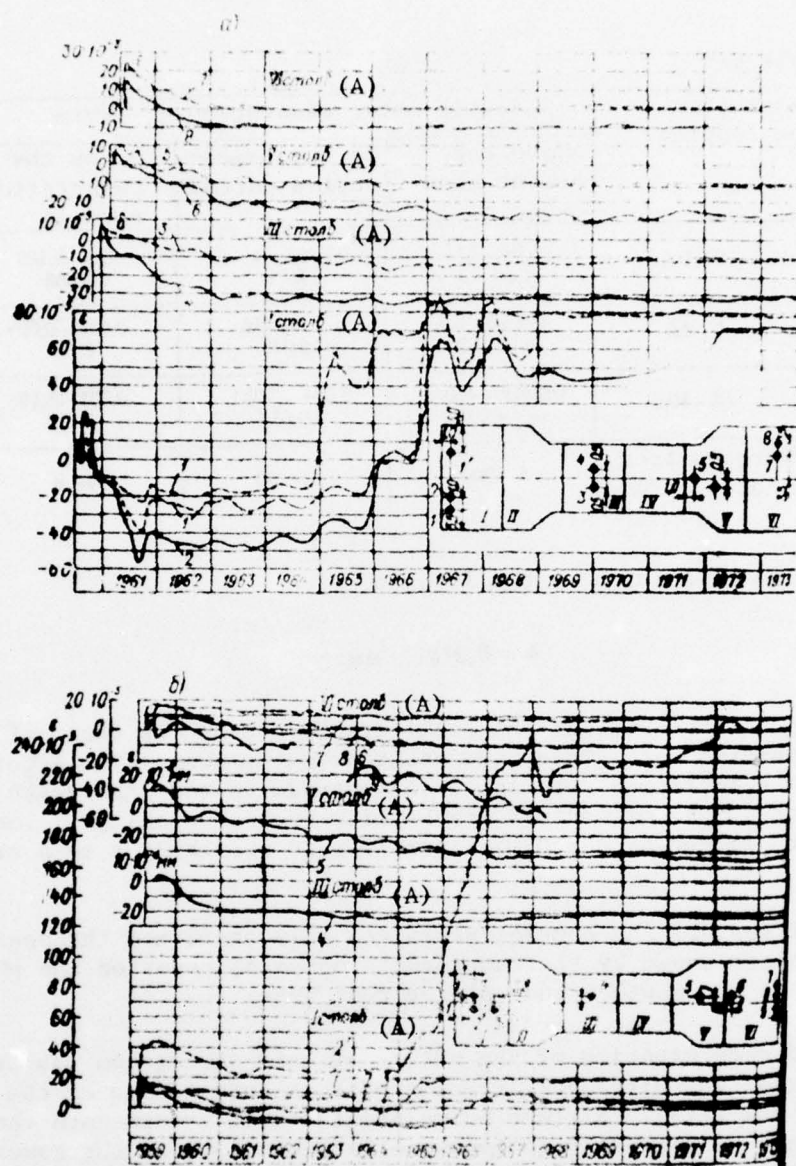


Figure 6-26. Deformations of the contact joints and the contact zone of the rock base: a -- section 30; b -- section 65 -- in the rock; --- at the contact.

Key; A. column...

and they are proposed uniformly distributed respect to depth in the zone. Inasmuch as the rock itself is water impervious, the pumped water is absorbed by the cracks. The width of the crack δ corresponding to the [deleted]

Table 6-9

Zones from the footing	Specific water absorption q , l/min		
	Above the cementation curtain	In the cemen- tation curtain	Below the cementation curtain
0-1 m	0.04-5.85 $q_{cp}=1.1$	0.0045-0.737 0.19	0.0-0.188 0.066
1-2.5	0.0033-0.93 $q_{cp}=0.26$	0.0-0.156 0.045	0.013-0.869 0.19
2.5-10.0	0.00039-0.037 $q_{cp}=0.012$	0.001-0.024 0.013	0.001-0.14 0.029
Flow rates from the holes, l/min	5-200	1-33	0-8

reduced q can be calculated by the formula

$$\delta = 0.27 q^{1/2}, \text{ mm.} \quad (6-32)$$

From (6-32) it is obvious that the small cracks can be the cause of significant water absorptions. Thus, the greatest water absorption according to Table 6-9, $q = 5.85$ liters per minute corresponds to one crack with opening on the order of 0.5 mm or several cracks with smaller openings. The designed specific water absorption $q = 0.02$ liters/minute corresponds to a crack 0.073 mm wide.

The results of testing the control holes not only confirmed the opening of the contact joints shown by the instruments but also revealed the phenomenon loss of seal of the contact zone of the rock base.

A more defined determination of the nature of this phenomenon was provided by the results of the ultrasonic studies of the contact zone of the first column of the dam [113]. Sixteen holes drilled 9-11 meters into the rock, cracks and zones of intense jointing were detected both at the contact and indirect proximity to it in the concrete and in the rock. The jointing in the 1-3 meter zone from the contact is especially intense. In addition, in the rock at different depths, including the 9-11 meter zone, there are individual large cracks and zones of increased and intensive jointing formed as a result of the fine, predominately subhorizontal cracks characteristic of the diabases. The cracks and the jointing zone were traced between adjacent holes.

The repeated geophysical studies performed in certain holes in 1973 demonstrated that part of the cracks were covered as a result of cementation. In addition, new cracks arose, including below the cementation zone.

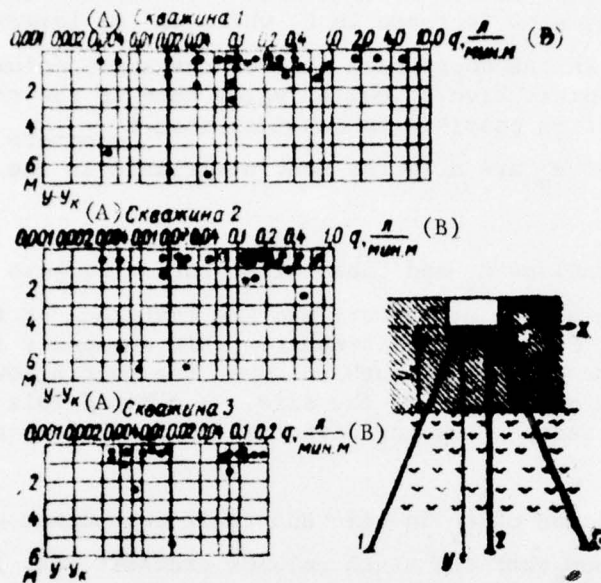


Figure 6-27. Specific water absorptions in the rock base of the first columns.

Key: A. hole... B. q, liters/min-meter

The results of the ultrasonic studies explain the high specific water absorption and increased counterpressure in a number of sections of the dam.

When constructing the dam, operations were performed with respect to surface (area) cementation of the base, the structure of the conjugate deep cementation curtains, beginning with the plan value of the specific water absorption of 0.02 liters/min-meter. The above discussed data from the natural observations indicate that even during the construction period the cementation curtains were cut by individual cracks and the jointing zones in the contact joint and at different depths of the rock. Judging by the readings of the contact remote strain gages, the reliability of which now cannot be doubted, the process of loss of seal in the contact zone of the rock base appeared at the beginning of 1965.

Let us consider the deformations of the contact zone under the remaining part of the dam (columns II-VI).

The horizontal deformations ϵ_x rated in the contact zone of the rock base are caused by the interaction of the latter with the concrete of the elastic clamped blocks next to the rock. Depending on the ratio $E_{\text{concrete}}:E_{\text{base}}$ in the increment diagram for the $\Delta\epsilon_x$ either is similar to the temperature diagram or is its mirror image.

The increase in natural weight of the columns is accompanied by intensive growth of the shortening (compressive) deformations. The hydrostatic load on the dam causes further, already slow increase in ϵ_y which is the largest in the

fifth columns and the least in the downstream face of the sixth column. The deformations in the contact joints have a smaller value than in the rock under them as a result of which it is possible to consider that $E_{\text{concrete}} > E_{\text{base}}$.

The seasonal fluctuations of ϵ_y are also the most noticeable in the fifth columns (Figure 6-26).

The magnitude of the deformations ϵ_y and their distribution on both sides of the transverse axis section 65 are different, and the [deleted] of the contact joints under the first columns are different. This obviously is explained by the discontinuity in time by 1 to 2 months between the pouring of the concrete for the halfblocks on both sides of the axis. A defined role is also played by the slope of the section and the direction of the left bank (see § 5-1).

On the graphs for the variation of ϵ_y in time and their dependence on the headwater level it is obvious that the sixth columns transmit less load to the base than the fifth columns (with the exception of one, probably, accidental point) which corresponds to the magnitude of the stresses σ_y in the blocks next to the rock of columns V and VI (see above).

6-8. Theoretical and Experimental Studies of the Stressed State of the Contact Zone of the Dam during Its Joint Operation with the Base

The phenomenon of the opening of the contact joints and the loss of the seal by the rock base of the first column detected at the dam of the Bratsk Hydroelectric Power Plant and previously not [deleted] in the literature on dam building, has attracted a number of theoretical and experimental investigations.

In 1970 the OMIN VNII~~G~~ Laboratory used the methods of mathematical theory of elasticity to investigate the stresses in the contact zone of the Bratsk Hydroelectric Power Plant dam. The basis for the calculation is the methods of determining the contact stresses in the concrete gravity dams operating jointly with the halfplane of another material from the contour loads [103, 104] and from the force effect of the water seeping through the base developed previously at the laboratory.

The calculation of the stresses from the hydrostatic pressure on the natural weight is performed for three cross sections: contact and the cross sections at 9 meters above and below the contact, for two ratios $\eta = E_{\text{concrete}} / E_{\text{base}}$, $\eta = 1$ and $\eta = 2$. The characteristic results of the calculations is the small compression at a depth of 9 meters in the rock which even when considering its natural weight does not exceed 2 kg-force/cm² for $\eta = 2$ and

is close to zero for $\eta = 1$. With respect to the vertical areas in the rock there are tensile stresses $\sigma_x = 5-6 \text{ kg-force/cm}^2$.

For the contact cross section it is assumed that the total stresses from the force effect of the seeping water are made up of the counterpressure stresses with the diagram of the latter with respect to the SN-123-60 and stresses from the water pressure in the bed of the reservoir calculated by the special program on a digital computer.

The summary stresses on the contact cross section under the pressure face for all loads are for $\eta = 1$ and $\eta = 2$ respectively $\sigma_y = 10 \text{ kg-force/cm}^2$ and $\sigma_y = 7.5 \text{ kg-force/cm}^2$ (tensile). The region of tensile stresses is propagated approximately to half the length of the first column.

In 1973 the OMIN VNIIG Laboratory calculated the stress-strain state of the Bratsk dam by the method of finite elements [106]. The procedure developed at the laboratory for calculating the dams jointly with the base simulating the linearly deformable media (the halfplane, periodically loaded with a halfbase) [106] was used. By this procedure the calculation by the method of finite elements is performed for the dam itself, and the elastic properties of the base are considered analytically by introducing the corresponding rigidity matrices into the calculation.

The following assumptions were adopted. The displacement and stress distribution with respect to thickness of the sections is constant. The difference of the cross section of the sections from rectangular was taken into account by the variable Young's modulus $E_{pl} = E\ell/L$ where $E_{pl} = 2 \cdot 10^5 \text{ kg-force/cm}^2$, L is the space between the axes of the section, ℓ is the thickness of the sections in the investigated cross section.

The base operates under the conditions of planar deformation, and it is simulated by the halfplane with the Young's modulus $E_{base} = 1.6 \cdot 10^5 \text{ kg-force/cm}^2$; $v_{base} = v_{dam} = 0.16$.

The calculation is performed for the effect of the natural weight of the concrete, the hydrostatic pressure for normal backwater level and the headwater level equals 116 meters, seasonal variations of the temperature (the cosinusoidal component) and seepage in the base.

The quasistationary two-dimensional temperature field was determined by the method of finite differences considering the air temperature in the expanded joints.

In order to consider the force effect of the seeping water a study is made first of the stress-strain state of the base as a free halfplane under the effect of the volumetric forces of the seepage ($-\gamma = \text{grad } h$) applied to the internal points of the halfplane and the surface forces $\gamma = h(x)$ at the contact, $h(x, y)$ is the piezometric head.

The calculation results in the form of the diagrams of the contact stresses σ_x , σ_y and τ_{xy} and the total load components are illustrated in Figure 6-28.

On the summary diagrams of σ_y , the two-dimensional diagram of the counter-pressure is superimposed with the ordinates: at the pressure face H, at the first drainage line 0, between drainage lines I and II, 0.2H and at the downstream face O.

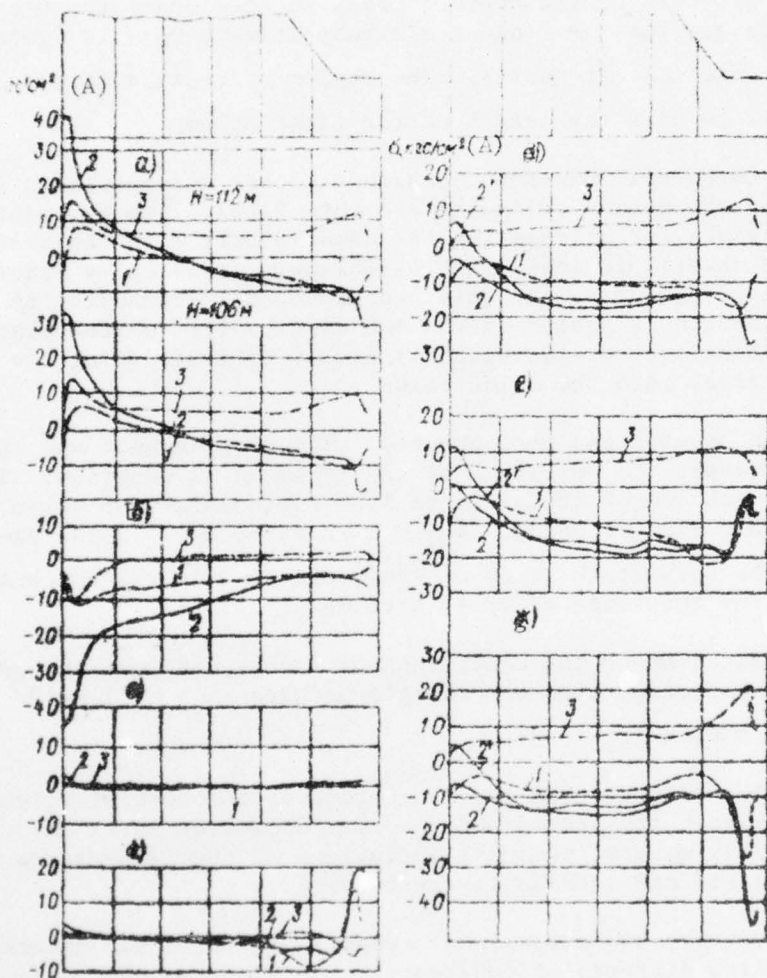


Figure 6-28. Stresses calculated by the method of finite elements near the contact cross section of the dam: a -- from hydrostatic loads; b -- from the natural weight; c -- from the seepage forces; d -- from the seasonal air temperature fluctuations; e -- summary without considering temperatures; f -- the same in the winter; g -- the same in the summer. 1 -- σ_x ; 2 -- σ_y ; 3 -- τ_{xy} ; 2' -- considering the counterpressure.

Key: A. kg-force/cm²

AD-A039 541 COLD REGIONS RESEARCH AND ENGINEERING LAB HANOVER N H F/G 13/13
FIELD STUDIES OF THE CONCRETE DAM AT THE BRATSK HYDROELECTRIC P--ETC(U)
APR 77 S Y EIDELMAN

UNCLASSIFIED

CRREL-TL-621

NL

3 OF 4
AD
A039541



Among the calculation results, the stressed state of the pressure face is of greatest interest.

In the contact cross section on the natural weight, the hydrostatic load, the normal backwater level and seepage forces the normal stress σ_y is $-2.2 \text{ kg-force/cm}^2$ (compression), and considering the counterpressure $+8.2 \text{ kg-force/cm}^2$ (tension). This compares quite well with the data from the analytical calculation presented above. The component from the seasonal variations of the temperature $\pm 3.4 \text{ kg-force/cm}^2$ gives $\sigma_y = 11.6 \text{ kg-force/cm}^2$ for the end of winter, and $4.8 \text{ kg-force/cm}^2$ for the end of summer. The amplitude of the fluctuations of σ_y is close to that calculated in § 6-7. The region of tensile stresses in the contact cross section is extended to 7-9 meters from the pressure face.

On drawdown of the reservoir by 6 meters the seasonal variations of σ_y take place within the limits from $-2.2 \text{ kg-force/cm}^2$ in the summer to $4.6 \text{ kg-force/cm}^2$ in the winter. At the 24 and 40 meter marks, σ_y on the pressure face remain compressive within the limits from 10 to 14 and 8 to 11 kg-force/cm^2 respectively.

The sharp fluctuations of σ_y in the vicinity of the downstream face were established by calculation. In the contact cross section these fluctuations are within the limits of¹ from -2.3 to $-101 \text{ kg-force/cm}^2$; at the 24 meter mark the fluctuations of σ_y are insignificant, and at the 40 meter mark the scale of the fluctuations is 54 kg-force/cm^2 which is quite close to the given contour observations (see § 6-5).

In the contact cross section within the limits of columns II-V with respect to the horizontal and vertical areas there are compressive stresses that are distributed approximately uniformly and increasing gradually in the direction of the downstream face. The sharp variations in the stresses and also τ_{xy} are observed in the downstream half of the sixth column, and at the 40 meter mark, in the 6-8 meter section, from the downstream face.

The problem of the stressed state of the contact zone has special significance for the dam at the Ust'-Ilim Hydroelectric Power Plant built on denser databases than the Bratsk dam and having a more compressed profile by comparison with the latter. Therefore, for the Ust'-Ilim dam model and theoretical studies were made which it is appropriate to discuss in this section.

¹This amplitude of the fluctuations which have no probability for this region was obtained in connection with the fact that when calculating the temperature field the presence of water in the tailrace of the hydroelectric power plant building were not taken into account.

First of all it is necessary to note the experimental and theoretical studies of the contact stresses with respect to the footing of the Ust'-Ilim dam from the weight of the water in the headrace.

In the dam of monolithic profile under the pressure face a region of tensile stresses arise with a magnitude at the contact of $3-5 \text{ kg-force/cm}^2$ propagated at a depth of more than 15 meters. Under the midsection of the footing there are compressive stresses $2-3 \text{ kg-force/cm}^2$, and near the downstream face, tensile stresses on the order of 1 kg-force/cm^2 . In the theoretical part of this work it is demonstrated that under the effect of the calculated loads and the seepage forces under the first columns a region of tensile stresses arose extending 6.5 meters with the stress under the pressure face of $4.3 \text{ kg-force/cm}^2$ and the possibility of opening of the contact joint [107].

The studies on the models of the Ust'-Ilim large scale dam (1:40) made of brittle materials gave the following results. The stressed state of the greater part of the profile of the monolithic dam is entirely favorable. In the vicinity of the lower part of the dam on the pressure face and the base in front of it and under operating loads, the tensile stresses arise on the order of $5.4 \text{ kg-force/cm}^2$ [108].

Thus, both the theoretical and experimental studies indicate that considering the joint operation of the dam with the base, the stressed state of the contact part of its profile planned with observation of the requirements of the SN-123-60 norms turns out to be unfavorable.

The calculated studies performed for the Bratsk Hydroelectric Power Plant dam confirmed the regularity of the drop established by the natural studies. For strong little-jointed rock bases the strength of the concrete-rock contact is determined by the strength of the concrete [39], and if we consider that $R[\text{deleted}] = 0.5R_p$, then the tensile stresses on the order of 10 kg-force/cm^2 are an actual prerequisite for the opening of the contact joints on the pressure face, especially if we consider that the adhesion along the concrete is frequently destroyed soon after pouring the concrete.

The tensile stresses with respect to the horizontal areas in the base of the first column of the dam on the dense little-jointed rock can involve opening of the contact joint without variation of the structure of the rock itself. The most probable cause of the loss of seal in the rock base of the first columns of the Bratsk Hydroelectric Power Plant dam is the combination of unfavorable stressed state at the contact zone of the dam with the characteristic peculiarity of the base. In addition to the system of primary joints, the Siberian trap rock is characterized by fine open cracks in which the rock is easily exfoliated under the effect of the [deleted] load (see § 1-1).

The cementation of the base was carried out during the erection of the sections of the dam, and the compressive load on the base increased. The fine, and especially the [deleted] cracks are not penetrated by the mortar and,

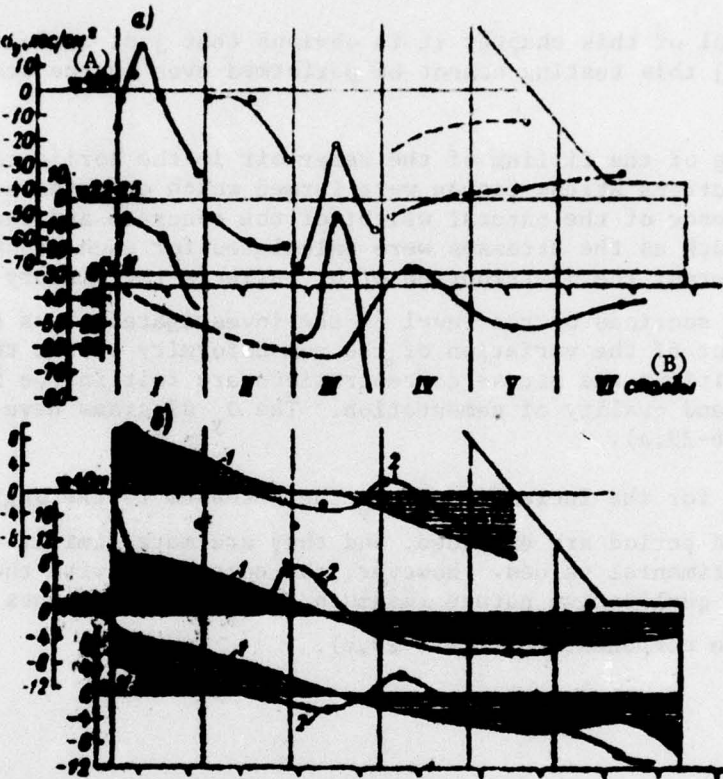


Figure 6-29. Diagrams of the normal stresses: a -- from the time of pouring the concrete for each block to 1 January 1968; b -- increments σ_y from 1 January 1964 to 1 January 1968. 1 -- according to the model investigation data; 2 -- measured.

Key: A. σ_y , kg-force/cm² B. columns

thus, being [deleted] increased in intensive jointing they remained uncemented. The load on the base previously compressed to a stress on the order of $\sigma_y = 40$ kg-force/cm², the pressure of the tensile stresses to 10 kg-force/cm² could involve opening of the fine and thin cracks. The redistribution of the stresses in the contact cross section for seasonal variations of the air temperature and also during rotations of the dam in the direction of the tailrace and headrace can promote instability of the rock structure with a gradual increase in the opening of fine and thin cracks.

It is of course expedient to compare the above presented calculated and experimental data with the corresponding field data. This goal was pursued when locating the remote strain gages along the horizontal transverse sections.

It was proposed that the calculated and field stress diagrams be compared and their correspondence to the external forces to determine the point of application of their resultant. In other words, it was proposed that the static calculation of the dam be checked.

From the material of this chapter it is obvious that just as in the construction period [19] this testing cannot be performed even in the stage of operation structure.

At the beginning of the filling of the reservoir in the horizontal cross sections of the sections stress fields were formed which occurred as a result of the total influence of the natural weight of the concrete and the temperature effects. Inasmuch as the stresses were calculated for each block at the time of its being poured, the distribution of σ_y reflects the history of the erection of the sections on the level of the investigated cross section and subsequent effect of the variation of the nonuniformity of the temperature fields. In addition, the stress concentrations are felt in the intercolumnar joints, cracks and quality of cementation. The σ_y diagrams have a complex nature (Figure 6-29,a).

In the diagrams for the increments of σ_y the stresses to the beginning of the investigated period are excluded, and they are more similar to the calculated or experimental values. However, the comparison with the latter has predominately a qualitative nature inasmuch as in the increments of σ_y there is a temperature component (Figure 6-29,b).

CHAPTER 7. CRACK FORMATION IN THE DAM BLOCKS

7-1. Crack Formation in Dams Built in Locations with Sharply Continental Climate

The problem of the control of the thermal crack formation arose simultaneously with the beginning of the mass application of concrete for the construction of dams. The primary measures to control crack formation in massive concrete with an insignificant number of cracks [109, 110] or without cracks [111] were developed 40 years ago. However, even in our time this problem cannot be considered solved; crack formation is observed in certain modern dams.

The control of crack formation has especially great significance for dams constructed in locations with sharply continental climate. The experience of Soviet construction of high concrete dams under such conditions pertains to locations with mean air temperature over many years from +2 to -4.9° C and the range of annual air temperature variations from 80 to [deleted]° C. The preservation of the monolithic future of the dams under such conditions is a highly complex manner.

In order to insure the monolithic nature of the dams, their plans provide for a set of technological process measures, the purpose of which is restriction of the temperature gradients in the erected concrete massifs: the zonal concrete with limited specific consumption of cement thermicity of the latter, fractionation of the fillers, cooling of the concrete mix, pipe cooling of the laid concrete, restriction of the difference in height of the adjacent columns, covering of the expanded joints. The structural design measures include the combined sectioning of the dams in order to limit the plan view and altitude dimensions of the concrete blocks that are poured in accordance with the thermal conditions and the methods of performing the operations [112].

At the dam for the Mamakanskaya Hydroelectric Power Plant, the cracks of a local nature are detected in 50% of the concrete blocks [90]; at the dam for the [deleted] Hydroelectric Power Plant, 100 local cracks occurred. Then a process of laying and cooling the concrete by long blocks was developed under microclimatic conditions created in the designed tents. In these blocks no cracks were detected [113]. At the Bratsk Hydroelectric Power

Plant dam, 2,777 surface cracks were located [114]. On the Krasnoyarsk the temperature regulation in the poured concrete was organized appreciably better than at the Bratsk dam, but crack formation was not avoided, the number of its crack amount to 1,289; 10% of them are [deleted] [115]. Pipe cooling is carried out on the Ust'-Ilim dam which is under construction; the height of the blocks is designated considering their [deleted] dimensions, the temperature of the base and the concrete mix, [deleted] by August 1974 with a volume of the poured concrete of 2,700,000 m³ [deleted] reckoned 1,480 cracks of which 16% were through cracks.

The crack formation of the massive concrete is a complex process which depends on a number of factors in which there is much that is unclear. In addition, it is necessary to recognize that the crack formation on the Soviet dams that have been constructed is caused to a significant degree by deviations from the design recommendations with respect to the temperature regulation of the poured concrete. As a result of the columnar [deleted] and the performance of design measures the cracks are in the majority superficial.

The design of the first Soviet dams (Mamakanskiy, Bukhtarminskiy and Bratsk) for severe climatic conditions was carried out in the absence of Soviet experience in the construction of such structures as applied to the data from foreign dam building under less severe climatic conditions. The observations of studies on the Soviet dams, the calculational and experimental studies connected with them have made it possible more clearly to formulate the requirements on the temperature regime of the concrete dams under severe climatic conditions. It is necessary to note the special field observations performed by the Siberian branch of the VNIIG Institute on the Krasnoyarsk dam [deleted]. On the basis of these and also other observations, practical recommendations have been developed on the modern level of knowledge in this field to insure crack resistance of the concrete blocks. The crack formation in the dam being built is also basically a consequence of deviations from the design requirements.

The location of the cracks on the open surfaces of the blocks usually performed visually with measurement of the opening of the cracks by optical or mechanical instruments does not offer the possibility of detecting internal cracks and establishing the relation between their occurrence and the stressed state of the blocks. The remote strain gage measurements greatly supplement the visual observations.

7-2. Remote Strain Gage as a Crack Formation Indicator

Depending on the nature of variation in time with the measured deformation in the operation of the remote strain gage it is possible to isolate three stages:

1. The instrument measures the deformation of the monolithic concrete. In this case by the measured deformations the stresses can be calculated considering the Poisson effect, the increase in the Young's modulus and the creep of the concrete.

2. The elongation deformation measured by the remote strain gage is close to the proposed limiting extensibility of the concrete. It is possible to assume that the instrument fixes the plastic deformation connected with the occurrence of microcracks [deleted]. In this case by the measured deformation it is impossible to calculate the stress, but it is also impossible to multiply it on the base of the instrument for calculating the open crack.

3. The elongation deformation significantly exceeded the limiting extensibility of the concrete, and a crack intersecting the axis of the instrument arose in it. Then the remote strain gage operated as a [deleted], measuring the opening of the crack. The least opening which can be measured depends on the length ℓ of the deformed part of the housing. For the remote strain gages of VNIIG and the KVU [18] ℓ is 100 and 165 mm, and the corresponding values of $\Delta\ell_{\min}$ per unit frequency modulation of the string are 0.15 and 0.5 microns. The maximum opening is limited by the strength of the string and can reach 1 mm for the VNIIG remote strain gages and 1.5 mm for the Czechoslovakian remote strain gages.

Inasmuch as the majority of the remote strain gages are located on [deleted] blocks, they often turn out to be in locations of the most probable formation of cracks. In many cases the cracks pass through the instrument which in this case fixes the time of its appearance and further opening.

Judging by which of the instruments from the tensometric rosette the crack intersects, it is possible approximately to determine its direction. In the cases where the crack does not intersect an instrument but passes near it, it changes the course of the deformation (relief) and in this way fixes the time of appearance of the crack.

In both of the indicated cases there is a possibility of establishing the stress preceding the occurrence of the crack at a point or in at a number of points.

7-3. Crack Resistance Criterion

The magnitude of the elongation deformation in monolithic concrete is limited by the limiting extensibility of the concrete. Inasmuch as free deformation does not cause the stressed state, the crack formation condition can be described as follows:

$$\varepsilon_{\text{meas}} < \varepsilon_{\text{lim}} + a\Delta T, \quad (7-1)$$

As was noted in § 6-1, the free deformation ε_0 , which is basically a thermal deformation is measured by the remote strain gage and the shrinkage cone and is known at each given point in time T ; therefore the condition (7-1) can be rewritten as follows:

$$\varepsilon_{\text{meas}}(T) - \varepsilon_0(T) < \varepsilon_{\text{lim}}(T). \quad (7-2)$$

Thus, the establishment of the time of occurrence of the crack when it intersects the axis of the strain gage presents no difficulties if $\varepsilon_{\text{lim}}(\tau)$ is known, but all of the difficulties if $\varepsilon_{\text{lim}}^*(\tau)$ is known, but all of the difficulty of the problem consists in the fact that the value of this deformation remains unknown.

The deformation $\varepsilon_{\text{meas}}$ measured by the remote strain gage in the given direction is the sum of the elastic deformations ε_y , the creep deformation ($\varepsilon_{\text{creep}}$) in the plastic deformation (ε_{p1}). The limiting deformation can be represented as the sum of the limiting values of the same information. Designating them $\varepsilon_{\text{lim}1}$, $\varepsilon_{\text{lim}2}$ and $\varepsilon_{\text{lim}3}$, it is possible to write the condition (7-2) as follows:

$$\varepsilon_{\text{meas}} = \varepsilon_y + \varepsilon_{\text{creep}} + \varepsilon_{p1} < \varepsilon_{\text{lim}1} + \varepsilon_{\text{lim}2} + \varepsilon_{\text{lim}3}. \quad (7-3)$$

For the uniaxial stress state

$$\frac{\sigma}{E} + \varepsilon_{\text{creep}} + \varepsilon_{p1} < \frac{\sigma}{E} + \varepsilon_{\text{lim}2} + \varepsilon_{\text{lim}3}. \quad (7-4)$$

Another part of the limiting extensibility $\varepsilon_{\text{lim}1}$ is determined most frequently by testing the samples for uniaxial stressed state. Inasmuch as the linear relation between σ and ε is retained almost to the rupture point (see § 3-4), it is possible to consider

$$\varepsilon_{\text{lim}1} = R_p/E. \quad (7-5)$$

The magnitude of R_p and E are determined usually by testing the laboratory samples. As for the values of $\varepsilon_{\text{lim}2}$ and $\varepsilon_{\text{lim}3}$, nothing in practice is known about them. Therefore when establishing the crack resistance criterion usually we begin with various assumptions. Thus, for example, P. I. Vasil'yev [118], beginning with the proposition that the region of plastic deformations is small proposes that the deformation with respect to the left-hand side of (7-4) be defined by solving the problem of linear creep, and the value of $\varepsilon_{\text{creep}}$ be taken equal to $\varepsilon_{\text{lim}2}$. As a result, he arrives at the known criterion of crack resistance:

$$\frac{\sigma(\tau)}{E} < \frac{\varepsilon'_{\text{lim}}(1)}{E} \quad (7-6)$$

Key: 1. $\varepsilon'_{\text{lim}}$

where $\varepsilon'_{\text{lim}}$ is the limiting elongation without considering creep obtained for the ordinary ruptured tests and is equal to about $(7-10) \cdot 10^{-5}$; k is the safety margin.

The limiting extensibility of ϵ_{lim}' depends on a number of factors: the composition of the concrete, its age, the submersion rate.

The magnitude of ϵ_{lim}' , according to our experiments (see Chapter 3), is within the limits of $(5-10) \cdot 10^{-5}$ with predominant values of $(5-7) \cdot 10^{-5}$. This coincides with the value of ϵ_{lim}' obtained by a number of authors.

For concrete similar with respect to type to 100, V-2, O. V. Kuntsevich obtaining the limiting extensibility from $(6-6.5) \cdot 10^{-5}$ to $7.65 \cdot 10^{-5}$, then he considers the lower limit more probable. With an increase in age from 28 to 180 days, ϵ_{lim}' increased by 15% [119].

The tests of the concrete of the Krasnoyarsk dam gave values of ϵ_{lim}' within the limits of $(4.8-8.1) \cdot 10^{-5}$ [119].

In the experiments of the central concrete laboratory of Bratskgesstroy when testing concrete samples for uniaxial tension to rupture, the instrument readings on the two opposite generatrices of the samples were recorded using a movie camera. It was established that ϵ_{liml} depends linearly on R_p ; identical ϵ_{liml} correspond to the concrete of equivalent strength based on gravel and rubble. The total deformation ϵ_{meas} according to (7-3) exceeds its elastic part ϵ_{liml} by 2 to 4 times. The difference $\epsilon_{meas} - \epsilon_{liml}$ called the "pseudoplastic" deformation depends randomly on the position of the sensors with respect to the zone in which initially the microruptures in the cracks are formed [120].

Under the conditions of the massive concrete blocks, the value of ϵ_{lim}' depends on a number of factors: the composition, the age, the stress state, the uniformity, the duration of the load, and so on.

There are a few data on the effect of the time factor on the magnitude of the limiting extensibility. Obviously the concept of the increase in the limiting extensibility to $(15-20) \cdot 10^{-5}$ is valid for slowly varying thermal stresses [121]. Thus, for example, the studies on the concrete of the Khayvossi dam established that with for a number of concrete the limiting extensibility would be about $\epsilon_{lim}' = 10 \cdot 10^{-5}$, for fast loading this value drops to $8 \cdot 10^{-5}$, and for slow loading the same concrete has limiting extensibility of $\epsilon_{lim}' = 16 \cdot 10^{-5}$ [111]. Judging by these data, the slow loading of the concrete can increase this limiting extensibility by 2 times by comparison with the fast loading.

The above presented values of ϵ_{lim}' were obtained by testing concrete samples under uniaxial tension. In the concrete massifs in the presence of thermal stresses, the limiting extensibility can vary sharply depending on the age of the concrete, the uniformity of the stress field and the rate of variation of the latter.

For the nonuniform stress state with large stress (strain) gradients frequently occurring in the open surfaces of the concrete block, the limiting extensibility $\epsilon_{lim\Gamma}$ depends on the deformation gradient Γ_1 , which increases with an increase in the latter. The field studies demonstrated that during cold weather the cracks occur with average deformation gradient of $(0.3-1.1) \cdot 10^{-5} \text{ cm}^{-1}$ measured in the surface layer 10 cm thick.

According to the data from the laboratory and field studies the relation was established in the limiting extensibility $\epsilon_{lim\Gamma}$ and the deformation gradients Γ_1 (Table 7-1) [115, 116].

Table 7-1

$\epsilon, 10^{-4} \text{ cm}^{-1}$	0	0.2	0.4	0.6	0.8	1.0	1.2	1.4	1.6	1.8	2.0
$\epsilon_{lim\Gamma}, 10^{-5}$	9.0	11.5	13.1	14.0	14.7	15.3	15.7	16.3	16.7	17.1	17.3

Thus, the limiting extensibility of the concrete with an increase in the deformation gradients can be doubled by comparison with its value for uniaxial tension and, consequently, in the concrete of [deleted] age, depending on the presence, the growth rate of the magnitude of the deformation gradients, the cracks can occur with small deformations on the order of $(5-7) \cdot 10^{-5}$ and lasts to deformations 2 to 3 times greater.

In Chapters 3 and 6, the significant increase in the limiting extensibility of the concrete in the frozen parts of the dam has already been noted.

When investigating the crack formation in concrete blocks of the Bratsk Hydroelectric Power Plant dam, we began with the analysis not only of the variable deformations of the concrete but also the nature of the buildup of the strength of the concrete and its stressed state. In addition to the measured deformations we also considered the instantaneous elastic deformations;

$$\frac{\epsilon_{im}}{\epsilon_{im}} = \frac{\epsilon(t)}{\epsilon_0} - \frac{\sum_{i=1}^n \Delta \epsilon_i(t) E_i(t)}{E_0} \quad (7-7)$$

Key: 1. lim

The cases where the deformations in the old concrete increase sharply to values on the order of $(8-10) \cdot 10^{-5}$ for which defined determination of the crack currents is difficult are the most difficult for the analysis.

It is necessary, however, to note that in the majority of cases the crack formation occurred under the conditions characteristic of brittle rupture with a sharp increase in the measured deformation from the small values to the values explicitly exceeding any possible limiting extensibility of concrete.

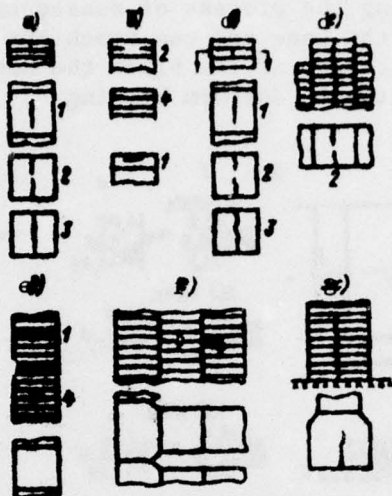


Figure 7-1. Classification of cracks: a -- vertical; b -- horizontal; c -- vertical crack as a result of overlap; d -- vertical for high rates of pouring the concrete; e -- horizontal in the form to concrete massif; f -- horizontal as a result of interaction on the columns; g -- continuation crack of the joint-notch. 1 -- internal; 2 -- surface; 3 -- through; 4 -- opening of the joint.

Beginning with the analysis of the crack formation in the blocks of the Bratsk Hydroelectric Power Plant dam [122], hereafter we shall adhere to the following classification of the cracks (Figure 7-1):

1. With respect to location: surface and internal
2. With respect to origin: a) cracks in the uncovered blocks, b) cracks connected with covering of the block; c) cracks with a high rate of concrete pouring; d) cracks in the massif made of old concrete.

7-4. Crack Formation in the Uncovered Blocks

When erecting the channel dam in a number of cases significant discontinuities were observed in the times of pouring the concrete of adjacent blocks with respect to height.

As experience shows, the most probable in the uncovered block are the vertical cracks running from the open horizontal surface deep into the block (Figure 7-1,a).

In Figure 7-2, A, B, we have the diagram for the temperature (1), deformations (2) and stresses (3) with respect to the vertical areas in the successively

poured uncovered blocks. Soon after pouring the concrete in the upper part of the block, a zone of small tensile stresses occurs with respect to the vertical areas which, during the process of subsequent cooling of the block increases with respect to the base and can reach the center of the block (Figure 7-3). In the lower part of the block the compression at the base decreases by comparison with the uniform heating.

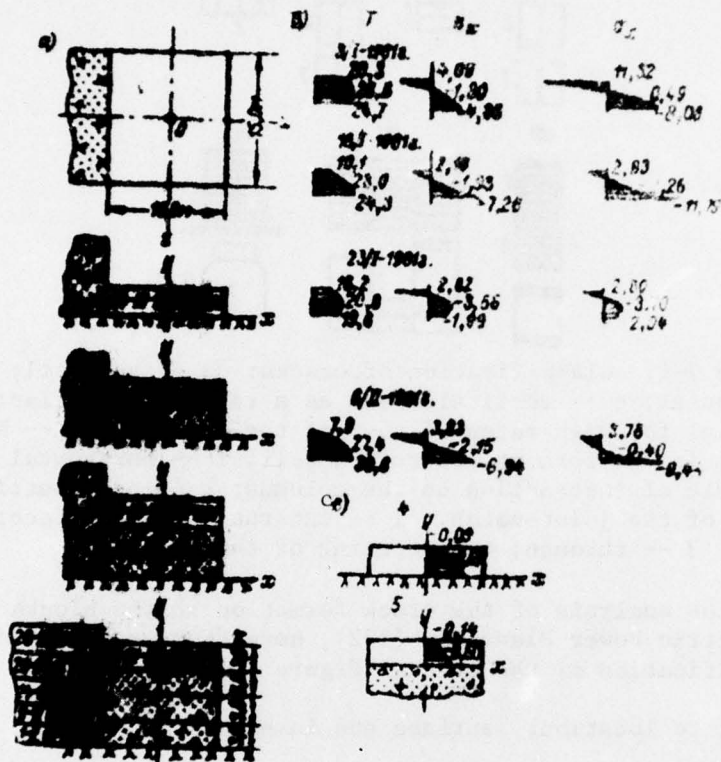


Figure 7-2A. Stress state of uncovered blocks of column III of section 30: a -- schematic of the block (plan view and section); b -- distribution with respect to height of the block of the temperature T , the measured deformations ϵ , stresses σ_x ; c -- theoretical stress diagram ϵ_x in the block uniformly heated with respect to the base in the fractions $E\alpha\Delta T/1 - v$ (4 -- for the block on the halfplane, 5 -- for the block on the halfstrip).

For intense cooling larger tensile stresses in the upper part of the block lead to the occurrence of vertical cracks. In the blocks poured in the summer these cracks are a consequence of the high exothermal heating of the concrete in the center of the block. In the winter blocks the cracks of this type occur as a result of intense cooling through the upper open surface. The block 65-V-9 was poured in July 1959 [deleted] between the previously

poured blocks of the adjacent columns (T [deleted] = $45.5^\circ C$, $T_{des} = 30^\circ C$). The maximum compressive stress at the center of the block $\sigma_x = 10 \text{ kg-force/cm}^2$. The cooling of the block took place equally through the upper horizontal surface on the average with an intensity of 6° per month. The deformation in the direction of the axis of the section measured in the center of the block made the transition from compression to tension a month after pouring the concrete, and after 10 [deleted] it increased sharply to $42 \cdot 10^{-5}$. A vertical crack occurred in the block parallel to the axis of the cross section with a value of the limiting measured deformation $\varepsilon_z' = 8 \cdot 10^{-5}$, a calculated stress of [deleted] kg-force/cm^2 and the corresponding elastic deformation $\varepsilon_z = 2 \cdot 10^{-5}$ (Figure 7-4,a).

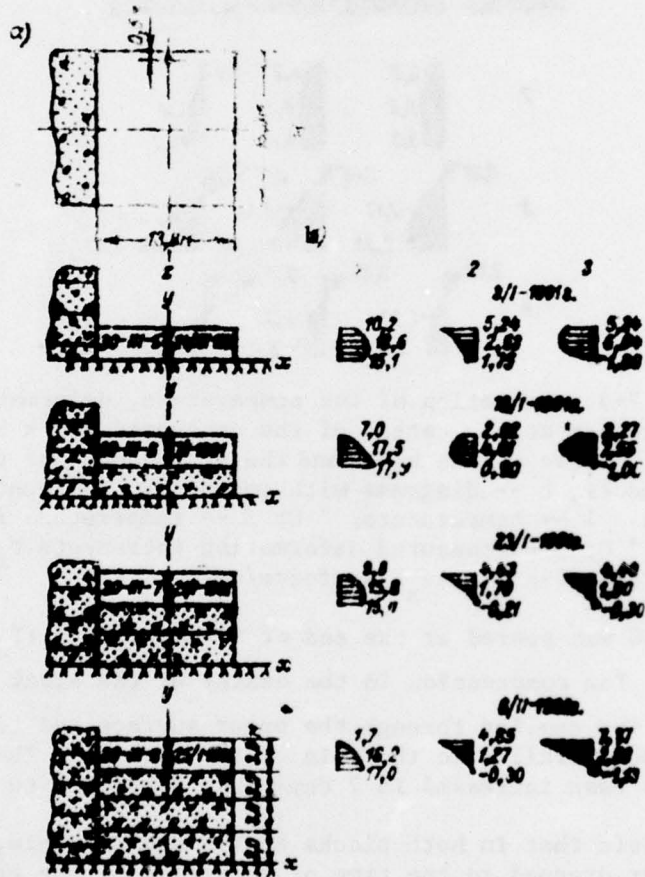


Figure 7-2B. Stressed state of uncovered blocks of III of section 30: a -- schematic of the blocks (plan view and sections); b -- distribution with respect to height of the block. 1 -- temperature; 2 -- measured deformations ε_x ; 3 -- stresses σ_x .

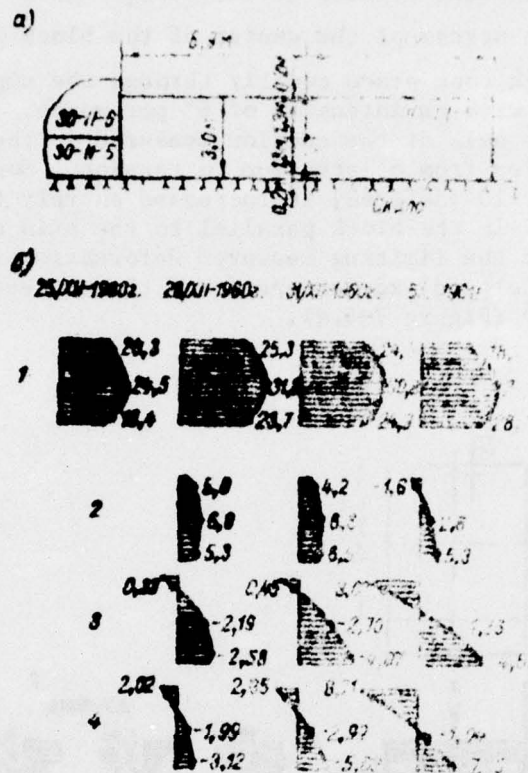


Figure 7-3. Variation of the temperature, deformations and stresses at the center of the uncovered block 30-II-5; a -- schematic of the block and the arrangement of the instruments; b -- diagrams with respect to the central section. 1 -- temperature, °C; 2 -- temperature increments, °C; 3 -- measured deformation increments $\sigma_x \cdot 10^{-5}$; 4 -- stress increment σ_x , kg-force/cm².

The block 51-IY-10 was poured at the end of November 1959 ($T_{\text{conc}} = 10\text{--}11^\circ \text{C}$, $T_{\text{max}} = 33.5^\circ \text{C}$). The compression in the center of the block did not exceed 6 kg-force/cm^2 . The cooling through the upper surface led to the occurrence of a vertical crack parallel to the axis of the section. The measured deformation in this case increased in 7 days from $1.23 \cdot 10^{-5}$ to $45 \cdot 10^{-5}$.

It is characteristic that in both blocks 65-V-9 and 51-IV-10, the temperature in the center dropped to the time of formation of the crack a total of 10-14° C.

The basic cause of the formation of the vertical cracks running through the center of the uncovered block is the nonuniformity of the temperature field vertically. However, for exothermal heating and subsequent cooling of the

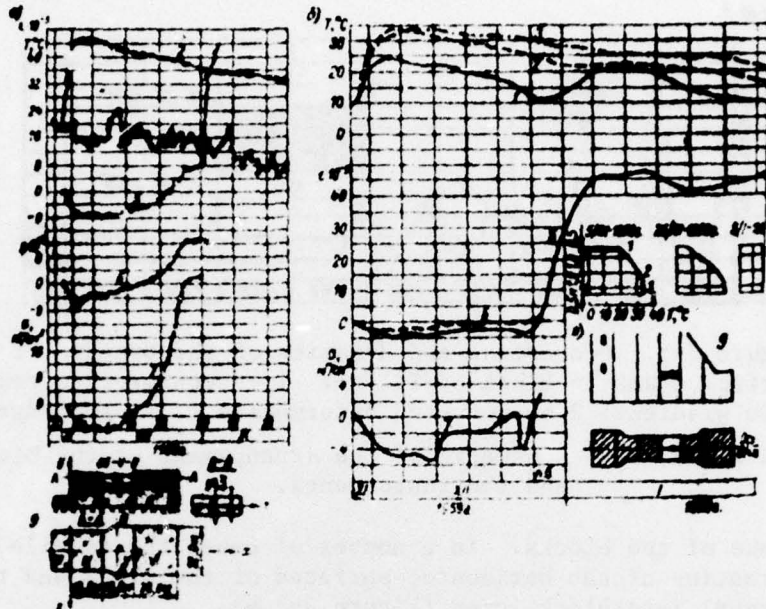


Figure 7-4. Occurrence of cracks in the center of the uncovered block: a -- [illegible], b -- 51-IV-10. 1,2,3 -- temperature of the concrete at the points with respect to the diagram: 4 -- air temperature; 5 -- measured deformation; 6 -- elastic deformation [illegible]/E; 7 -- stress σ_x ; 8 -- temperature diagrams, [illegible] of the block.

block usually the cooling takes place through the lateral faces.

The nonuniformity of the temperature field in the horizontal direction causes the occurrence of tensile stresses on the block faces with respect to the vertical areas perpendicular to these faces. These stresses can spread to the entire height of the block (Figure 7-2,b) and involve the occurrence of a vertical crack first of all on the lateral surface of the block. An example of this crack occurring 7 days after pouring the block for a center-face temperature gradient of 25° C is presented in Figure 7-5.

It is possible to say that in a number of cases the combination of the non-uniform temperature field vertically and horizontally can lead to a through crack.

The data that we obtained on the strain gage measurements permit us to determine the stress distribution with respect to horizontal areas during the period of exothermal heating of the uncovered block.

It is obvious from Figure 7-6, the stress diagrams with respect to the horizontal areas σ_y have a unique form. Common to them is the occurrence between the period of exothermal heating of a region of tensile stresses on the

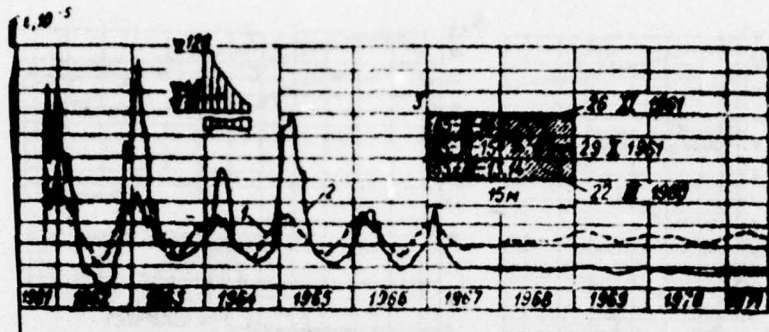


Figure 7-5. Occurrence and dynamics of the opening of the surface crack in block 65-III-15. 1 -- center-face temperature gradient; 2 -- measured deformation ϵ_x at the edge of the block; 3 -- schematic of the arrangement of the blocks and the instruments.

lateral surface of the blocks. In a number of cases the tensile stresses lead to deformation of the horizontal surfaces of the crack and the opening of the horizontal interblock joint (Figure 7-1,b).

The opening of the horizontal interblock joint is shown in Figure 7-7A. During the heating of the block its edges in the headwater and downstream face directions opened with an increase in the compression in the middle part of the joint. As the block cooled the edges began to close; at the center the joint opened so much that string of the strain gage broke. The same picture was observed also in other joints in the right bank sections.

The occurrence of tensile stresses with respect to the horizontal areas on the lateral surface of the block was caused by the positive temperature gradient between the center of the block and its lateral surfaces. The magnitude of the stresses increases with an increase in the nonuniformity of the temperature field.

As the exothermal heat dissipates, the tensile stresses on the edges of the blocks decrease and become compressive. The horizontal surface cracks close in this case.

In a number of cases the deformations measured by the remote strain gages indicate the occurrence of the horizontal internal cracks (Figure 7-7B).

The characteristic feature of the distribution of the vertical deformations and stresses with respect to the horizontal cross section of the blocks during the period of exothermal heating is a saddle nature of the diagram with the occurrence of the central part of the block of small compressive stresses or small tensile stresses (Figure 7-6,b) which, however, considering the low tensile strength of concrete and the early age, they can lead to the occurrence of cracks.

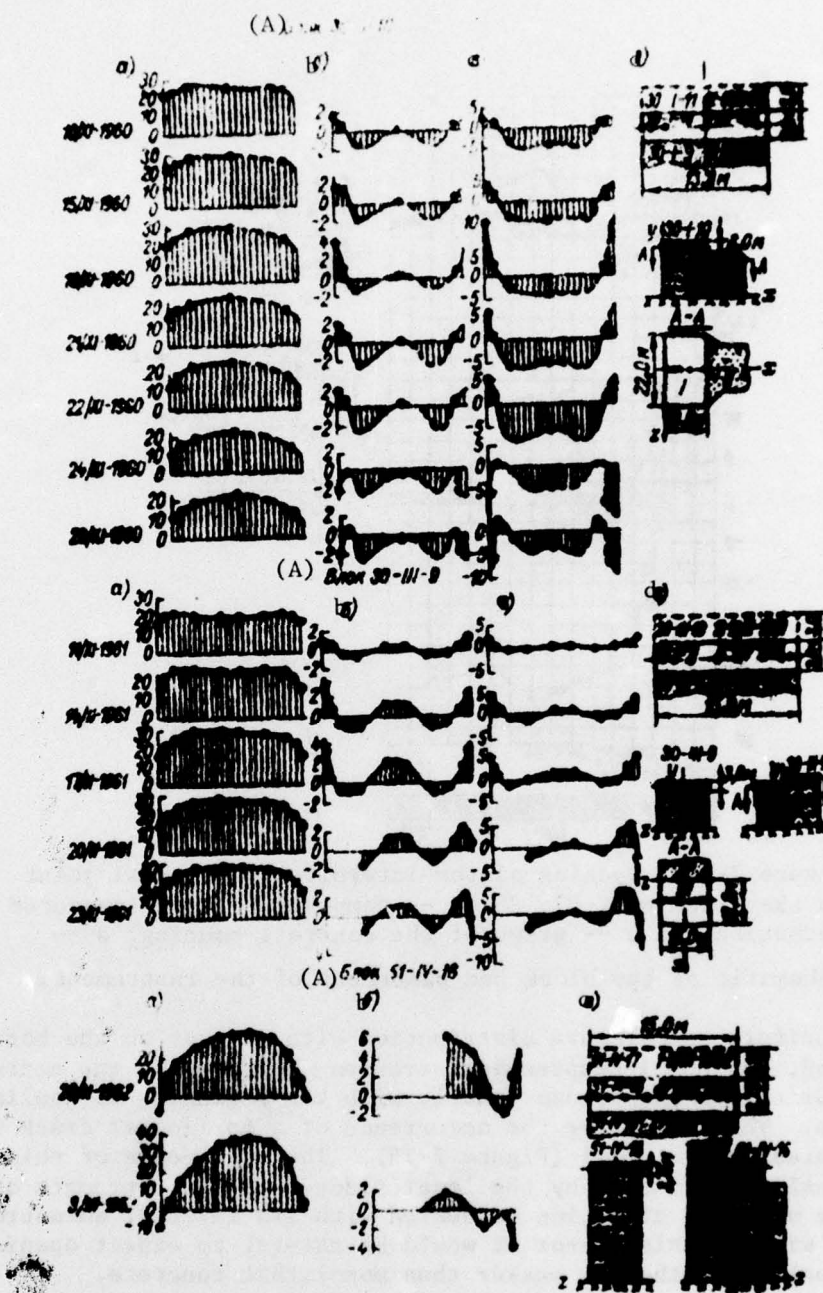


Figure 7-6. Distribution with respect to the horizontal axial cross section of the blocks (30-I-[deleted], 30-III-9, 51-IV-16): a -- temperature, T, °C; b -- measured deformations ε_y , 10^5 ; c -- stresses σ_y , kg-force/cm 2 ; d -- schematic of the block and placement of the instrument.

Key: A. block

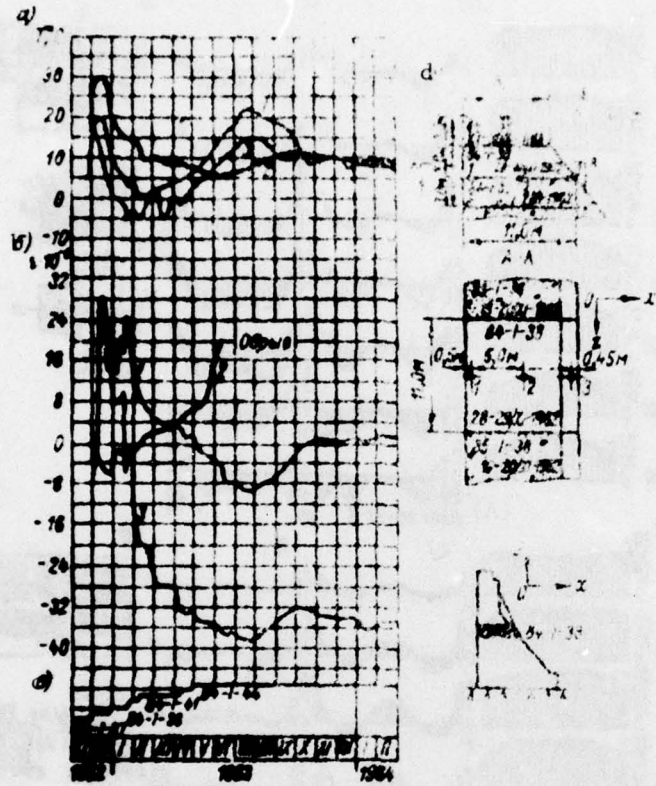


Figure 7-7A. Opening of the interblock horizontal joint in the block 84-I-37, 38; a -- temperature; b -- measured formation ϵ_y ; c -- graph of the concrete pouring; d -- schematic of the block and placement of the instrument.

For the nonuniform temperature distribution with respect to the horizontal cross section, the small compressive stresses occurring in the center of the block during heating become tensile with the beginning of cooling of the concrete. This can cause the occurrence of a horizontal crack if the initial compression is small (Figure 7-7B). The occurrence of this type of crack obviously is promoted by the local reduced tensile strength of the concrete in the vertical direction connected with its layered, anisotropic structure. Without this factor it would be natural to expect opening of the interblock joint, that is weaker than monolithic concrete.

7-5. Crack Formation Connected with Covering of the Blocks

The covering of the block is a highly important factor influencing its stressed state and monolithic nature. The occurrence of a vertical crack immediately after covering was noted in a number of blocks.

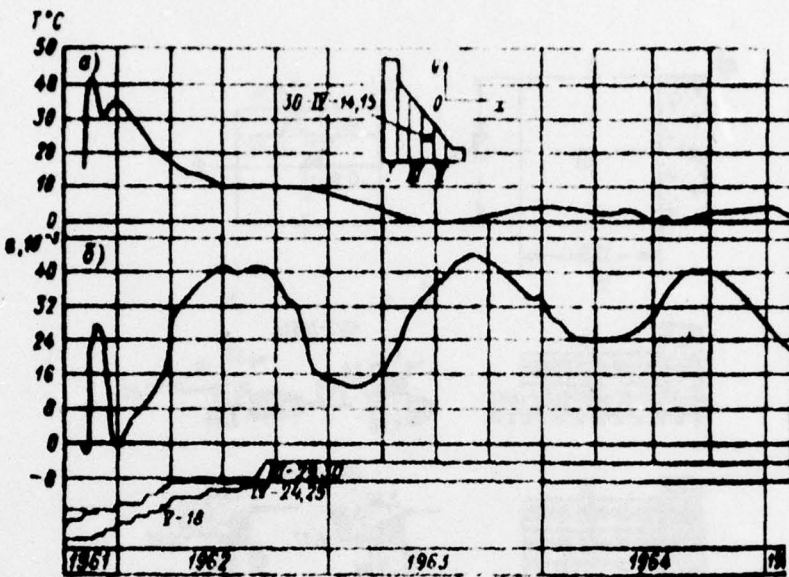


Figure 7-7B. Occurrence of a horizontal crack in the center of the block 30-IV-14, 15: a -- temperature, b -- measured deformation ϵ_y and concrete pouring schedule.

The covering of the block in which the dispersion of the exothermal heat has still not completed causes secondary rise in the temperature, a consequence of which is the hydrostatic compression in the central part of the covered block. This compression promotes closure of the internal cracks (Figure 7-7B).

With a long temperature interval between pouring the blocks and the covering, the exothermal heat in the covered block is dissipated, and the stressed state of this block changes under the effect of the exothermal heating of the top block. On static interaction between the heated upper block and the cooling, more rigid covered block, additional tensile stress occur in the latter frequently leading to the formation of vertical cracks or opening of the crack occurring in advance (see Figure 7-1,c). The probability of occurrence of this crack was greater the higher the thermal gradient between the two blocks. The cracks occur also in the upper block when it is cooling. The variation in nature of the stress distribution (deformations) with respect to the vertical areas by covering of the blocks is shown in Figure 7-8. For comparison in Figure 7-8,b we have the stress diagrams for the block uniformly heated with respect to the base constructed along the lines of influence for $E_l/E_{\text{meas}} = [deleted]$ [123].

For the case of the uniformly heated block the maximum tension connector at the boundary of the blocks, as was noted in § 6-3. Under natural conditions the tension in the upper part of the block decreases as a result of the compression caused by the heat fluxes from above; the maximum tension shifts to

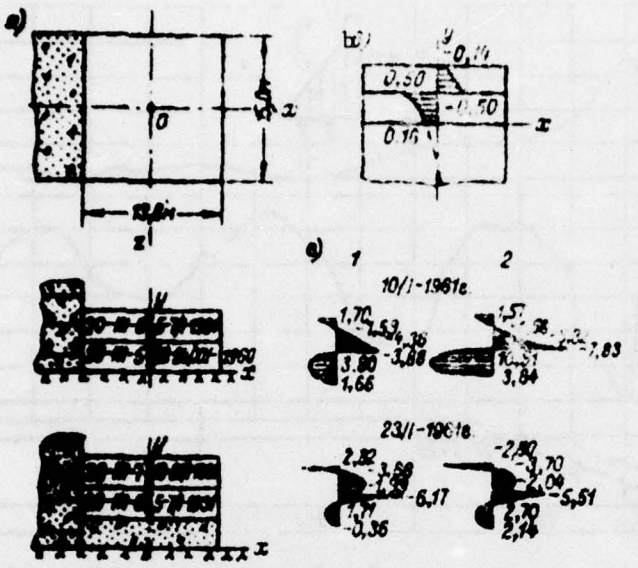


Figure 7-8. Effect of the covering on the stressed state of the block 30-III-5; a -- diagram of the block; b -- theoretical diagram of σ_x for the uniformly heated block in the halfband in fractions of $E\alpha\Delta T/1 - \nu$; c -- diagrams with respect to height of the block (1 -- measured deformations $\epsilon \cdot 10^{-5}$ occurring as a result of the covering, 2 -- measured σ_x).

the center of the covered block, and at the boundary of the blocks compressive stresses will occur which are propagated to some distance into the depth of the lower block (Figure 7-8,c).

On the edge of the blocks the region of tensile stresses after covering extends to the entire height of the covered block.

The nature of variation of the deformation and the stresses in the blocks after covering is shown in Figure 7-9.

The variation of the stresses with respect to the horizontal areas after covering of the block is also caused by the increase in the temperature [deleted] from the exothermal heating of the covering block.

In three blocks poured at different times and covered after 7-13 days, the effect of the covering turned out to be qualitatively identical was expressed in the occurrence of conversive stresses on the edge of the blocks. The horizontal cracks in this case were closed (Figure 7-6, 7-7). The effect of the compression on the edges of the block obtained in this way also established

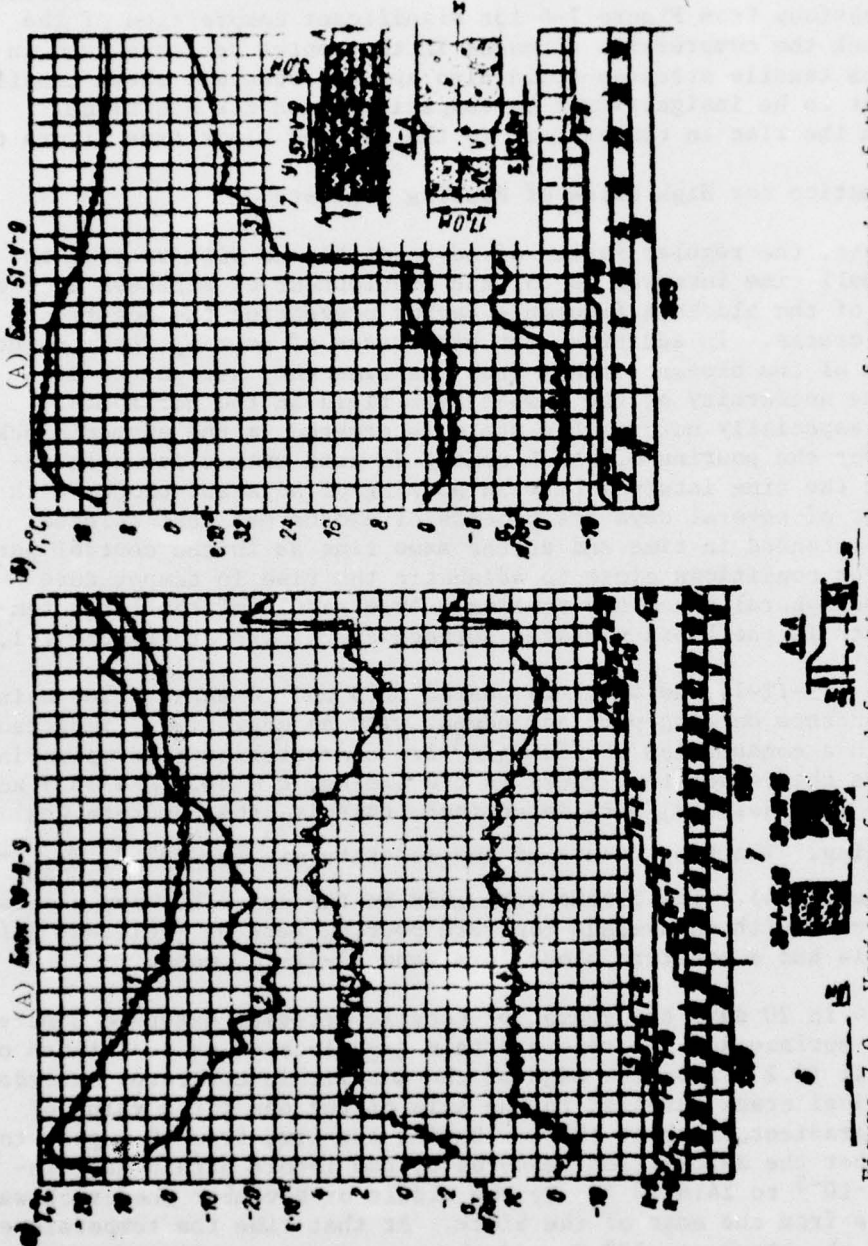


Figure 7-9. Variation of the deformations and stress after covering of the blocks: a -- block 30-II-9; b -- 51-V-9. 1 -- concrete temperature; 2 -- air temperature; 3 -- measured deformation ε_z ; 3' -- elastic deformation $\varepsilon_z = \sigma_z/E$; 4 -- stress σ_z ; 5 -- graphs of the concreting of the columns; 6 -- schematic of the arrangement of the blocks in the instruments on the date the concrete is poured; [deleted].

Key: A, block

for other investigations [deleted] has a practical significance especially for the edges of the blocks of the pressure face dam (see Chapter 6).

On the occurrence of the compressive stresses with respect to the horizontal areas on the edges of the block in the center small tensile stresses should appear. As is obvious from Figure 7-6 for significant compression of the edges of the block the compressive stresses in the center decrease, and in a number of cases tensile stresses could also appear; however, these tensile stresses turn out to be insignificant by comparison with the additional compression from the rise in temperature in the covered block (see Figure 6-6).

7-6. Crack Formation for High Rates of Pouring Concrete

As was noted above, the regular laying of adjacent blocks with respect to height with a small time interval is for the development of stresses in the central regions of the blocks a favorable factor preventing the occurrence of the internal cracks. In addition, for high rates of pouring the concrete the stress state of the blocks already from the time they are poured is determined by the uniformity of the temperature field in the horizontal direction. The especially unfavorable state is created in the summer blocks (July, August) for the pouring of which cement is used with a low heat release rate. For the time interval between pouring of adjacent blocks with respect to height of several days the process of exothermal heat release turns out to be extended in time and at the same time as in the central part of the block under conditions close to adiabatic the rise in temperature continues, the peripheral zones are cooling. As a result of the large temperature gradients in the block vertical surface cracks appear (Figure 7-1,d).

The blocks 45-II-14 and 47-II-14 poured on 9 and 14 August 1960 using type 100, V-2 concrete on slag portland cement with an activity of [deleted] kg-force/cm² with a consumption of 180 kg/m³ are characteristic examples in this respect. As the temperature rises in the blocks, $q = 68.2$ and 73.9 kcal/kg, $A_{20} = 0.408$ and [deleted] were determined, that is, the concrete was gradually hardening. The temperature of the concrete mix was 20° C, $T_{\max} = 46^\circ$ C (see Figure 4-4). The blocks were laid in the space between blocks I and III of columns with an average concrete pouring rate of [deleted] 9m/month. The block 45-II-14 had a concrete block form, and 47-II-14, wood.

In block 45-II-14 in 20 days the region of tensile stresses extended 3 meters from the lateral surface and the remote strain gage located at a distance of 0.9 meters from it (0.2 m from the edge of the monolithic concrete) recorded the surface vertical crack parallel to the axis of the dam for a value of the temperature gradient of about 19° C. During the time from 30 August to [deleted] September the deformation measured by the remote strain gage increased from $8.3 \cdot 10^{-5}$ to $24.6 \cdot 10^{-5}$. By the middle of November the crack was spread 4.5 meters from the edge of the block. At that time the temperature in the center of the block was 37° C, and the temperature gradient reached 33° C.

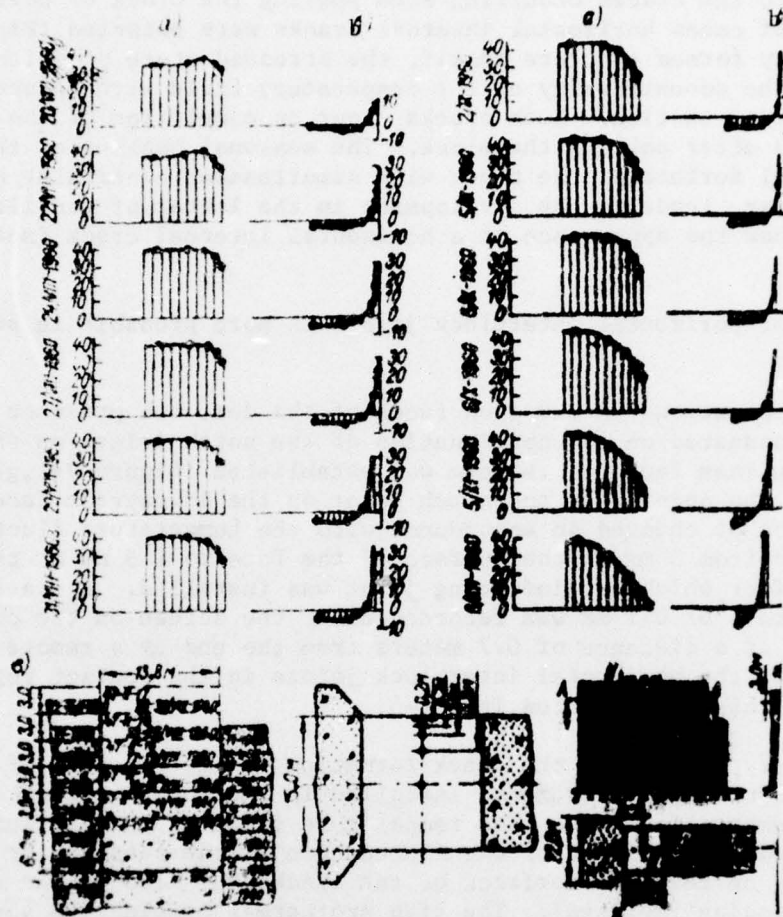


Figure 7-10. Distribution with respect to axial horizontal cross section of the block 47-II-[deleted]. a -- temperature, $T^{\circ} C$; b -- stresses σ_z , kg-force/cm 2 ; c -- schematic for arrangement of the blocks and the instruments.

In 47-II-14 the vertical surface crack ($\varepsilon_x = [deLETED] 28 \cdot 10^{-5}$) occurred at a distance of 0.2 meters from the lateral surface of the block 12 days after it was pouged for a temperature gradient of $15^{\circ} C$. During the subsequent 8 days the crack extended to 1.8 meters from the edge of the block, and by the beginning of January it penetrated to 3.8 meters into the block. The temperature in the center of the block at that time was $34^{\circ} C$, and the temperature gradient was $36^{\circ} C$ (Figure 7-10).

7-7. Crack Formation in the Concrete Massif made of Old Concrete

In addition to the cracks occurring when pouring the block or covering it, in a number of cases horizontal internal cracks were detected (Figure 7-1,e) in the already formed concrete massif, the stressed state of which is determined by the nonuniformity of the temperature field with respect to the horizontal cross section. Such cracks occur on completion of the first winter period after pouring the block. The seasonal heating of the concrete on the lateral surface of the block with simultaneous continuing cooling of the central part leads to the development in the latter of tensile stresses which can cause the appearance of a horizontal internal crack (see Figure 7-11).

The opening of horizontal interblock joints is more probable in such cases (Figure 7-7).

By visual observations on the open faces of the dam, the presence of a number of cracks propagated on the continuation of the notch joints on the pressure and the downstream faces of the dam was established (Figure 7-1,g). Thus, for example, the opening of the notch joint on the downstream face of the dam in section 65 changed in accordance with the temperature fluctuations and decreased from 3 mm on the surface of the face to 1.3 mm at the end of the joint, after which a reinforcing joint was installed. A crack with opening on the order of 0.1 mm was recorded after the screen on the continuation of the joint at a distance of 0.7 meters from the end by a remote strain gage. The opening of the horizontal interblock joints in the contact region between the adjacent columns was noted in § 6-5.

It is necessary to discuss the crack formation in the concrete of the sectional part of the dam. The instruments installed in the lower part of section 36 recorded a number of cracks. The temperature field of the station sections was formed under the effect of the fluctuation at the outside air temperature not only on the open surfaces of the blocks but also on the internal region surrounding [deleted]. The high exothermal heating (to 45-50° C) of the summer blocks was replaced by cooling of them where the outside surfaces of the blocks and the steel shell cooled more intensely than the inside regions of the comparatively thin concrete cross sections as a result of which significant temperature gradients arose in the latter.

The occurrence of cracks in the concrete around the conduit is illustrated by Figure 7-12. Soon after covering, annular and longitudinal cracks arose in the blocks which is indicated by the sharp increase in the elongation deformations of the concrete to value of [deleted] 10^{-5} and more leaving no doubt about the occurrence of the crack formation. The greatest crack opening is noted at a distance of 2 meters from the shell, that is, beyond the limits of the annular reinforcing.

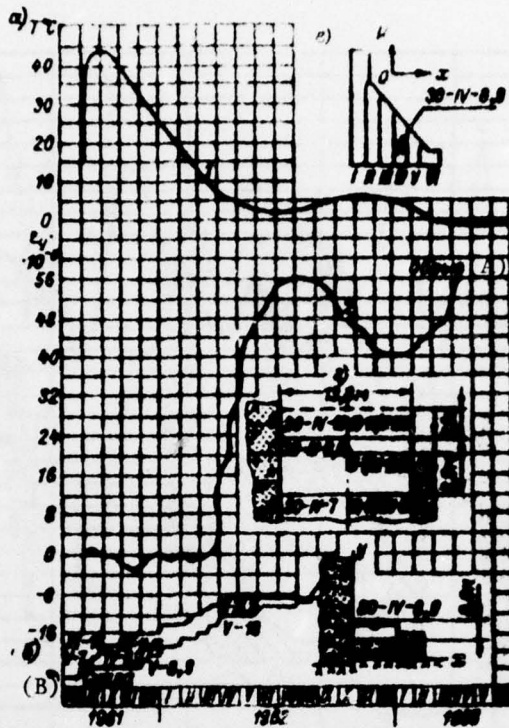


Figure 7-11. Occurrence of horizontal internal cracks in blocks 30-IV-8, 9: a -- temperature (1) and measured deformation ϵ_y (2); b -- concrete pouring charge; c,d -- schematics for arrangement of the blocks and the instruments.

Key: A. separation B. rock

7-8. Variation of the Opening of the Cracks in Time

From what has been discussed in § 7-4-7-7 it is obvious that the greater part of the cracks occurring in the dam blocks are with respect to origin cracks from the construction period. Accordingly, the dynamics of their opening in the various pores are determined by the rose and the rate of covering of the blocks, the laying of the blocks of adjacent columns, the heat protective properties of the forms and the time of removal of the forms. As the exothermal heat is scattered and the temperature is equalized with respect to height of the massif the dynamics of the crack opening are determined more and more by the nonuniformity of the temperature field with respect to the horizontal cross section.

The most widespread are the vertical surface cracks. The dynamics of the opening of such cracks soon after their appearance are beginning to be determined primarily by the center-face gradient. The opening of the

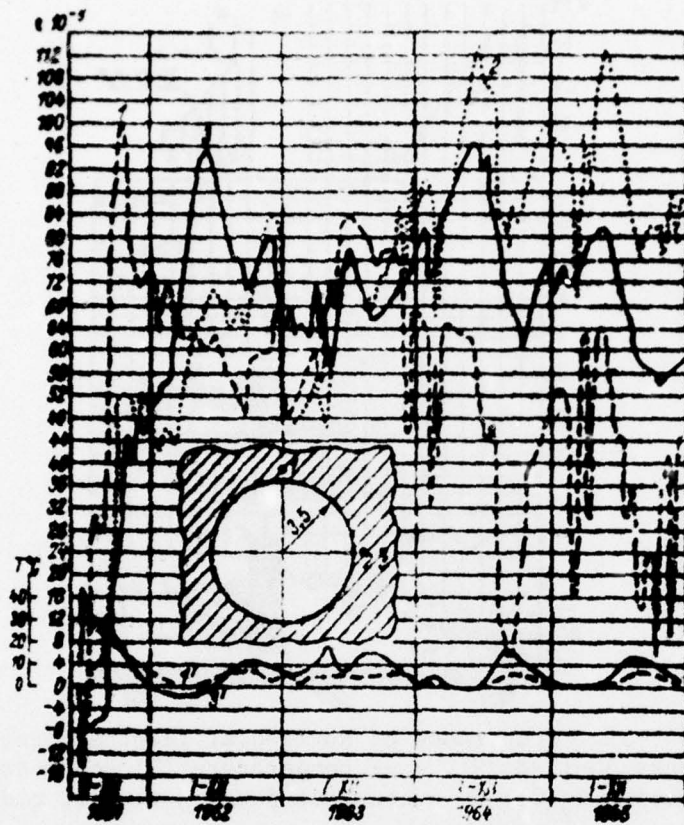


Figure 7-12. Crack formation around the turbine conduit of section [deleted] of the dam. Deformations in the concrete measured in the following directions: 1 -- annular, 0.9 m above the shell; 2 -- longitudinal, 0.9 m to the right; 3 -- annular 2 meters to the right; 1' and 3' -- temperature at points 1 and 3 (see the schematic).

vertical surface cracks varied in time periodically in accordance with the nature of the temperature gradient (Figure 4-7). The maximum openings occurred during the period of minimum temperatures of the concrete (December-March); in the summer the cracks are completely or partially closed.

The greatest opening of the cracks appeared either in the first winter after pouring the concrete or in the second winter. Then the opening of the cracks diminished as the center-face temperature gradient dropped and the temperature on the open surface of the columns rose. After covering of the expanded joints the amplitudes of the fluctuations of the openings decreased sharply, and the cracks either closed (Figure 7-5) or they stabilized with respect to some partial opening.

The opening of the horizontal surface crack and the interblock joint begins to diminish immediately after the exothermal peak and also after covering the block. As was noted in Chapter [deleted] the variations of the temperature gradient between the center of the block and the open surfaces are felt more noticeably on the stresses with respect to the horizontal areas σ_y than vertically. Accordingly, the decrease in the temperature gradient promotes closure of the horizontal surface cracks more than the vertical. Inasmuch as in the open surfaces of the blocks which merge in the expanded joints and on the pressure face, a gradual increase in the compressive stresses σ_y was observed, the horizontal surface cracks and opening interblock joints were closed (Figure 7-6).

The variation in opening of the internal vertical longitudinal cracks (the perpendicular cross sectional axes) is connected with variation of the non-uniformity of the temperature distribution with respect to the horizontal cross sections. In accordance with the variation of the stresses σ_z in the columns of the free zone (Figure 6-10, 6-11) the amplitude of the variations in the closure of these cracks decreases, and the mean magnitude of the opening either remains stable or under the effect of the hydrostatic load on the pressure face it diminishes somewhat if the covering of the expanded joints of the opening of these cracks is stabilized [see Figure 7-13].

The opening of the internal vertical cracks parallel to the section is basically connected with the gradual cooling of the central zone of the blocks and can increase. Depending on the location of the investigated block and the point at which the deformations were measured, the nature of the variation of the openings is different. For example, in the block 30-III-5 which is next to the rock the opening of the transverse crack increased discontinuously in the warm of the year when during the process of equalization of the temperature with respect to the longitudinal cross section of the block its distribution becomes uniform, and the temperature gradient least. The magnitude of the summer increments of the opening gradually decreased, and after covering the expanded joints the opening of the cracks stabilized at a value much less than the maximum opening (see Figure 7-14, 2).

In the block of the extracontact zone (51-V-9), periodic variations of the opening of the transverse crack were observed with a decrease in the amplitude and insignificant change in the mean opening. From 1967 the opening of this crack stabilized at a value on the order of 0.7 of the maximum opening.

The variation of the opening of the cracks in the section of the stationary dam is determined by the combined effect of the variations of the outside air temperature of the air in the expanded joints and the water temperature in the conduit. Accordingly, the extremal seasonal values of the opening are connected with the shift in time with the maximum and minimum water temperature at the level of the water intake. The opening of the transverse cracks increases; the longitudinal (annular) ones decrease (Figure 7-14, and 9-2). The water pressure in the conduit has some effect on the opening of

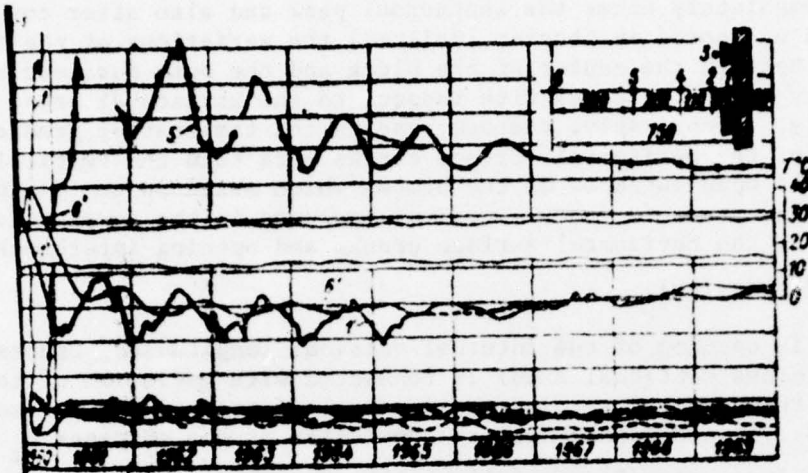


Figure 7-13. Variation of the opening of the internal longitudinal crack in block [deleted] 1' and 6' -- temperature at points 1 and 6; 1 and 5 -- deformation Δ_x at points 1 and 5; crosshatched -- limits of deformation at points 2, 3, 4 and 6.

the cracks. The filling and emptying of the latter is accompanied by discontinuous variations of the crack openings.

The opening of the horizontal cracks occurring as a result of the interaction of the columns (see Figure 7-14) decreased as the irreversible horizontal displacements of the dam increased, but significant seasonal variations of these openings are observed during operation.

The maximum magnitude of the opening of the cracks fixed by the remote strain gages is small and does not exceed 0.35-0.4 mm for the vertical surface cracks, and for the internal ones, 0.3 mm. The opening of the horizontal internal cracks is insignificant with the exception of the interblock joints in the region close to the toothed coupling where the openings are measured to [illegible] (Figure 7-14,5).

7-9. Observations of the Surface Cracks

The data presented above were obtained by the processing of the strain gage measurements in 40 blocks of the dam. How characteristic these data are for the entire dam can be determined when comparing them with the results of the systematic 7 year observations of the surface cracks. These observations were performed by the [illegible] of Orgenergostroy (V. P. Shkaran) and encompassed about [illegible] million m^3 of concrete.

The observations were performed both by direct examination with measurement of the opening by the PB-2 measuring microscope and by examination through binoculars [114].

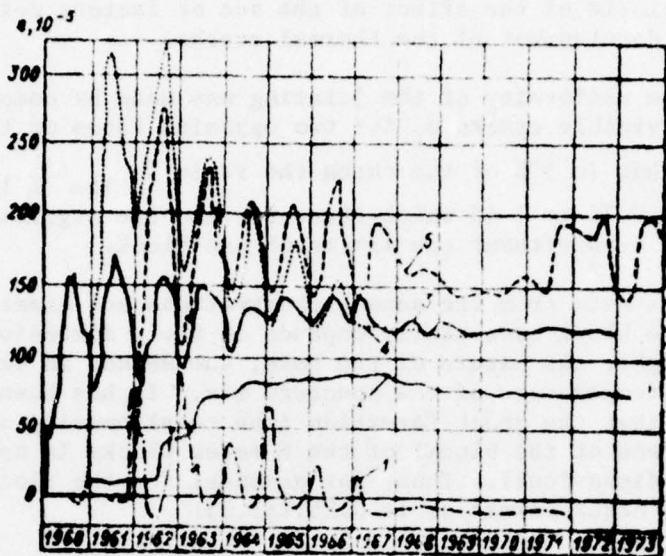


Figure 7-14. Variation of the openings of standard cracks.
 1 -- surface, vertical longitudinal; 2 -- internal, vertical transverse in the block next to the rock; 3 -- internal, vertical transverse; 4 -- internal, vertical longitudinal;
 5 -- internal horizontal interblock joint.

The total number of cracks recorded on the open surfaces of the channel part of the dam, including the inspection tunnels and the hydroelectric power plant buildings amounted to 3,544 of which 238 and 135 were on the pressure and downstream faces respectively.

The cracks occurred during the first ten days after pouring the concrete when the center-face gradient was only 10 to 15° C. The basic number of cracks belongs to the period of the first winter cooling; later crack formation is observed [illegible].

The limiting crack opening is 3.2 mm. The mean mean maximum opening was within the limits from 0.2 to 0.5 mm, and the most frequently encountered openings were 0.1 to 0.2 mm.

The extent of the cracks usually did not exceed 3 meters (1 block) with a maximum length of 24 meters (8 blocks). Half of the cracks were located near the middle of the base of the block.

The opening of the thermal cracks increased with a reduction in the outside air temperature and an increase in the center-face temperature gradient. During the process of seasonal fluctuations the maximum opening was observed somewhat later than the maximum temperature gradient (see Figure 7-5); the amplitude of the variations gradually decreased, and the average opening decreased to a value on the order of [deleted] to 0.6 of the maximum. No functional relation was established between the maximum and final or residual

opening of the cracks. According to [114] this is explained by the statistical characteristic of the effect of the set of factors determining the occurrence and development of the thermal cracks.

The study of the uniformity of the jointing was made by comparing the total opening of the visible cracks δ_{Σ} for two opposite faces of the same blocks.

It turned out that in 50% of the cases the ratio $\delta_{\Sigma \text{ lim}} : \delta_{\Sigma \text{ left}}$ varies within the limits from 0.75 to 1.45 which characterizes the significant nonuniformity of the jointing even without the limits of one block.

According to the data from the annual observations and examination, the crack formation in the block essentially depends on their dimensions in the [deleted], the height, the nature of the base, the season in which the concrete is poured, the temperature of the concrete mix. It has been pointed out more than once that the crack formation (the total opening of all apparent cracks on the face of the block) of the 6 meter blocks is appreciably greater than the three-dimensional. Thus, for example, for the blocks 1.5, 3 and 6 meters high the crack formation is 0.25:1:1.35.

The statistical processing of the observation data with respect to a large number of facts made it possible to formulate the effect of a number of factors on the crack formation.

The data presented in Table 7-2 characterized the effect of the season in which the blocks are poured on the probability of crack formation. Above all it is necessary to know the general high percentage of blocks with cracks even in the period is favorable with respect to temperature of the concrete mix (April, October). The established opinion of the increased crack formation of the blocks poured in the summer is not confirmed in general. Although the temperature of the concrete mix in the summer blocks only averaged 11° C greater than in the blocks of the other seasons (see Table 4-3, 4-4), the difference in the number of summer blocks with the cracks and the blocks poured at another time of year turned out to be much less than it was possible to expect.

Table 7-2

Observation point	Blocks with cracks by month in which they were poured, %												Ave- rage for year	No. [de- leted]
	I	II	III	IV	V	VI	VII	VIII	IX	X	XI	XII		
Lateral surfaces of blocks in the expanded joints.														
Length of face 13.8 m	73	74	72	72	70	80	65	65	70	71	65	65		
Walls of the inspection tunnels.	94	100	82	81	95	88	67	100	95	95	95	95		
Length of face 22 m														

A more detailed analysis shows that the season in which the concrete is poured influences the crack formation differently depending on other factors. For example, with a length of face less than 11 to 12 meters, the season in which the concrete is poured (the temperature of the concrete mix) has no

effect on the crack formation. In the summer blocks of the first columns on the old (age greater than 30 days) concrete the crack formation turned out to be 2 to 2.5 times greater than in the same spring blocks.

The plan dimensions (length of face) and nature of the base (Table 7-3) have the greatest effect on the crack formation in the blocks. As is obvious from the table, with respect to effect on the crack formation the old concrete differs little from the rock. In the three meter blocks with the face length of 13.6 meters the probability of crack formation in practice does not depend on the nature of the base; for a face length of 22 meters it is close to 100%.

The crack formation in the block is caused by the length of the face. Thus, [deleted] the walls of the drainage tunnels of the station part of the dam, the blocks of which are distinguished only by the length of the face, the crack formation characteristics were obtained which were presented in Table 7-4 [114].

Table 7-3

Observation point	Length of face, m	Base	Faces with cracks, %
Direct effect of outside air			
Drainage tunnels of the shore part of the dam	7	Rock	67
Pressure face	11	Rock Concrete $\tau > 30$ da Concrete $\tau < 30$ da	100 96 65
Attenuated effect of the outside air			
Expanded joints	13.8 22	Rock Concrete $\tau > 30$ day Concrete $\tau < 30$ day Concrete	80 79 74 100
Walls of the inspection and cementation tunnels	11	Concrete $\tau < 30$ day	40
Walls of the inspection tunnel	22	Concrete $\tau > 30$ day Concrete $\tau < 30$ day	91 90

With respect to the situation in March 1965, 79% of all of the recorded cracks pertain to the channel dam and 16% to the shore dams; [deleted] % pertain to the hydroelectric power plant building. Out of the 2,777 cracks in the channel dam 40% go to the inspection tunnels and 30% to the expanded joint (Table 7-5). As was pointed out in Chapter 4, the former were in communication by the expanded joints and the temperature regime in them was

not regulated, and the latter remained opened and their temperature for a prolonged time remained close to the outside air temperature. The crack formation was appreciably less on the surfaces of the shore part of the dam emerging into the expanded joints. In the left bank dam the blocks were poured with open expanded joints. The number of cracks was 105, and the maximum opening was 1.9 mm. In the right bank part of the dam the blocks for the inside region were poured in the summer of 1962, and the joints were covered in the fall of the same year. There were 44 cracks and a maximum opening of 0.9 mm. In the cementation tunnel not having exits to the expanded joints, the crack formation is insignificant.

Table 7-4

Characteristics	Length of the face,		
	7.6	13	18
No of blocks with cracks, %	54	75	100
Total opening, mm	0.55	1.38	2.9
Opening of the largest cracks, mm	0.55	0.88	1.43

Table 7-5

Location of surface	No of cracks in March		
	1965	1969	1972
Pressure face	238	—	—
Downstream face	135	178	—
Tunnels: cementation	26	26	29
inspection	943	1294	1644
through	179	194	279
transverse	12		
drainage	208		
Expanded joints	53	500	
Intercolumnar joints	129		
Horizontal surfaces of the blocks	40		
		2 2777	

The examination of the cracks in 1969 (NIS Institute of Orgenergostroy) and 1971 and 1972 (the hydraulic shop of the Bratsk Hydroelectric Power Plant) demonstrated the changes caused by the finding of new, previously detected cracks and closure of the cracks recorded during the preceding examinations. Thus, in 1969 the number of cracks in the expanded joints decreased (by comparison with 1965) by 243, which is explained by the covering of the expanded joints. The new cracks were detected: on the pressure face (above the headwater level) there were 51, on the downstream face there were 53, in the inspection tunnels there were 88, in the through tunnels there were 21. Judging by the openings $\delta_{ave} = 0.04-0.07$ mm and $\delta_{ave}^{max} = (0,0[deleted] to 0.11)$ mm newly detected cracks in the inspection tunnels [deleted] new and previously not noted. In the through tunnels ($\delta_{mean} = 0.14$ mm; $\delta_{mean}^{max} = 0.6$ mm) the

cracks obviously are new. By 1972 the number of cracks in the tunnels increased by 103 and reached 279 total with an average opening of 0.27 mm (data from the hydraulic shop of the Bratsk Hydroelectric Power Plant).

So far as it is possible to determine new data, the crack formation process on the surface with a face length of 22 meters under the direct effect of the outside air still was not stabilized.

7-10. Probability of Through Crack Formation in the Blocks

We have at our disposal data on 12 blocks of the inside region in which there are longitudinal sections of the remote strain gages. Only in one of them (20-III-5) it is possible to suspect the presence of a through crack. In the remaining blocks in the central region the compression deformations remain with respect to vertical areas.

The cracks in the longitudinal direction, the surface and inside cracks gradually were closed, and since 1967 the openings have stabilized (Figure 7-13, 7-14). Beginning with this fact and all of the nature of the variation in time of the stresses σ (see Chapter 6), it is possible to consider the development of the available longitudinal surface cracks into through ones to have low probability. The stresses σ_z and the cracks in the transverse direction and the columns of the inside region also stabilized, and there are no reasons to expect an increase in the openings under operating conditions.

In [114] the probability of the through cracks in the longitudinal direction was estimated at 12%. The through cracks were also detected in the thin elements and the blocks of elongated shape and plan view (piers, the tunnel walls for the technical equipment, long blocks in section 4). The presence of cracks in the central region of the columnar blocks was established by inspecting the surface of the calex hole [124]. There are no more defined data on the through cracks in the dam, and it is possible to show that if such cracks exist, the number is insignificant.

It is necessary especially to discuss the seepage cracks of the transverse direction in the first columns of the dam which are through at least to the inspection tunnels.

A number of cracks recorded on the pressure face was 238; of them there were about 210 seepage cracks in 1963.

The occurrence of the transverse cracks coming from the surface of the pressure face is caused by nonuniformity of the temperature distribution in the transverse direction. The variation and time of the opening of these cracks is analogous to the variation of the opening of the surface longitudinal cracks (Figure 7-5) which during the process of the seasonal variations closed gradually. Accordingly, the flow rate of the seepage through the cracks in the pressure face have a seasonal nature and gradually decrease.

The seepage intensity was caused by the same factors as the jointing of the blocks. According to the data of [114], for the face length to 12 meters the weak seepage was observed in no more than 10% of the blocks next to the rock and it was absent in the block made of fresh and old concrete. For a face length of 22 meters the seepage was observed in all of the blocks made from old concrete. The greatest seepage flow rate through one crack was noted in the summer of three meter block placed on a concrete base about 6 months old. In March 1963 with a crack opening of 1.2 mm the flow rate through it was 19.7 liters per minute; after two years it decreased to 1.5 liters per minute, and after two years to 0.01 liters per minute (the hydraulic shop data).

In March 1963 there were about 210 cracks with noticeable water emission; the flow rate which could be measured in only 122 cracks was 53.4 liters per minute. By March 1965 the number of cracks decreased to 58 and 29 respectively, and the flow rate decreased to 19.2 liters per minute. In March 1967 there were 26 seepage cracks; the flow, which was measured in nine of them amounted to 6 liters per minute. During the 1967-1971 period, the flow measured in the 12 cracks was within the limits of 5-12 liters per minute.

The total seepage flow rate through all of the cracks in the pressure face decreased in two years (1963-1965) from 924 to 80 liters per minute. This is basically a consequence of the closure of the cracks under the effect of the temperature variations. In addition, a decrease in the seepage was promoted by the colmatation of the cracks by the products of the bleaching out of the cement and their carbonization. The number of cracks with pressure filtration to 1967 decreased with a simultaneous increase in the number of cracks with traces of moisture and removal of salts and also dry cracks.

It is necessary to note that the observations of the condition and the seepage flow rate on the pressure face of dam have not been organized as they should have been. Only at the end of 1973 and the beginning of 1974 were devices built to measure the flow rates through the three cracks with pressure seepage and 20 drainage holes. According to the available data it is possible, however, to establish a trend toward an increase in the number of cracks with weak seepage, the flow of which cannot be measured. Obviously this is explained by the process of corrosion of the concrete although the water in the reservoir is considered nonaggressive for it. In many locations in the dam, especially in the inspection tunnels at the 45 and 63 meter marks, the removal of the products of bleaching out of the cement is observed, the layer of which is accumulated on the floor of the tunnel.

By the initiative and under the direction of K. B. Alekseyev in December 1973, in March and May of 1974 the calcium content in the water which seeped through three cracks on the pressure face and also in the drainage collectors and in the measuring spillways encompassing the entire seepage flow through the pressure face was measured. The calcium content in the water from the cracks amounted to 2 to 4 mg per liter, and the total amounted to 8-10 mg per liter. With a seepage flow rate of 18-20 liters per minute, the total amount of

calcium washed out of the body of the dam by the seepage water turned out to be 150 to 200 mg per second or 13 to 18 kg per day. With a concrete volume on the pressure front of the channel part of the dam 616,000 m³ and a calcium content of 87 kg per m³, the intensity of the removal of the calcium is of no direct danger to the life of the dam, but the effect of this intensity on the state of the cracks and the seepage through them and the joints requires further systematic study.

It is of interest to compare the data presented above with the results of the field observations of the crack formation at the Krasnoyarsk dam [115]. These observations, encompassing about two million m³ of concrete were performed by the same methods as at the Bratsk dam.

The number of blocks with through cracks does not exceed 10% of their total number. The basic cause of the through cracks is the clamping in the cooling concrete base. All of the remaining cracks are caused by high nonuniformity of the temperature distribution with respect to the horizontal direction where the majority of them (75%) occurred in the blocks where the forms were removed at an early age during preparation for the pouring of the adjacent block.

Some 25% of the cracks in the blocks in the free zone belong to the old blocks from 3 to 4 months to 2-3 years old which have the forms removed during the warm time of the year at a concrete temperature to 10-20° C. During the first winter no surface without cracks remained in such blocks.

The majority (66%) of the cracks caused by clamping occurred in the winter and spring blocks. The jointing ($\Sigma \delta_{\text{mean}}$) essentially depends on the length of face. The length of face, the season in which the concrete is poured and the temperature of the concrete mix have little effect on the crack formation.

As was noted above, in the dam being built at the Ust'-Ilim Hydroelectric Power Plant in the summer of 1974, 1,480 cracks were recorded of which no less than 16%, in all probability, were through cracks. The openings of the cracks were within the limits from fractions of mm to 3 mm with an extent on the vertical faces to 6-9 meters and on the horizontal faces to 22 meters. About 45% of all of the cracks occurred during the period of transition from the summer conditions to winter conditions and vice versa, as a result of untimely or insufficient thermal insulation of the open surfaces.

The probability of crack formation in the blocks laid on the old ($\tau > 30$ days) base is 1.5 times greater than in the blocks in the younger base. The crack formation in the three-meter blocks with planned dimensions of 22 × 13 meters is 2.5 times more frequent than in the blocks 11 × 12 meters in size. The age of the base is felt here. The most frequent crack formation is observed in the blocks of the first columns in which the inspection tunnels run.

The data with respect to the two operating dams are not comparable as a result of the different grouping of the cracks during statistical processing of the observation data. In addition, the conditions of holding the blocks

created by the presence of the expanded joints in the Bratsk dam and their absence in the Krasnoyarsk dam are also different. The smaller plan dimensions of the blocks, the smaller number of lateral surfaces subject to prolonged effects of outside air and the better organized pipe cooling cut the number of cracks in the Krasnoyarsk dam to about one-third by comparison with the Bratsk dam. The pipe cooling essentially reduced the crack formation. In three-fourths the blocks without cracks pipe cooling has been carried out and in two-thirds of the blocks with cracks it had not been carried out.

The data on the Ust'-Ilim dam are still incomplete, but they confirm some of the conclusions which can be drawn from the observations of the first two dams.

1. Under the conditions of the unregulatable temperature regime the direct effect of the outside air on the open faces of the blocks on the rock with the old concrete implies intense crack formation with a face length exceeding 11 to 12 meters. For the three-meter blocks with a face length of 13.6 and 22 meters the probability of the crack formation is close to 75-80% and 90-100% respectively, independently of the nature of the base.
2. The season in which the concrete is poured (the temperature of the concrete mix) has a noticeable effect on the crack formation in the blocks on the rock or on the old concrete, and it has little effect on the crack formation in the blocks of the free zone.

CHAPTER 8. OPENING OF THE CONSTRUCTION AND STRUCTURAL JOINTS OF THE DAM

8-1. Conditions of Making the Dam Monolithic

According to the plan, the monolithic nature of the dam at the Bratsk Hydroelectric Power Plant with columnar sectioning of it is insured by cementation of the temporary longitudinal joints for which more than 180 cementation cards of $15 \times 9 \text{ m}^2$ in size were made monolithic. This very serious problem was complicated by the fact that the solution of it on such scales was accomplished in the Soviet Union for the first time.

The plan provided for the cementation of the intercolumnar joints at a temperature of the concrete massifs of $2-3^\circ \text{ C}$ close to the mean annual operating temperature of the dam. The cementation had to be carried out with a cementation solution pressure in the joint of $2-4 \text{ kg-force/cm}^2$ with maximum additional opening of the joint at this pressure not exceeding 0.5 [deleted]. The minimum specific absorption of the cementation solution was 1.85 kg/m^2 which corresponds to opening of the joint on the order of 1.5 mm . The cementation of the joints in the massifs with negative temperature was not permitted.

Inasmuch as the temperature regulation of the columnar massifs began to be carried out with a delay, achievement of temperature to 3° C in the required time turned out to be impossible. This caused a lag in the cementation operations behind the schedule coordinated with the time for starting up the first units at the Bratsk Hydroelectric Power Plant, and therefore in 1961 the following cementation temperatures were adopted for the intercolumnar joints: 10° C for the extracontact zone (more than 12 to 15 meters from the rock base) and from 10 to $2-4^\circ \text{ C}$ on approaching the rock. The temperature of monolithing the dam was raised to 10° C after the calculations indicating that with subsequent cooling of the concrete no additional opening of the cracks occurred as a result of the effect of the hydrostatic load on the dam.

The construction control of the temperature was performed by the Gidrospets-sroyekt using the electrical resistance thermometers installed at the center of the middle of the blocks on both sides of the cementation card. The

least opening for which successful cementation is still possible was considered to be 0.5 mm [15].

In the plan the openings of the intercolumnar joints as a result of free deformation of the two adjacent columns during cooling to expanded joints were calculated. These openings for the central and peripheral regions of the cards were within the limits of 0.9 to 2.7 mm and 4.6 to 5.6 mm respectively.

The greatest openings of the joints occurred in the cases where the blocks of the adjacent columns forming the joints are poured with concrete with minimum possible lapse in time. During construction, for one reason or another, greater lapses between the times of pouring adjacent columns are permitted, and it was possible to expect a significant decrease in the opening of the intercolumnar joints.

Under these conditions, the control of the actual opening of the joints acquires special significance, in accordance with which the author organized the installation of remote crevice gages in the longitudinal joints which were not provided for by the plan. The observations encompassed [deleted] cementation cards of the experimental sections in which more than 110 remote crevice gages located at 6 marks were installed, approximately every 18 meters with respect to height. The instruments were installed perpendicular to the plane of the joint and measured the horizontal component of the mutual displacements of the adjacent columns. The crevice gages installed in the two cards perpendicularly to the plane of the faces of the toothed couplings, failed after two years of operation.

Depending on the height position of the joint the observations were performed for 10 to 12 years, and their results offer the possibility of determining the behavior of the joints under various temperature conditions before and after cementation. These observations have special significance because they are the first and most prolonged observations of the opening of the intercolumnar joints on a high gravity dam in our country.

8-2. Maximum Opening of the Intercolumnar Joints

All of the intercolumnar joints, depending on the cause of their opening can be divided into the following groups:

1. The joints, the opening of which is determined directly by the effect of the temperature.
2. The joints, the opening of which is connected with the horizontal displacements of adjacent columns with respect to each other and also having a temperature origin.
3. The joints, the opening of which is determined simultaneously by several causes.

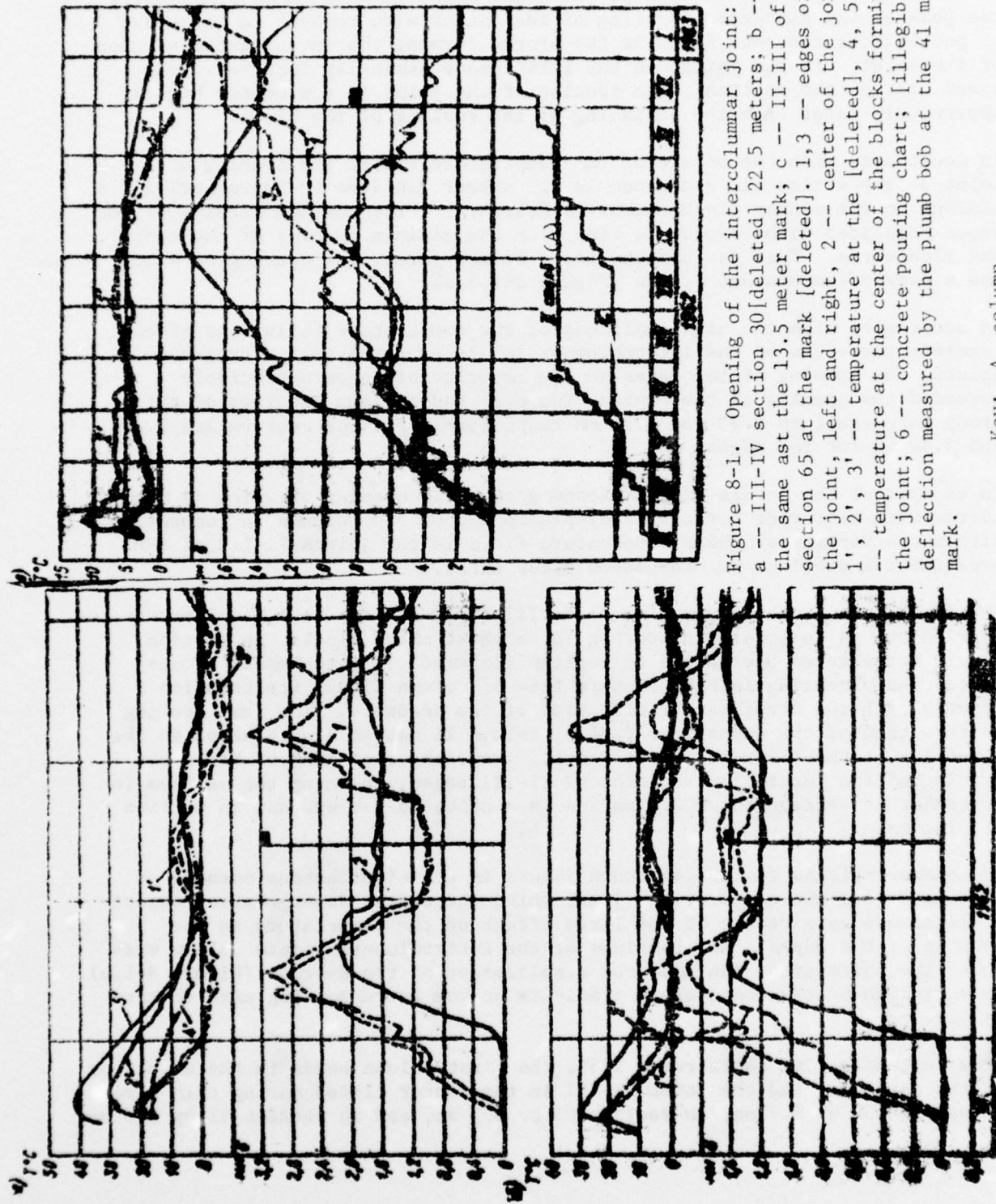


Figure 8-1. Opening of the intercolumnar joint:
 a -- III-IV section 30 [deleted] 22.5 meters; b --
 the same ast the 13.5 meter mark; c -- II-III of
 section 65 at the mark [deleted]. 1,3 -- edges of
 the joint, left and right, 2 -- center of the joint;
 1', 2', 3' -- temperature at the [deleted], 4,
 5 -- temperature at the center of the blocks forming
 the joint; 6 -- concrete pouring chart; [illegible],
 deflection measured by the plumb bob at the 41 m
 mark.

Key: A. column...

In the joints of all three groups the edges began to open immediately after the peak of the exothermal heating of the latter with respect to the order of pouring the concrete from the two blocks forming the investigated section of the joint. In the joints in the first group basically located in the lower part of the sections, the opening of the joint in the center begins appreciably later than the beginning of the cooling of the block.

In accordance with the nature of the temperature field, the opening of the joint at the center had a maximum in the summer (in June to September) and a minimum in the winter (in December to February). The maximum opening of the edges coincided with respect to time with the minimum opening of the center and vice versa. This is characteristic of the joint, the opening of which has a purely temperature origin (Figure 8-1,a,b).

In accordance with the high amplitude of the temperature variations of the concrete the edges of the intercolumnar joints emerging in the expanded joints, the opening of the edges in the majority of cases appreciably exceeded the opening of the center. The mean and maximum openings of this group were equal to 0.93 and 2.16 mm respectively for the centers and 1.21 and 3.40 mm for the edges.

An example of the joints of the second group, the opening of which is connected with different horizontal displacements of the columns in connection with nonuniformity of their temperature field is the joints II-III of the experimental sections at the 58-60 meter marks.

The intense concrete pouring in column III (from January to April 1962 was carried out as follows: in section 30, 8 three meter blocks, in section 51, 10 three meter blocks and in section [deleted], 7 three meter blocks) caused sharp heating in the pressure face of column II and its rotation jointly with the first in the direction of the headrace. The fast cooling at this time of the downstream face of column II caused its rotation in the direction of the tailrace. As a result, since the beginning of March the opening of the intercolumnar joint of II-III began, reaching the maximum in September in section 30 at 2.2 mm and in section 65 1.9 mm, and in section 51, 1.1 mm.

The characteristic feature of these joints is the simultaneous opening of the center and the edges of the joint which thereafter diverge with respect to magnitude as a result of the large effect of the temperature on the opening of the edges. The openings of the intercolumnar joints follow with some time shift after the measured displacement of the section (Figure 8-1,c) or variation of the temperature gradients on the corresponding mark (Figure 8-2,a).

From September 1962 to February 1963, the first column bends in the direction of the tailrace, and the joint II-III in the center closed during this time: in section 30 by 0.7 mm, in section 65 by 0.5 mm, and in section 51 by 0.3 mm.

The magnitude of the closure of the joint which is significantly less than the opening is explained by the following causes:

From September 1962 to February 1963, the temperature gradients in the columns had different signs and the second column inhibited the displacement of the first in the direction of the tailrace. In the same period as a result of the general cooling of the concrete, the opening of the joint increased at the edges and decreased in the center. The opening of the joint was limited by the newly concreted blocks of the third column and its cementation at the marks 54-63 meters executed at the end of 1962.

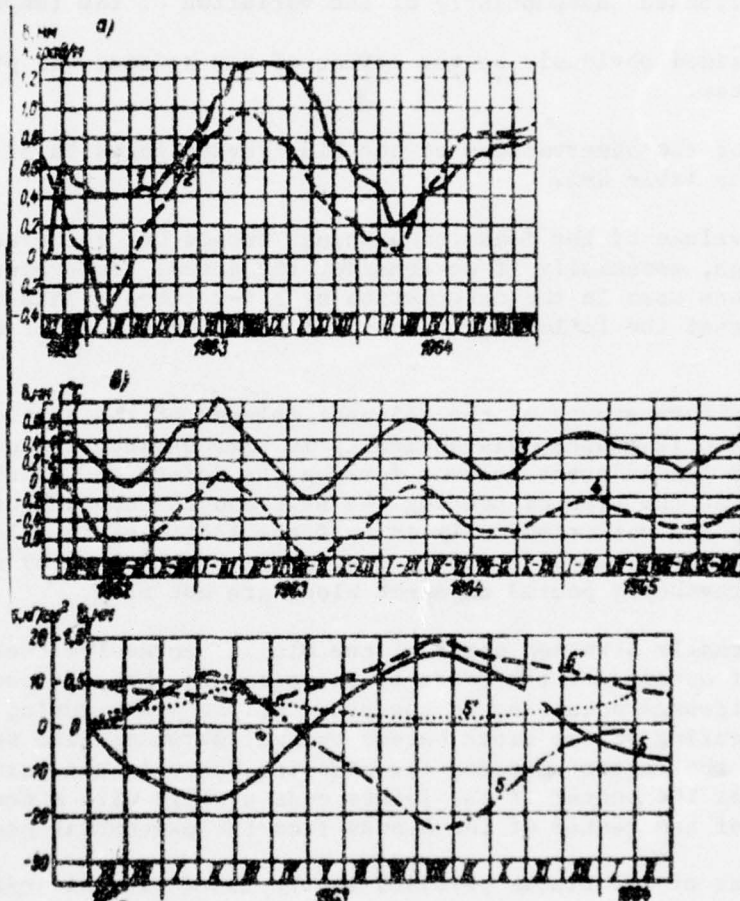


Figure 8-2. Relation between the openings of the intercolumnar joints and temperature are as follows: a -- joint I-II of section 30 at the 101 meter mark; b -- joints III-IV of section 51 at the 43.5 m mark. 1 -- opening of the joint; 2 -- temperature gradients of column I; 3 -- center-face temperature gradient. 4 -- difference in openings of the edges and centers; 5 -- stress σ_T calculated by the temperature diagram in the plane of the joint 1 meter from the edge; 6 -- the same in the center of the joint; 5', 6' -- measured openings in the joint at the same points.

Key: A. deg/m

The joints of the second group are located in the zone where the temperature gradients in the columns are high (above the 45 meter mark). The third group includes the joints, the opening of which is determined by the different factors: the variation in temperature, the deflections of the columns, the hydrostatic pressure of the headrace water.

Among the joints it is necessary especially to discuss the joints between the first and second columns (I-II). From Figure 8-3 it is obvious that the opening of the lower part of the joint does not vary, but the joint is closed. In the rest of the height of the joint it either was closed or open; it gradually decreased independently of the variation of the temperature.

This is explained obviously by the effect of the hydrostatic pressure of the reservoir water.

The results of the observations of the 113 crevice gages in 37 joints are illustrated in Table 8-1.

The maximum values of the measured openings turned out to be appreciably less than by design, especially if we consider the actual temperature exceeded the temperature used in the calculation by 1.5-2 times. This can be explained by the fact that the following factors are taken into account by the calculation:

1. The nonuniform growth of the adjacent columns of the sections. With significant (to 12 months) discontinuity in time between the concreting of the blocks of the adjacent columns forming the joint, one of them succeeded in [deleted] at the time of pouring the next and the opening of the joint was caused by the variations only in half the length of the block. The cases where the cooling of the poured block is accompanied by seasonal heating of the previously poured adjacent block are not rare.
2. The thermally stressed state of the blocks decreasing their free deformations. For opening of the joint it is necessary that the compressive (deformation) stresses occurring in the plane of the joint during the period of exothermal heating of the block became thermal stresses also suited the total magnitude of the latter exceeded the coupling force in the joint. Therefore the opening of the center of the joints ends usually with a decrease in the temperature of the center of the blocks from the exothermal peak by 5-15° C.
3. The effect of the cracks parallel to the intercolumnar joints. As was demonstrated in Chapter 7, the openings of the surface in internal vertical longitudinal cracks varies with the same periodicity of the opening of the edges in the center of the joints respectively which naturally decrease the opening of the latter.
4. The deformation in the columns with respect to the hydrostatic pressure with partial enclosure of the uncemented joints.

These factors must be considered when calculating the magnitude of the opening of the intercolumnar joints.

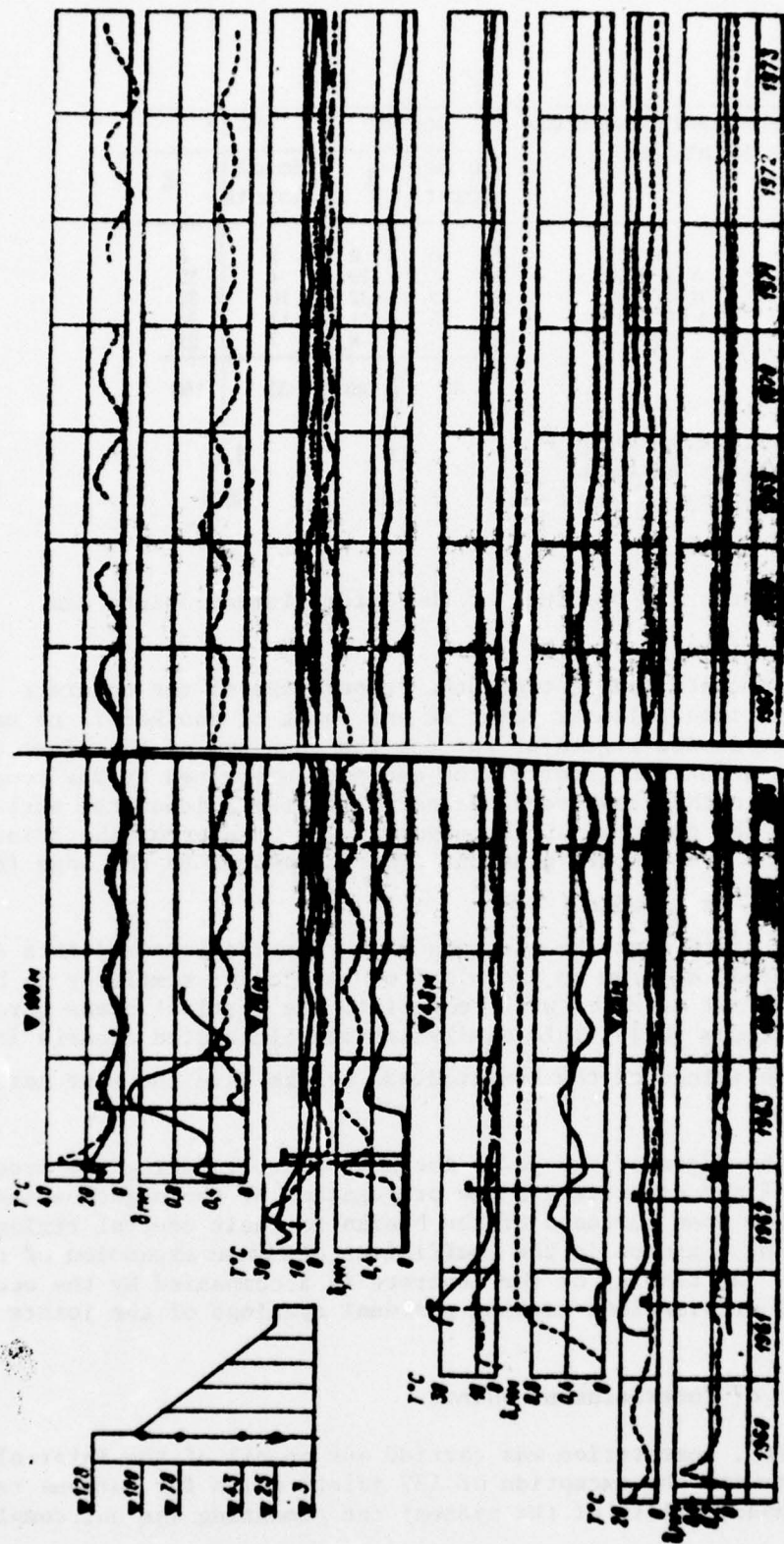


Figure 8-3. Opening of the center of the intercolumnar joint I-II at the marks on the graphs (the solid line -- section 30, the dotted line section 65, [illegible]).

Table 8-1

Maximum measured opening of the joint, mm	Center		Edge	
	No of joints	%	No of joints	%
0.1	6	6	1	3
0.11 - 0.50	7	19	4	12
0.51 - 1.00	12	32	10	31
1.01 - 2.0	15	41	11	33
2	3	8	7	21
	37	100	33	100
Average opening		1.0		1.4
Largest measured opening of joint, mm		2.84		3.15

8-3. Relation Between the Openings of the Intercolumnar Joints and Temperatures

As the analysis demonstrated, between the temperature of the concrete and the opening of the intercolumnar joint at one point or another is no unique relation. For the inside region of the dam the openings of the edges and the center of the joint are interrelated and are determined by the temperature distribution in the cross sections normal to the axis of the section. The difference in the openings of the edges and the center of the joint is proportional to the temperature gradient from the center to the edge (Figure 8-2,b) $\delta_{cr} - \delta = A(T_c - T_{edge})$.

It is possible to state that the openings of the intercolumnar joints are caused by the thermal diagram in the plane of the joints similarly to how this occurs for normal stresses with respect to the vertical areas parallel to the axis of the dam (σ_x). This similarity is illustrated clearly in

Figure 8-2. The openings of the longitudinal cracks have the same nature (Figure 7-14).

The openings of the edges of the joint increase sharply during the process of the freezing of the concrete and the propagation of the negative temperature range from the open surfaces of the blocks to their central regions which was caused by a growth in the coefficient of linear expansion of the frozen concrete. The thawing of the concrete is accompanied by the occurrence of residual deformations causing residual openings of the joints (Figure 8-1,a,b).

8-4. Cementation of Intercolumnar Joints

During 1961 to 1963, cementation was carried out on all of the intercolumnar joints of the dam with the exception of 139 joints which for various reasons (closed joint, impossibility of the system) the cementing was not completed.

The cementation of the intercolumnar joints in the dam in the first stage began to be executed in sufficient height only in the right bank part of the dam (sections 58 to 66). In the remaining sections, the top of the cemented cards was at a distance from the headwater level. At the beginning of the summer 1961 when the headwater level reached the 65 meter mark, from the 30 sections the cementation level corresponded to the planned level: with respect to joint I-II 10 sections, with respect to joint II-III in 8 sections, with respect to joint III-IV in 3 sections. In the joints of the remaining sections the lag was within the limits of 29-55 meters.

The cementation of the joints of the sections in which the instruments are installed was carried out for openings from 0 to 1.9 mm on the edges and from 0 to [deleted] mm in the center; 16% of the joints were closed in the center on cementation; for 13% the openings were within the limits of 0.1 to 0.3 mm; [deleted] % of the joints were cemented for openings of 0.5 mm and higher (see Table 8-2). The average opening was 0.7 mm.

The temperature in the centers of the joints on the date of cementation, being in the majority of cases approximately the average between the temperature and the center in the adjacent blocks forming the joint, was predominantly (72%) within the limits of 0-10° C. In 6% of the cases the cementation was performed at negative temperature (to [deleted]° C at the edges and -5.5° C at the center), and in 21% of the cases at a temperature in the center of the joint greater than 10° C.

These data obtained by the readings of the remote strain gages installed next to the remote crevice meters compare satisfactory with the data of Gidrospetsproyekt Institute on the temperature of monolithing the dam measured by the remote thermometers in each cementation card (Table 8-3).

The specific absorption of the cement by the joint was within the broad limits from 0 to 70 kg/m² and on the average for the entire dam it was about 8 kg-m². The effort to establish the relation between the absorption of the cement and the opening of the joints and also the temperature on the date of monolithing for 37 cards with the instruments did not have results. The absorption of the cement obviously depended not only on the opening of the joint but to a great degree on the presence of open horizontal joints and cracks in the blocks on both sides of the joint and also other causes (leaks). For a large number of the joints the relation between the absorption of the cement and the concrete temperature on the date of cementation was obtained by dividing the total amount of cement used to cement the cards and a defined temperature range by the total area of these cards (Table 8-3). For the monolithing temperature in the range of 0 to 10° C the specific absorption of the cement was 8.9 kg/m² [125].

The cards with defects in the cementation system were cemented through holes drilled from the tunnels or the expanded joints to the intersection with the intercolumnar joints. In the case of 6 to 9 such holes in a card, the average specific absorption of cement was 5.7 kg/m², and the cost per square meter reached 20 to 25 rubles which is five times more than when cementing through the pipe system.

Table 8-2

Opening of joints of date of cementation, mm	No of cards pces.	Absorption of cement, kg/m ³
0-0.1	6	15.8
0.1-0.3	5	13.3
0.3-0.5	5	13.3
0.5-1.0	10	26.3
1.0-1.5	10	26.3
1.5-2.0	1	2.6
2.0	1	2.6
Total	38	100

Table 8-3

Monolithing temperature, °C	No of cards pces.	Absorption of cement, kg/m ³
0	20	12.8
5-10	20	12.8
10-15	20	12.8
15-20	20	12.8
20-25	20	12.8
>25	20	12.8
Total	100	12.8

The thermal conditions in the uncovered expanded joints, the freezing of the concrete in the columns of the inside region gave rise to a zonal nature of the operations with respect to cementation of the intercolumnar joints. The work was performed in the period May to November where at the beginning and end of this period on the lateral faces of the blocks there were regions of frozen concrete (see Figure 4-7). With a depth of this region greater than 2 meters, to eliminate the ice lenses 4 to 9% solution of calcium chloride was passed through the joints, and then cementation was performed using non-freezing mortars. This experiment was performed on 14 cards, and gave an average absorption of cement of 2 kg/m². This absorption of the cement was obtained in 19 blocks in which heating of the concrete in the vicinity of the joint by rod taped electric heaters was performed on the order of an experiment [125]. In two of cards the electric heating elements in the form of coils made of iron wire were tested which were melted in the plane of the joints. The experiment demonstrated that for specific power of 1 kilowatt per m² it is possible to increase the concrete temperature by 8-12° C during [deleted] while maintaining a positive temperature in the joint 2 to 3 days after disconnecting the electric heater [19].

In the joints with poor passability, the experimental cementing in the application of activated solutions prepared in the high speed turbulent mixer designed by the VNIIG Institute was used. The mean absorption of the cement of 6.8 kg/m² achieved obviously could be explained by the increase to penetrating capacity of these solutions.

The results of the experiments performed on cementation of the dam indicate the means of eliminating the seasonal nature and improvement of the quality of the operations with respect to monolithing analogous structures.

8-5. Quality of Cementation

At the present time there is experience in the mass cementation operations on the Ladzhanuri arch dam [14] and the gravity dams of Bratsk Hydroelectric Power Plant [15, 125] and Krasnoyarsk Hydroelectric Power Plant [126].

The schematics in the cementation systems of the designs for the projections and the process for carrying out the cementation have been developed. The basic difficulty in performing these operations arises from the small, non-uniform openings of the intercolumnar joints which in turn depend on the concrete operations, especially for the severe climatic conditions.

The studies of the hydraulics of the cemented cards with exact [deleted] with opening of 2 mm demonstrated the very nonuniform distribution of the pressure gradients with respect to area of the card. Even on the [deleted] made of organic glass with smooth surfaces the effective filling of the joint was about 50%. This gave rise to the idea of the linear protrusions and the method of filling the joints [127] where even with their variation, the presence of a sufficiently large opening of the joint is required, and the use of finely disperse mortars is recommended.

The cementation of the intercolumnar joints is a completely [deleted] operation. There is no reliable direct method of monitoring and evaluating the efficiency of this work, and usually the following indirect methods are used to estimate its quality: with respect to the fulfillment of the design requirements, the results of the control drilling and measurements using the crevice meters of the openings of the joints before and after cementation [128].

The first method is to a significant degree subjective and therefore unreliable. For example, according to the reports of the Bratsk expedition of the Gidrospetsproyekt Institute at the beginning of 1965 760 cars (46%) were considered cemented with high quality and 862 cards (52.5%) with low quality. Then the criteria for evaluation and the evaluation itself were changed and according to [125] the general results of cementation of the joints are far from satisfactory although this conclusion does not follow from the results of the control drilling.

According to the report data from the Gidrospetsproyekt Institute out of the 648 intersections, there were 245 cores with the presence of traces of cement rock (deleted %) including 52 monolithic (8%). Without cement rock there were 403, including 10 monolithic. According to the data of [125] out of 60° cores 42 were with cemented monolithic concrete (7%) and 179 (29%) nonmonolithic cores with cement film and (3.5%) cores with monolithic concrete without cement rock. The remaining 367 cores (60%) obviously were without traces of cement rock and were not monolithic. However, it is possible that part of these cores were destroyed during shot drilling of the holes 168 mm in diameter.

In spite of the application of the pipe cooling to the Krasnoyarsk dam, the openings of the intercolumnar joints during cementation of them were within the limits from 0.13 to 2.3 mm with an average value of 1.2 mm [126]. The temperature of the concrete corresponded to the technical conditions. The absorption of the cement was 2-12 kg/m² and on the average 5-6 kg/m². The control drilling using the special bits gage in 71 intersections 79% of the cores with cement rock from which 7% were monolithic. The intersections of

the joint with the filling and without it were encountered in the same card. During shot drilling (91 intersections) the cement rock was detected in 79% of the cores.

At the Bratsk and Krasnoyarsk dams, the surface ultrasonic sounding was used to monitor the quality of the cementation of the intercolumnar joints [129-130]. At the Bratsk dam the test performed on 23 sections of the intercolumnar joints near their edges emerging in the expanded joints demonstrated that the openings of these joints make up 0.25-0.5 mm. The very nonuniform filling of the joints with the mortar was established. Such tests gave the best results at the Krasnoyarsk Hydroelectric Power Plant.

Let us consider the third method of quality control of the cementation. As the observations demonstrated with respect to the remote split gages, the cementation of the joints did not prevent opening of their edges. This is explained by the fact that in the majority of cases the cementation was carried out during the warm part of the year (May to October) when on the edges of the joints the maximum temperature and minimum openings were observed.

Inasmuch as the opening of the joint, the absorption of the cement and the temperature in the joint during cementation is not the criterion for its efficiency, the latter can be determined by the opening of the central part of the joints after cementation. The well cemented joint at the proper temperature should not open, and especially close after cementation.

An example of the satisfactorily cemented joint is the joint III-IV of section 65 at the 40.5 meter mark. Five crevice gages located in this joint make it possible to construct the diagram of the openings (see Figure 8-4).

The discontinuity in time between the dates of pouring the blocks forming the joints at this mark was 4 months. The joint began to open in February 1962 and at the cementation time (August 1962) its opening at the center had reached 0.53 mm. The absorption of the cement was 3.17 kg/m². The opening of the center of the joint after cementation did not exceed 0.2 mm, and after a year it was stabilized at a value of 0.7 mm. The region of insignificant openings encompasses the central zone extending approximately half the width of the joint. In the peripheral regions to 4 meters from the edges of the joint periodic variations of the openings occurred in correspondence with the variations of the center-face temperature gradient. It is possible, therefore, to note that the concept of the well-cemented joint in the dams with expanded joints must pertain to the middle section of the card. The edges of the joint continued to open and close independently of the quality of the cementation.

After investigation of this example it is possible to proceed to evaluation of the quality of the cementation of the joints in which the remote crevice gages are placed. Along with the joints, the openings of which after cementation were insignificant (0.1-0.2 mm), there were joints in which large openings were observed and which behaved like the uncemented ones. In several joints after cementation closure of the center took place by an amount 0.3 to 0.9 mm which indicates the absence of the cement rock in the joint or insufficient thickness of it.

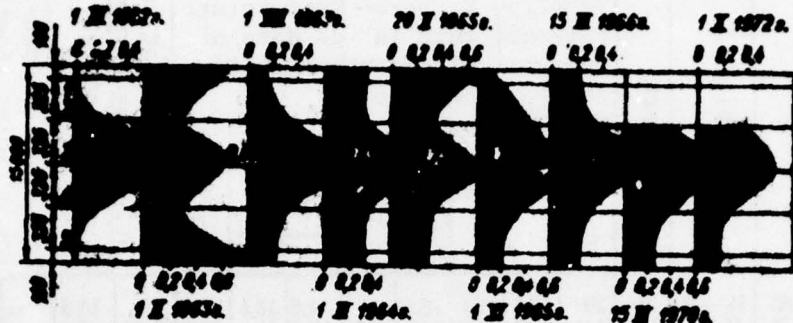


Figure 8-4. Diagrams of the opening of the joint III-IV of section 65 at the mark at 40.5 meters.

Thus, the cementation in a number of cases turned out to be inefficient, which is explained by its execution: at a block temperature significantly exceeding $5-10^{\circ}\text{C}$ (Table 8-4), for in practice closed joints, or in the wintertime.

Out of the 34 cards only in seven cards (21%) did the joints not in practice open or close after cementation (Figure 8-7). Cementation during the summer with maximum opening of the joints is characteristic of them. In four cards the temperature on the date of cementation did not exceed 5.5°C , and in three, $(7-10)^{\circ}\text{C}$ (Table 8-5). In the remaining cards the cementation took place in different intermediate stages of opening, and we considered the joints to be cemented with poor quality in which the opening of the joint at the beginning of cementation was less than 0.3 mm and also the joints which after cementation closed or opened more than 0.3 mm. By these criteria, out of the 37 joints with instruments, repeated cementation was required in 16 joints (43%). By the criteria of the Gidroprospectsprojekt Institute there were also 16 of these joints, but in a number of cases the estimates did not coincide.

The repeated cementation through the drilled holes was performed in 1966 and 1967 in part of the cards of joint I-II and in all joints V-VI and VI-VII, and in all in 400 cards. The average cement absorption was $0.7-0.8 \text{ kg/m}^2$.

As was noted above, the openings of the edges of the joints periodically varied in accordance with the fluctuations of the air temperature in the expanded joints. In the winter of 1964-1965 they became asymmetric with the large values from the direction of the partially open expanded joints. After their final closure the variations in the openings of the edges of the joints were stabilized at an insignificant amount on the order of 0.1-0.2 (Figure 8-5).

In the central region of the joints, periodic variations of the openings were observed with amplitudes differing in different cards and increasing in the direction of the crest of the dam. During the process of equalization of the temperature, the amplitude of the oscillations diminished and at the

Table 8-4

Section	Joint	Mark	Temperature at center of blocks °C	Temperature in blocks at beg. of open. blks. °C	Temperature on date of cementation, °C		Opening of joint on date of cement., mm	Absorption of cement of cem. mix., kg/m³	Increment of opening of joint after cementation, mm			
					in jnt							
					I	II						
63	IV-V	42	39	10.5	9.5	18.5	-	9.5	18.5			
	II-III	61.5	44	13.0	10.5	34	23	12.5	18.5			
	IV-V	39	40.5	17.0	8.5	20.0	19	9.5	19.0			
	V-VI	22.5	38.0	17.0	14.5	34.0	-	11.0	11.0			
	I-II	26.0	26.0	7.0	11	15	14	6.0	9.5			
51	II-III	61.5	44.0	1.5	0.5	35.5	18.0	12.0	12.0			
	III-IV	43.5	36.0	5.0	4	34.5	14.0	8	13			

Note. Numbering of the blocks is in the order of pouring. The temperature in the first block is presented for the date T_{\max} in the second block.

Table 8-5

Section	Joint	Mark, meters	Cementation date	Temper-ature in the joint, °C	Open-ing of joint, mm	Specific absorption of cement, kg/m³
63	I-II	40	16/IX 1961	10	0.7	34
63	II-III	78	3/VII 1963	3.5	1.2	34
51	II-III	78	26/VIII 1963	2.5	1.2	34
63	II-III	78	3 IX 1963	1.5	1.2	34
30	II-IV	40	12/VII 1962	5.5	0.8	34
30	III-IV	40	28/VIII 1962	7.0	0.8	34
30	IV-V	14	14/IX 1962	8.0	0.7	34

time of normal operation the variations in the openings either ceased or were insignificant (Figure 8-3, 8-5, 8-6).

In Chapter 6 it was noted that the increments of the normal stresses σ_x are approximately equal to γH . As a result of these stresses, the intercolumnar joints had to close as the headwater level rose. As the remote crevice gages indicate, in a number of joints gradual decrease in the mean annual openings was observed (see Figure 8-4). Thus, in the lower part of the sections (to mark 27) the full closure of joints I-II and II-III, reckoning

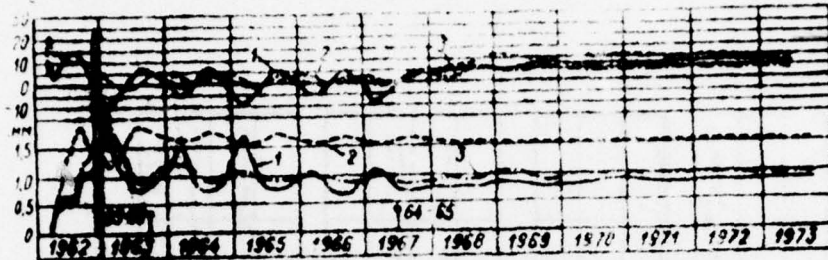


Figure 8-5. Opening of the joint II-III in section 65 at the 3.5 meter mark. 1 -- left edge; 2 -- center; 3 -- right edge. Flag -- cementation date; circle -- covering of the expanded joint.

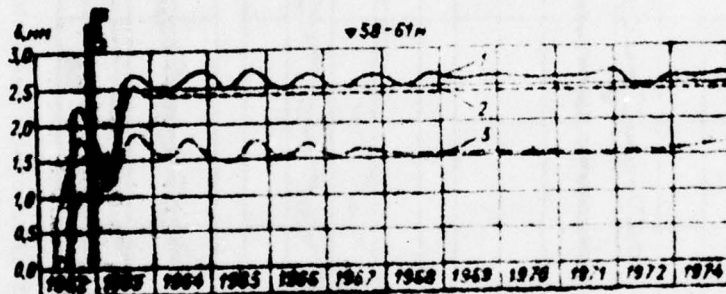


Figure 8-6. Opening of joint II-III at the center. 1 -- section 30; 2 -- section 51; 3 -- section 65.

from maximum opening, is within the limits from 0.1 to 1 mm, on the average amounting to 0.55 mm, from which after cementation, 0.2 mm.

With respect to openings of the intercolumnar joints it is necessary especially to isolate the region adjacent to the downstream face of the sections. The crevice gages installed at a distance vertically of 8-12 meters from the face demonstrated the significant variation in the openings of the centers of the cards with an annual difference reaching 1.3 mm (Figure 8-7). In the upper part of this region in joints I-II and under the conditions of constant operation, the variations of the openings are observed with an annual difference to 0.7 mm in the center of the joints and to 0.7 mm on the edges with a corresponding annual temperature difference of the concrete on the order of 7-10° C (Figure 8-8). In the remaining, lower lying part of the joints the annual difference in the openings does not exceed 0.1 mm, and it is possible to consider that the intercolumnar joints of the dam under the conditions of constant operation are closed.

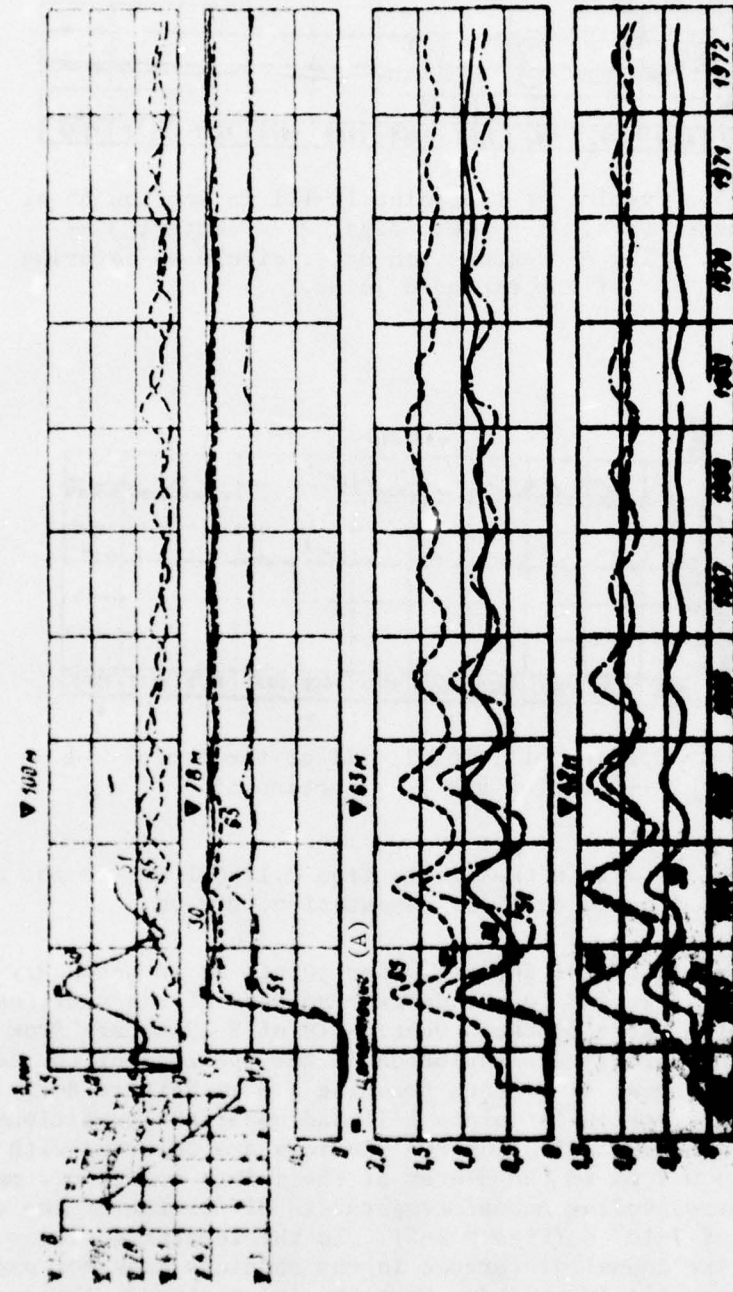


Figure 8-7. Opening of the joints near the downstream face of the sections [legend deleted].

Key: A. cementation

8-6. Role of the Toothed Couplings

The intercolumnar joints cemented for a temperature exceeding 10° C were opened after cementation by an amount to 1.9 mm (Table 8-4), and they did not completely close under the effect of the temperature variations and the hydrostatic load. The stabilized openings of the joints in a number of cases exceeds 0.5-1.0 mm of the openings of these joints on the cementation date. From this, however, it does not follow that the opening intercolumnar joints remained in the dam.

Above, it was pointed out that the remote crevice gages measure the horizontal component of the opening of the joint and, consequently, by the term "opening of the joint" we mean the magnitude of the divergence of the vertical planes of the two adjacent blocks with respect to the horizontal direction. This magnitude, which is more easily measured than others, does not take into account the work of the toothed couplings, and it does not characterize the force interaction of the adjacent columns through the joint.

Beginning with the configuration of the teeth (Figure 8-8) it is possible to state that the transfer of forces from column to column takes place as a result of the contacts along the inclined areas and in the presence of small horizontal opening of the joint.

The openings of the joints with respect to the inclined and vertical areas are different both with respect to magnitude and with respect to intensity of growth. This is obvious from the readings of the crevice gages normal to these areas for two years of their operation at the Bratsk dam and the crevice gages especially installed in the Ust'-Ilim dam for studying the opening of the joints.

The process of erecting the dam with columnar section and tooth profile leads to significant difference in the height of the column which combined with the local peculiarities of the geotechnical characteristics of the base determines the difference in settling of the columns (see Figure 5-4). The same cause can be considered also for the nonuniform settling in the longitudinal direction. In addition, for a number of years there was a bend in the sections in the direction of the tailrace under the effect of the hydrostatic load with deflection of the crest to 30-40 mm and also a bend in the section in the direction of the colder expanded joint reaching 5 mm in their upper part. The nonuniform settling and bending of the sections and also their horizontal displacements cause deformations of the toothed couplings commensurate with the openings of the joints insignificant with respect to the magnitude and nonuniformly distributed with respect to height and width of the sections.

There is no doubt that as a result of these deformations at any point in time, independently of the presence of cementation, there are contacts along the toothed couplings in the intercolumnar joints through which transfer of forces from column to column is realized by which the stressed state of the profile as a whole is determined.

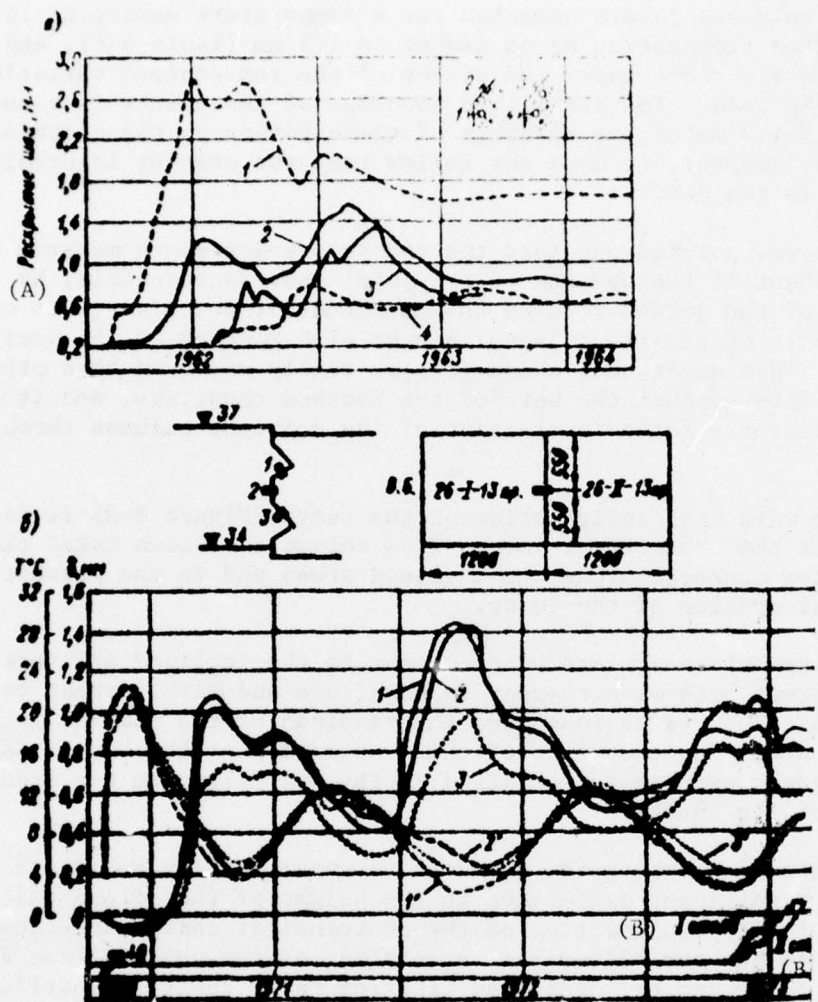


Figure 8-8. Openings of the intercolumnar joints with respect to vertical and inclined areas: a -- Bratsk dam (1 -- section 51 at the 79.5 meter mark, vertical area, 2 -- the same inclined area, 3 -- section 65 at the 76.5 meter mark, inclined areas, 4 -- the same vertical area); b -- Ust'-Ilim dam section 26 at the 35 meter mark (1,2,3 -- areas (see the schematic)).

Key: A. opening of the joint, mm
B. column...

The presence of the contact is indicated by the monolithic cores without traces of the cement mortar drilled from the plane of the joints, impassibility of the cards during hydraulic testing and weak opening of the joints

during cementation. The presence of the contacts is also supported by the stress concentration in the toothed couplings noted in Chapter VI. The joint operation of the adjacent columns is obvious from the nature of development of the stresses on both sides of the intercolumnar joints (see Figure 8-9).

For a favorable static operation of the dam it is expedient to orient the faces of the teeth along the trajectory of the principal directions. For this purpose the configuration of the teeth must be variable with respect to height of the dam. At the Bratsk dam the configuration of the teeth is constant on all of the intercolumnar joints. This is convenient in production respects, but it leads to the occurrence of the [deleted] stresses along the surface of the teeth, especially where the areas of the teeth are deflected significantly with respect to orientation from the trajectory of the principal normal stresses and also the time when these trajectories calculated for the complete set vary with an increase in the headwater level to the normal backwater level.

The tensile strength and shearing strength of the joint 2 mm thick even under laboratory conditions do not exceed 3.7 and 2 kg-force/cm² [131]. The sliding stresses with respect to the areas of the teeth significantly exceed this magnitude, and it is possible to assume that the stresses are perceived by the contact surfaces of the teeth even in the absence of a thin layer of cement mortar between them.

In the practice of foreign dam construction, examples are known of the erection of gravity dams with vertical and inclined uncemented intercolumnar joints. At the Suddagan dam 75 meters high built in Japan in 1955, the vertical intercolumnar joints were not submitted. The measurements by means of 230 remote strain gages and 35 remote crevice gages placed in the dam demonstrated that during the filling of the reservoirs the distribution of the normal stresses with respect to the horizontal cross sections is close to the calculated value. It is noted that the shear resistance of the longitudinal joints is so great that it insures joint operation of the columns and monolithic nature of the dam [58]. In the experimental work of MISI Institute [132] a study was made of the problem of the effect of various cases of attenuation of the monolithic nature of the dam 100 meters high on its stressed state and strength. It was established that for "smooth" longitudinal joints at the base of the pressure face (point A) tensile stresses of $\sigma = 11.5$ kg-force/cm² occur. For the toothed surface of the joints in which there is no coupling, the tensile stress point A decreased by 2.8 times by comparison with the "smooth" (untoothed) surface of the joints. If with respect to height of the joints the monolithic nature of the dam is destroyed only in individual sections (to [deleted] of the surface), no increase in stress at point A is observed in practice in comparison with the monolithic profile.

Thus, also from this experiment it follows that the longitudinal construction joints opened over a great extent are dangerous for the [deleted] operation of the dam [132]. This possibility is considered, however, to have low probability.

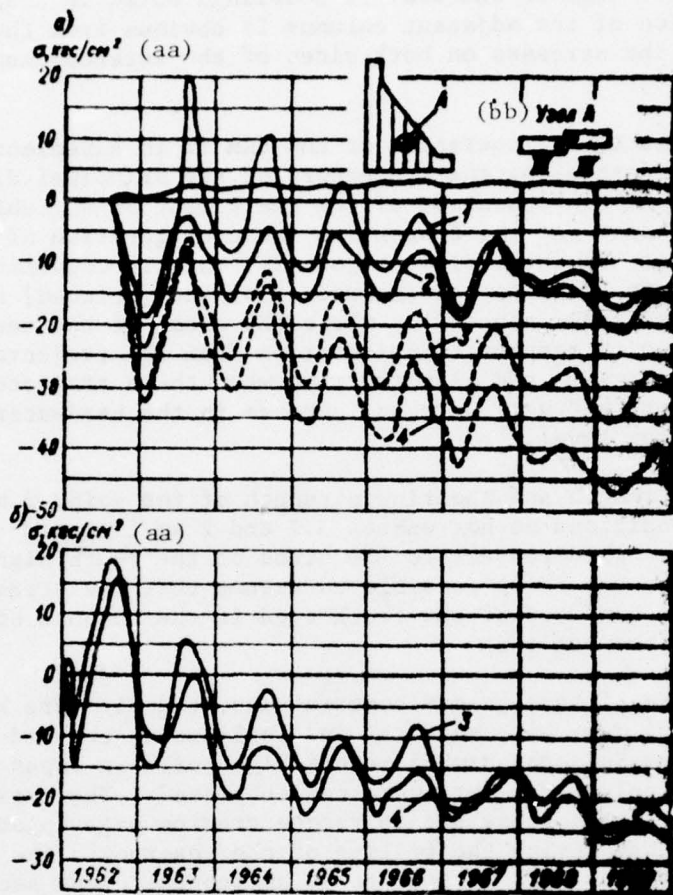


Figure 8-9. Normal stresses on both sides of the intercolumnar joints: a -- III-IV of section 65 and the 40.5 meter mark; b -- II-III of section 30 at the 40.5 meter mark. 1 -- σ_x at block III of the column; 2 -- the same at block IV of the column; 3 -- σ_y in block IV of the column; 4 -- the same in block III of the column.

Key: aa. σ , kg-force/cm² bb. assembly A

The openings of the intercolumnar joints which depend on a number of factors do not vary regularly with respect to height, but they have a random [deleted] nature caused by the conditions of the performance of the concrete operations. For this reason the sections of the joints of great opening with high quality cementing alternate with sections of less opening or ineffective cementation. This discontinuous condition of the joints has little effect on the stressed state of the dam by comparison with the monolithic profile (see Chapter 6), especially if we consider the operation of the toothed couplings.

In 1967 the Commission of Experts of the Technical Council of the Ministry of Power Engineering and Electrification of the USSR, under the chairmanship of Doctor of Technical Sciences, Professor Yu. A. Nilender, investigated the problem of the stressed state of the Bratsk Hydroelectric Plant dam and the necessity for repeated cementation of the intercolumnar joints. Beginning with the results of the field studies of the stressed state of the dam, the technical council decided to limit the repeated cementation of the intercolumnar joints to the 400 [deleted] noted above. Its necessity for the remaining [deleted] must be established by the results of the field observations of the condition of the dam.

The data presented above do not provide a basis for doubting that the degree of monolithic nature of the Bratsk dam achieved by cementation of the joints is sufficient and there is no necessity for repeated cementation of the intercolumnar joints.

8-7. Intersectional Joints

The observations of the opening of these joints is of interest for determining the operation of the waterproof packing in the first columns and also other means of controlling the operation of the section independent of each other (absence of "pile-up").

The observations of the openings of the intersectional joints are carried out using the uniaxial crevice gages (see § 2-2) installed in the inspection tunnels of the first columns in 16 joints on both sides of section 30, 36, 40, 45, 51, 58, 65 and 66. In addition, in the intersectional joints on the shore adjoinings, biaxial crevice gages were installed. The observations were started as the crevice gages were installed in the period from September 1961 to the beginning of 1964.

Inasmuch as the beginning of the readings with respect to individual instruments and groups of instruments were displaced in time, the principal difference between the extremal ordinates of the graph of the readings of the crevice gage for the investigated time period from the beginning of the observations was taken as the opening of the joints.

The openings of the intersectional joints were determined by the thermal state of the [deleted] columns which depended on the conditions and the order of pouring the concrete, the water temperature of the reservoir and the air temperature in the expanded joints. The air temperature in the inspection tunnels, the nonuniform distribution and variations of which give the graphs of the openings of the joints a [deleted] nature and complicate the establishment of a relation between the openings of the joints and the temperature had a noticeable effect.

The maximum openings of the intersectional joints occurred during the first and second winters after pouring the first columns at the corresponding marks. The first observations by 35 crevice gages installed at three marks by the winter of 1961 to 1962 demonstrated that the greatest openings from

the beginning of measurements (to 4 mm) were noted at the 45 meter mark where by the pouring conditions a higher exothermal heating temperature occurred. Here, according to the data of the NIS Institute of Orgenergostroy the increased jointing was recorded.

In accordance with the seasonal temperature fluctuations of the concrete of the first columns the openings of the intersectional joints assumed the periodic nature, decreasing in the warm time of the year and increasing during the cold part of the year with a shift with respect to the extremal values of the air temperature by 1 to 4 months. The annual differences in the openings increased in the direction of the crest of the dam, and at each given mark the openings decreased with time (Figure 8-10, Table 8-6).

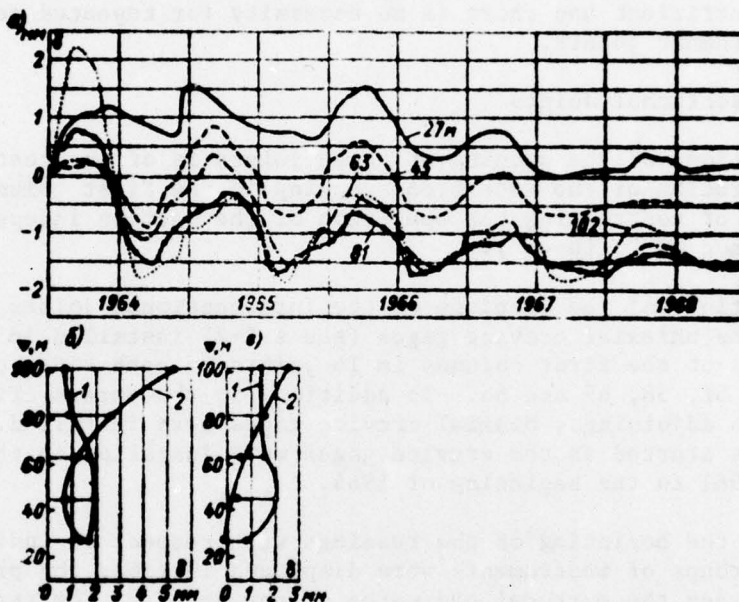


Figure 8-10. Opening of the intersectional joints: a -- variation in time of the openings of the joint 30-31 at the marks indicated on the graphs for the opening diagram with respect to height of the sections; b -- 58; c -- 30. 1 -- from the direction of the joint with the pylon; 2 -- from the direction of the joint without the pylon.

The air temperature in the expanded joints and the fluctuations of it have a significant effect on the magnitude of the opening of the intersectional joint. The difference in temperature regime of the expanded joints on both sides of each section (covered and partially covered) caused different openings of the intersectional joints.

In addition to the openings of the intersectional joints from the direct effect of the temperature, openings were observed which were caused by the phenomenon of the bending of the columns of the longitudinal direction in the direction of the colder expanded joint (with a pylon) with deflection

at the upper marks on the order of 5-6 mm. The bending of the columns was accompanied by an increase in the opening of the intersectional joint of the warm side of the section and a decrease on the colder side. This gave rise to the measured maximum opening of the intersectional joints (at the 102 meter mark above 6 mm) and their asymmetric nature on both sides of the sections (Figure 8-10,b, Table 8-6). After covering the expanded joints the phenomenon [illegible] of the sections in the direction of the axis of the dam in practice ceased.

Table 8-6

Marks, meters	Annual difference in openings (mm) by years				
	Maximum	1965	1967	1968	1972
27	<u>0.7-2.3</u> <u>1.51</u>	<u>0.4-2.3</u> <u>0.97</u>	<u>0.3-0.75</u> <u>0.47</u>	<u>0.4-1.2</u> <u>0.52</u>	<u>0.0-0.4</u> <u>0.14</u>
45	<u>1.3-3.2</u> <u>2.13</u>	<u>0.4-2.7</u> <u>1.51</u>	<u>0.1-1.8</u> <u>0.81</u>	<u>0.1-0.5</u> <u>0.38</u>	<u>0.1-0.5</u> <u>0.18</u>
63	<u>1.7-2.8</u> <u>1.95</u>	<u>0.7-2.45</u> <u>1.54</u>	<u>0-0.9</u> <u>0.67</u>	<u>0.2-0.6</u> <u>0.31</u>	<u>0-0.2</u> <u>0.16</u>
81	<u>0.9-2.75</u> <u>1.85</u>	<u>0.6-2.25</u> <u>1.34</u>	<u>0.4-1.2</u> <u>0.75</u>	<u>0.2-0.9</u> <u>0.48</u>	<u>0-0.3</u> <u>0.18</u>
102	<u>1.5-6.25</u> <u>2.50</u>	<u>0.9-5.2</u> <u>2.0</u>	<u>0.75-3.0</u> <u>1.44</u>	<u>0.3-1.6</u> <u>1.16</u>	<u>0-1.0</u> <u>0.50</u>

Note. The limits of the annual difference appear in the numerator, and the mean values for 8 joints in the denominator.

Under the conditions of normal operation and maintenance, the annual variations of the openings of the intersectional joints are insignificant (0.1-0.25 mm, with the exception of the upper marks where they reach 1 mm).

The average opening of the intersectional joints on both sides of each section is the difference in free temperature of deformation and deformation connected with the thermally stressed state. During the operating period, the stress σ_z in the first columns varies little, and the annual difference in the openings is close to the calculated value by the temperature difference at the corresponding marks.

8-8. Joint Between the Dam and the Hydroelectric Power Plant Building

The observations of the mutual displacements of the dam and the hydroelectric power plant building were organized by the author in 1963 in connection with the problem of the operation of the escarpment with vertical cut to 11 meters high in the base of the dam in the section of adjoining to the building [133]. A study was made of the proposition of the possibility of

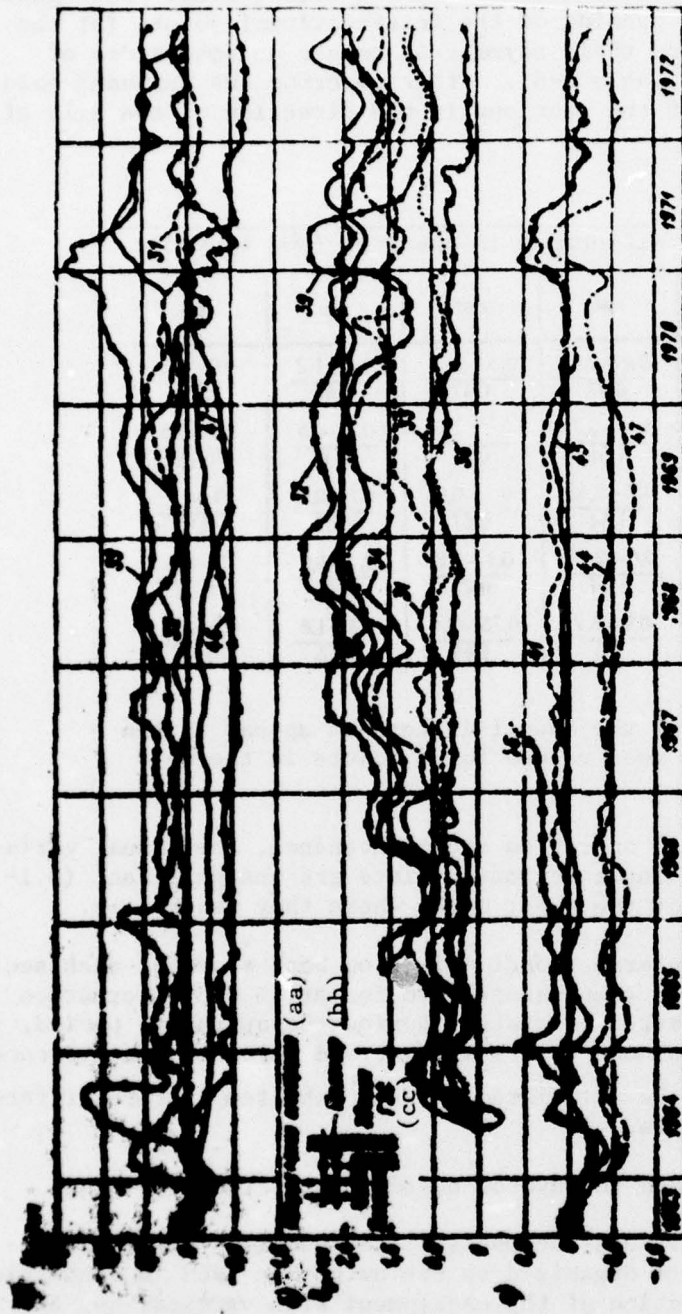


Figure 8-11. Mutual displacements of the dam and the hydroelectric power plant building: a -- horizontal component; b, c -- vertical component. The numbers on the graphs are the section numbers.

Key:

- aa. displacement stress
- bb. crevice gage
- cc. hydroelectric power plant building

the sliding of the dam with respect to the jointed zones inside the rock massif at the level of the escarpment with increasing horizontal load on the hydroelectric power plant building.

On the structural joint 20 mm in thickness between the dam and the hydroelectric power plant building at the level of the floor of the transformer tunnel, the biaxial crevice gages were installed one per section by means of which the vertical and horizontal components of the mutual displacement of the dam and the hydroelectric power plant buildings are recorded. The observations for 9 years (Figure 8-11) indicate that the vertical components in part of the section are insignificant and do not go beyond the limits of one mm. In the other part of the sections these components built up with time, changing discontinuously at the beginning of the warm period of the year and at the end of winter when the dam changes the direction of seasonal inclination in the direction of the headwater and tailrace. The vertical component reached a maximum on the order of 2-3 mm in 1968 and then stabilized with large or smaller seasonal variations.

The horizontal component does not exceed 2 mm with respect to magnitude and with respect to nature of variation in time as connected with the vertical component.

In the dam and the hydroelectric power plant building there are two sections of amplitude marks which offers the possibility of determining the nonuniformity of the settling of each of these structures. Beginning with the available data it is possible to assume that the picture of the mutual displacements with respect to Figure 8-9 is caused by the difference in settling of the dam and the hydroelectric power plant building in the vicinity of the joint between them. It is possible to consider it established that the horizontal displacements in the joint do not have a comprehensive and building nature and, consequently, the dam does not shift in the direction of the hydroelectric power plant building. The four sections at the left bank where along with the seasonal fluctuation the tendency is also observed toward an insignificant increase in the components, predominately the vertical components, constitute an exception.

CHAPTER 9. STRESSES IN THE TURBINE CONDUIT

9-1. Calculated Loads. Calculated Stresses from the Internal Water Pressure

Calculating the pipeline, the following loads were assumed: the static head $H = 105$ m, the internal pressure considering the increase with relief of the load $H_{\text{calc}} = 130.5$ meters, the seepage pressure for the shell of the pipeline $P_{\phi} = 4 \text{ kg-force/cm}^2$, the pressure on cementation $P_{\text{cem}} = 4 \text{ kg-force/cm}^2$.

The calculated stresses from the internal pressure are determined in the "boil" formula which is equal for the lower horizontal inclined states 1840-1890 kg-force/cm². The admissible stress (σ) = 0.9 of σ_{cur} .

The stress in the shell from the internal seepage pressure was determined by calculation for a plate elastically attached on two and four sides (between the stiffening ribs) and reaches 1830 kg-force/cm². The stiffening ribs were calculated for a pressure of the inclosing concrete of 5 tons-force/cm² of the pipe surface which gives 3.82 tons per running meter of the rib with a stress of [deleted] kg-force/cm².

Distressing occurring in the concrete around the conduit from the natural weight of the concrete and the hydrostatic pressure of the water on the pressure face of the dam were calculated according to the paper by S. G. Gutman [deleted].

The stress distribution over the surface of the cylindrical [deleted] of the radius of $r = a$ was determined by the formula

$$\sigma_{\beta} = \frac{N \cos^2 \alpha}{2} (1 - 4 \sin^2 \theta) \quad (9-1)$$

for the region from $r = a$ to $r = r_1$;

$$\sigma_{\beta} = \frac{N \cos^2 \alpha}{2} \left[1 + \frac{a^2}{r_1^2} - \left(1 - 3 \frac{a^2}{r_1^2} \right) \cos 2\theta \right], \quad (9-2)$$

where σ_{β} is the tangential stress; α is the angle of inclination of the axis of the pipeline; β is the coordinate reckoned from the upper part of the cylinder, N is a principal stress.

The calculation of the stresses from the inside pressure during joint operation of the shell with the concrete is performed in accordance with the solution for the halfplane attenuated by the circular hole under the uniform pressure. It was established that the shell takes 10% of the internal pressure q , and 90% of q goes to the concrete. The maximum tensile stresses in the shell and in the concrete are 190 and $30.3 \text{ kg-force/cm}^2$ respectively.

The cross section of the reinforcing is selected beginning with $[\sigma] = 1800 \text{ kg-force/cm}^2$ for total stresses from natural weight, hydrostatic loading on the pressure face and internal pressure. In the regions where the total stresses turned out to be compressive, the tensile stresses from the internal pressure were used in the calculation. The operation of the concrete under tension was taken into account.

9-2. Thermal Stresses

In order to determine the stresses in the concrete surrounding the conduit from the difference in temperature of the free face and the water flowing in the conduit, some simulation studies were performed at the VNIIG Institute in 1959. It was established that on the outline of the halfcircle turned toward the downstream face, during the winter tensile stresses are developed up to 5 kg-force/cm^2 , and in the summer compressive stresses develop after 2 kg-force/cm^2 . On the outline of the opposite halfring turned toward the massif of the dam the stresses in the concrete fluctuate within the limits from 4 kg-force/cm^2 of compression in the winter to 1 kg-force/cm^2 of tension in the summer.

The temperature stresses during the construction period were considered when calculating the conduit. In addition, their effect prevails over the stresses from the calculated loads.

During the period on the order of 2.5 years the conduit was not filled with water and the stresses measured during this period had predominately thermal origin.

The blocks of section 36 in which the conduit was poured in the measuring cross section section were poured in the summer with a temperature of the concrete mix of $17-23^\circ \text{ C}$ and the temperature at the peak of exothermal heating was $43-50^\circ \text{ C}$. The cooling of the concrete occurred with a density of 4-5 deg/month, and in the field adjacent to the steel shell, with a density of 5-6 deg/month. In the cooling process between the various zones of the concrete blocks and the shell a temperature gradient that is variable along the radius is maintained, which, for example, for the point 2.75 meters from the block reached 20° C . Beginning with the winter period after dispersion of the exothermal heat, the concrete temperature varied periodically with a temperature reading in the summer to 10° C (the shell temperature is higher).

In November 1962 the thermal regime of the shell began to differ from the regime established during the process of the seasonal variations. Instead

of the usual transition to a negative temperature at that time obviously for reasons of a production nature (penetration of heat from a machine room) warming of the shell to 2-6° C occurred, and in April 1963, to 15-25° C with the maximum value at the upper generatrix of the conduit. The heating of the concrete which, for example, at the point 0.9 meters from the shell was 3 to 15° C was observed simultaneously. In May 1963, the temperature began to drop and then the variations acquired the usual periodic nature with an annual period. By the end of 1963, the temperature distribution with respect to the radial cross sections became in practice uniform within the limits from 0 to 5° C.

The temperature variations in the shell and the surrounding concrete were accompanied by the development and significant temperature stresses.

The intense cooling and the large temperature gradients of the measured points with respect not only of the peripheral regions of the blocks but also the shell led to a sharp increase in the tensile stresses in the concrete with the occurrence of cracks. In a number of cases the cracks went through the strain gages which demonstrated that the cracks appeared soon after pouring the concrete or after 2 to 3 months (see Figure 7-12). The cracks occurred also during the period of the above noted heating of the shell and the surrounding concrete in April 1963 (see Table 9-1).

Table 9-1

Date	Deformation $\epsilon \times 10^{-5}$ at the section points [illegible]					
	0.9 m from shell			2 m from shell		
	ϵ_x	ϵ_y	ϵ_z	ϵ_x	ϵ_y	ϵ_z
63 II						
II	1.5	4.5	8.70	6.00	7.13	9.90
IV	4.5	9.2	6.70	6.30	11.40	
V	3.5	7.1	4.37	7.42	13.60	
VI	2.5	21.5	1.70	4.37	9.55	
VII	4.5	20.5	2.75	5.20	16.0	
VIII	3.5	34.5	4.75	4.45	25.0	
IX	2.5	34.5	4.95	4.75	29.0	

The symbols ϵ_x , ϵ_y and ϵ_z are used to denote the relative deformation in the direction of the flow, in the direction of the radius of the shell and in a circle respectively.

The data in Table 9-2 leaves no doubt of the occurrence of a crack directed along the upper generatrix of the conduit. The instruments recorded such cracks in another cross section (b-b) and annular cracks in both cross sections. The opening of the cracks along the axis of the section then increased, and the annular crack decreased.

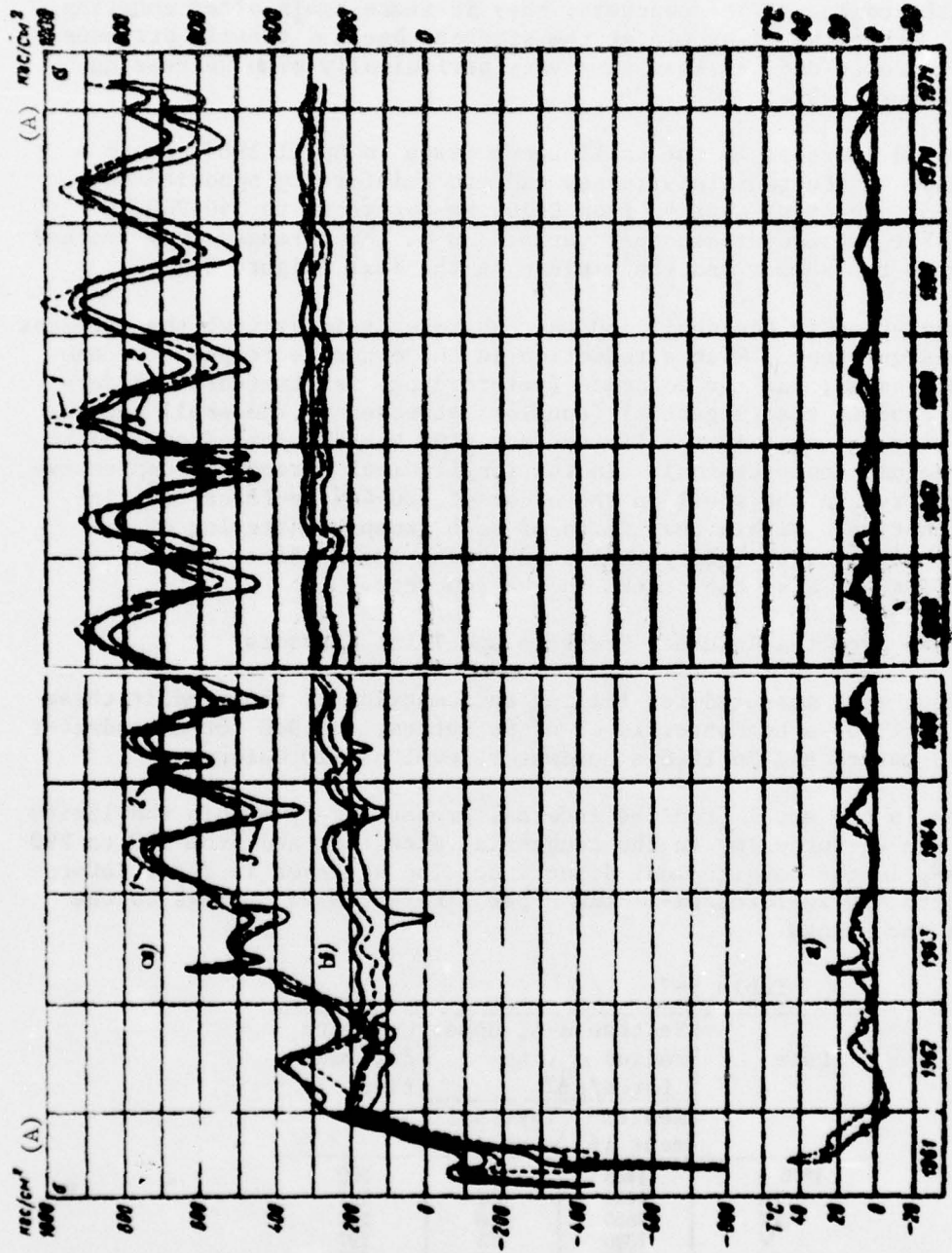


Figure 9-1. Stresses in the annular reinforcing of the section [deleted]: a -- temperature; b -- lower point of the cross section; c -- upper point of the cross section.
1, 2, 3 -- [deleted] of the reinforcing.

Key: A. kg-force/cm²

In the annular reinforcing, compressive stresses of up to [deleted]-600 kg-force/cm² occurred during the exothermal heating period which began to decrease with cooling of the concrete; they increase again after covering the blocks. After the first winter the stresses became tensile stresses 200 to 400 kg-force/cm² and then they vary periodically with decreasing amplitude (Figure 9-1).

The above noted increase in the shell temperature in April 1963 caused a sharp increase in the tensile stresses and the reinforcing opposite the upper point of the cross section from 0-100 kg-force/cm² to 540-900 kg-force/cm². For subsequent seasonal variations of the stresses they reached the maximum in the summer and the minimum in the fall (Figure 9-2).

For joint operation in the shell and the concrete (reinforcing) the stresses of opposite sign occur. With a reduction in the concrete temperature the shell is compressed, and the concrete (reinforcing) is stretched. Before filling the conduit the tangential (annular) stresses in the shell and the stiffening ribs were within the limits from +100 kg-force/cm² (tension) to -250 kg-force/cm² (compression). In the longitudinal direction compressive stresses occurred in the shell on the order of 100-400 kg-force/cm², increasing with time. Within the limits of each group, scattering of the stresses was observed obviously explained by the local effect of the stiffening ribs and also the cracks in the concrete.

9-3. Stresses from the Internal Pressure and Total Stresses

These stresses were measured for filling and emptying of the conduit three times: in 1964 for a headwater level of 96 meters, in 1966 for a headwater level of 110 meters and in 1968 a headwater level of 120 meters.

The stresses in the shell from the internal pressure were within the limits from 26 to 188 kg-force/cm² in the tangential direction and from 170 to 290 kg-force/cm², in the longitudinal direction. The stresses in the reinforcing were 25 to 420 kg-force/cm². The upper stress limits belongs to the point close the cracks.

Table 9-2

Date	Section a-a, upper radius α_a , kg-force/cm ²		Concrete deformation, 10^{-5}
	Instrument 16	Instrument 17	
1970. I	1400	766	202
	1485	832	221
	1655	950	242
	1390	775	197
	1440	802	195
	1223	635	163
	932	416	127
	805	350	123
	Maximum	1736	310

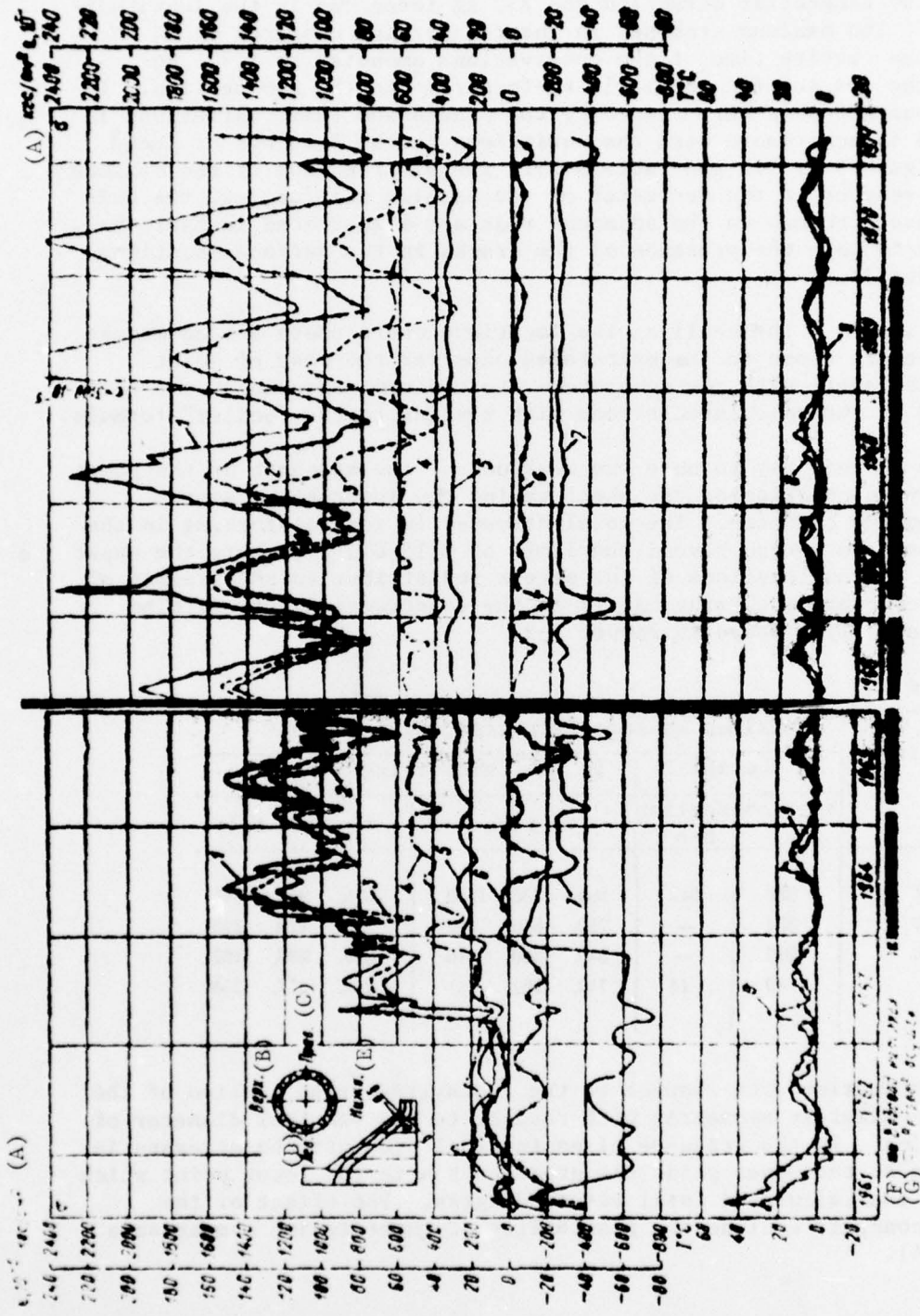


Figure 9-2. Maximum measured stresses in the shell, the reinforcing and deformations of the concrete. 1 -- deformation of the concrete at the upper point of the cross section 2 m above the shell; 2 -- [deleted]; 3 -- stresses in the annular reinforcing, upper point of the cross sections; 4 -- annular stresses in the shell, top; 5 -- the same, right side; 6 -- longitudinal stresses in the shell, right; 7 -- the same at the top; 8 -- shell temperature, top; 9 -- the same concrete; at the bottom [deleted] No 6. B. top C. right D. left, E. bottom, F. conduit filled G. conduit drained.

The maximum value of the total stresses measured on the shell is 642 kg-force/cm² in the tangential direction and 250 kg-force/cm² in the longitudinal direction. The maximum stresses in the reinforcing measured by 24 devices during the entire time of the observations amounted to 1,736 kg-force/cm² in the a-a section and 1,016 kg-force/cm² in the b-b section. In both cases these stresses were caused by the cracks and their variations in time increased in accordance with the variations in the openings of these cracks (see Figure 9-1, 9-2 and Table 9-2). The distribution of the maximum stresses with respect to the perimeter of the annular reinforcing, the uniformity of these stresses in the adjacent rods are illustrated in Table 9-3. It is possible to note the presence of the cracks in the various locations in the cross sections.

The actual stresses in the shell at the locations where there are no cracks in the concrete are close to the calculated ones for the case of joint operation of the shell with the concrete. The maximum measured stress does not exceed 1/3 of the calculated stress with respect to the "boiler" formula.

It is possible in this way to note the weak use of the strength of the sheet steel closed by calculation of the shell taking the internal pressure separately from the concrete. The total stresses in the reinforcing in the majority of cases do not go beyond the limit of 0.15-0.5 [σ] where the upper limit pertains to the locations of the stress redistribution as a result of cracks in the concrete occurring mainly in the construction period. The mean stresses are illustrated in Figure 9-3.

Table 9-3

Radius	Maximum measured stresses, kg-force/cm ²						
	In the shell		In the reinforcing				
	section a-a	section b-b	section a-a			section b-b	
Upper	250	642	890,	1736,	1550	1016,	910, 945
Lower	334	—	710,	640,	316	380,	270, 323
Right	272	—	340,	300,	316	870,	936, 162
Left	40	14	710,	262,	325	244,	277, 248

The stress distribution with respect to the transverse cross section of the conduit is approximately symmetric with respect to the vertical diameter of the cross section. In the presence of an internal pressure the stresses in the reinforcing at the upper point are greater than in the lower point which corresponds to the calculated total stress diagram. The effect of the cracks in the concrete exclude the possibility of quantitative comparisons (see Figure 9-4).

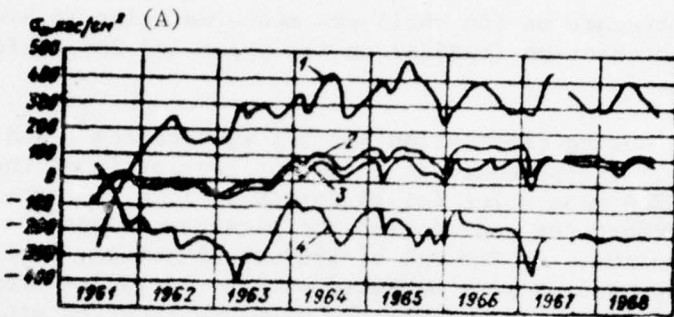


Figure 9-3. Average stresses with respect to sections a-a and b-b (Figure 2-9). 1 -- in the annular reinforcing; 2 -- in the shell with respect to the annular direction; 3 -- in the stiffening rib; 4 -- the same with respect to the longitudinal direction.

Key: A. kg-force/cm²

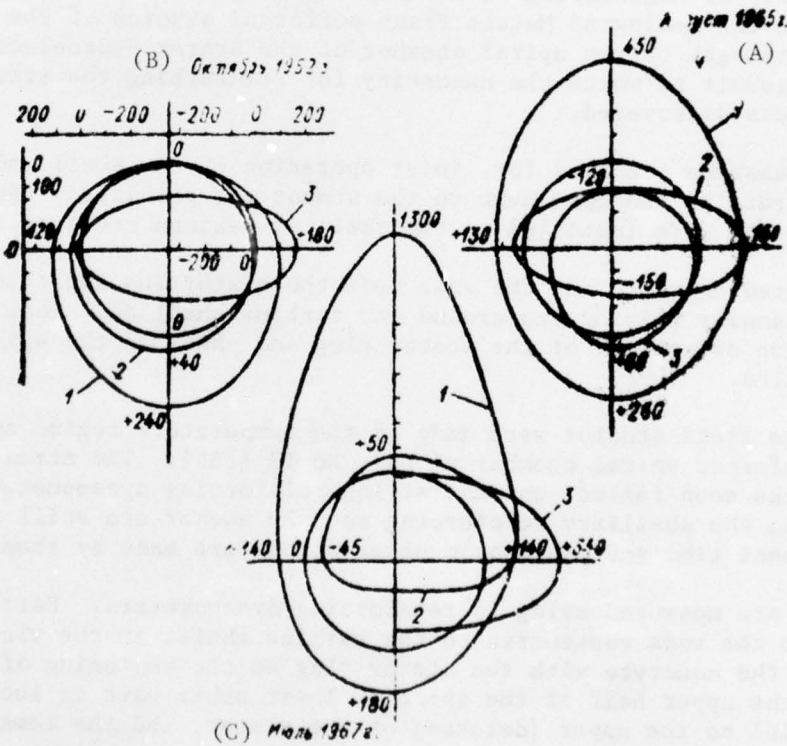


Figure 9-4. Stress diagrams with respect to section a-a.
1 -- in the reinforcing; 2 -- in the shell; 3 -- in the stiffening rib.

Key: A. August 1965; B. October 1962; C. July 1967

9-4. External Pressure on the Conduit Shell.

The external water pressure on the shell was measured using 16 piesodynamometers located in each section (radius) on the upper and lower sides of the stiffening rib.

The maximum pressure during cementation was $3.1 \text{ kg-force/cm}^2$, and the minimum $0.9 \text{ kg-force/cm}^2$. The pressure at the upper generatrix of the shell was equal to zero. The mean value for 16 points is $1.28 \text{ kg-force/cm}^2$. After cementation, before the end of 1965 the pressure dropped to a value of $0.00-1.30 \text{ kg-force/cm}^2$. At the end of 1969 at 15 points, including the upper points, small pressures were measured within the limits from 0 to $0.46 \text{ kg-force/cm}^2$, and only at one point was the pressure reported equal to $1.41 \text{ kg-force/cm}^2$. From this, it is possible to conclude that with respect to the casing around the shell there is great seepage pressure as a result of leakage of the water along the conduit from the top or as a result of leakage of the water through any local leaks in the shell.

9-5. Stresses in the Concrete and Reinforcing Around the Shell of the Spiral Chamber

The Laboratory of Engineering of Structural Designs of the VNIIG Institute jointly with the Leningrad Metals Plant performed studies of the stressed state and strength of the spiral chamber of the Bratsk Hydroelectric Power Plant as a result of which the necessity for reinforcing the structure of the spiral was discovered.

Among the measures provided for, joint operation of the shell and the reinforced concrete in the zone next to the stator was permitted; the additional stiffening ribs were installed on the shell of maximum cross sections.

The reinforced concrete and the zone near the stator was additionally reinforced by annular reinforcing around the turbine shaft and along the conduit in the region of contact of the stator ring and shell of the spiral anchors were installed.

In 1962 some field studies were made of the temperature regime and stresses in the reinforced spiral chamber of unit No 13 [135]. The strain gages used in this work soon failed, and the string reinforcing dynamometers that were installed in the auxiliary reinforcing and the anchor are still operating at the present time and systematic observations are made by them.

Distresses are measured using 14 reinforcing dynamometers. Part of them are welded into the rods concentric to the turbine shaft, in the vicinity of the contact of the concrete with the stator ring to the beginning of the felt insert on the upper half of the spiral. Their other part is located in the rods parallel to the upper [deleted] of the stator, and the remaining part in the anchor.

The stresses vary periodically with maximum compression in the summer and maximum tension in the winter. This periodicity is caused by the temperature

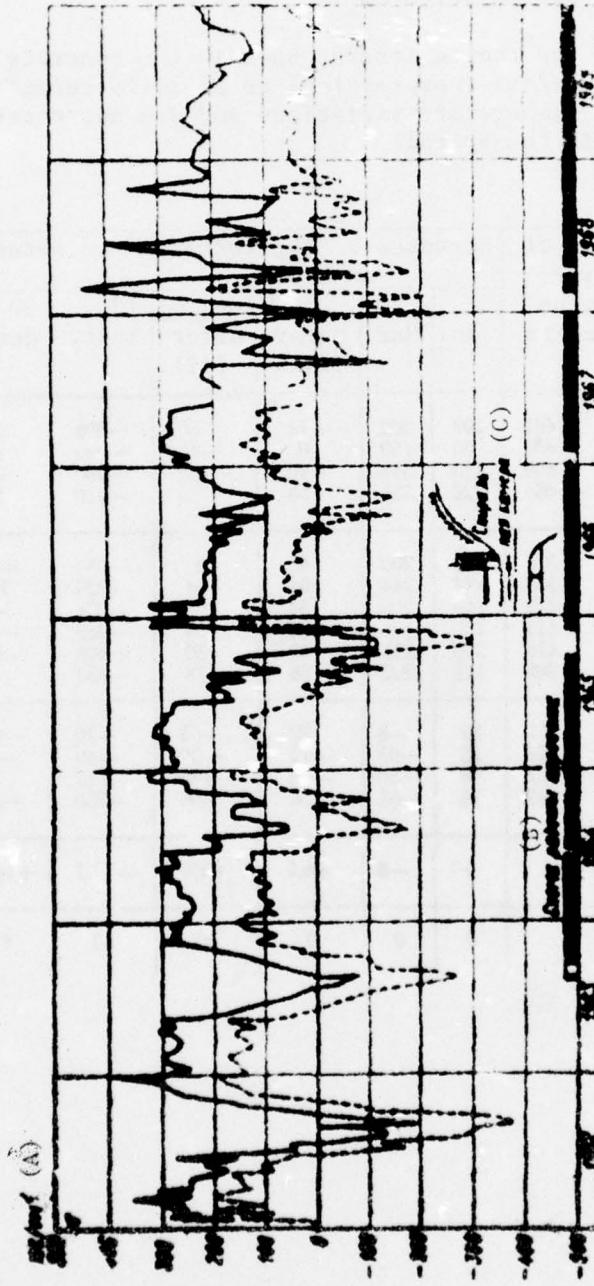


Figure 9-5. Stresses in the reinforcing of the spiral chamber.

Key: A. kg-force/cm²
 B. schematic of the operation of the unit
 C. spiral chamber

fluctuations in the concrete depending on the water temperature. The measured stresses are basically thermal stresses (Figure 9-5), the effect of the internal pressure is felt insignificantly (Table 9-4). The maximum measured tensile stresses do not exceed 400 kg-force/cm², and the maximum compressive stresses are 550 kg-force/cm².

The stresses measured by the remote strain gages in the concrete were within the limits from -8 kg-force/cm² (compression) to 22 kg-force/cm² (tension). They corresponded to the temperature variations and did not react to the internal water pressure in the spiral.

Table 9-4

Location of the reinforcing	No of instruments	Stresses σ (kg-force/cm ² on dates in 1962)					
		30 Jan.	20 Mar.	20 June before fill.	20 June after fill.	10 Sept.	30 Oct.
Turbine shaft	461	207	302	-14	-66	-108	72
	463	85	150	0	-45	-280	45
	469	210	343	-90	-135	-290	-5
	464	220	355	55	20	-210	20
Operating reinforcing above the shell around the stator	375	140	200	45	0	-380	-26
	363	184	244	104	94	-226	104
	422	166	200	54	65	-154	-4
	411	136	136	-24	-34	-439	-84
	410	220	298	40	30	-405	-75
	369	143	292	88	78	-353	12
Anchor rods	251	52	-8	22	-68	-70	-140
	429	52	-62	-12	-90	-40	-70
	257	98	-56	-60	-186	-115	14
	263	76	-31	-56	-96	-250	-168
Temperature in concrete, °C		+7	-8	+6.2	+4.8	+17.2	+10.2
Head, meters		0	0	0	59	63	68

CHAPTER 10. LEAKAGE REGIME IN THE BASE AND IN THE BODY OF THE DAM

10-1. Leakage Head in the Contact Zone

The experimental study of the leakage flow in the base of a concrete dam was performed at the percolation laboratory of the VNIIG Institute on two-dimensional models of the base with nonuniform permeability of the layers of the rock. The studies indicated that the most effective means of reducing the counterpressure on the underground contour of the dam are the expanded joints and the first series of drainage holes. The second series of drainage holes has a weak influence on the counterpressure.

The cementation curtain in the presence of the drainage holes of the first series is ineffective. It lowers the counterpressure in sections 28-58 poorly and increases it in sections 59 to 66.

The design counterpressure diagram provides for a drop in the seepage head according to linear law from H under the pressure face to 0 on line I of the series of drainage holes with reduction of the head to 0.20 H between rows I and II of the drainage with a drop to zero under the downstream face of the footing (see Figure 10-2).

The drilling of the drainage holes of rows I and II was completed with respect to the entire pressure front at the beginning of 1964. In many of the holes the depth was less than planned. The examination of the drainage system at the end of 1964 demonstrated its poor condition. Among the inspected wells only 40 to 50% were in the operating state; the rest were plugged or frozen.

The pie ometric network of the dam which reached 158 pieces in 1963 gradually failed as a result of the freezing of the concrete and damage, and for example, on the beginning of 1965 1/3 of the pie ometers were not working. Then the number of piesometers was increased, but part of them remained in nonworking condition for various reasons.

The cleaning of the drainage holes, the drainage tunnels and the expanded joints was started at the end of 1966 and completed by September 1967.

The established positive temperature in the cavitys of the expanded joints and their reinforcing completed the process of reducing the drainage system of the base to the operating state.

During the period from the beginning of April to the middle of December 1968 the expanded joints in the dam were drained. In 1968 they began to work on cementing the base of the first columns.

The buildup of the headwater level to the normal backwater level which took 6 years, the condition of the drainage network and the work on cementation resulted in the nonsteady state percolation regime during the entire observation period. In this regime it is possible to note three steps: the first at the beginning of 1967 was characterized by a progressive worsening of the condition of the drainage system, and the second with gradual worsening and the third with destruction of the percolation regime of a number of sections in connection with the drilling operations and cementation.

The first observations on the piesometers in the middle of 1962 indicated that in a majority of cases the piezometric levels of the contact zone beyond the cementation curtain are close to the tailrace level (or below it) as a result of pumping water out of the expanded joints. Nevertheless, in sections 28-32 in the left bank adjoining the reduced percolation heads are within the limits of 25 to 47%, which could be explained by the absence of drainage holes in the section. However, after reinforcing cementation and the construction of drainage lines according to plan, the heads in certain sections continued to rise. The regions of increased heads by comparison with the other sections, although they did not go beyond the limits of the planned values appeared in the central part with the channel (sections 41 to 42) and in the right bank abutments (section 67) (Table 10-1 and Figure 10-1).

Section No.	Reduced heads and percentages before dates						
	MV mm	1/1 1964	1/1 1965	1/1 1966	1/1 1967	20/IV 1967	20/III 1968
28	26	30.0	30.5	43.0	50.8	47.5	50.0
29	26	30.5	30.4	25.5	28.2	23.4	23.4
30	26	27.8	27.8	24.6	25.6	35.6	22.4
31	26	20.6	20.6	37.0	48.4	41.5	37.2
32	26	11.7	11.7	22.6	51.5	45.8	75.0
33	26	3.5	3.5	9.6	35.8	31.9	-
34	26	20.4	20.4	37.0	33.4	50.9	-
35	26	13.6	13.6	84.0	87.0	92.6	36.0
36	26	-	10.8	20.2	62.5	41.4	15.6
37	26	-	-	53.5	74.8	81.5	81.0
38	26	26.8	26	26.4	22.7	22.7	22.0

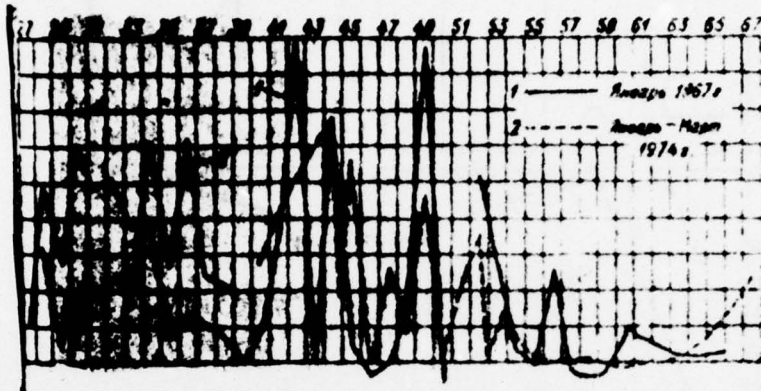


Figure 10-1. Distribution with respect to longitudinal section of the maximum piezometric heads h_a in the base of the dam on the downstream side of the cementation curtain; 27-67 -- section numbers.

Key: 1. January 1967
2. January-March 1974

In 1965 a sharp increase in the piezometric heads began to be observed which in individual sections reached 80 to [deleted] H. In 1967, in connection with cleaning the drainage holes the heads dropped somewhat, but in sections 28, 31, 32, 33, 41, 42, and 49 high values of them remained.

The cause of the increase piezometric heads in the area of sections 28-32 can obviously be considered to be the inflow of water into the base of these sections below the cementation curtain from the aquifer above the trap rock through vertical cracks in the shore slope. This is confirmed by the observed sharp drop in the piezometric levels in the winter when the [deleted].

Sections 41 and 42 are located at the beginning of the section of increased jointing of the diabases and at the butt of the deep and conjugate cementation curtains.

The increased heads in section 67 probably are explained by the seepage around the trap rocks.

It is necessary to note the significant difference in the readings by the row of contact piezometers located at one mark characterizing the nonuniform permeability of the traprock.

The high percolation heads appearing in sections 42 and [deleted] in 1965 increasing with time and spreading to a number of sections are explained by

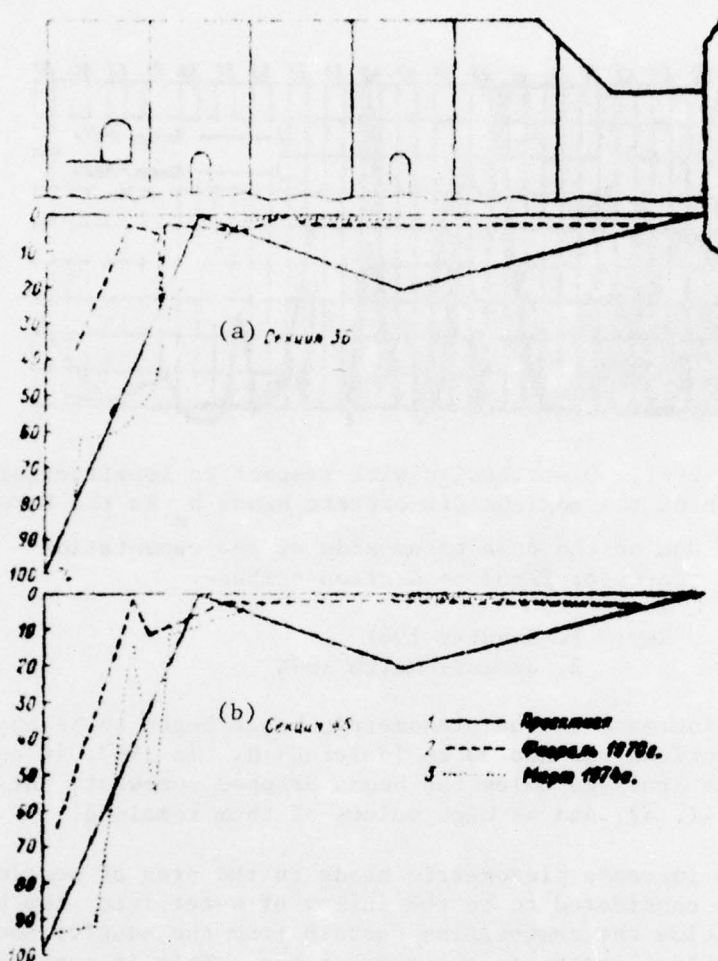


Figure 10-2. Distribution with respect to transverse sections of the piezometric heads in the base of the dam.

Key:	a. section 36	1. design
	b. section 45	2. February 1970
		3. March 1974

the phenomenon of opening of the contact joints and loss of seal in the rock base of the first columns which was exhibited by the readings of the contact remote strain gages at the beginning of 1965 (see § 6-7).

Seven of the transverse sections of the piezometers located along the [deleted] channel dam (see § 2-3) permit determination of the distribution of the percolation heads along the axis of the sections.

Common to all of the diagrams is the extinguishing of a significant part of the percolation head to the cementation curtain. The low permeable trap-rocks in the headwaters of the dam are a natural upstream flow. The total effect of the latter and the cementation curtain removes the basic part of the percolation head (to 80-100%), and the first line of the drainage holes removes the basic head. In some of the sections a reduction of the head to 10-20% in the section between the drainage holes was observed (see Figure 2-5, 10-2). In general the piezometric heads at the footing of the sections beginning with the second columns did not go beyond the limits of the designed diagrams with the exception of several sections.

10-2. Effect of the Cementation on the Counterpressure in the Base of the First Column

The data of the last column in Table 10-1 pertained to the beginning of the normal operation of the dam. In April 1968 the expanded joints were drained, and the drainage water was pumped out. In the base of several of the sections control holes and cementation holes were drilled. After flooding of the expanded joints the piezometric level in columns II-VI were restored approximately to the tailrace level, however, in the section before drainage of the first line in the series of sections the counterpressure built up independently of the tailrace level which indicated the continuing loss of seal in the base of the first columns.

The operations with respect to cementation of the base under the first columns were started in 1968, and they continued, encompassing the series of new sections to 1974. The cementation was carried out to a depth of up to 10 meters with respect to the direction from the cementation tunnel to the pressure face through 5 series of radial holes in a row [deleted] zones with subsequent approach of the holes in the [deleted]. The ordinary portland cement is used with a consistency of the mortar from 20 to 0.6 and a pressure exceeding the percolation head in the given zone by 5 atmospheres.

The absorption of the cement increases from units of kg/meter in rows I and II to hundreds of kg/meter in the rows close to the pressure face.

The control drilling before and after cementation performed by the Angara Expedition of Gidroproyekt Institute demonstrated that the water permeability of the rock as a result of cementation was decreased to the recorded values. The cementation usually led to a reduction in the counterpressure (Table 10-2). In a number of sections the effect of the cementation turned out to be short-lived, and the piezometric heads gradually dropped for 2-3 years. The especially intense rise was observed in the winter of 1971 to 1972 when after prolonged and high fall flooding the headwater level was at the ~120 meter mark. The instruments on the pressure face indicated additional opening of the contact joint at this time (see Figure 6-26).

With respect to nature of reduction of the counterpressure it is possible to divide the sections of the dam into two groups. In part of the section either the stable position was maintained or there was a monotonic increase

Table 10-2

Section	Cementation date	Amt. of absorbed cement	Reduced percolation head, %		Beyond cementation curtain							
			By design	Actual maximum	Before	After	Feb.	Mar.	Before	After	Feb.	Mar.
			cement-	cemen-	1972	1973	cemen-	cemen-	1972	1973	1972	1973
22	IX 1968 - IV 1969	20.2	88	-	-	7	46	41	20	32	28	28
22	IX 1968 - I 1969	4.5	76	74	92	-	46	61	15	12	11	11
33	IV - VI 1970	3.1	93	87	94	-	46	73	7	24	16	10
33	V - XI 1970	7.8	118	118	118	-	46	56	11	16	18	18
33	V - XI 1971	11.8	118	118	118	-	46	42	-	3	-	-
33	V 1970 - III 1971	6.7	84	82	94	-	46	20	7	23	12	12
33	V - V III 1971	3.4	72	70	94	-	46	53	9	23	7	7
47	V - VII 1970	5.3	80	46	95	-	31	38	3	17	43	43
47	V - V 1970	4.7	81	47	95	-	31	45	10	17	17	17
47	V 1970 - V 1971	7.7	86	87	95	-	61	76	8	36	6	6
47	non topo										31	1
47	V 1971										32	1
47	V 1972										32	1
47	IV - VIII 1970	2.3	82	82	82	-	23	41	-	-	-	-
47	I - IV 1970	6.5	82	82	82	-	36	46	1	8	8	8
47	XII 1971 - V 1972	10	82	82	82	-	36	46	1	8	8	8
47	VII 1971 - III 1972	4.8	82	82	82	-	36	46	1	8	8	8

Note. The ordinate of the design diagram at the location of the water receiver of each piezometer was taken as the design head.

in the counterpressure. In the other part of the sections, its variation had a seasonal nature with a summer minimum and winter maximum drawing with time (Figure 10-3). These variations coincided with respect to phase with the temperature variations. This nature of variation of the counterpressure can be explained by varying the opening of the cracks in the case of seasonal variations of the stresses σ_x and σ_y (see § 6-7). Beginning with this proposition it is necessary to consider the best time for cementation through the winter period when the opening of the crack is the greatest. The monotonic buildup of the counterpressure obviously is connected with gradual opening of the fine and thin cracks in which usually the cement mortar does not penetrate.

In 1973 Gidroproyekt Institute performed some repeated ultrasonic and electrometric studies in the base of the first columns with a number of sections, including the sections in which these studies were performed in 1969. It was established that as a result of cementation, the properties of the rock became worse in the sections previously having increased jointing. In addition, the appearance of new cracks was noted both within the limits of the cemented zones and below them and also in the holes where the cementation did not occur. The penetration of the cement mortar only into the large cracks was confirmed. In six sections (32, 35, 36, 40, 53 and 55) the absence of zones of increased jointing was recorded.

In 1973 alone in some of the sections a small spring increase in counterpressure was observed. In the spring of 1974 this increase was observed in a number of sections where up to that time the headwater level was held above the 120 meter mark for more than 7 months.

Thus, the process of stress relief of the rock base of the first columns continues as a result of which the performed cementation only has a temporary effect.

10-3. Nature of Percolation Flow in the Traprocks

In six sections bundles of piezometers were builtin on both sides of the cementation curtain with the water receivers at three levels: in the roof of the diabases (5-8 meter marks), in their midsection (28-23 meter mark) and in the subdiabase sandstones. The measured piezometric levels make it possible to determine the widespread nature of the percolation flow and its form.

Table 10-3 has the values of the piezometric heads in the indicated three horizons with respect to the state on 1 February 1964 and 1965. The head distribution to depth of the base during constant operation is illustrated in Figure 10-4.

The piezometric heads in sections 46, 56 and 65 with deep cementation drop sharply beyond the curtain (to 0-11%) in the contact zone and in the series of diabases; in sections 28, 30, 67 located outside the region of deep cementation, beyond the curtain 28-33% of the defective head was maintained. In the sandstone region the effect of the curtain in practice was not felt.

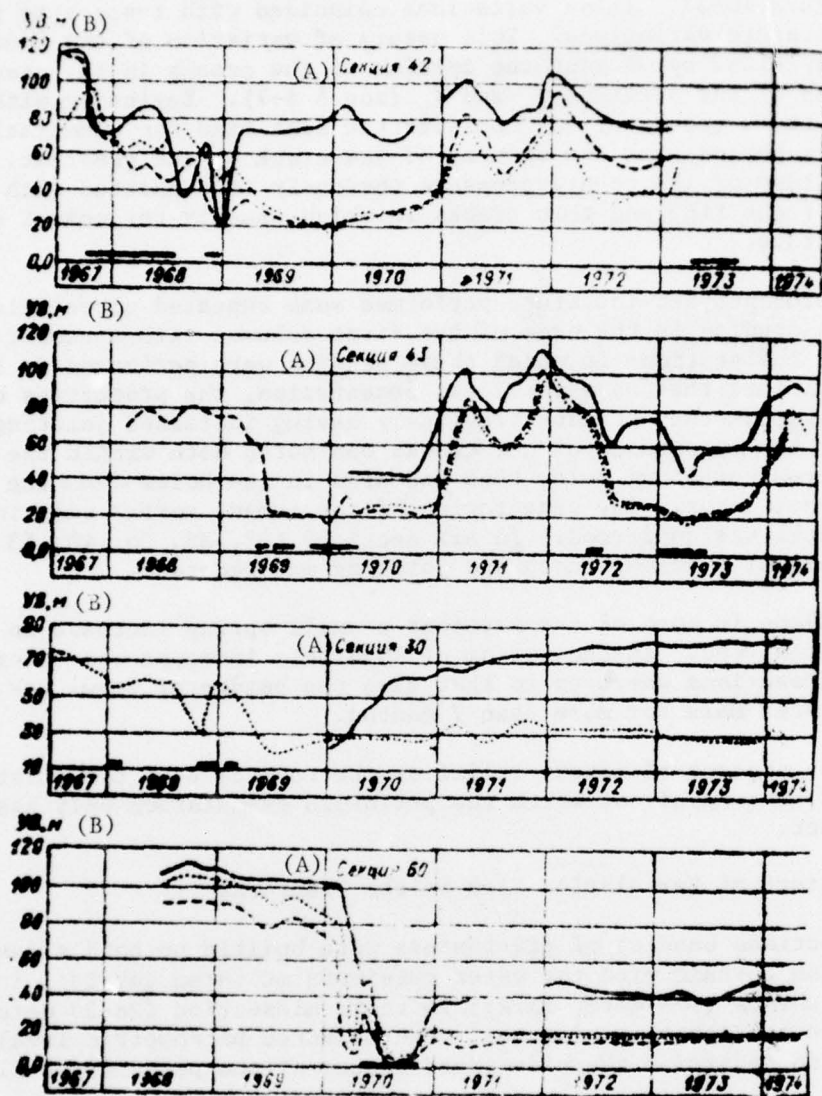


Figure 10-3. Variation of the piezometric levels before and after cementation of the base of the first columns.

Key: A. section...
B. level, meters

The piezometric heads in sandstones were within the limits of 0-10% and varied little during the process of the filling of the reservoir. It is possible to state that the feed of the percolation flow in the sandstones occurs outside the limits of the dam, and it is an aquifer which depends

Table 10-3

Sections	Horizon	Percolation head in % of the head			
		1 Feb. 1964		1 Feb. 1965	
		Before curtain	After curtain	Before curtain	After curtain
28	Upper	60.0	—	4.0	38.0
	Middle	17.2	20	30.0	33.2
	Lower	7.2	15.5	12.1	—
30	Upper	61.0	15.0	—	27.8
	Middle	8.7	1.0	0	1.0
	Lower	1.0	7.5	7.5	7.8
45	Upper	39.0	1.5	—	0
	Middle	3.1	0.0	25	0
	Lower	6.5	2.4	4.8	2.7
56	Upper	16.4	0	28.0	0
	Middle	44.0	0	42.0	0
	Lower	4.2	0	2.4	0
65	Upper	45.5	3.0	—	7.4
	Middle	35.7	7.0	—	11.0
	Lower	2.7	4.2	—	3.7
67	Upper	52.0	29.0	—	26.0
	Middle	40.0	32.0	—	28.0
	Lower	5.0	5.0	—	—

little on the percolation flow in the diabases located above.

The head in the diabases varied noticeably during the filling of the reservoir. From the pressure side of the curtain in all sections the percolation flow is directed from the contact to the body of the diabases. From the low side of the curtain the head distribution is different. In the sections at the left bank (28, 30, 36 and 45) the maximum values of the head occur in the contact zone. In the remaining sections the head is distributed vertically either uniformly or it increases somewhat in the direction from the contact into the body of the diabases.

The discharge of the flow from the body of the diabases in the right bank sections takes place in the first and second columns, and in the remaining sections somewhere downstream.

10-4. Effectiveness of the Cementation Curtain and the Drainage Structures

It was noted above that the total effect of the cementation curtain and the natural upstream floor removes the greater part of the percolation head under the first columns of the dam. The great drop in head at the contact and the

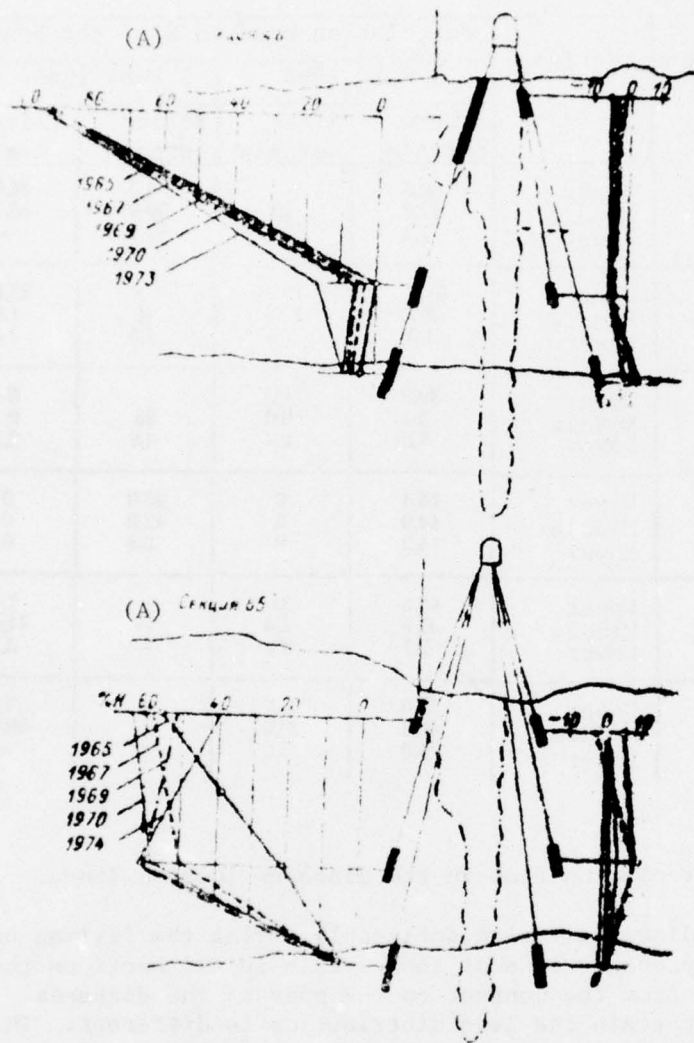


Figure 10-4. Distribution of the piezometric heads with respect to depth of the base.

Key: A. section...

body of the diabases in the sections with deep cementation curtain by comparison with the sections outside the deep cementation zone was noted. In Table 10-4 values were presented for the piezometric heads in the contact zone on both sides of the cementation curtain and their difference by which it is possible quantitatively to estimate the effect of the natural upstream floor and the curtain on the extinguishing of the head.

Table 10-4 primarily characterizes the nonsteady state percolation regime during the first years of constant operation of the dam caused by drilling of the control and cementation holes. Using the data in 1968 when the upstream level was close to the normal backwater pressure and the drilling of the holes had a local nature it was possible to note the following.

The drop in the head on the natural upstream floor is within broad limits from 8 to 41%. In section 46 where this drop is maximal, the deep curtain removes the head completely, and in section 65 where it is maximal, the deep curtain completely removes the entire remaining part of the head. However, this phenomenon is observed also in the sections without a deep curtain (29, 30 and 31). Therefore the defined determination of the effectiveness of the latter still is difficult. It is possible only to note that this efficiency is less than was proposed in the plan. The flow in the curtain sandstone has little effect on the percolation flow.

For determination of the effect of the drainage system of the base let us consider the data on the percolation flow rates.

The measurement of the specific discharges in the head piezometers characterizes the weak water permeability of the traprock. In the majority of cases the discharges are small and commensurate with the specific water absorptions of the diabases. The measured discharges are within the limits of 0.001-2.8 liters per minute. In the control group made up of 11 piezometers the quarterly measurements indicate the discharges in the range from 0.003 to 0.47 liters per minute. Here the discharges with an upper limit of 0.32 to 0.47 belong to the three contact piezometers at the pressure face and at 8 points at a distance of 10 to 15 meters from the face the discharges are 0.003 to 0.19 liters per minute.

The cementation reduces the discharges sharply in the piezometers. Thus, in 11 piezometers of four sections the discharges of 0.007 to 0.8 liters per minute dropped after cementation to 0.0003 to 0.01 liter per minute.

By the investigations using the EHDA method the specific percolation flow with normal backwater level in the section with natural hydraulic floor was estimated at 1 liter per second per meter which for the length of the pressure front gives about $1 \text{ m}^3/\text{sec}$. The actual flowrates remain appreciably less for the entire observation time.

The first measurements of the flow rates were performed at the end of 1968 with a headwater level of about 120 meters by three methods, and they turned out to be equal to the following: 1) on filling of the receiving pits of the pumping stations with drained expanded joints of 52 liters per second; 2) with respect to intensity of filling of the expanded joints after reduction of the pumping of 42 liters per second, and 3) with respect to the measurements on the spillways of the pumping stations (the operating schematic of the measurements) 21 liters per second. Judging by these data it was possible to estimate the percolation flow rate at about 50 liters per second.

Table 10-4

Sections	Measurement location	Reduced head (%) by years						
		1967	1968	1969	1970	1972	1973	1974
28	Before curtain	77.0	73.2	55.2	10.5	61.2	46.1	61.5
	Beyond curtain	46.0	39.2	31.5	26.0	30.2	29.1	30.2
	Difference	31.0	34.0	23.7	-15.5	21.0	18.0	31.3
29	Before curtain	83.0	70.0	74.5	78.0	86.0	85.0	-
	Beyond curtain	22.0	10.0	7.4	8.0	14.4	13.7	-
	Difference	61.0	60.0	67.1	69.5	71.6	71.3	-
30	Before curtain	64.5	47.0	piezometer defect		53.5	61.5	62.7
	Beyond curtain	56.5	5.6			16.0	12.7	14.7
	Difference	8.0	41.4			37.5	48.9	48.9
31	Before curtain	64.0	54.5	21.5	23.0	92.0	86.0	-
	Beyond curtain	6.0	4.4	0.1	0	14.1	13.2	-
	Difference	58.0	50.1	21.4	23.0	77.9	72.8	-
32	Before curtain	66.0	77.0	23.1	44.0	64.8	47.4	67.5
	Beyond curtain	46.5	62.0	0.7	13.5	24.1	10.8	20.1
	Difference	19.5	15.0	22.4	30.5	40.7	36.5	47.4
48	Before curtain	92.0	93.5	96.2	96.0	96.0	97.5	-
	Beyond curtain	-4.0	0	-3.0	-3.3	-3.2	-3.2	-
	Difference	96.0	93.5	99.2	99.3	99.3	-	-
65	Before curtain	58.5	61.0	51.5	64.0	65.2	41.0	63.9
	Beyond curtain	-2.5	1.0	0.7	1.5	7.4	6.5	4.1
	Difference	61.5	60.0	50.8	62.5	57.8	34.5	59.9
67	Before curtain	68.2	62.6	65.5	64.5	-	-	-
	Beyond curtain	22.9	21.0	22.5	24.5	-	-	-
	Difference	35.3	41.6	43.0	40.0	-	-	-

The measurement of the flow rates using the spillways of the pumping stations performed during the period from 1969 to 1972 monthly gave a value of the filtration flows exceeding 20 to 25 liters per second, decreasing during the summer months almost to zero. The testing of the system of operating measurements performed in 1972 demonstrated the absence of significant errors. From this it follows that the drainage system does not catch the entire percolation flow through the base of the dam; part of the percolation flow is discharged directly to the tailrace. The high piezometric heads which occur in a number of sections before cementation of the base of the first columns were not accompanied by variation of the percolation flow rates. The cracks of the first columns which are the cause of these heads obviously are not through cracks and do not have a hydraulic connection with the drainage system.

The absence of the region of increased heads under the footing of columns II-VI of the sections indicates the sufficient effectiveness of the drainage system at the base.

In general the filtration regime of the base of the channel dam in 1973 after the performed cementation operations in the majority of sections corresponds to the design proposals. The conclusions regarding the effectiveness of the deep curtain must be more precisely defined by the observations under the conditions of steady state percolation.

10-5. Percolations through Concrete of the First Columns of the Dam

When designing the concrete gravity dams beginning with the M. Levi rule it was proposed that the water cannot penetrate into the body of the dam if the main compressive stresses at the point at the pressure face exceed the hydrostatic pressure of the water at this point.

With respect to the later ideas [136] the water penetrates into the concrete and is filtered through it independently of the magnitude of the effective stress.

With certain ideas, the presence on the pressure face of the dam of an open horizontal joint or crack is accompanied by penetration of water in them causing counterpressure with redistribution of the stresses in the plane of the joint or the crack. In order to avoid opening of the horizontal joints, the occurrence or opening of the previously occurring horizontal cracks, the effective norms of SN. 123-60 provide for insurance on the pressure face of the minimum principal stress no less than $0.25\gamma H$, where H is the hydrostatic pressure in the investigated cross section without considering the counterpressure.

The field investigations demonstrated that at a number of dams the counter pressure in the interblock joints is absent. On some of the dams a counter-pressure was detected which decreases from the full head on the pressure face to zero in the drainage [137].

Thus, under defined conditions it is possible to avoid penetration of the water into the concrete and the development of counterpressure in the latter.

The quality of part of the piezodynamometers turned out to be (see § 2-10), and one-third failed soon after raising the upstream level to the corresponding marks. This, to a significant degree, decreased the value of observations performed by the results of which during the period from 2 to 9 years it is possible to establish the following.

The pressure in the monolithic concrete measured by 22 instruments did not exceed the limits of accuracy of the measurements and, therefore, it is possible to consider that in practice there is no counterpressure in the monolithic concrete.

The water impermeability of the horizontal interblock joints is different depending on the age of the lowest of the blocks forming the joints. In the joints between the block with a small time interval, the counterpressure either is insignificant or absent.

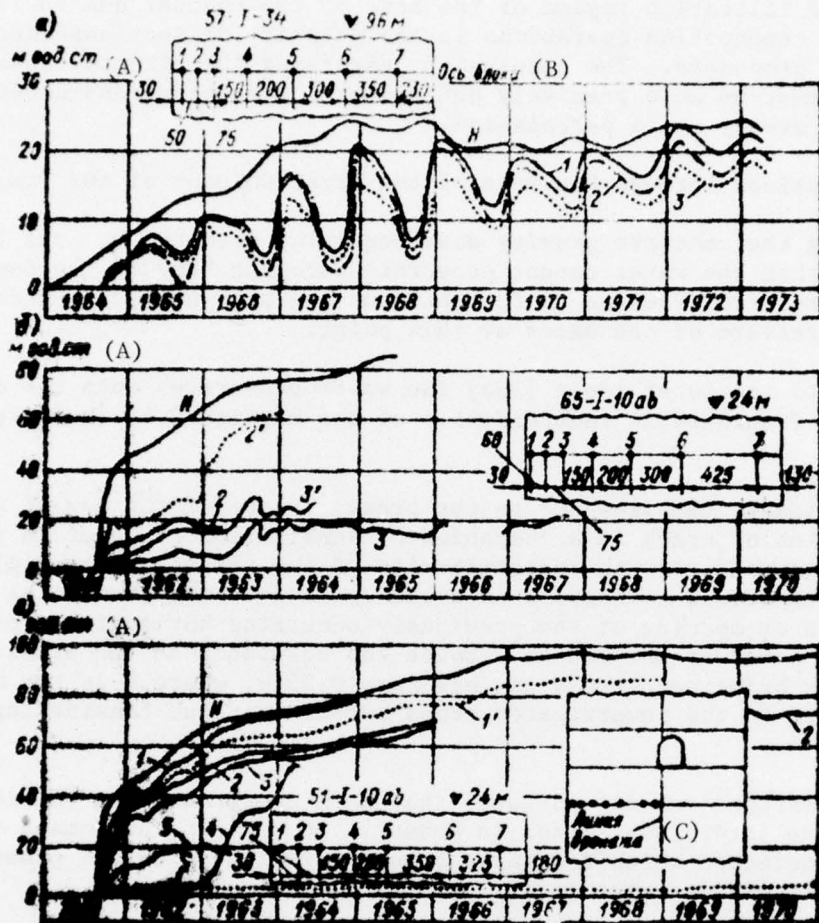


Figure 10-5. Pressure of the percolated water in the horizontal interblock joints of the first columns. 1 -- head; numbers on the graphs correspond to the measured points on the schematics without a stroke -- in the halfblock a, with a stroke in the halfblock b.

Key; A. meters of water
 B. axis of the block
 C. drainage line

In the joints between the blocks poured with a large discontinuity in time (4 to 8 months), the water pressure increases with an increase in the head H, constituting a smaller proportion of it, the farther the investigated point is from the pressure face. The pressure face remains at the 90 to 100% of H level, and for drainage it does not exceed 0-2%. In some cases also after the drainage the pressure remains 2 to 4% H (Figure 10-5).

At points of the duplicated sections identically removed from the pressure face, the water pressure is different, and in the points of one section it is nonuniform. This characterizes the water permeability of the joint which is nonuniform with respect to area (Figure 2-5). The nonuniformity of the pressure along the section gradually decreases and its distribution can be approximately considered linear.

With respect to nature of variation of the pressure in the joint with time it is possible to note two cases. At the lower mark the pressure in the joint increases monotonically with the discontinuous measurements in individual cases. In the section closest to the crest of the dam, the pressure variation in the joint near the pressure face (0.25 to 1.5 meters) has a sharply periodic nature, decreasing in the summer time and increasing in the winter. Judging by the variation in temperature in the joint and the nature of variation of the oscillation amplitude it is possible to assume that the latter are caused by openings of the joint under the combined effect of measurements of the headwater level and temperature. It is possible that to some degree the openings of the intercolumnar and interblock joints on the downstream face are felt.

It is necessary to note another case of pressure variation in the joints. At the 40 meter mark of section 51 in the section made up of six measuring points a sharp increase in pressure in the joint began to be observed in the beginning of winter, and the same sharp drop at the beginning of spring. The pressure distribution was extraordinary. It decreased regularly from the maximum at the point which is located at a distance of 2 meters beyond the drainage line to the minimum at the pressure face.

The blocks forming the joint were poured with an interval of 5 days and on the pressure face side the water did not penetrate into the joint. The rise in pressure in the joint was demonstrated by the instruments at the beginning of 1964, that is, 2.5 years after the rise in headwater level to the setting of the instruments with a head above 50 meters.

The extraordinary pressure distribution can be explained by penetration of the water through the vertical cracks into the bypass of the section of instruments with spread of it into the joint from the inspection tunnel side. This proposition is confirmed by the fact that after coverage of the expanded joint in October 1966 the periodic variations of pressure in the joint ceased although the pressure distribution remained.

The absence of the counterpressure in the horizontal joints of the first columns between the blocks poured with a small time interval is the most significant practical conclusion from the observations made.

CHAPTER 11. CONCLUSIONS AND PROPOSITIONS

11-1. State of the Dam

The construction of a high gravity dam in a location with severe climatic conditions faces the builders with a number of difficult problems. For the construction of the Bratsk Hydroelectric Power Plant these problems were complicated by the fact that they were solved under especially severe conditions and they were solved for the first time.

In a comparatively short time the Bratskgesstroy collective built the first concrete gravity dam in the USSR 126 meters high in which about 4.3 million cubic meters of concrete were used. Exactly at the planned time -- 1 September 1961 -- the filling of the reservoir was started, the waterlevel in which in September 1967 had reached the 122 meter mark that is, the normal backwater level. Eighteen out of 20 of the hydraulic units with a power of up to 225 megawatts each were installed and started up; during the temporary operation period they generated more than 60 billion kilowatt-hours with power.

In September 1967 the Bratsk Hydroelectric Power Plant was put into industrial operation and by order of the Presidium of the Supreme Council of the USSR it was named the Bratsk Hydroelectric Plant imeni 50th Anniversary of Great October Revolution. In the six years of industrial operation (on 15 May 1974) the Bratsk Hydroelectric Power Plant had provided 220 billion kilowatt-hours of power.

The condition of the concrete dam at the end of 1973 is characterized by the following field observations data.

The settling of the channel dam caused by compression of the subdiabase sandstones has built up directly proportionally to the level (weight) of the water in the reservoir, and after reaching the normal backwater level it stabilized at an amount within the limits from 72 to 73 mm in the central part of the channel to 50 mm in the shore cuts.

The magnitude of the settling approximately corresponds to the calculation considering the deformative properties of the two-layer base and the weight of the water in the reservoir.

Under the effect of the hydrostatic load the dam jointly with the contact zone at the rock base shifted in the direction of the tailrace by an insignificant amount on the order of 4 mm. For the horizontal displacements of the sections with respect to the base (bending) the irreversible deformations in the direction of the tailrace from the hydrostatic load were summed which at the level of the dam crest amounted to 30 to 35 mm, and the periodic variation of the temperature origin were noted. Under the conditions of normal operation the relative horizontal displacements vary seasonally. During the warm part of the year the sections bent in the direction of the headrace and in the cold part of the year, in the direction of the tailrace. The magnitude of the seasonal fluctions is 15 to 18 mm, and the temperature component predominates in it. The effect of the drawdown of the reservoir on the deflection of the crest with a magnitude of the latter not exceeding 5.5 meters is insignificant (on the order of 1 mm per meter).

The Young's modulus calculated by the measured deflections of the dam, as a single structure, is $(1.5-2.0) \times 10^5$ kg-force/cm². This value which characterizes the rigidity of the structure with large numbers of horizontal inter-block joints and by comparison with other analogous dams appears to be satisfactory.

The thermal state of the dam arises from the water temperature in the reservoir, the air temperature in the expanded joints and the air temperature on the downstream face side. The complete covering of the expanded joints of the dam in the summer and their flooding to the level of the tailrace increased the temperature in the columns of the inside region and eliminated the phenomenon of annual freezing in them. The air temperature in the expanded joints varies seasonally within the limits of 4 to 5° C in the lower part to 3-10° C in the upper part. The temperature in the special cross sections of the columns of the internal region is 5 to 8° C; the center-face temperature gradients are insignificant (1-3° C). According to the data from the strain gage measurements in the lower part of the three sections of the dam the stressed state in this part is entirely satisfactory. With respect to the horizontal areas on the pressure face normal compressive stresses are retained which during the periods of seasonal minima exceed the normative 0.25γH.

In the axial cross sections of the columns of the internal region there are significant compressive stresses which increase in the intercolumnar joints and especially toward the lateral surfaces. In the latter, significant compressions are observed also with respect to the vertical areas parallel to the axis of the dam. The principal compressive stresses at the downstream face of the sections vary seasonally from 50 to 60 kg-force/cm² in the summer to 8-10 kg-force/cm² in the winter when the horizontal inter-block joints open up on the face.

The condition of the base of the first columns in the contact zone differ significantly from the plan. On the pressure face even in 1965 the rock-concrete contact joints began to open up and the process of loss of seal in the rock under the first column began with the occurrence in it of jointing

zones and individual large cracks. This condition, which presents no threats to the stability of the dam requires constant measures in the operating process with respect to maintaining the counterpressure in the base on the planned level. Beginning in 1968, under the first columns of the channel section of the dam reinforcing cementation occurs.

The condition of the pressure face basically is good. The horizontal joints are compressed. The majority of the cracks filtering into the inspection tunnels closed. A small amount of leakage is observed in the individual cracks. The total flow of water percolating through the pressure face is 15 to 20 liters per second. This water removes up to 150 to 200 mg/sec of calcium from the concrete. It is appropriate to organize inspection of the effect of this removal on the condition of the concrete and the percolation through it.

The surface cracks under longitudinal direction existing in the dam in large number were closed as the temperature gradients from the center to the face decreased, and after covering of the expanded joints the remaining small openings (0.2 to 0.3 mm) stabilized. The same thing can be said of the internal longitudinal cracks. The presence in the columns of through cracks of longitudinal direction most dangerous for the static operation of the dam was not detected; if such cracks exist their number is small, and their propagation is insignificant.

The internal local cracks in the transverse direction closed, but they had little effect on the static operation of the dam.

Part of the intercolumnar joints of the dam opening after cementation subsequently, under the effect of the hydrostatic pressure and a decrease in the temperature gradients closed completely or partially. After covering the expanded joints the openings of the intercolumnar joints stabilized with seasonal situations on the order of 0-0.1 mm having no practical significance. The intercolumnar joints reaching the downstream face of the dam where seasonal fluctuations on the order of 0.2 mm at the center of the joint and up to 0.7 mm on their edges are observed at the upper marks constitute an exception.

The condition of the intercolumnar joints, the analysis of the horizontal displacements and the stresses on both sides of the intercolumnar joints on the downstream face indicate that the dam operates as if it were monolithic.

The low-permeable diabases in the headrace jointly with the cementation curtain reduced the counterpressure on the footing of the dam to the limits of the design diagram. The increased piezometric heads observed in a number of sections are a consequence of the stress relief of the diabase under the first columns. The cementation of the base performed here in 17 sections lowers the counterpressure to the designed value, but the effect of the cementation is called short term (1 to 5 years) inasmuch as the ordinary cement flow rate does not occur into the fine and thin cracks. In 1973

colloidal solutions with plastification-active materials were used for cementation.

The stress relief of the base of the first columns has no effect on the percolation regime of the base. The percolation flow rates reaching the base through the drainage systems do not exceed [deleted] to 25 liters per second.

With respect to the set of results of the field observations it is possible to consider the state of the concrete in the dam in the constant operating regime entirely satisfactory. The state of the contact joint of the base of the first columns requires further observation and investigation for development of measures with respect to a prolonged insurance of the design value of the counterpressure.

11-2. Effect of the Technological Factors on the Monolithic Nature of the Dam

The crack formation in the dam was caused by the thermally stressed state of the concrete massifs in the process of their erection which depends on the conditions of formation of the temperature fields. The field studies that were performed indicate the decisive effect which the construction-process factors have on this formation.

Among the design measurements with respect to the control of the thermal crack formation only the structural part of them were fully performed -- the columnar sectioning into the block for pouring the concrete and decreasing the length of the blocks of the first columns in the contact zone of the dam by construction of a transverse joint. The technological process point of the design measures was only partially carried out.

The concrete in the lower part of the dam in a volume of about 2.5 million m³ was poured without performing any measures to regulate the temperature. The cooling of the concrete mix by the addition of crushed ice was used in insignificant volume. The tubular cooling of the poured concrete was carried out simultaneously in the first and second stages of the upper half of the height of the dam. Superheating in the concrete plant of the winter concrete was permitted. A significant part of the concrete was poured in 6 meter blocks and at the same time in the summer on old concrete. The pouring of the blocks had no regular nature -- both high rates and long breaks in pouring the blocks adjacent with respect to height and also in plan view were permitted. The regulation of the temperature in the inspection tunnels was not systematic. The expanded joints of the dam remained open for the entire construction period.

These deviations from the plan recommendations with respect to the regulation of the concrete temperature include the following: high maximum temperature in the blocks, large temperature gradients from the center to the face connected with intensive cooling of the open surfaces with insufficient heat protection properties of the forms, large temperature gradients between the

blocks and their base and, as a consequence, intensive crack formation. The crack formation was promoted to a defined degree by the physical-mechanical properties of the concrete: the thermicity exceeding the normative, intensive buildup and high magnitude of the Young's modulus with small relative strength in an early age, low specific extensibility in brittle nature of rupture and also significant nonuniformity.

Among the technological factors promoting the intensive crack formation it is necessary especially to note the large discontinuities in the pouring of the adjacent blocks with respect to height. As the strain gage measurements indicate, the occurrence of the internal vertical cracks in the blocks of the contact and extracontact zone is connected with the thermal regime of the long-uncovered block. The high temperature gradients vertically led to the formation of cracks both in the covered block and in the block being covered poured on a cooled (old) base. The majority of the leakage cracks on the pressure face of the dam occurred in the blocks poured on old concrete. The counterpressure of the percolation water reached a high magnitude in the horizontal joints of the first columns between the old and the fresh concrete and in practice is absent in the joints between the blocks poured with a small time interval.

The greater part of the thermal surface cracks in the blocks occurred in the first winter after pouring the concrete as a result of the supercooling of the peripheral regions of the blocks subjected directly to the effect of outside air with the formation of high temperature gradients with respect to the horizontal directions. This was promoted by significant discontinuities in the pouring of the blocks of the adjacent columns with a difference in their height exceeding the admissible amount by the design. The large temperature gradients occurring in the columns intensely poured without tubular cooling with one open face caused bending of the columns in the direction of this face with opening of intercolumnar joints and also interblock joints in the toothed couplings.

The intense cooling of the lateral surfaces of the blocks of the inside region of the dam was caused by the air temperature regime in the uncovered expanded joints of the dam. The seasonal through freezing of the columnar massifs caused by this regime while maintaining a positive temperature with respect to their longitudinal cross section for only 2 to 4 months annually to a significant degree complicated the operation with respect to monolithing the dam, giving them a seasonal nature. This combined with the absence of the measures with respect to the temperature regulation to values permitting cementation of the intercolumnar joints led to the lagging of the cementation behind the planned schedule tied with the reservoir filling regime.

11-3. Conclusions with Respect to the Problems of Planning, Design and Construction

1. The control of the thermal crack formation in the high dams built under severe climatic conditions is a complex problem of the successful solution of which depends on the correctness of the adopted sectioning of the structure into blocks to be poured in concrete and performance of the measures

corresponding to this sectioning with respect to regulating the concrete temperature.

The columnar sectioning of the Bratsk dam turned out to be entirely expedient and efficient and as a result of it, the crack formation in the dam blocks was limited to the surface cracks without the occurrence of significant through cracks. Under the conditions of weak performance of the planning measures with respect to temperature regulations the dimensions of the three-meter block of $13.8 \times 15 \text{ m}^2$ are close to limiting. The probability of crack formation in the blocks with a face length of 22 meters turned out to be close to 100%.

The experimental pouring of the concrete in long blocks carefully done under constant inspection of the scientific research organization provided no positive results. In the blocks poured in the cold part of the year and in the summer blocks with temperature regulation, in spite of the low maximum temperature of the concrete close to the design temperature, it was not possible to avoid cracks of long length. Considering all of the analogous experience at the Krasnoyarsk Hydroelectric Power Plant it is necessary to consider that with respect to the conditions of crack resistance the application of the sectional sectioning under severe climatic conditions with ordinary methods of performing the operations is inexpedient.

2. The construction of expanded joints in the dam is expedient. They reduce the volume of concrete, they decrease the counterpressure on the footing of the dam and they promote dispersion of the exothermal heat and achievement of the monolithing temperature of the dam. The submersion of the expanded joints in water provided for by the plan insures that a positive temperature will be maintained within the columns of the internal regions of the dam without artificial heating of the air in the cavities of the joints. However, leaving the expanded joints for a number of years uncovered led to great difficulties in the cementation of the intercolumnar joints and failure of the drainage system in the base of the dam during the temporary operation of the hydroelectric power plant. In addition, the cleaning out of the expanded joints to remove the construction waste that had fallen in them over a number of years require great expenditure of labor.

All of these facts must be taken into account when designing analogous dams with consideration of the possibility of constructing permanent and temporary coverings of the expanded joints at defined concrete pouring levels.

3. The Bratsk dam has been in an entirely satisfactory state during the first years of normal operation in spite of the departure from the design measures with respect to regulating the temperature of the concrete permitted during its erection. It does not follow from this that it is possible to relax the control of the thermal crack formation but the necessity for re-examination of certain of the principles used as the basis for the development of these measures arises.

During the 15 years after compiling the technical plan for the Bratsk Hydroelectric Power Plant, a number of theoretical and experimental studies were performed with respect to the problems of the formation of the temperature field and the thermally stressed state of the concrete massifs and their crack resistance. Methods of calculation have been developed using a digital computer to calculate the thermal and thermally stressed state of the concrete massifs during the process of their erection considering the basic factors, their defining factors. This combined with the results of the field observations on the dams that have been built or are under construction offers the possibility of clearly formulating the requirements on the thermal regime of the blocks for pouring the concrete and development of the set of measures with respect to regulation of it. As the foreign and Soviet experience indicates, the most universal and flexible of these measures is the tubular cooling of the poured concrete. In case of the necessity of a contact zone substantiated by the calculation, cooling of the concrete mixes must be used.

It is necessary to give special attention to establishment of the sufficient (but not excessive) heat protective properties of the forms in order to limit the temperature gradients in the blocks and the intensity of the cooling of their peripheral zones. It is just as important to insure regular pouring of adjacent stages of the concrete with the designation of their height or times of covering depending on the planned dimensions of the blocks and the temperature conditions. The plan measures must include the regulation of the temperature in the inspection tunnels of the dam. At the Bratsk dam 40% of all of the cracks in the dam are associated with these tunnels.

The progress in the matter of controlling crack formation can be achieved only when departures from the plan measures with respect to temperature control are not permitted in the construction process.

4. The calculation of the strength of the gravity dam by the formulas of extracentral compression without considering the joint operation of the dam with the base does not reflect the effective stressed state of the contact zone of the structure. In connection with the opening of the contact joints and the stress relief of the rock base of the first columns of the Bratsk dam for the latter and also for the Ust'-Ilim dam a number of calculational and experimental studies were performed. It is established that when considering the properties of the base, the percolation forces of the weight of the water in the reservoir in the contact cross section on the pressure face significant tensile stresses occur which predetermine the opening of the contact joints and are propagated into the depths of the base.

For the design of high gravity dams it is necessary to establish the necessity and nature of the structural measures in the vicinity of the base of the pressure face.

5. The important role of the thermal effect on the stressed state of the dams is at the present time undisputed. For consideration of these effects in the planning practice, further development of the methods of quantitative evaluation of the these effects is needed: the thermal state and opening of

the joints on the downstream face, the thermal state of the cavities of the expended joints and the thermal reduction of the pressure face. The measures with respect to increasing this reduction [102] must be coordinated with the requirements with respect to insuring crack resistance of the concrete. When considering the thermal effects, the variations in the physical mechanical properties of the concrete of the structures at negative temperature must be taken into account.

6. The characteristic conditions for cementation of the intercolumnar joints of the dam were their small openings on the average amounting to 1 mm (1.2 mm on the Krasnoyarsk dam). The cementation in part of the cards was performed at the concrete temperature significantly exceeding the admissible value, and they then opened. This in combination with the disturbances of the process of the impossibility of the system and other causes reduce the effectiveness of cementation to a value of on the order of 50%. The cementation significantly lagged behind the water level on filling the reservoir, especially in the dam of the first stage.

In order to increase the opening of the joints and the cementation efficiency it follows to:

- a) Increase the length of the blocks;
- b) Permit the maximum possible concrete temperature in accordance with the crack resistance conditions;
- c) Not permit prolonged breaks between the pouring of the blocks on both sides of the cementation cards;
- d) Not perform the cementation at a temperature essentially exceeding the admissible;
- e) For small openings of the joints to apply special mortars with greater penetrating capacity than in the ordinary ones;
- f) In case of the possibility of freezing of the blocks provide for electric heating of the concrete near the joints;
- g) When the cementation operations lag behind the level of filling of the reservoir, the cementation must be carried out on every other card, with cementation of the skip cards in the second round in case of necessity.

11-4. Conclusions with Respect to Procedural Problems

1. Since the beginning of installation of the remote instruments in the Bratsk dam 15 years have gone by. Part of the instruments in the concrete of the first columns and also in the concrete and rock of the contact zone have been under the effects of water percolating under the head of up to 100 meters for 13 years. The fact that more than 80% of the total number of instruments have been preserved indicates the satisfactory and sufficiently reliable (with small exceptions) construction of the instruments, the type of

cable and the methods of joining it used. The conservation of the instruments in the Bratsk dam turned out to be higher than for the same instruments in the Bukhtarma, the Ladzhanurskaya, Krasnoyarsk and Ust'-Ilim dams. This indicates the more expedient organization of work with respect to preparation and installation of the instruments in the Bratsk dam.

2. Experience in operating and maintaining the dam permits us to estimate the correspondence of the established system of measuring and control equipment to the requirements of the operation and maintenance control. The total number of remote instruments, although providing very valuable information, exceeds the requirements for this control and the possibilities of the hydraulics shop with respect to processing and analyzing the operation data. In addition, the number of instruments at the locations most important for the operating inspection -- the pressure face and the downstream face -- is insufficient. This is explained by the fact that in the planning of the placement of the measuring and control equipment in the dam (just as in other plans for measuring and control equipment compiled by the VNIIG Institute) the problem of the operating control instruments was not specially considered.

Beginning with this fact, when planning the placement of the measuring instruments in a high gravity dam it is recommended first of all that the instruments be especially isolated for dealing with the problems of operating control of the strength and stability of the structure. These problems must be considered to include observations of the following:

- a) The overall displacements;
- b) The percolation counterpressure in the base;
- c) The thermal regime of the dam;
- d) The primary stresses on the pressure face at a sufficient number of points with respect to height of the profile and also in the concrete and in the rock of the contact zone. Special attention must be given to the region of contact of the pressure base with the base;
- e) The deformations of the horizontal interblock joints on the pressure face, including the joint at the contact with the base and also in the horizontal joints on the downstream face;
- f) The principal stresses at the downstream face;
- g) The state of the intercolumnar joints with placement of the crevice gages normally to the areas of the toothed couplings oriented with respect to the trajectory of the principal compressive stresses.

The groups of instruments for the observations according to items c-f must be placed in 25% of the sections of the dam.

AD-A039 541 COLD REGIONS RESEARCH AND ENGINEERING LAB HANOVER N H F/G 13/13
FIELD STUDIES OF THE CONCRETE DAM AT THE BRATSK HYDROELECTRIC P--ETC(U)
APR 77 S Y EIDELMAN

UNCLASSIFIED

CRREL-TL-621

NL

4 OF 4
AD
A039541

END

DATE
FILMED
6-77

3. The field observations during the construction period have as their purpose the control of the effective measures with respect to regulating the temperature and the process of performing the concrete operations. These observations (the temperature regime, the thermally stressed state, crack formation) have a temporary nature, and the results depend on a number of construction-technological factors. Therefore, they must be organized so that the role of these factors cannot be clearly discovered. In the majority of cases such studies are expediently performed in individual blocks for which it is easier to insure the required temperature regime and boundary conditions. The placement of the instruments for observations of the construction control is carried out locally and by the course of the operations.

4. The observations of the settling of the dam and the absolute horizontal displacements of it must be carried out in all sections and, in addition, along the shore part of the reservoir within the limits of the subsidence crater. It is necessary to encompass 20 to 25% of the sections by the observations of the relative horizontal displacements of the sections using the direct plumbs in the part of the dam next to rock and the direct plumbs in the upper part.

The experience in the application of the sectional-optical method of measuring the horizontal displacements on the Bratsk dam indicates its inexpediency for all cases where the optical observations must be performed under the conditions of the unstable temperature regime. The string-optical instruments are simple and reliable.

In addition to the direct and indirect plumbs it is necessary to use the shear gages, the long based deformation meters and other devices for determination of the vertical displacements with respect to the various layers of the base. The anchors for the indirect plumbs must be placed at a number of levels of the rock and must reach a depth which is sufficient for determining the active zone of the base of the dam. When measuring the deformations of the rock in the contact zone it is expedient to use the long base remote strain gages with determination of the location of their deformation modulus of the rock using stamps or indentation meters.

5. In the design of the dam provision must be made for a special tunnel along the first columns (the monitoring and measuring equipment tunnel) in which during the construction period all of the observations (piezometric, geodetic) and the reading by remote instruments must be concentrated.

For the temporary commutation panels special closed niches must be built. In the monitoring and measuring equipment tunnel there must be structural mechanisms and equipment and all kinds of communications. The through passage along the tunnel during the construction period must be closed.

For operating observations in the plan there must be provision for the device for remote readings located in a special facility. It is necessary to investigate the possibility of increasing the reliability of the remote switches for placement of them directly in the blocks by which up to 80 to 90% of the cable can be saved and the labor consumption of the readings decreased.

6. The determination of the physical-mechanical properties of the concrete on the laboratory moisture insulated samples gives a general determination of the nature of the investigated properties of the concrete and their variation with time. As a result of the difference from the natural conditions of hardening and the temperature regime of the laboratory samples the results of testing them are approximate.

In order to improve the procedure for determining the physical-mechanical properties of the concrete it is expedient to practice the following:

- a) A significant increase in dimensions of the transverse cross section of the sample;
- b) Maintenance in the laboratory samples of a heat and moisture regime as analogous as possible to the concrete regime at the investigated point of the structure;
- c) Determination of the deformative properties of the concrete directly in the structure by statistical tests and also ultrasonic methods;
- d) Determination of the coefficients of stress relaxation by direct measurement with simultaneous study of the creep characteristics of the concrete as needed;
- e) Measurement of the limiting extensibility of the concrete with determination of its plastic part by laboratory tests and also determination under natural conditions of the limiting extensibility as a function of the deformation gradients.

7. The tensometric method is up to not the only universal means of studying the nature of the occurrence and the development of the stresses in the concrete blocks. As a result of the conditionality of the characteristics of deformativeness of the concrete obtained by testing the laboratory samples, to one degree or another the stresses that are calculated by the measured deformations are provisional, which, however, does not decrease their great scientific and practical significance.

With a large number of tensometric groups and many years of observations the very difficult calculations of the stresses by the measured deformations in practice are possible only using a digital computer. With their help a determination can be made of the component displacements and stresses entering the construction period.

8. It is necessary to introduce dynamometers into the practice of our field investigations for direct measurement of the compressive stresses in the concrete (of the Karlson dynamometer type) especially convenient for operational control of the stresses with respect to the principal areas of the space of the dam. The parallel use of these dynamometers and the tensometric measurements is a means of controlling the accuracy of the latter and establishing the effect of the concrete creep.

9. Special attention must be given to the work of the toothed couplings of the intercolumnar joints. The study of the openings of the latter especially with respect to the areas of the main compressive stresses has great significance not only from the point of view of establishing the relation between the variations of the openings and the temperature but also as an objective means of monitoring the quality and the efficiency of cementation and also establish the force interaction between the adjacent columns. Therefore, for the toothed couplings it is necessary also to install the strain gage rosettes for determining the magnitude and nature of variation of the normal and tangential stresses.

During the cementation of the intercolumnar joints it is recommended that the pressure of the cementation mortar in the plane of the joints be measured using remote dynamometers.

10. The plan for the arrangement of the measuring instruments in the devices in a large concrete dam must be compiled in accordance with the general program of the field investigations developed on the basis of the design materials, static calculations, the model investigation data and the plan for the performance of the concrete operations.

In the general program the field studies and observations of different purpose must be tied together, and the required accompanying experimental studies and tests with them are planned to encompass all problems of the operation of the structure. In the program it is necessary to provide for the organization form of the field studies.

11. The operating experience of the group (the groups and sections) with respect to installation of monitoring and measuring equipment organized for the construction administrations cannot be called successful. Without constant guidance by a qualified co-worker of the Scientific Research Institute these groups do not insure the required quality of the installation of the monitoring and measuring equipment.

The problem of the form of organization of the operations with respect to installation of the monitoring and measuring equipment at the construction sites requires reexamination.

It is possible that it is expedient to transfer the performance of these operations to the specialized installation organization.

BIBLIOGRAPHY

1. M. N. Levitskiy, "Plan for the Bratsk Hydroelectric Power Plant on the Angara River," HYDROENGINEERING CONSTRUCTION, No 2, 1962, pp 1-8.
2. R. R. Tizdel', "Engineering-Geological Conditions of the Construction of the Bratsk Hydroelectric Power Plant," HYDROENGINEERING CONSTRUCTION, No 2, 1962, pp 8-14.
3. P. D. Yevdokimov, D. D. Sapgin, STRENGTH, RESISTANCE TO SHEAR AND DE- FORMATIONS OF THE FOUNDATIONS OF STRUCTURES ON ROCK, Moscow-Leningrad, Energiya Press, 1964, 169 pages with illustrations.
4. N. A. Ogorodnikov, "Concrete Dams of the Bratsk Hydroelectric Power Plant," HYDROENGINEERING CONSTRUCTION, No 4, 1962, pp 1-7.
5. BRATSK HYDROELECTRIC POWER PLANT IMENI 50TH ANNIVERSARY OF THE GREAT OCTOBER REVOLUTION, TECHNICAL REPORT ON THE PLANNING, DESIGN AND CON-STRUCTION, VOL 1, BASIC STRUCTURES, DRAWING COLLECTION, Moscow, Energiya Press, 1970, 68 pages.
6. I. P. Denisov, EXPERIENCE IN ERECTING A CONCRETE CHANNEL DAM WITH TOOTHING ON THE BRATSK HYDROELECTRIC POWER PLANT, Moscow, Informenergo, 1971, 55 pp with illustrations.
7. A. M. Gindin, "Organization of Concrete Work on the Construction of the Bratsk Hydroelectric Power Plant," CONCRETE OPERATIONS TECHNOLOGY IN THE CONSTRUCTION OF HYDROELECTRIC POWER PLANTS, Moscow-Leningrad, Gosenergoizdat Press, 1962, pp 29-39.
8. K. V. Alekseyev, "Hydroengineering Concrete of the Dam at the Bratsk Hydroelectric Power Plant," HYDROENGINEERING CONSTRUCTION, No 12, 1962, pp 13-18.
9. G. L. Gershmanovich, "Winter Grading of Fillers at the Bratskgesstroy Trust," HYDROENGINEERING CONSTRUCTION, No 2, 1963, pp 10-16.
10. K. V. Alekseyev, "Design Requirements on the Concrete at the Bratsk Dam considering the Crack Resistance of the Concrete and Comparison of them with the Natural Observation Data," COLLECTION OF REPORTS FROM THE MEETING ON THE CONSTRUCTION OF HIGH CONCRETE DAMS ON A ROCK FOUNDATION, GPKEIE Press, 1964, 16 pp.
11. V. A. Terant'yev, S. K. Akhran, "Performance of Concrete Operation in the Construction of the Bratsk Hydroelectric Power Plant," HYDROENGINEER-ING CONSTRUCTION, No 11, 1962, pp 5-12.
12. INSTRUCTIONS FOR THE PLANNING AND DESIGN OF THE COMPOSITION OF HYDRO- ENGINEERING CONCRETE, GPKEIE Institute Press, Glavniiproekt Institute, Moscow, Gosenergoizdat Press, 1963, 83 pp.

13. K. V. Alekseyev, "Some Preliminary Results of Testing the Design and Pouring of the Concrete for the Bratsk Hydroelectric Power Plant Dam," HYDROENGINEERING CONSTRUCTION, No 1, 1964, pp 11-16.
14. Ye. S. Baranos, A. N. Meshcheryakov, "Monolithing Concrete Dams," HYDROENGINEERING CONSTRUCTION, No 12, 1964, pp 1-4.
15. B. F. Fomin, "The Flow Chart for Performing the Operations of Cementing the Construction Joints of the Bratsk Hydroelectric Power Plant Dam," MATERIAL FROM THE CONFERENCE ON THE CONSTRUCTION OF HIGH CONCRETE DAMS ON A ROCK FOUNDATION, GPKEIE Institute, 1964, 12 pp.
16. K. A. Knyazev, V. N. Sinitzin, "From the Experience in Operating the Bratsk Hydroelectric Power Plant imeni 50th Anniversary of the Great October," HYDROENGINEERING CONSTRUCTION, No 3, 1971, pp 3-6.
17. M. S. Murav'yev, "Observation by Geodetic Methods of the Shifts of the Hydroengineering Structures with Respect to Their Base," NEWS OF THE INSTITUTION OF HIGHER LEARNING. SECTION 4, GEODETICS AND AERIAL PHOTOGRAPHIC SURVEYING, No 5, 1968.
18. S. Ya. Eydel'man, FIELD STUDIES OF CONCRETE HYDROENGINEERING STRUCTURES, Gosenergoizdat Press, 1960, 210 pp with illustrations.
19. S. Ya. Eydel'man, FIELD STUDIES OF THE BRATSK HYDROELECTRIC POWER PLANT DAM, Leningrad, Energiya Press, 1968, 255 pp with illustrations.
20. S. Ya. Eydel'man, Z. I. Solov'yeva, "Observations of the Operating Section as the Concrete Dam of the Bratsk Hydroelectric Power Plant," NEWS OF THE ALL UNION SCIENTIFIC RESEARCH INSTITUTE OF HYDRAULIC ENGINEERING, Vol 100, 1972, pp 270-291.
21. S. Ya. Eydel'man, "Construction of Devices for Studying Hydroengineering Structures," ANNOTATIONS OF SCIENTIFIC RESEARCH WORK COMPLETED IN 1959 ON HYDROENGINEERING, Leningrad, Gosenergoizdat, 1960, pp 54-55.
22. S. Ya. Eydel'man, "Processing and Analysis of the Materials from Observations by the Monitoring and Measuring Equipment installed in the Concrete Structures of the Kakhovskiy Hydroengineering Combines," ANNOTATIONS OF SCIENTIFIC RESEARCH WORK ON HYDRAULIC ENGINEERING, Leningrad, Gosenergoizdat, 1960, pp 86-88.
23. S. Ya. Eydel'man, "Field Studies of the Normal Stresses in the Footing of Concrete Hydroengineering Structures of the Kakhovskiy and Novosibirsk Hydroengineering Complexes," WORKS OF THE COORDINATION CONFERENCES ON HYDRAULIC ENGINEERING, No III, 1962, pp 84-104.
24. J. Bolf, Z. Cermak, L. Mejzlik, P. Marcan, O. Tavoda, NEW METHODS OF FIELD MEASUREMENTS, Slovenska Akademia vied Bratislava, 1959.

25. S. Ya. Eydel'man, TECHNICAL SPECIFICATIONS WITH RESPECT TO INSTALLING THE MEASURING AND MONITORING INSTRUMENTS IN CONCRETE HYDROENGINEERING STRUCTURES, THE PERFORMANCE OF READINGS AND PRIMARY PROCESSING OF (PLAN), Leningrad, Energiya Press, 1964, 124 pp with illustrations.
26. A. G. Levelev, "Development and Introduction of Reliable Methods of Field Studies and the Monitoring of the State of the High Head Hydro-engineering Structures," SCIENTIFIC RESEARCH ON HYDRAULIC ENGINEERING IN 1970, Leningrad, Energiya Press, 1971, pp 158-160.
27. K. A. Mal'tsov, A. M. Arkhipov, I. B. Sokolov, P. G. Staritskiy, "Effect of Water on the Strength of Concrete," REPORTS OF THE USSR ACADEMY OF SCIENCES, Vol 125, No 2, 1959, pp 359-362.
28. V. V. Stol'nikov, A. S. Gubar', V. B. Sudakov, "Effect of the Age of the Hydroengineering Concrete on the Basic Properties," NEWS OF THE ALL UNION SCIENTIFIC RESEARCH INSTITUTE OF HYDRAULIC ENGINEERING, Vol 64, 1960, pp 55-65.
29. V. V. Stol'nikov, V. P. Sudakov, "Problem of Determining the Tensile Strength of Concrete," NEWS OF THE ALL UNION SCIENTIFIC RESEARCH INSTITUTE OF HYDRAULIC ENGINEERING, Vol 60, 158, pp 55-66.
30. B. G. Skramtayev, M. YU. Leshchinskiy, STRENGTH TESTING OF CONCRETE IN SAMPLES, PRODUCTS AND STRUCTURES, Moscow, Gosstroyizdat Press, 1964, 176 pp with illustrations.
31. Ts. G. Ginzburg, D. F. Yershov, "Analysis and Comparison of the Design and Actual Data on the Concrete of the Bratsk Hydroelectric Power Plant Dam," MATERIALS FROM THE CONFERENCE ON THE CONSTRUCTION OF HIGH CONCRETE DAMS ON A ROCK FOUNDATION, GPKEIE Institute, 1964, 16 pp with illus.
32. A. V. Shvetsov, "Approximate Method of Determining the Natural Stresses in Concrete Considering the Variability of its Deformative Properties," HYDROENGINEERING CONSTRUCTION, No 8, 1952, pp 23-27.
33. N. N. Chalyy, "Practical Methods of Calculating the Stress in the Concrete by the Measured Deformations," WORKS OF THE COORDINATION CONFERENCES ON HYDROENGINEERING, No 49, 1969, pp 42-60.
34. P. I. Vasil'yev, "Approximate Method of Considering the Creep Deformations of Determining the Thermal Stresses in Concrete Massive Slabs," NEWS OF THE ALL UNION SCIENTIFIC RESEARCH INSTITUTE OF HYDRAULIC ENGINEERING, Vol 47, 1952, pp 120-128.
35. V. V. Stol'nikov, V. B. Sudakov, "Adiabatic Calorimeter of the All-Union Scientific Research of Hydraulic Engineering," NEWS OF THE ALL UNION SCIENTIFIC RESEARCH INSTITUTE OF HYDRAULIC ENGINEERING, Vo 79, 1965, pp 71-79.

36. I. D. Zaporozhets, S. D. Okorokov, A. A. Pariyskiy, HEAT GENERATION OF CONCRETE, Leningrad-Moscow, Stroyizdat Press, 1966, 314 pp with illus.
37. L. P. Trapeznikov, "Determination of the Heat Generation Characteristics of the Concrete of Bratsk Dam by the Data from the Field Observations," WORKS OF THE COORDINATION CONFERENCES ON HYDRAULIC ENGINEERING, No 29, 1966, pp 106-113.
38. G. M. Makedonskiy, S. Ya. Eydel'man, "Pouring the Concrete for Experimental Long Blocks in the Construction of the Bratsk Hydroelectric Power Plant," MATERIALS FROM THE CONFERENCE ON THE CONSTRUCTION OF HIGH CONCRETE DAMS ON A ROCK FOUNDATION, GPKEIE Institute, 1964, [deleted].
39. V. I. Dubintskiy, "Thermophysical Characteristics of the Concrete of the Experimental Sections of the Bratsk Hydroelectric Power Plant Dam," HYDROENGINEERING CONSTRUCTION, No 2, 1963, pp 17-18.
40. Sh. N. Plat, A. S. Kats, "Experimental Study of the Strength and Deformative Characteristics of Concrete at a Negative Temperature," NEWS OF THE ALL UNION SCIENTIFIC RESEARCH INSTITUTE OF HYDRAULIC ENGINEERING, Vol 83, 197, pp 180-194.
41. A. Kats, "Study of the Deformative and Strength Properties of Concrete at Negative Temperature," Author's Review of Dissertation in Defense of the Scientific Degree of Candidate of Technical Sciences, All Union Scientific Research Institute of Hydraulic Engineering, 1969, 40 pp
42. V. M. Moskvin, M. M. Kapkin, B. M. Mazur, A. M. Podval'nyy, STRENGTH OF CONCRETE AND REINFORCED CONCRETE AT NEGATIVE TEMPERATURE, Moscow, Stroyizdat Press, 1967.
43. V. V. Stol'nikov, THEORETICAL PRINCIPLES OF THE RESISTANCE OF CEMENT ROCK AND CONCRETE TO ALTERNATING CYCLES OF FREEZING AND MELTING, Leningrad, Energiya Press, 1970, 67 pp with illus.
44. V. N. Durcheva, "Field Studies of the Free Thermal Deformations of Concrete in the Blocks of the Bratsk Hydroelectric Power Plant Dam under the Prolonged Effect of Negative Temperatures," HYDROENGINEERING STRUCTURE, No 6, 1967, pp 28-33.
45. S. Ya. Eydel'man, V. N. Durcheva, "Effect of the Negative Temperature on the Young's Modulus of the Concrete," NEWS OF THE ALL UNION SCIENTIFIC RESEARCH INSTITUTE OF HYDRAULIC ENGINEERING, Vol 88, 1969, pp 279-286.
46. S. Ya. Eydel'man, V. N. Durcheva, "Young's Modulus of Concrete using Gravel and Crushed Rock for Negative Temperatures," NEWS OF THE ALL UNION SCIENTIFIC RESEARCH INSTITUTE OF HYDRAULIC ENGINEERING, Vol 96, 1971, pp 182-190.

47. V. I. Durcheva, "Effect of Negative Temperature on the Deformation of the Loaded Concrete," NEWS OF THE ALL UNION SCIENTIFIC RESEARCH INSTITUTE OF HYDRAULIC ENGINEERING, Vol 103, 1973, pp 216-220.
48. M. I. Leantskiy, "Design for the Bratsk Hydroelectric Power Plant and Requirements for the Dam Concrete," CONCRETE OPERATIONS TECHNOLOGY IN THE CONSTRUCTION OF HYDROELECTRIC POWER PLANTS, Moscow-Leningrad, Gosenergoizdat Press, 1962, pp 18-29.
49. Ye. N. Terent'yev, "Methods of Regulating the Properties of the Concrete in Order to Increase its Crack Resistance Adopted in the Design for the Bratsk Hydroelectric Power Plant and their Practical Implementation," SCIENTIFIC AND TECHNICAL CONFERENCE ON THE INVESTIGATION OF THE PROPERTIES OF THE CONCRETE DETERMINING ITS CRACK RESISTANCE IN MASSIVE HYDROENGINEERING STRUCTURES, NTOEP, Leningrad, Gosenergoizdat Press, 1963, pp 29-32.
50. K. I. Chikvandze, "Application of Ice for Cooling a Concrete Mix," HYDROENGINEERING CONSTRUCTION, No 10, 1964, pp 16-18.
51. B. V. Pospelov, "Crack Formation in the Concrete Dam of the Bratsk Hydroelectric Power Plant and Its Basic Causes," CONFERENCE ON THE CONSTRUCTION OF HIGH CONCRETE DAMS ON A ROCK FOUNDATION, GKEIE Institute, 1964, 398 pp with illus.
52. P. I. Vasil'yev, Yu. I. Kolonov, THERMAL STRESSES IN CONCRETE BLOCKS, LPI Institute imeni Kalin Press, 1969, 120 pp with illus.
53. A. M. Tsybin, "Study of the Thermal and Thermally Stressed State of Concrete Hydroengineering Structures with Cavities (Massive-Counterforce Dam, Dam with Expanded Joints)," AUTHOR'S REVIEW OF DISSERTATION IN DEFENSE OF THE SCIENTIFIC DEGREE OF CANDIDATE OF TECHNICAL SCIENCES, ALL UNION SCIENTIFIC RESEARCH INSTITUTE OF HYDRAULIC ENGINEERING, Leningrad, 1970, 36 pp.
54. R. M. Rapport, "Boussinesque Problems for a Layered Electric Halfplane," WORKS OF THE LGI INSTITUTE, 1948.
55. R. R. Tizdel', "Engineering-Geological Conditions of the Concrete Dam of the Bratsk Hydroelectric Power Plant," COLLECTION OF WORKS FROM THE CONFERENCE ON THE CONSTRUCTION OF HIGH DAMS ON THE ROCK FOUNDATION, GKEIE Institute, 1964, 21 pp.
56. R. R. Tizdel', "Settling of the Rock Foundation of the Bratsk Hydroelectric Power Plant," HYDROENGINEERING CONSTRUCTION, No 9, pp 18-19.
57. A. W. Simons, J. T. Richardson, "Observed Structural Performance of Large Concrete Dams of the Bureau of Reclamations," VI CONGRESS ON LARGE DAMS, Q. 21, R. 122, New York, 1958, p 33.
58. "Present Status of Measurement of Structural Behavior of Dams in Japan," THE VI CONGRESS ON LARGE DAMS, Q. 21, R. 25, New York, 1958, p 57.

59. M. B. Ginzburg, "Measurement of the Deflections, Settling and Displacements of Dams," PLANNING, DESIGN AND CONSTRUCTION OF LARGE DAMS, Moscow-Leningrad, Gosenergoizdat Press, 1962, pp 290-352.
60. S. A. Frid, THERMAL STRESSES IN CONCRETE AND REINFORCED CONCRETE STRUCTURAL ELEMENTS OF HYDROENGINEERING STRUCTURES, Moscow-Leningrad, Gosenergoizdat Press, 1959, 72 pp with illus.
61. S. Ya. Eydel'man, "Field Study of the Thermal Regime, Deformations and Stresses in the Bratsk Hydroelectric Power Plant Dam," MATERIALS OF THE CONFERENCE ON THE CONSTRUCTION OF HIGH DAMS ON A ROCK FOUNDATION, GPKEIE, 1964, 55 pp with illus.
62. S. Ya. Eydel'man, "Some Results of the Field Studies of the Static Operation of the Bratsk Hydroelectric Power Plant Dam," HYDROENGINEERING CONSTRUCTION, No 10, 1964, pp 21-28.
63. N. P. Zhuravlev, V. N. Sholin, "Some Factors Influencing the Settling of the Foundation of the Bratsk Hydroelectric Power Plant," HYDROENGINEERING CONSTRUCTION, No 5, 1966, pp 6-9.
64. B. N. Barshevskiy, "Comparison of the Results of Calculating the Settling of the Bratsk Hydroelectric Power Plant Dam with the Field Observation Data," NEWS OF THE ALL UNION SCIENTIFIC RESEARCH INSTITUTE OF HYDRAULIC ENGINEERING, 1968, Vol 87, pp 323-324.
65. S. Spagnoletti, "Un decennio di osservazioni alla diga di Morasco," L'ENERGIA ELETTRICA, No 2, 1960, pp 99-138.
66. S. Spagnoletti, "Sui comportamento di un tipo di diga a gravi alleggerita elementi cavi. I-II Comportamento teorico," L'ENERGIA ELETTRICA, No 10, 1960, pp 877-907.
67. V. N. Durcheva, "Effect of a Negative Temperature in the Concrete on the Nature of Operation of a High Concrete Dam," HYDROENGINEERING CONSTRUCTION, No 3, 1973, pp 26-29.
68. S. Ya. Eydel'man, "Study of the Deformation of Stresses in Concrete Dams," PLANNING, DESIGNING AND CONSTRUCTION OF LARGE DAMS ACCORDING TO THE MATERIALS OF THE VI INTERNATIONAL CONGRESS OF ON LARGE DAMS, Moscow-Leningrad, Gossenergoizdat, 1962, pp 175-260.
69. A. F. Silveira, J. O. Da Pedro, QUANTITATIVE INTERPRETATION OF THE RESULTS OBTAINED IN THE OBSERVATION OF CONCRETE DAMS, Laboratorio de Engenharia Civil, Lisbon, 1965.
70. A. Marzia, "Analisi statistiche sul comportamento di una grande diga nei primi dell'esercizio," L'ENERGIA ELETTRICA, No 4, 1965.
71. R. Widmann, "Evaluation of Deformation Measurements Performed on Concrete Dams," IX CONGRESS ON LARGE DAMS, Q. 34, R. 38.

72. S. Leliavsky, "Gravity Dam Deflections," THE ENGINEER, July 9, 1954, pp 41-45.
73. S. P. Timoshenko, ELASTICITY THEORY, ONTI Institute, 1927, 451 pp.
74. N. S. Rozanov, "Statement of Model Studies of the Thermal Stresses in Cooling Blocks," NEWS OF THE ALL UNION SCIENTIFIC RESEARCH INSTITUTE OF HYDRAULIC ENGINEERING, Vol 73, 1963, pp 173-192.
75. P. I. Vasil'yev, Yu. I. Kononov, "Effect of the Temperature of Hardening on the Growth of the Modulus of the Instantaneous Deformations of Concrete," NEWS OF THE ALL UNION SCIENTIFIC RESEARCH INSTITUTE OF HYDRAULIC ENGINEERING, Vol 75, 1964, pp 123-142.
76. S. Ya. Eydel'man, "Determination of the Elasticity and Creep Characteristics of Concrete in Structures," HYDROENGINEERING CONSTRUCTION, No 5, 1952, pp 12-16.
77. S. Ya. Eydel'man, "From the Experience of the Field Studies of Concrete Hydroengineering Structures at Hydroelectric Power Plants," MATERIALS FROM THE SYMPOSIUM ON EXPERIMENTAL STUDIES OF ENGINEERING STRUCTURES, LOSNTO, No 11, 1965, pp [deleted].
78. [deleted] Snjat [remainder of last name deleted], "Measurements of Strains and Stresses inside Cementation Materials," PROCEEDINGS OF THE CONFERENCE ON EXPERIMENTAL METHODS OF INVESTIGATING STRESS AND STRAINS IN STRUCTURE, Prague, October 5-8, 1965, Part I.
79. M. Rocha, IN SITU STRAIN AND STRESS MEASUREMENTS. STRESS ANALYSIS, RECENT DEVELOPMENT IN NUMERICAL AND EXPERIMENTAL METHODS, John Wiley & Sons, Ltd, London, New York, Sydney, 1965.
80. N. N. Chalyy, "Preliminary Results of Setting the Effect of the Base in the Rigidity of the Installed Strain Gages on the Accuracy of the Measurement of the Concrete Deformations," WORKS OF THE COORDINATION CONFERENCE ON HYDRAULIC ENGINEERING, No 49, 1969, pp 68-81.
81. S. Ya. Eydel'man, "Study of the Static Operation of Hydroengineering Structures, Bases and Foundations, Testing and Study of the Properties of Construction Materials (General Report and Conclusions)," WORKS OF THE SYMPOSIUM. EXPERIMENTAL STUDIES OF STRUCTURES, Leningrad, Energiya Press, 1967, pp 87-115 and 239-246.
82. Sh. N. Plyat, L. B. Sapozhnikov, "Calculations on a Digital Computer of a Thermal Field of Concrete Massifs in the Erection State," NEWS OF THE ALL UNION SCIENTIFIC RESEARCH INSTITUTE OF HYDRAULIC ENGINEERING, Vol 79, 1965, pp 113-126.
83. Sh. N. Plyat, N. Ya. Sheynker, T. T. Ovsinikova, "Development of the Method of Calculating the Thermally stressed State of Concrete Massifs in the Construction Period," SCIENTIFIC STUDIES OF HYDRAULIC ENGINEERING IN 1970, Leningrad, Energiya Press, 1971, pp 30-32.

84. K. I. Dzuba, "Development of the Method and Programs for Calculating the Thermally Stressed State of Dams," SCIENTIFIC STUDIES OF HYDRAULIC ENGINEERING IN 1970, Leningrad, Energiya Press, 1971, pp 56-57.
85. A. V. Shvetsov, M. S. Lamkin, "Development of Practical Methods of Calculating the Stress-Strained State of Dams for Various Methods of Erecting Them including Dams with Preliminary Reduction of the Pressure Face," TECHNICAL REPORT OF THE ALL UNION SCIENTIFIC RESEARCH INSTITUTE OF HYDRAULIC ENGINEERING, State Registration No 71064718, Leningrad, 1973, 56 pp with illus.
86. V. G. Orekhov, A. M. Medovikov, B. I. Konzli, "Planning of Design of Instruments for Measuring Stresses in a Concrete Dam," WORKS OF THE MOSCOW CONSTRUCTION ENGINEERING INSTITUTE, Moscow, No 29, 1958.
87. TEMPORARY INSTRUCTIONS FOR INSURING MONOLITHIC NATURE OF CONCRETE HYDRO-ENGINEERING STRUCTURES ERECTED IN AREAS WITH SHARPLY CONTINENTAL CLIMATE, Moscow-Leningrad, Energiya Press, 1964, 71 pp.
88. A. A. Khrapkov, "Some Results of the Static Calculation of Individual Types of Structures on the Ural-2 Digital Computer," NEWS OF THE ALL UNION SCIENTIFIC RESEARCH INSTITUTE OF HYDRAULIC ENGINEERING, Vol 81, 1966, pp 155-169.
89. L. P. Trapeznikov, L. A. Ugol'nikov, "Thermal Stresses in Concrete Blocks on a Concrete Base," NEWS OF THE ALL UNION SCIENTIFIC RESEARCH INSTITUTE OF HYDRAULIC ENGINEERING, Vol 92, 1969, pp 105-124.
90. Ye. L. Budnikov, "Some Results of Field Studies in the Construction of the Mamakanskaya Hydroelectric Power Plant," MATERIALS ON THE CONFERENCE ON THE CONSTRUCTION OF HIGH DAMS ON THE ROCK FOUNDATION, GPKEIE Institute, 1964, 21 pp.
91. L. P. Trapeznikov, "Study of the Thermal and Destressed State of Concrete Massifs of Hydroengineering Structures," AUTHOR'S REVIEW OF DISSERTATION IN DEFENSE OF THE SCIENTIFIC DEGREE OF CANDIDATE OF TECHNICAL SCIENCES, ALL UNION SCIENTIFIC RESEARCH INSTITUTE OF HYDRAULIC ENGINEERING, 1971, 26 pp.
92. B. K. Frolov, "Experience of the Land Improvement Office of the United States of America in Planning Measures to Prevent Crack Formation in Massive Concrete Structures," HYDROENGINEERING CONSTRUCTION, No 10, 1966, pp 52-56.
93. P. I. Vasil'yev, "Determinations of the Spacing Between the Thermal Joints in Concrete Dams," NEWS OF THE ALL UNION SCIENTIFIC RESEARCH INSTITUTE OF HYDRAULIC ENGINEERING, Vol 64, 190, pp 33-54.
94. S. Ya. Eydel'man, G. M. Madomskiy, "Thermally Stressed State of Experimental Data of the Blocks of the Bratsk Hydroelectric Power Plant Dam in the Construction Period," HYDROENGINEERING CONSTRUCTION, No 5, 1968, pp 17-23.

95. N. S. Rozanov, "Procedure for Studying the Effect of Vertical Construction Joints on the Stressed State of the Massive Concrete Dams," NEWS OF THE ALL UNION SCIENTIFIC RESEARCH INSTITUTE OF HYDRAULIC ENGINEERING, Vol 71, 1962, pp 133-160 with illus.
96. N. S. Rozanov, V. N. Makrushin, "Study of the Effect of the Uncemented Joints on the Stressed State of the Concrete at the Bratsk Hydroelectric Power Plant," NEWS OF THE ALL UNION SCIENTIFIC RESEARCH INSTITUTE OF HYDRAULIC ENGINEERING, Vol 76, 1964, pp 43-54.
97. G. L. Khesin, V. N. Sevast'yanov, N. N. Kuz'mina, "Effect of Crack Formation on the Stressed State of the Gravity Dams with Expanded Joints," WORKS OF THE MOSCOW INSTITUTE OF CONSTRUCTION ENGINEERS, No 40, 1962, pp 109-118.
98. N. I. Chalyy, "Basic Results of the Four-Year Observations of the Buh-tarminskaya Concrete Dam," MATERIALS ON THE CONFERENCE ON CONSTRUCTION OF HIGH DAMS ON ROCK FOUNDATIONS, GPKEIE Institute, 1964, p 14.
99. E. K. Aleksandrovskaya, "Stresses in the Dam at the Krasnoyarsk Hydroelectric Power Plant during the Periods of Construction and Temporary Operation," HYDROENGINEERING CONSTRUCTION, No 4, 1971, pp 19-24.
100. MESSUNGEN, BEOBACHTUNGEN UND VERSUCHE AN SCHWEIZERISCHEN TALSPERREN, 1919-1955, Schweizerische Talsperrenkomission, Bern, 1946.
101. G. L. Khesin, V. L. Sevost'yanov, "Simulation of the Thermoelastic Problems for Gravity Dams with Expanded Joints," HYDROENGINEERING CONSTRUCTION, No 6, 1967, pp 37-41.
102. M. S. Lankin, Sh. N. Plyat, A. A. Khrapkov, "Stressed State of the Massive Concrete Dam Considering Crack Formation on the Downstream Face," NEWS OF THE ALL UNION SCIENTIFIC RESEARCH INSTITUTE OF HYDRAULIC ENGINEERING, Vol 100, 1972, pp 232-247.
103. S. Ya. Eydel'man, "Opening the Contact Joints and Stress Relief of the Rock Foundation under the First Columns of the Channel Dam of the Bratsk Hydroelectric Power Plant," NEWS OF THE ALL UNION SCIENTIFIC RESEARCH INSTITUTE OF HYDRAULIC ENGINEERING, Vol 94, 1970, pp 140-153.
104. A. A. Khrapkov, "Dissipation of the Contact Stresses in the Splitting of the Gravity Dam Caused by the Force Effect of the Percolating Water," NEWS OF THE ALL UNION SCIENTIFIC RESEARCH INSTITUTE OF HYDRAULIC ENGINEERING, Vol 87, 1969, pp 104-121.
105. L. A. Rozin, METHOD OF FINITE ELEMENTS, Moscow, Energiya Press, 1971, 214 pp.
106. A. A. Gotlib, "Algorithm and Program Calculating the Gravity and the Counterforce Dams Jointly with the Base by the Method of Finite Elements," MATERIALS FROM THE SYMPOSIUM ON THE GES 73 COMPUTER, Leningrad, Energiya Press, 1973.

107. A. A. Khrapkov, B. N. Barshevskiy, L. A. Uvarov, "Theoretical and Model Studies of Contact Stresses with Respect to the Footing of the Dam at the Ust'-Ilim Hydroelectric Power Plant," SCIENTIFIC RESEARCH IN HYDRAULIC ENGINEERING IN 1970, Leningrad, Energiya Press, 1971, pp 15-16.
108. A. V. Karavlev, A. V. Vovkushevskiy, L. S. Kirillova, "Study of the Strength Models of the Stressed State of the Ust'-Ilim Dam in the Presence of Opened Intercolumnar Joints," ALL UNION CONFERENCE. METHODS OF DETERMINING THE STRESSED STATE AND STABILITY OF THE HIGH-HEAD HYDRO-ENGINEERING STRUCTURES AND THEIR FOUNDATIONS IN THE CASE OF STATIC AND DYNAMIC LOADS, MOSCOW, Moscow Institute of Construction Engineers imeni V. V. Kuybyshev, 1972.
109. Blanks, Meissner, Lowhouser, "Cracking in Mass Concrete," JACL, Vol III-IV, 1938.
110. W. R. Wough, "Experience in Controlling Temperatures and Cracking in Mass Concrete Dams," TRANS. THE VI CONGRESS ON LARGE DAMS, New York, 1958, Q. 21, R. 93.
111. Roy R. Clar, "Mss Concrete in Detroit Dam," JACL, June.
112. G. M. Makedoyaskiy, B. P. Matveyev, et al., SECTIONING MASSIVE STRUCTURES INTO CONCRETE POURING BLOCKS, Moscow, Energiya Press, 1969, 151 pp with illus.
113. B. M. Erakhtin, "Crack Formation in Temperature Regime of the Dam at the Bukhtarminskaya Hydroelectric Power Plant During the Construction Period," HYDROENGINEERING CONSTRUCTION, No 6, 1962, pp 5-11.
114. V. P. Shkarin, "Field Studies of the Thermal Crack Formation in the Concrete Bratsk Hydroelectric Power Plant," WORKS OF THE COORDINATION CONFERENCES ON HYDROENGINEERING, No 49, Leningrad, Energiya Press, 1969, pp 18-22.
115. L. M. Garakun, "Experimental Studies of the Thermal Crack Formation in the Blocks of Concrete Dams Erected under Severe Climatic Conditions," AUTHOR'S REVIEW OF DISSERTATION IN DEFENSE OF SCIENTIFIC DEGREE OF CANDIDATE OF TECHNICAL SCIENCES, Leningrad Polytechnic Institute, 1973, 26 pp.
116. A. P. Yepifamov, L. M. Garkul, L. M. Petrova, FROM THE EXPERIENCE IN REGULATING THE THERMAL REGIME OF THE MASSIVE CONCRETE OF THE DAM OF THE KRASNOYARSK HYDROENGINEERING COMPLEX DURING THE CONSTRUCTION PERIOD, Moscow, Informenergo Press, 1972, 39 pp with illus.
117. K. A. Mal'kov, "Discontinuity of the Concrete Structure," NEWS OF THE ALL UNION SCIENTIFIC RESEARCH INSTITUTE OF HYDRAULIC ENGINEERING, Vol 67, 1961, pp 163-180.

118. P. I. Vasil'yev, "Thermally Stressed State of Concrete Massifs and the Control of the Crack Formation in Concrete Dams," WORKS OF THE COORDINATION CONFERENCE ON HYDROELECTRIC ENGINEERING, No IV, Leningrad, Gosenergoizdat Press, 1962.
119. O. V. Kuntsich, "Tensile Strength and Extensibility of Concrete at a Low Cement Content," SCIENTIFIC AND ENGINEERING CONFERENCE ON THE STUDY OF THE PROPERTIES OF CONCRETE DETERMINING ITS CRACK RESISTANCE, NTOEP, Gosenergoizdat Press, 1963, pp 67-69.
120. M. A. Sadovich, "Limiting Extensibility of Concrete Considering the Pseudoplastic Deformations," HYDROENGINEERING CONSTRUCTION, No 7, 1973, pp 23-27.
121. S. A. Frid, "Basic Principles of Insuring the Crack Resistance of Massive Concrete Dams under Conditions of Siberia," HYDROENGINEERING CONSTRUCTION, No 1, 1964, pp 8-10.
122. S. Ya. Eydel'man, L. P. Trapeznikov, "Crack Formation in the Blocks of the Bratsk Hydroelectric Power Plant Dam," NEWS OF THE ALL UNION SCIENTIFIC RESEARCH INSTITUTE HYDRAULIC ENGINEERING, Vol 79, 1965, pp 41-70.
123. L. P. Trapeznikov, "Line of Effect for Normal Stresses in the Halfband," NEWS OF THE ALL UNION SCIENTIFIC RESEARCH INSTITUTE OF HYDRAULIC ENGINEERING, Vol 73, 1963, pp 271-278.
124. A. I. Adamovich, M. S. Lamkin, "Examination of the Crack Formation in the Concrete of the Bratsk Hydroelectric Power Plant Dam by Drilling Special Holes," WORKS OF THE COORDINATION CONFERENCE ON HYDROELECTRIC ENGINEERING, No IV, Leningrad, Gosenergoizdat Press, 1962, pp 265-288.
125. V. A. Ashikhmen, B. G. Fomin, "An Experiment in Monolithing of the Bratsk Hydroelectric Power Plant Dam," POWER ENGINEERING CONSTRUCTION, No 5, 1971, pp 43-46.
126. A. P. Dolmatov, V. L. Pavlov, A. I. Plosk, "Cementation of the Joints of the Krasnoyarsk Hydroelectric Power Plant Dam," HYDROENGINEERING CONSTRUCTION, No 7, 1970, pp 11-15.
127. V. A. Murzanov, V. A. Ashikhmen, I. G. Sovalov, Yu. G. Khayutin, "Problem of Monolithing Concrete Dams," HYDROENGINEERING CONSTRUCTION, No 10, 1968, pp 17-19.
128. B. G. Fomin, "Methods of Estimating the Quality of Cementation of Construction Joints," HYDROENGINEERING CONSTRUCTION, No 1, 1973, pp 7-10.
129. G. Ya. Pochtovick, A. S. Nikol'skiy, A. V. Mizonov, "Use of Ultrasound to Estimate the Condition of the Concrete Pouring Joints in Massive Concrete Structures," HYDROENGINEERING CONSTRUCTION, No 3, 1968, pp 30-32.

130. S. A. Tul'skiy, B. I. Sal'nitskiy, V. N. Shakhalev, "Application of Ultrasound for Monitoring the Quality of the Monolithing of the Construction Joints of the Massive Concrete Dams," POWER ENGINEERING CONSTRUCTION, No 5, 1971, pp 46-47.
131. A. N. Adamovich, "Efficient Methods of Monolithing the Concrete of High Dams by Cementation of the Construction Joints," MATERIALS ON THE CONFERENCE ON CONSTRUCTION OF HIGH CONCRETE DAMS ON A ROCK FOUNDATION, GPKEIE, 1964.
132. G. I. Shimel'nik, "Effect of the Attenuated Monolithic Nature of the Massive Concrete Dams on their Strength and Stability," NEWS OF THE INSTITUTIONS OF HIGHER LEARNING. CONSTRUCTION AND ARCHITECTURE, Novosibirsk, No 7, 1971, pp 135-139.
133. P. D. Yevdokimov, S. Ya. Eydel'man, L. N. Fradkin, "Study of the Displacements of the Stability of the Concrete Dam of the Bratsk Hydroelectric Power Plant," NEWS OF THE ALL UNION SCIENTIFIC RESEARCH INSTITUTE OF HYDRAULIC ENGINEERING, Vol 86, 1967, pp 171-187.
134. S. G. Gutman, "Calculation of Tunnels, Halfplane Weakened by a Circular Hole under Uniform Pressure," NEWS OF THE ALL UNION SCIENTIFIC RESEARCH INSTITUTE OF HYDRAULIC ENGINEERING, Vol 25, 1939, pp 148-168 with illus.
135. A. M. Arkhipov, S. Ya. Eydel'man, A. N. Kazachenko, "Field Studies of the Strength of the Spiral Chamber of the Bratsk Hydroelectric Power Plant," ANNOTATIONS OF THE SCIENTIFIC RESEARCH WORK ON HYDROENGINEERING COMPLETED IN 1962, Leningrad, Energiya Press, 1964, pp 37-40.
136. M. M. Grishin, HYDROENGINEERING STRUCTURES, Moscow, Gosstroyizdata Press, 1954, 499 pp with illus.
137. M. B. Ginzburg, K. A. Mal'tsov, I. B. Sokolov, DETERMINATION OF THE MAGNITUDE OF THE COUNTERPRESSURE IN THE CONCRETE OF HYDROENGINEERING STRUCTURES, Moscow-Leningrad, Gosenergoizdat, 1959, 67 pp with illus.
138. B. K. Frolov, REGULATION OF THE TEMPERATURE REGIME OF CONCRETE IN DAM STRUCTURES, Moscow, Energiya Press, 1964, 168 pp with illus.
139. D. P. Protukhin, S. A. Frid, L. K. [illegible], ROCK FOUNDATIONS OF HYDROENGINEERING STRUCTURES, Leningrad, Stroyizdat Press, 1971, 192 pp with illus.